


For Reference

NOT TO BE TAKEN FROM THIS ROOM

Ex LIBRIS
UNIVERSITATIS
ALBERTAENSIS





Digitized by the Internet Archive
in 2023 with funding from
University of Alberta Library

<https://archive.org/details/Kosar1983>

THE UNIVERSITY OF ALBERTA

THE EFFECT OF HEATED FOUNDATIONS ON OIL SAND

by



KEITH MICHAEL KOSAR

A THESIS

SUBMITTED TO THE FACULTY OF GRADUATE STUDIES AND RESEARCH
IN PARTIAL FULFILMENT OF THE REQUIREMENTS FOR THE DEGREE
OF MASTER OF SCIENCE IN GEOTECHNIQUE

DEPARTMENT OF CIVIL ENGINEERING

EDMONTON, ALBERTA

SPRING , 1983

ABSTRACT

The extraction and upgrading of bitumen at surface mining projects require the construction of heat generating structures. In some cases these structures must be situated above oil sand strata. Oil sand expands upon heating with the amount of expansion dependent on the amount of drainage of water and bitumen from the heated zone. The expansion can cause large surface movements which can have adverse effects on the structures.

Laboratory work consisted of the measurement of geotechnical properties of oil sand subjected to high temperatures. Detailed information was collected with regard to the influence of temperature on properties such as permeability, compressibility and volume change. Laboratory work also involved the preparation of high quality undisturbed oil sand test samples from frozen core.

Analytical studies involved utilizing information derived from the laboratory testing program to investigate theoretical methods for predicting volume change and pore fluid development of oil sand subjected to increases in temperature. Numerical methods were employed to analyze the rate at which heat flows through an oil sand mass and the rate at which excess pore fluid pressure resulting from an increase in temperature dissipates. A method was developed to couple the above processes (heat transfer and fluid flow).

Undrained heating of oil sand to 200 °C will result in a volume increase of about 6 percent. Most of this increase, over 5 percent, is due to the pore fluids, water and bitumen, with the bitumen expanding slightly more than water. The remainder of the volume increase is due to the thermal expansion of the sand grains. The dense, impenetrative structure of in situ oil sand will show a negligible amount of thermal volume change by itself.

The analytical model presented in this study investigated the effect of heat flow from a 80 m diameter storage tank on underlying oil sand strata. The tank was assumed to rest on a conventional crushed rock and sand foundation pad, 2 m in thickness, and held at a constant temperature of 175 °C.

The results of the theoretical analysis showed that although the rate of pore fluid flow was slower than that of heat flow, it was sufficient to provide a significant amount of drainage. The pore fluid pressure developed during heating of the oil sand strata was found to drain fast enough to negate large volume changes associated with the undrained condition. A maximum differential heave of 14 cm was observed after 30 years of heating. The amount of differential heave predicted from the analysis appears manageable when incorporated into a structural design of a storage tank.

ACKNOWLEDGEMENTS

The author is deeply indebted to his supervisor, Dr. J.D. Scott, for the conception of this research topic and for his guidance and encouragement throughout the study.

The author would also like to thank Dr. N.R. Morgenstern and Mr. J.G. Agar for providing invaluable advice, suggestions and guidance.

Special thanks are extended to Mr. Denis Gagnon for giving freely of his technical expertise in the laboratory.

The author is grateful for the technical assistance provided by Steve Gamble, Gerry Cyre, Rod McKenzie and Scotty Rogers. Gratitude is extended to Heinz Friedrich and Ken Ellis for constructing and modifying the laboratory apparatus.

Appreciation is expressed to the Natural Sciences and Engineering Research Council and the Department of Civil Engineering for providing financial support for this study.

Table of Contents

Chapter	Page
1. INTRODUCTION	1
1.1 Statement of Problem	1
1.2 Scope of Thesis	2
1.3 Organization of Thesis	6
2. LITERATURE REVIEW	8
2.1 The Athabasca Oil Sands	8
2.2 Characteristics of the Athabasca Oil Sands	8
2.3 Surface Mining Projects	13
2.4 Effect of Heat on Oil Sands	14
3. ANALYTICAL CONCEPTS	21
3.1 Influence of Heat on Oil Sands	21
3.1.1 Expansion	21
3.1.1.1 Expansion Under Fully Drained Conditions With no Effective Confining Pressure	21
3.1.1.2 Expansion Under Completely Undrained Conditions With Constant Effective Stress	23
3.1.2 Volume of Pore Fluid Expelled under Fully Drained Conditions with No Effective Confining Pressure	24
3.1.3 Heat Consolidation	26
3.1.3.1 Increase in Pore Fluid Pressure ...	26
3.2 Analysis of Fluid Flow	31
3.2.1 Introduction	31
3.2.2 Two Dimensional Transient Fluid Flow Beneath a Heated Foundation by Finite Elements	39
3.3 Analysis of Heat Flow	40

3.3.1	Introduction	40
3.3.2	Two Dimensional Transient Heat Flow Beneath a Heated Foundation by Finite Differences	44
3.4	Coupling of Heat and Fluid Flow	51
3.5	Conclusions	52
4.	LABORATORY APPARATUS AND PROCEDURES	54
4.1	Introduction	54
4.2	Laboratory Apparatus	55
4.2.1	Oedometer	55
4.2.2	Axial Loading and Back Pressure Systems ...	58
4.2.3	Heating System	58
4.2.4	Measuring Devices - Data Logger System	60
4.2.5	Insulation	61
4.3	Test Procedures	61
4.3.1	Thermal Expansion of Water	61
4.3.2	Thermal Expansion of Bitumen	64
4.3.3	Thermal Expansion of Compacted Tailing Sand	65
4.3.4	Thermal Expansion of Oil Sand	66
4.3.4.1	Sample Preparation	66
4.3.4.2	Undrained Test Procedure	69
4.3.4.3	Drained Test Procedure	71
4.4	Conclusions	71
5.	EXPERIMENTAL RESULTS	73
5.1	Thermal Expansion of Water	73
5.1.1	Introduction	73
5.1.2	Test Results	73

5.2	Thermal Expansion of Bitumen	76
5.2.1	Introduction	76
5.2.2	Test Material	77
5.2.3	Test Results	77
5.3	Thermal Expansion of Compacted Tailing Sand	81
5.3.1	Introduction	81
5.3.2	Test Material	81
5.3.3	Test Results	83
5.4	Thermal Expansion of Oil Sand	87
5.4.1	Introduction	87
5.4.2	Test Material	88
5.4.3	Test Results	88
5.4.4	Theoretical Analysis to Predict the Undrained Behavior of Oil Sand	99
5.5	Conclusions	102
6.	NUMERICAL ANALYSIS	106
6.1	Introduction	106
6.2	Heat Flow	107
6.3	Drainage	111
6.4	Volume Change	138
6.5	Conclusions	144
7.	SUMMARY AND CONCLUSIONS	150
7.1	Summary	150
7.2	Conclusions	152
7.3	Recommendations for Future Work	159
	BIBLIOGRAPHY	161
	APPENDIX A - THEORETICAL DEVELOPMENT	166

APPENDIX B - DETAILED DESCRIPTION OF APPARATUS	181
APPENDIX C - LABORATORY CALIBRATIONS	188
APPENDIX D - DATA REDUCTION CALCULATIONS	202
APPENDIX E - COMPUTER PROGRAMS	213

List of Tables

Table	Page
5.1 Test and Sample Data.....	89
6.1 Thermal Properties Used in Numerical Analysis.....	109

List of Figures

Figure	Page
1.1 Heated Bitumen Storage Tank on Oil Sand.....	4
2.1 Oil Sands Deposits of Alberta.....	9
2.2 Composition of In Situ Oil Sand.....	11
2.3 Grain Size Distribution for Athabasca Oil Sand.....	12
2.4 Surface Mineable Area of the Athabasca Oil Sands Deposit.....	15
3.1 Time Variant Flow Through an Element of Fully-Saturated Soil	34
3.2 Typical Nodal Arrangement for a Portion of the Region Beneath a Heated Foundation.....	46
3.3 Energy System Assigned to a Interior Node.....	47
3.4 Energy System Assigned to a Node along Axis of Symmetry.....	47
3.5 Energy System Assigned to a Node at Ground Surface.....	47
4.1 Drawing of Laboratory Apparatus.....	56
4.2 Laboratory Apparatus.....	57
4.3 Back Pressure System and Temperature Controller Unit.....	59
4.4 Data Logger System.....	62
4.5 Laboratory Apparatus Enclosed in Insulating Shell.....	63
4.6 Trimming Sample to Correct Diameter.....	68
4.7 Notching Sample.....	68
4.8 Machining Sample Ends Flush.....	70
5.1 Thermal Expansion of Water: Test 1.....	74
5.2 Thermal Expansion of Water: Test 2.....	75
5.3 Thermal Expansion of Bitumen.....	78

Figure	Page
5.4 Thermal Expansion of Bitumen (Experimental Results) vs. Water (Theoretical Curves).....	79
5.5 Thermal Expansion of Bitumen: Change in Density with Temperature.....	80
5.6 Grain Size Distribution of Oil Sand Tailings.....	82
5.7 Thermal Expansion of Sand at Different Densities....	84
5.8 Thermal Expansion of Sand: Change in Density With Temperature.....	85
5.9 Thermal Expansion of Oil Sand Samples.....	90
5.10 Thermal Expansion of Oil Sand: Change in Density With Temperature.....	91
5.11 Thermal Expansion of Sand Grains and Soil Structure in Drained Oil Sand Tests.....	92
5.12 Drained Oil Sand Tests in Terms of Dry Density.....	93
5.13 Thermal Volume Change of Soil Structure.....	97
5.14 Coefficient of Thermal Expansion of Soil Structure..	98
5.15 Thermal Volume Change of Oil Sand.....	101
5.16 Theoretical Expansion of Bitumen.....	103
6.1 Finite Element Mesh Utilized for Thermal Analyses..	110
6.2 Isotherm Plot after 3 Months.....	112
6.3 Isotherm Plot after 6 Months.....	113
6.4 Isotherm Plot after 9 Months.....	114
6.5 Isotherm Plot after 1 Year.....	115
6.6 Isotherm Plot after 5 Years.....	116
6.7 Isotherm Plot after 10 Years.....	117
6.8 Isotherm Plot after 15 Years.....	118
6.9 Isotherm Plot after 20 Years.....	119

Figure	Page
6.10 Isotherm Plot after 25 Years.....	120
6.11 Isotherm Plot after 30 Years.....	121
6.12 Computer Program Vartest5.....	123
6.13 Excess Pore Pressure after 3 Months.....	127
6.14 Excess Pore Pressure after 6 Months.....	128
6.15 Excess Pore Pressure after 9 Months.....	129
6.16 Excess Pore Pressure after 1 year.....	130
6.17 Excess Pore Pressure after 5 years.....	131
6.18 Excess Pore Pressure after 10 years.....	132
6.19 Excess Pore Pressure after 15 years.....	133
6.20 Excess Pore Pressure after 20 years.....	134
6.21 Excess Pore Pressure after 25 years.....	135
6.22 Excess Pore Pressure after 30 years.....	136
6.23 Heave Beneath Tank Due to Pore Fluid Pressure.....	140
6.24 Heave Beneath Tank Due to Thermal Volume Change of Sand Grains and Soil Structure.....	142
6.25 Total Heave Beneath Tank.....	143
A.1 Coefficient of Thermal Expansion of Oil Sand Components.....	167
A.2 Coefficient of Compressibility of Oil Sand Components.....	170
A.3 Dynamic Viscosity of Methane Saturated Bitumen.....	172
A.4 Dynamic Viscosity of Carbon Dioxide Saturated Bitumen.....	174
A.5 Dynamic Viscosity of In Situ Bitumen.....	175
A.6 Dynamic Viscosity of Bitumen, Water and Fluid.....	176
A.7 Unit Weight of Bitumen, Water and Fluid.....	178

Figure	Page
A.8	Hydraulic Conductivity of Oil Sand with Temperature180
C.1	Calibration Curve for 7.0 MPa Pressure Transducer..189
C.2	Calibration Curve for 2.0 MPa Pressure Transducer..190
C.3	Calibration Curve for Diaphragm Air Cylinder.....191
C.4	Calibration Curve for Linearly Varying Displacement Transducer.....193
C.5	Compression of Apparatus for Different Temperatures196
C.6	Vertical Expansion of Apparatus with Temperature...198
C.7	Piston Friction for Different Pressure Levels and Temperatures.....200

1. INTRODUCTION

1.1 Statement of Problem

The purpose of this thesis is to examine the influence that temperature increases from heated foundations have on the foundation performance of oil sand and to determine whether unacceptable foundation movement could be caused to overlying structures. The aim of the study is also to determine what temperatures are allowable in the oil sand or what rate of temperature increase in the oil sand from heated foundations is allowable before alteration of the physical properties of the oil sand occurs.

To analyze this problem, it is necessary to assess the rate at which heat generated by the structure propagates through the underlying oil sand strata and evaluate the amount of drainage which occurs. If drainage occurs at a rate greater than or equal to that of heat flow, the oil sand mass will be fully drained and thermal volume changes are due to the sand grains and soil structure. If drainage occurs at a rate less than that of heat flow the oil sand mass will be partially drained and thermal volume changes are due to the sand grains, soil structure and pore fluids (bitumen and water).

To perform the heat flow analysis, the heat flow parameters are required. These include thermal conductivity, density and specific heat. Oil sand subjected to an increase in temperature will experience: an increase in volume; a

change in viscosity of the pore fluids; and an increase in pore fluid pressure.

To determine the state of drainage it is necessary to assess: the distribution of pore pressure increase; permeability (which is dependent on viscosity); increase in volume of pore fluid; compressibility of pore fluid; and the change in volume of soil structure.

The amount of heave and differential heave occurring beneath the heated structure are calculated from the volume changes taking place in the oil sand mass.

1.2 Scope of Thesis

Undisturbed oil sand satisfies the fundamental requirements necessary for a good foundation material. Owing to its extremely dense interpenetrative structure, oil sand in situ has a high resistance to shearing failure (Chapter 2) and is virtually incompressible enabling it to support massive structures with minimal settlements. To illustrate the latter, consider a storage tank 80 m in diameter containing $100,000 \text{ m}^3$ of bitumen (density = 1.05 Mg/m^3) resting on a layer of oil sand 80 m in thickness. From the theory of elasticity (Lambe and Whitman, 1969) the stress at mid-layer (tank center) induced by the uniform normal stress of 205 kPa ($1.05 \text{ Mg/m}^3 \times 100,000 \text{ m}^3 \times 9.81/3.14 \times [40 \text{ m}]^2$) is 131 kPa (0.64×185). Assuming a coefficient of volume change of $5 \times 10^{-7} \text{ kPa}^{-1}$ (Dusseault, 1980) the settlement under the center of the tank would be

5.2 mm.

Oil sand subjected to temperature increases will expand with the interstitial fluids (water, bitumen and gases) contributing to the majority of the volume increase. As heat from the foundation propagates through the oil sand, the thermal expansion will produce heaving beneath the foundation. The severity of the heaving is dependent on the compositional nature of the oil sand, local stratigraphy, foundation temperature and whether or not sufficient drainage of pore fluids can take place.

The structure considered in the analyses is an 80 m diameter bitumen storage tank maintained at a constant temperature of 175 °C (Figure 1.1).

When examining the foundation performance of the oil sand beneath a heated structure, the possibility of shear failure, lateral movement and settlement must also be considered. The possibility of shear failure is governed by the lateral confining pressure on the oil sand beneath the structure, the relative density of the oil sand and the size of the foundation. In the surface mineable area the minor principal stress is believed to be vertical from the surface to a depth of approximately 330 m and is one-third that of the horizontal stress to a depth of about 100 m (Dusseault, 1977b). The relative density of in situ oil sand is extremely high (chapter 3). Since the size of the foundation considered in this study is extremely large and the lateral confining pressure and relative density high, the

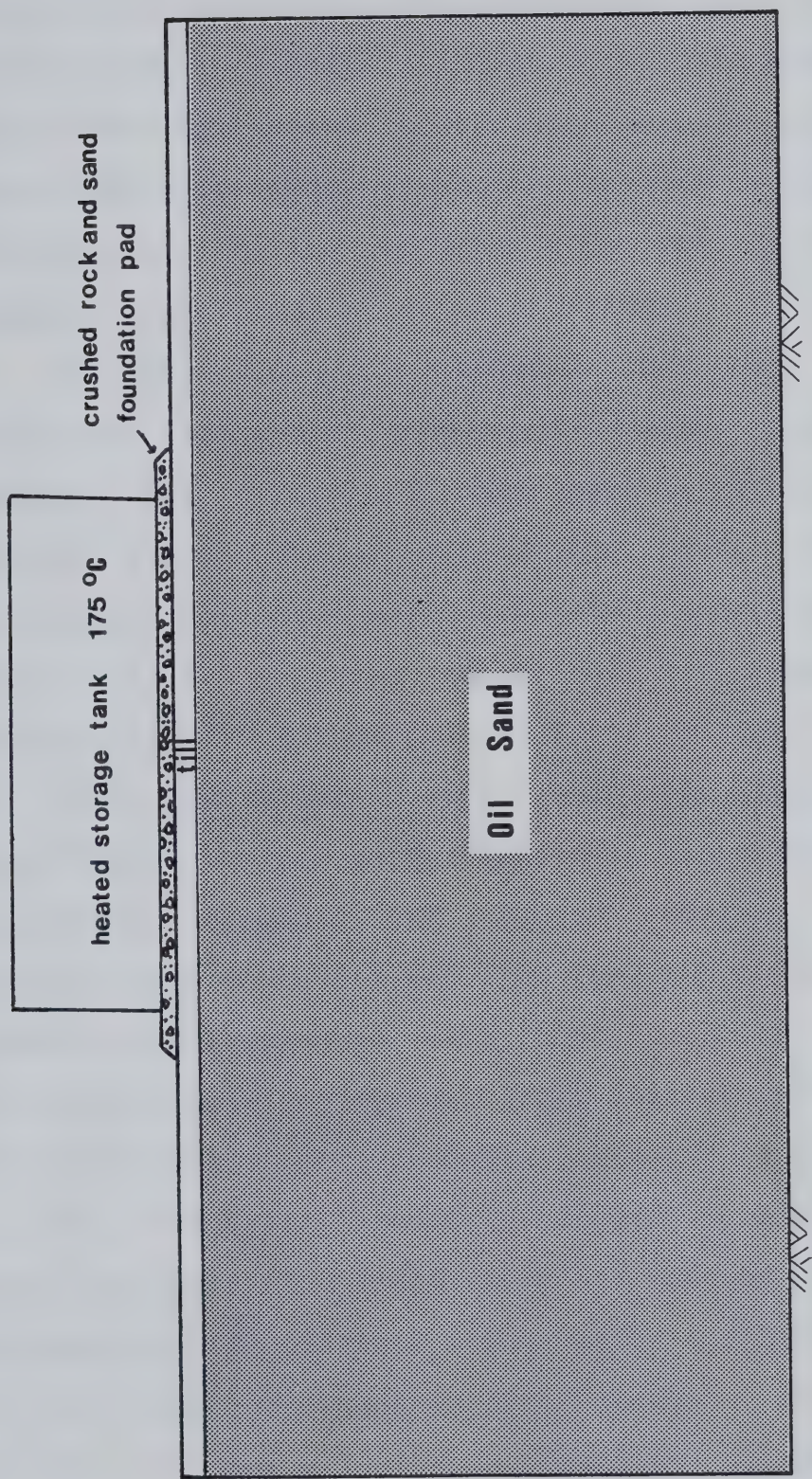


Figure 1.1 Heated Bitumen Storage Tank on Oil Sand

possibility of shear failure is extremely remote. These factors also negate the possibility of the oil sand and structure moving laterally. Results of this study will also show that settlement of the structure does not take place even under successive heating and cooling cycles. Heave and differential heave is the sole factor affecting the foundation performance of the oil sand.

The magnitude of expansion that oil sand and its individual constituent components undergo with temperature increase was determined experimentally in the laboratory. Thermal volume change experiments were performed on undisturbed oil sand under completely undrained and drained conditions to temperatures of 200 °C. Each component contributing to volume change; water, bitumen, sand grains, and soil structure were examined separately. The experimental values were compared to theoretical models for completely undrained and drained states. Experimental thermal constants derived from the testing of the oil sand constituent components were also used to examine the validity of existing formulations, theoretically derived for the prediction of pore pressure generation in heated soils.

The analytical model developed in this study couples heat flow theory to fluid flow to assess the state of drainage in the oil sand strata below the heated foundation and calculate the change in pore pressure and the volume change (or heave). The propagation of heat from the overlying structure through the oil sand strata was

determined analytically utilizing numerical heat transfer techniques. With consideration to changes in permeability, coefficients of thermal volume change and compressibility, dynamic viscosity, density, thermal generation rate and specific storage coefficient of oil sand with temperature and pressure, the amount of pore pressure drainage was also examined by numerical methods.

The analytical model used in this study was developed for the two-dimensional case. Although the model is easily adapted to the three-dimensional case, results of this study will show that the increase in accuracy would not justify the large computational effort and expense.

1.3 Organization of Thesis

Published information concerning the characteristics of the Athabasca Oil Sands (including compositional nature and engineering properties), surface mining projects, and studies relevant to heated foundations on oil sand is presented in Chapter 2.

Chapter 3 contains a discussion of the analytical concepts utilized in this study. These concepts include: the influence of heat on oil sands (expansion and drainage); analysis of heat flow; analysis of fluid flow; and the coupling of heat and fluid flow.

A description of the laboratory apparatus and test procedures employed in the experimental program are given in Chapter 4. The experimental results and discussion of

results are contained in Chapter 5.

Numerical analysis simulating heat flow into an oil sand foundation from a hot bitumen storage tank is given in Chapter 6. Also in this chapter analytical techniques are used to predict the amount of drainage which may occur. The resulting volume change of the oil sand foundation from the numerical analyses is also given.

Chapter 7 contains observations made during the study and conclusions drawn from the research.

The engineering properties of the oil sand constituent components which were required as input for the numerical analyses are given in Appendix A. This appendix outlines the source of the data used to derive each property (experimental testing or published information) and how each property varies with temperature and pressure.

Appendix B provides a detailed description of the apparatus used in the experimental testing program. Appendix C outlines the laboratory calibrations used and Appendix D provides the data reduction calculations.

Appendix E contains listings of the available computer programs used in the study.

2. LITERATURE REVIEW

2.1 The Athabasca Oil Sands

The Athabasca Oil Sand Deposit is located in northeastern Alberta (Figure 2.1) underlying an area of approximately 32,000 square kilometers with estimated inplace reserves of 146.5 billion cubic meters (Outrim and Evans, 1978; Mossop, 1980). Athabasca, the largest of the four major oil sands deposits in Alberta, is unique in that a portion of the reserves (about 10 percent) have less than 50 m of overburden (figure 1.1) and is exploitable by surface mining methods (Mossop, 1978).

In contrast to the other Alberta oil sand deposits, the Athabasca reserves are limited for the most part to one reservoir unit, the McMurray Formation. Mossop (1980) describes the McMurray Formation as a Lower Cretaceous unit consisting of uncemented quartz sand with interbedded shales. In general, the entire McMurray Formation bears oil with the well sorted, shale free oil sand layers having porosities of up to 35 percent and oil saturations of 18 weight percent (Carrigy and Kramers, 1974; Mossop, 1978).

2.2 Characteristics of the Athabasca Oil Sands

The vast majority of reserves of the Athabasca Deposit are found in the sands of the Lower Mannville McMurray Formation. The McMurray Formation in the area of concern averages between 40 and 60 m in thickness (Mossop, 1980). In



Figure 2.1 Oil Sands Deposits of Alberta

the area of the present mining operations, the overburden varies in thickness from 0 to about 35 m.

Oil sand typical of the Athabasca deposit consists of approximately 95 percent quartz, 2 to 3 percent feldspar grains, 2 to 3 percent mica and clay minerals, and traces of other minerals (Mossop, 1978). The grains are primarily subangular with moderate sphericity (Mossop, 1980). The high grade oil bearing sands in Athabasca are predominantly fine to medium grained and uniformly graded quartz sand (Dusseault, 1977).

The sand grains are surrounded by a thin film of water, with the remaining pore space occupied by the oil (Figure 2.2). The water and the oil form continuous phases (Mossop, 1980). The majority of clay particles in the oil sand matrix are contained in the water envelope usually attached directly to the sand grains. Substantial portions of gases (mostly methane and carbon dioxide) are dissolved within the liquid phase of the oil sands (Dusseault, 1977).

Dusseault (1977; 1980) reports saturated bulk densities for uniformly graded, rich oil sand (the ore bearing zones of the Middle and Lower McMurray Formation) of 2.05 to 2.18 Mg/m³ and porosities of 28 to 36 percent. Mossop (1978) reports oil and water saturations of rich oil sands in the Athabasca Deposit of 18 and 2 weight percent, respectively. The grain size distribution for Athabasca oil sand is given in Figure 2.3.

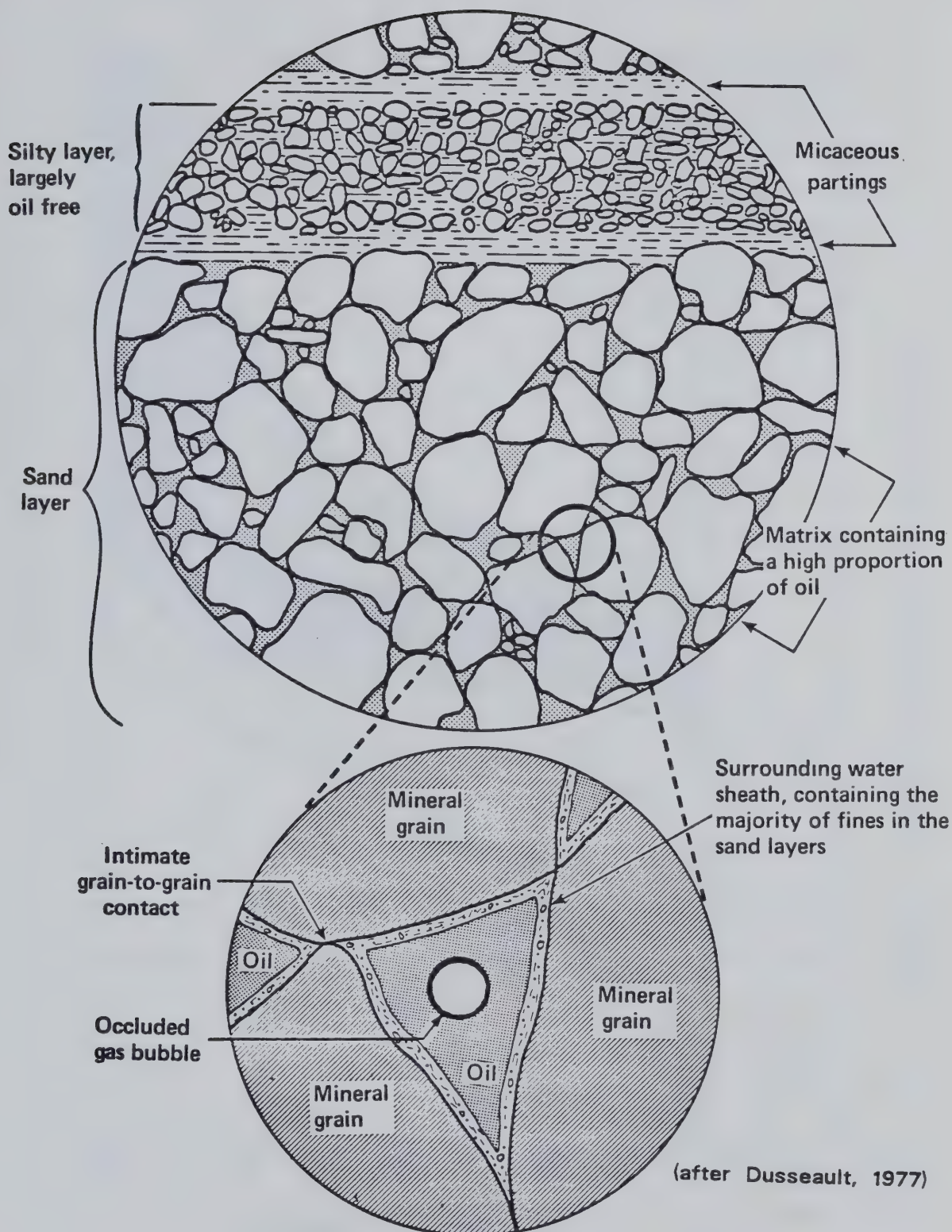


Figure 2.2 Composition of In Situ Oil Sand

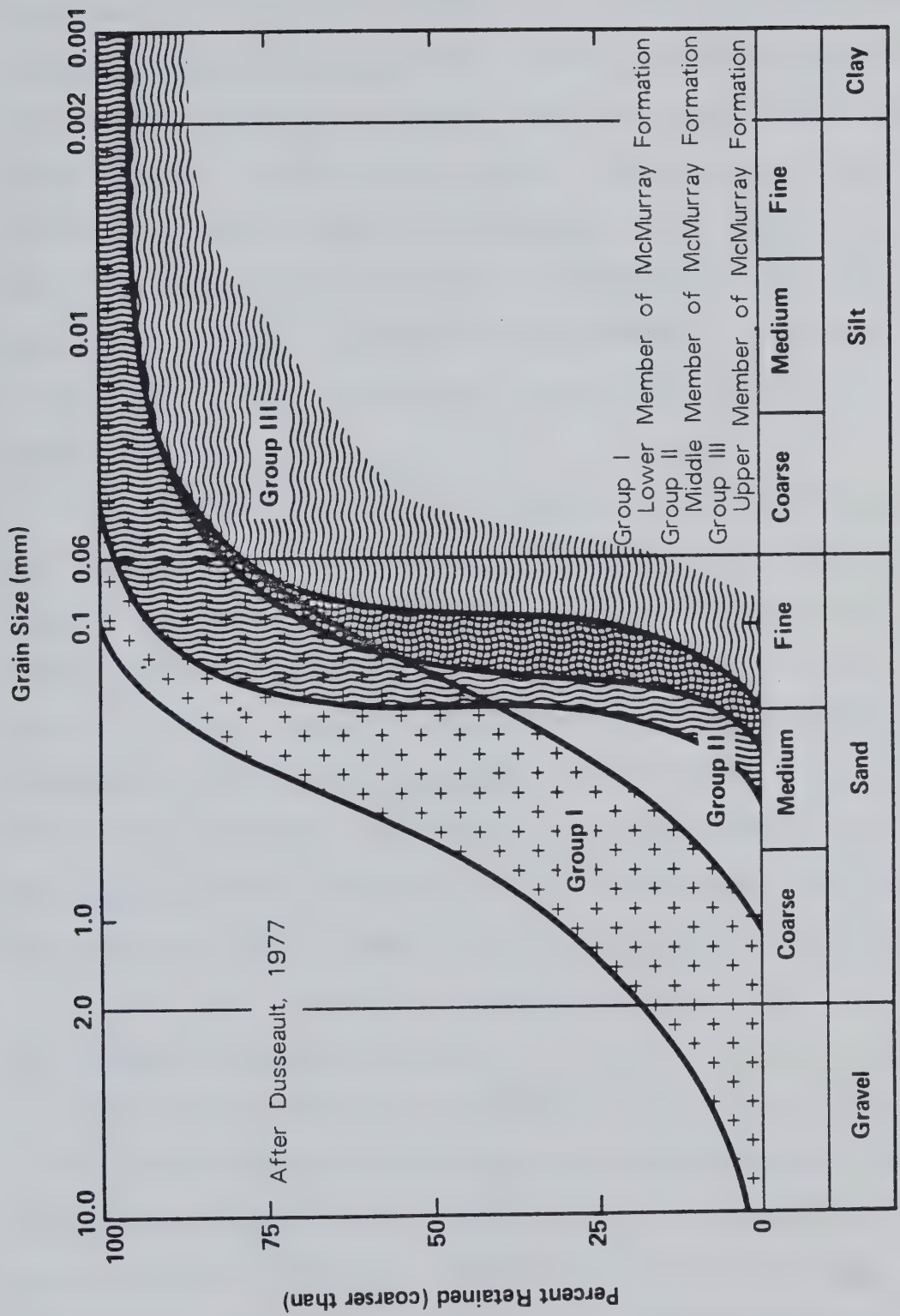


Figure 2.3 Grain Size Distribution for Athabasca Oil Sand



Undisturbed oil sand exhibits extremely high shear strengths and dilatancy compared to normal dense sand of similar mineralogy. Dusseault (1977) provides evidence from thin section and scanning electron microscope investigations which show oil sand, unlike typical dense sands, has a large number of concavo-convex and straight (or long) contacts. This interpenetrative structure developed during the time of burial in which diagenetic processes occurred with dissolution and recrystallization of quartz at grain boundaries.

Undisturbed oil sands exhibit curvilinear Mohr failure envelopes. The internal angle of friction is high at low normal stresses, reflecting high rates of dialation but as normal stresses increase dilatancy is reduced as more shear occurs through grains and surface asperities. The rate of curvature in the failure envelope decreases as the residual angle of shearing resistance is approached (33 to 36° (Dusseault, 1977)). Dusseault (1977) expresses the failure envelopes for undisturbed oil sand as a power law functions.

2.3 Surface Mining Projects

Of the 11.8 billion cubic meters of reserves which lie within the surface mineable area of the Athabasca Deposit only 6.4 billion cubic meters are recoverable by current surface mining methods, resulting in 4.3 billion cubic meters of synthetic crude oil (Outtrim and Evans, 1978). Figure 2.4 illustrates the surface mineable area of the

Athabasca oil sand deposit indicating the location of the two existing commercial operations (Suncor Inc. and Syncrude Canada Ltd.). A third surface mining project was proposed by the Alsands Consortium and was to be located 70 km north of Fort McMurray (Figure 2.4).

Suncor began surface mining of oil sand with bucket wheel excavators in 1963 and is currently producing about 8000 cubic meters of synthetic crude oil per day. The surface mining activity at the Syncrude site commenced in 1977 with draglines and is currently producing approximately 20,000 cubic meters of synthetic crude oil per day. The proposed Alsands project was planned to mine oil sand with draglines and was projected to produce approximately 22,000 cubic meters of synthetic crude oil per day.

2.4 Effect of Heat on Oil Sands

Only recently, upon the construction of the Syncrude Canada Ltd. commercial production facility was the necessity for erecting heated structures on oil sand strata considered. As a result, little information exists in the published literature concerning the behavior of oil sands beneath heated foundations.

Boga, et al. (1980) conducted a study to explore the stability of oil sand exposed to excessive heating beneath hot bitumen storage tanks. The investigation centered on the proposed installation of four additional hot storage tanks 12 m above oil sand at the Syncrude plant site. The study

was intended to provide an optimum thermal foundation design for the hot bitumen storage tanks.

Utilizing a finite element thermal model Boga, et al. (1980) investigated the propagation of heat from the tanks in the subsurface material. Triaxial testing of oil sand samples under drained and undrained conditions to temperatures of 90 °C were also conducted. The oil sand used in the testing program were obtained from block samples taken from the Syncrude mining operation. Since no precautions were taken to guard against expansion of the oil sand from in situ conditions, the samples could be assumed to be at a considerably lower density and thus be considered disturbed. The in situ horizontal stress in this study was assumed to be one-half the vertical in the Syncrude mine area. In the surface mineable area, however, the horizontal stress is believed to be three times the vertical stress to a depth of about 100 m (Dusseault, 1977b; section 1.2). Such conditions suggest one-dimensional testing (zero lateral strain) is more representative of actual field conditions.

The triaxial tests conducted in this study indicate that under fully drained conditions oil sand did not display any softening or failure to temperatures of 90 °C. The triaxial tests conducted under fully undrained conditions, however, displayed a significant increase in pore fluid pressure at 60 °C and softened and subsequently failed at 70 °C. It was concluded from these tests that under undrained conditions the strength of oil sand is adversely affected at

temperatures exceeding approximately 45 °C.

Boga, et al. (1980) noted in their investigation that considering the slow rate of heat flow into the oil sand foundation beneath the heated storage tank, some dissipation of pore fluid pressure was possible. However, since the amount of pore pressure dissipation from drainage could not be calculated, a maximum limiting temperature of 45 °C (based on undrained tests) for the oil sand beneath the tank was assumed for design purposes. This limiting temperature, combined with the thermal analysis, provided a foundation design for the proposed tanks.

Harris and Sobkowicz (1977) developed a mathematical model to analyze the undrained behavior of oil sand to changes in temperature (and/or stress). The model has the capability of dealing with either one-dimensional compression (no lateral strain) or two-dimensional, plane strain. The model does not, however, incorporate the effect of fluid pressure drainage which occurs during the time of heat propagation into the oil sand layer. As a result, the model may exaggerate the magnitude of potential heave which may occur as the temperature of the oil sand beneath the hot foundation increases with time.

Byrne, et al. (1980) provide a procedure for estimating the undrained behavior of oil sand resulting from changes in temperatures and loads. The method involves use of the computer program *OILSTRESS* (developed by Byrne and Grigg [1980]). The program utilizes finite element techniques and

has the capability to deal with both plane strain and axisymmetric conditions. The program assesses volume changes occurring in the pore fluid and couples it with that of the sand matrix to maintain volumetric compatibility. An iterative procedure is used to obtain compatibility in the sand skeleton and fluid phases in terms of volumetric strain. Gas laws are used to calculate changes in pore pressures. In the analysis the sand skeleton is considered non-linear elastic. The program also considers volume changes arising from shear dilatation:

Although Byrne, et al. (1980) have not applied the computer program *OILSTRESS* directly to heated foundations on oil sand, it has been used successfully in predicting the behavior of one-dimensional stress relief of oil sand. The procedure has also been utilized to predict the response of a deep shaft in oil sand. When applied to cylindrical openings in elastic and elastic-plastic materials the results obtained from the analysis compare favourably with closed form solutions.

Charlwood, et al. (1980) modified the computer model put forth by Byrne, et al. (1980) (which only considers temperature influence on the gas phase of oil sand) to include transient heat transfer and thermal expansion effects. The model is intended for use in mine assisted in situ (MAIS) design applications.

The computer model proposed by Charlwood et al. (1980) was not used for this study for several reasons. The model

assumes in its pore pressure generation term for undrained conditions that water and bitumen are incompressible. It will be shown in this study that the compressibility of bitumen and water is similar to that of the soil structure. The pore pressure generation term also does not include thermal expansion of pore fluids.

The forces associated with temperature are calculated in this model based on a single value of thermal expansion coefficient and therefore fails to differentiate between drained and undrained thermal expansion. Therefore, if an undrained thermal expansion coefficient were used in the analysis, the stress distribution in the oil sand strata would only be correct if all elements remain fully undrained throughout the analysis. Should any of the elements reach a temperature in which the permeability was such to permit drainage of pore fluids, these elements would have to be manually altered to the correct drained volume in order to produce the proper stress distribution. In other words, the computer program does not account for mass transfer during simultaneous thermal expansion and drainage because it cannot automatically differentiate between drained and undrained coefficients of thermal expansion. As a result, use of the program for the purposes required for this study would be extremely difficult.

The geotechnical aspects of oil sand behavior due to temperature changes and the concept of heat-consolidation (the time rate of drainage during heating) are discussed by

Morgenstern (1981).

A theoretical analysis for predicting volume changes in soils resulting from temperature variations and pore pressure changes due to undrained heating have been developed by Campanella and Mitchell (1968) and examined further by Mitchell (1976). These theoretical expressions are discussed in Chapter 3.

3. ANALYTICAL CONCEPTS

3.1 Influence of Heat on Oil Sands

3.1.1 Expansion

A theoretical analysis for predicting volume changes in saturated soils subjected to temperature changes was put forth by Campanella and Mitchell (1968). This analysis is extended herein to consider oil sand which contains two pore fluids (bitumen and water). The analysis presented here assumes the pressure of the pore fluids is sufficient to prevent gas exsolution and pore fluid vapourization or distillation. The influence of possible gas exsolution is discussed in the conclusions of Chapter 6.

3.1.1.1 Expansion Under Fully Drained Conditions With no Effective Confining Pressure

Under fully drained conditions the volume change of oil sand subjected to increases in temperature under no effective confining pressure arises from the expansion of the individual sand grains and structural changes in the sand skeleton.

Campanella and Mitchell (1968) theorize that when a homogeneous sand with grains in particle to particle contact undergoes a temperature change, each mineral experiences the same volumetric strain and the entire structure will experience the same volumetric strain ($\alpha_s \Delta T$). It is believed that subsequent volume changes

may arise from changes in intergranular forces due to temperature which entails relative movement or reorientation of particles to allow the sand mass to support the same effective stress. Campanella and Mitchell (1968) denote this change in volume by $(\Delta V_{s,t})_{\Delta T}$. As a result the net volume change of an oil sand mass subjected to a change in temperature under fully drained conditions is:

$$(\Delta V_m)_{\Delta T} = \alpha_s V_m \Delta T + (\Delta V_{s,t})_{\Delta T} \quad 3.1$$

where:

α_s = volumetric coefficient of thermal expansion of the sand grains

V_m = volume of oil sand mass

ΔT = change in temperature

The structural volume change of the sand structure due to a change in temperature may be expressed as:

$$(\Delta V_{s,t})_{\Delta T} = \alpha_{s,t} V_m \Delta T \quad 3.2$$

where:

$\alpha_{s,t}$ = coefficient of structural volume change of sand structure due to change in temperature

Combining equations 3.1 and 3.2 gives:

$$(\Delta V_m)_{\Delta T} = (\alpha_s + \alpha_{s,t}) V_m \Delta T \quad 3.3$$

3.1.1.2 Expansion Under Completely Undrained Conditions With Constant Effective Stress

Under completely undrained conditions the volume change of oil sand subjected to increases in temperatures under a constant effective stress arises from the expansion of the individual sand grains and pore fluids as well as structural changes in the sand skeleton.

The volume change of pore fluids experiencing a change in temperature can be stated mathematically as:

$$(\Delta V_F)_{\Delta T} = \alpha_w V_w \Delta T + \alpha_b V_b \Delta T \quad 3.4$$

where:

α_w = coefficient of thermal volume change of water

V_w = volume of pore water

ΔT = change in temperature

α_b = coefficient of thermal volume change of bitumen

V_b = volume of pore bitumen

The total volume change of an oil sand mass subjected to a change in temperature under completely undrained conditions (effective stress held constant)

is:

$$(\Delta V_m)_{\Delta T} = (\Delta V_F)_{\Delta T} + (\Delta V_m^d)_{\Delta T} \quad 3.5$$

where:

(ΔV_m^d) = net volume change of an oil sand mass subjected to a change in temperature under fully drained conditions

Combining equations 3.3, 3.4, and 3.5 gives:

$$(\Delta V_m)_{\Delta T} = \alpha_w V_w \Delta T + \alpha_b V_b \Delta T + (\alpha_s + \alpha_{s,t}) V_m \Delta T \quad 3.6$$

3.1.2 Volume of Pore Fluid Expelled under Fully Drained Conditions with No Effective Confining Pressure

The volume of pore fluid drained (under no confining stress) from a fully saturated oil sand sample experiencing a change in temperature can be expressed as:

$$(\Delta V_d)_{\Delta T} = (\Delta V_F)_{\Delta T} + (\Delta V_s)_{\Delta T} - (\Delta V_m)_{\Delta T} \quad 3.7$$

where:

$(\Delta V_s)_{\Delta T}$ = volume change of the sand grains due to change in temperature

The volume change of the sand grains due to change in temperature can be expressed mathematically as:

$$(\Delta V_s)_{\Delta T} = \alpha_s V_s \Delta T \quad 3.8$$

Combining equations 3.3, 3.4, 3.6 and 3.7 gives:

$$(\Delta V_d)_{\Delta T} = \alpha_w V_w \Delta T + \alpha_b V_b \Delta T + \alpha_s V_s \Delta T - \alpha_s V_m \Delta T - \alpha_{s,t} V_m \Delta T \quad 3.9$$

or:

$$(\Delta V_d)_{\Delta T} = \alpha_w V_w \Delta T + \alpha_b V_b \Delta T - \alpha_s \Delta T (V_m - V_s) - \alpha_{s,t} V_m \Delta T \quad 3.10$$

where:

$V_m - V_s$ = volume of the voids

Put simply into words, the amount of fluid expelled from an oil sand sample during a drained thermal expansion test is the sum of the volume change of the fluids less the change in void volume and structural volume change. If the structure expands $[\Delta V_{s,t}]_{\Delta T}$ is positive and would be subtracted or contrastingly if the structure contracts $[\Delta V_{s,t}]_{\Delta T}$ is negative and would be added.

3.1.3 Heat Consolidation

The amount of expansion an oil sand mass experiences due to temperature changes depends on the amount of pore fluid which is permitted to drain. To evaluate the quantity of fluid flowing from oil sand subjected to temperature increases it is necessary to assess the relative rates of pore pressure generation and dissipation.

Campanella and Mitchell (1968) provide a theoretical analysis for predicting pore water pressure changes in saturated soils subjected to temperature changes. This analysis is extended here to consider oil sand which contains two pore fluids (bitumen and water). Gas exsolution and pore fluid vapourization is not considered in the analysis.

3.1.3.1 Increase in Pore Fluid Pressure

Under undrained conditions the combined volume changes of the oil sand constituents (bitumen, water and sand grains) resulting from changes in pressure and temperature must balance the combined changes of the entire oil sand mass resulting from changes in pressure and temperature, i.e.:

$$(\Delta V_b)_{\Delta T} + (\Delta V_w)_{\Delta T} + (\Delta V_s)_{\Delta T} + (\Delta V_b)_{\Delta p} + (\Delta V_w)_{\Delta p} + (\Delta V_s)_{\Delta p} = (\Delta V_m)_{\Delta T} + (\Delta V_m)_{\Delta p} \quad 3.11$$

where:

ΔV_b = volume change of pore bitumen

ΔV_w = volume change of pore water

ΔV_s = volume change of sand grains

ΔV_m = volume change of oil sand mass

The volume changes of the oil sand constituents due to pressure changes can be written as:

$$(\Delta V_b)_{\Delta p} = m_b V_b \Delta u \quad 3.12$$

$$(\Delta V_w)_{\Delta p} = m_w V_w \Delta u \quad 3.13$$

$$(\Delta V_s)_{\Delta p} = m_s V_s \Delta u + m_s' V_s \Delta \sigma' \quad 3.14$$

where:

m_b = compressibility of bitumen

Δu = change in pore fluid pressure

m_w = compressibility of water

m_s = compressibility of sand grains under an all round pressure

m_s' = compressibility of sand grains when grains are subjected to concentrated loadings

$\Delta \sigma'$ = change in intergranular (effective) stress

The volume change of the total oil sand mass due to pressure changes can be written as:

$$(\Delta V_m)_{\Delta p} = m_v V_m \Delta \sigma' \quad 3.15$$

where:

m_v = compressibility of oil sand mass

The change in volume of pore water, pore bitumen and sand grains due to temperature change are expressed as:

$$(\Delta V_w)_{\Delta T} = \alpha_w V_w \Delta T \quad 3.16$$

$$(\Delta V_b)_{\Delta T} = \alpha_b V_b \Delta T \quad 3.17$$

Substituting equation 3.8 and equations 3.12 through 3.17 into the governing equation for undrained conditions (equation 3.11) gives:

$$\alpha_b V_b \Delta T + \alpha_w V_w \Delta T + \alpha_s V_s \Delta T + m_b V_b \Delta u + m_w V_w \Delta u + m_s V_s \Delta u + m_s' V_s \Delta \sigma' = (\Delta V_m)_{\Delta T} + m_v V_m \Delta \sigma' \quad 3.18$$

rearranging terms yields:

$$\alpha_b V_b \Delta T + \alpha_w V_w \Delta T + \alpha_s V_s \Delta T - (\Delta V_m)_{\Delta T} = m_v V_m \Delta \sigma' - m_b V_b \Delta u - m_w V_w \Delta u - V_s (m_s \Delta u + m_s' \Delta \sigma') \quad 3.19$$

The change in effective stress may be expressed as:

$$\Delta\sigma' = \Delta\sigma - \Delta u$$

where: $\Delta\sigma$ = change in total stress

The change in total stress at depth d may be represented as:

$$\Delta\sigma = \Delta\gamma_{s,t}d$$

or,

$$\Delta\sigma = (V_b/V_m)\Delta\gamma_b d + (V_w/V_m)\Delta\gamma_w d + (V_s/V_m)\Delta\gamma_s d$$

Since the unit weight of the sand grains does not vary with temperature or pressure ($\Delta\gamma_s = 0$) then:

$$\Delta\sigma = (V_b/V_m)\Delta\gamma_b d + (V_w/V_m)\Delta\gamma_w d$$

As a result, equation 3.19 becomes:

$$\alpha_b V_b \Delta T + \alpha_w V_w \Delta T + \alpha_s V_s \Delta T - (\Delta V_m)_{\Delta T} = m_v V_m (V_b \Delta\gamma_b d / V_m + V_w \Delta\gamma_w d / V_m - \Delta u) - m_b V_b \Delta u - m_w V_w \Delta u - V_s (m_s \Delta u + m_s' [V_b \Delta\gamma_b d / V_m + V_w \Delta\gamma_w d / V_m - \Delta u]) \quad 3.20$$

Assuming m_s and m_s' do not differ greatly and are very small as compared to m_v , m_b and m_w , no significant error is introduced by setting $m_s = m_s' = 0$, as a result

equation 3.19 can be rewritten as:

$$\alpha_b V_b \Delta T + \alpha_w V_w \Delta T + \alpha_s V_s \Delta T - (\Delta V_m)_{\Delta T} = m_v V_m (V_b \Delta \gamma_b d / V_m + V_w \Delta \gamma_w d / V_m) - m_v V_m \Delta u - m_b V_b \Delta u - m_w V_w \Delta u \quad 3.21$$

Since $V_m = V_b + V_w + V_s$ and $(\Delta V_m)_{\Delta T} = \alpha_s V_m \Delta T + \alpha_{s,t} V_m \Delta T$ (section 3.1.1) equation 3.21 becomes:

$$\alpha_b V_b \Delta T + \alpha_w V_w \Delta T - \alpha_s V_b \Delta T - \alpha_s V_w \Delta T - \alpha_{s,t} V_m \Delta T = m_v V_m (V_b \Delta \gamma_b d + V_w \Delta \gamma_w d) - m_v V_m \Delta u - m_b V_b \Delta u - m_w V_w \Delta u \quad 3.22$$

Assuming the oil sand mass is fully saturated, the extent to which the voids are filled by bitumen or water (bitumen and water porosities) can be expressed as:

$$n_b = V_b / V_m \text{ and } n_w = V_w / V_m \quad 3.23$$

equation 3.22 may be rewritten as:

$$\Delta u = n_b \Delta T (\alpha_b - \alpha_s) + n_w \Delta T (\alpha_w - \alpha_s) - \alpha_{s,t} \Delta T - m_v (n_b \Delta \gamma_b d + n_w \Delta \gamma_w d) / m_v + n_b m_b + n_w m_w \quad 3.24$$

It should be noted that α_s , α_b and α_w are positive in the above equations since an increase in temperature results in an increase in volume; whereas, m_v , m_b and m_w are negative because volume decreases with increasing pressure. The coefficient $\alpha_{s,t}$ is positive when an

increase in temperature produces an increase in volume of the sand structure and negative when a decrease in volume of the sand structure occurs.

3.2 Analysis of Fluid Flow

3.2.1 Introduction

To evaluate the rate at which excess pore fluid pressure resulting from an increase in temperature dissipates from an oil sand mass, the rate of fluid flow must be examined. One dimensional fluid flow through a saturated soil is governed by Darcy's observational law which is represented by the equation:

$$v = -ki \quad 3.25$$

or

$$q = - kiA \quad 3.26$$

where:

v = flow velocity

k = hydraulic conductivity

i = hydraulic gradient

q = flow rate

A = cross-sectional area of soil normal to the direction of

flow

The value of the hydraulic conductivity for a soil is influenced by the properties of the permeant and the soil. The Kozeny-Carman equation provides a good assessment of the hydraulic conductivity in uniform sands (Mitchell, 1976) and illustrates the effect soil and permeant properties have on permeability. The Kozeny-Carman equation is expressed in the following manner

$$k = \gamma e^3 / K_0 S^2 \mu (1 + e) \quad 3.27$$

where:

k = the Darcy hydraulic conductivity

γ = unit weight of permeant

e = void ratio

K_0 = pore shape factor

S = the specific surface per unit volume of particles

μ = viscosity of permeant

It is apparent from the Kozeny-Carman equation that the hydraulic conductivity is dependent, in part, on the viscosity and the unit weight of the permeant. Temperature changes influence both the viscosity and the unit weight (or density) of the permeant and therefore the hydraulic conductivity also varies with temperature. It is useful to

express hydraulic conductivity in terms of absolute permeability K (a coefficient dependant on the properties of the soil skeleton only) by the equation:

$$k = K (\gamma[\Delta T] / \mu[\Delta T]) \quad 3.28$$

Lambe and Whitman (1969) outline the soil characteristics which affect hydraulic conductivity. These characteristics include void ratio, particle size, fabric, composition and degree of saturation. When considering an oil sand mass subjected to a change in temperature changes in particle size, void ratio and fabric can be expected.

Consider the time variant flow through an element of fully-saturated soil having dimensions dx , dy and dz with flow occurring in the x,y plane only (Figure 3.1). The volume of fluid entering the element during a time Δt is:

$$(v_x - [\partial v_x / \partial x] dx / 2) dy dz \Delta t + (v_y - [\partial v_y / \partial y] dy / 2) dx dz \Delta t$$

where:

v_x, v_y = components of velocity at the central point P ($x = y = z = 0$) of the element

$[\partial v_x / \partial x], [\partial v_y / \partial y]$ = change of velocity in the x and y directions

$dy dz, dx dz$ = cross-sectional areas

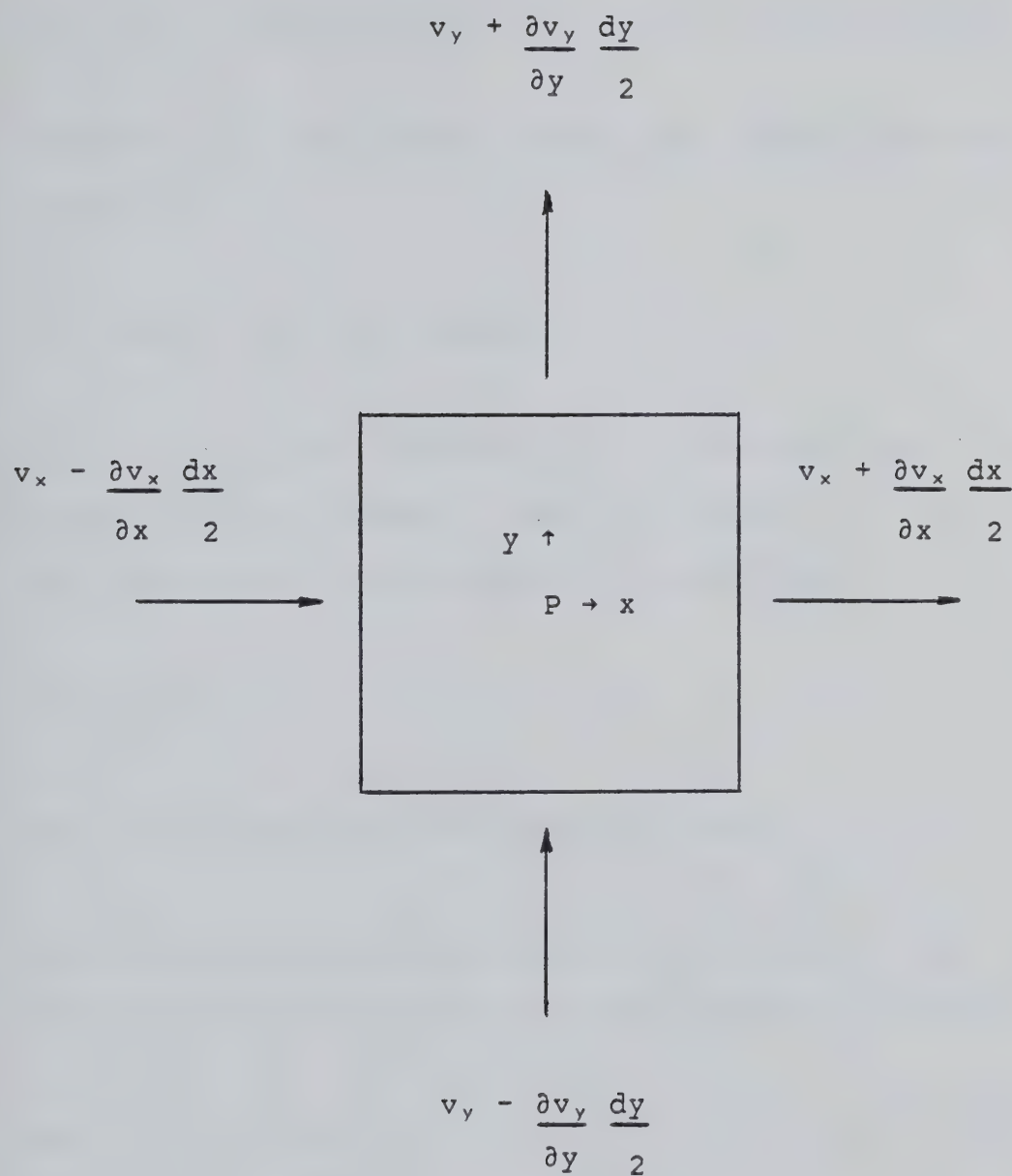


Figure 3.1 Time Variant Flow Through an Element of Fully-Saturated Soil

The volume of fluid leaving the element during a time Δt is:

$$(v_x + [\partial v_x / \partial x] dx / 2) dy dz \Delta t + (v_y + [\partial v_y / \partial y] dy / 2) dx dz \Delta t$$

Therefore, the net volume leaving the element during a time Δt is:

$$([\partial v_x / \partial x] + [\partial v_y / \partial y]) dx dy dz \Delta t$$

During the time increment Δt , the total head at point P increases by ΔH and as a result the volume of fluid taken into storage due to the change in total head is:

$$S_s dx dy dz \Delta H$$

where: S_s = specific storage coefficient

The volume being generated within the element due to the thermal expansion of the pore fluid during the time Δt is:

$$Vg\Delta t = g' dx dy dz \Delta t$$

where: g' = thermal generation rate

From the principle of continuity (conservation of volume) the above three quantities must sum to zero, hence:

$$([\partial v_x / \partial x] + [\partial v_y / \partial y]) dx dy dz \Delta t + S_s dx dy dz \Delta H + g' dx dy dz \Delta t = 0 \quad 3.29$$

substituting:

$$v_x = -k_x [\partial H / \partial x]$$

and

$$v_y = -k_y [\partial H / \partial y]$$

into equation 3.28 and rearranging terms yields:

$$\partial / \partial x (k_x [\partial H / \partial x]) + \partial / \partial y (k_y [\partial H / \partial y]) + g' = S_s [\partial H / \partial t] \quad 3.30$$

Smith and Chapman (1983) identify two driving forces which causes fluid to flow in a thermal regime, piezometric head differences and a buoyancy force due to differences in fluid densities. When considering a heated foundation on oil sand, however, the direction of fluid flow is opposite to that of heat flow. As a result, the density of the pore fluid decreases in the direction of fluid flow and therefore, the driving force associated with buoyancy effects does not exist. The effect of the fluid density decreasing towards the heat source as occurs in this problem is included in the analytical procedure developed.

The generation rate (g') is the ratio of the amount of fluid expelled from an element of oil sand subjected to an increase in heat to the original volume of the element, i.e.:

$$g' = (\Delta V_d)_{\Delta T} / V_m$$

$$= (\alpha_w V_w \Delta T + \alpha_b V_b \Delta T - \alpha_s \Delta T (V_m - V_s) - \alpha_{s,t} V_m \Delta T) / V_m \quad 3.31$$

Since $V_w + V_b + V_s = V_m$, $n_b = V_b / V_m$ and $n_w = V_w / V_m$

$$g' = n_w \alpha_w \Delta T + n_b \alpha_b \Delta T + \alpha_s \Delta T (n_b + n_w) - \alpha_{s,t} \Delta T \quad 3.32$$

The specific storage coefficient, S_s , is defined as the volume of fluid expelled per unit volume of aquifer in response to an unit decrease in total head. The pore volume compressibility, the compressibility of fluid, the density of fluid and porosity all contribute to specific storage. The specific storage coefficient can be expressed as:

$$S_s = ((\Delta V_w)[\Delta H = 1] + (\Delta V_b)[\Delta H = 1] - (\Delta V_m)[\Delta H = 1]) / V_m \quad 3.33$$

where: H = total head, which is the sum of the pressure head (u/γ_f) and the elevation head (z)

The change in total head may be written as:

$$\Delta H = \Delta u / \gamma_f + \Delta z$$

Since for a specific element of oil sand $\Delta z = 0$ the change in total head is:

$$\Delta H = \Delta u / \gamma_f$$

For a unit change in total head ($\Delta H = 1$)

$$1 = \Delta u / \gamma_f \text{ or } \Delta u = \gamma_f$$

$$\text{Since } (\Delta V_w)_{\Delta p} = m_w V_w \Delta u$$

$$\text{then } (\Delta V_w)[\Delta H = 1] = m_w V_w \gamma_w$$

and similarly

$$(\Delta V_b)[\Delta H = 1] = m_b V_b \gamma_b \text{ and } (\Delta V_m)[\Delta H = 1] = m_v V_m \gamma_f$$

As a result equation 3.32 can be rewritten as:

$$S_s = (m_w V_w \gamma_w + m_b V_b \gamma_b - m_v V_m \gamma_f) / V_m \quad 3.34$$

$$\text{Letting } n_b = V_b / V_m \text{ and } n_w = V_w / V_m$$

then,

$$S_s = n_w m_w \gamma_w + n_b m_b \gamma_b - m_v \gamma_f \quad 3.35$$

The above expressions allow the rate at which excess pore fluid pressure resulting from an increase in temperature dissipates from an oil sand mass to be evaluated. When heat flow theory is coupled to equation 3.30 (the fluid flow expression), the state of drainage or heat consolidation can be determined.

3.2.2 Two Dimensional Transient Fluid Flow Beneath a Heated Foundation by Finite Elements

The solution to the governing differential fluid flow equation for two dimensional transient fluid flow beneath a heated foundation (equation 3.30) was determined utilizing the finite element technique. Unlike the conventional governing differential equation representing transient seepage, equation 3.30 includes a term which accounts for generation of pore fluid due to increases in temperature. As a result, existing finite element programs designed to solve the conventional governing differential equation prove inadequate. Since heat transfer governing equations are compatible to the analysis of seepage problems and an analogy can be made between the thermal generation rate (developed in this study) and the internal heat generation rate included in the heat transfer governing equation, an existing computer program which evaluates problems of heat conduction by the finite element method can be employed. When utilizing a heat transfer computer program to solve a

fluid flow problem, the appropriate analogous variable must be used. The analogy between variables include:

temperature \Rightarrow total head

thermal conductivity \Rightarrow hydraulic conductivity (permeability)

specific heat \Rightarrow specific storage

Using the above analogous variables, the heat transfer program ADINAT (*A Finite Element Program for Automatic Dynamic Incremental Nonlinear Analysis of Temperatures*) was employed directly for the analysis of the fluid flow problem (Chapter 6). Bathe (1977) provides a summary of the finite element theory as well as the ADINAT program solution capabilities and the numerical techniques employed.

This study determines the solution for fluid flow beneath a heated storage tank. Due to symmetry only one half of the tank is considered with no flow occurring across the axis of symmetry. The phreatic surface is assumed to be at the ground surface, below which the pore fluid is assumed to initially be static (hydrostatic conditions). The foundation material is also assumed to be fully saturated.

3.3 Analysis of Heat Flow

3.3.1 Introduction

The conduction of heat from one mass to another or from one portion of a mass to another is governed by two

fundamental laws of thermodynamics. The first law states that the thermal energy of a system is conserved (i.e., the thermal energy flowing into the system and the thermal energy generated inside the system must balance the energy flowing out of the system and the thermal energy stored inside the system). The equation which describes this concept is:

$$E_{in} + E_g = E_{out} + E_s \quad 3.36$$

where:

E_{in} = rate of energy flow into the system

E_g = rate of thermal energy generated inside the system

E_{out} = rate of energy flow out of the system

E_s = rate of energy storage inside the system

The second law of thermodynamics states that heat will flow only when a temperature differential exists and that the flow of heat will take place from the point of the greatest temperature to the point of the least temperature. In other words, the flow of heat occurs only when a temperature gradient exists and occurs in the direction of diminishing temperature. The major processes of energy transfer are conduction, convection, thermal energy storage and energy generation.

Conduction is the transmission of heat through substances without motion of the conducting body as a whole. The rate at which heat flows by conduction can be expressed as follows:

$$q = -k A (dT/dx) \quad 3.37$$

where:

k = thermal conductivity

A = area normal to direction of heat flow

T = temperature

x = distance

Convection refers to the transference of heat between a solid and a circulating fluid. The rate at which heat flows by convection is given by the following expression:

$$q_c = h A_s (T_s - T_f) \quad 3.38$$

where:

h = heat transfer coefficient

T_s = surficial temperature of solid

T_f = ambient fluid temperature

A_s = surficial area

Thermal energy storage occurs when a solid is subjected to a time dependant increase in temperature. The rate of energy storage in a solid can be expressed as follows:

$$E_s = \rho V c (dT/dt) \quad 3.39$$

where:

ρ = density

V = volume

c = specific heat

t = time

Thermal energy generation occurs in solids when other types of energy are transformed into thermal energy. The rate of thermal energy generation is commonly described by the following:

$$E_g = g V \quad 3.40$$

where:

g = thermal generation per unit volume

V = volume

Performing an energy balance in two dimensions equating the time rate change of energy stored to the sum of net heat

transfer due to conduction and the heat generated yields the governing differential heat - conduction equation:

$$c\rho(dT/dt) = \partial/\partial x(k_{xx}[\partial T/\partial x]) + \partial/\partial x(k_{xy}[\partial T/\partial y]) + \partial/\partial y(k_{xy}[\partial T/\partial x]) + \partial/\partial y(k_{yy}[\partial T/\partial y]) + g \quad 3.41$$

The above equation is for non homogeneous and anisotropic heat flow, and simplifies for homogeneous, isotropic material where the thermal conductivity is constant to:

$$dT/dt = (k/\rho c)([\partial^2 T/\partial x^2] + [\partial^2 T/\partial y^2]) + g/\rho c \quad 3.42$$

The governing differential heat-conduction equation neglects the influence fluid flow has on the rate of heat flow. The amount of heat loss through convection is small considering that little fluid flows from the oil sand strata. Ignoring the effects of convection results in a slight over estimation of the rate at which heat flows into the oil sand strata and the amount of pore fluid pressure and volume change that would occur.

3.3.2 Two Dimensional Transient Heat Flow Beneath a Heated Foundation by Finite Differences

The solution to the heat flow equation for two dimensional transient heat flow beneath a hot foundation was determined utilizing the finite difference technique. When

the second order derivatives of the heat equation are finite difference a system of ordinary differential equations (equations containing derivatives of a single independent variable) is obtained. A solution to this set of equations is determined numerically as a function of time.

This study determines the solution for heat flow beneath a heated storage tank. Due to symmetry only one half of the tank is considered with no energy conducted across the axis of symmetry. The tank and ambient air temperatures are assumed constant at 175 and 10 °C, respectively. The initial foundation soil temperature was assumed to be 5 °C.

The initial stage in the finite difference formulation involves establishing a system of nodes which divide the area into a finite number of elements. A typical nodal arrangement for a portion of the region under consideration is illustrated in Figure 3.2.

Figure 3.3 shows the energy system assigned to the interior node positioned at the coordinates (X_m, Y_m) along with the appropriate energy terms. For the prescribed system energy flow occurs by conduction through each side and thermal energy storage within the system.

The energy balance may be expressed as:

$$E_{in} = E_{out} + E_s$$

or,

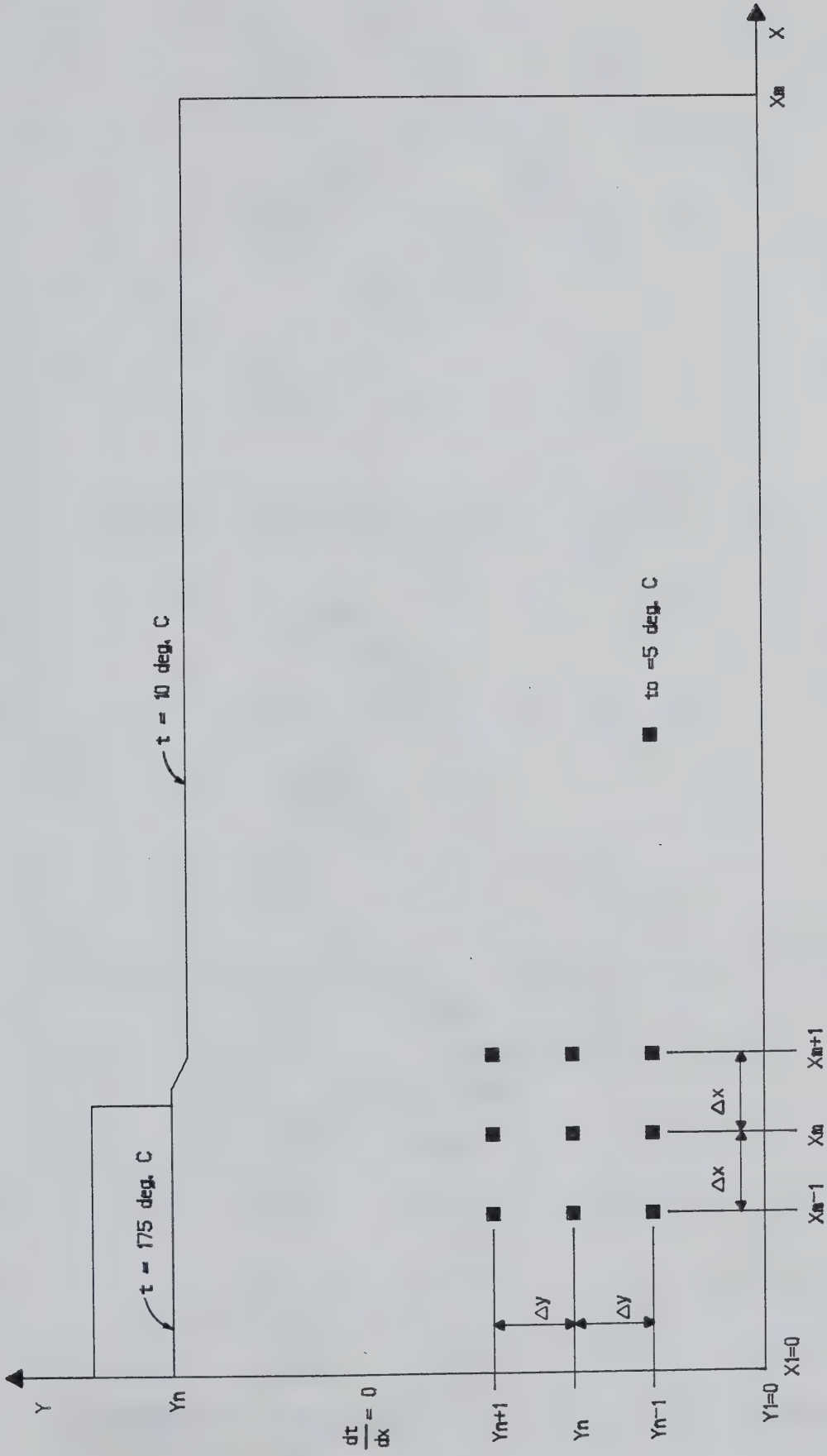


Figure 3.2 Typical Nodal Arrangement for a Portion of the Region Beneath a Heated Foundation

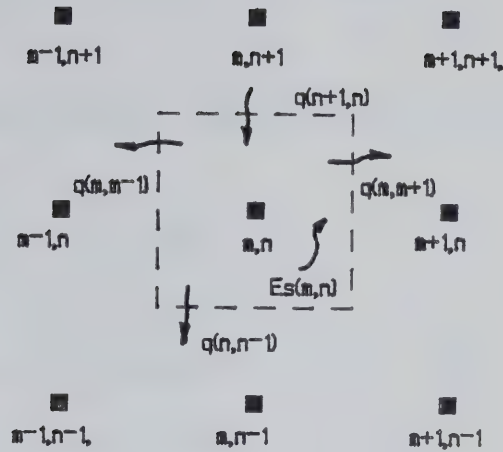


Figure 3.3 Energy System Assigned to an Interior Node

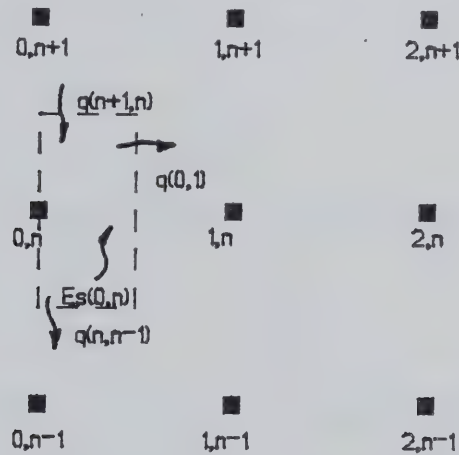


Figure 3.4 Energy System Assigned to a Node along Axis of Symmetry

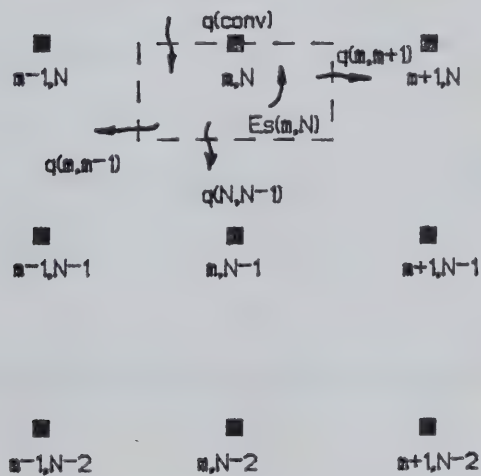


Figure 3.5 Energy System Assigned to a Node at Ground Surface

$$q_{n+1} = q_{m,m-1} + q_{m,m+1} + q_{n,n-1} + Es_{m,n}$$

The rate equations may be approximately stated as:

$$q_{n+1,n} = k\Delta x(T_{m,n+1} - T_{m,n})/\Delta y$$

$$q_{m,m-1} = k\Delta y(T_{m,n} - T_{m-1,n})/\Delta x$$

$$q_{m,m+1} = k\Delta y(T_{m,n} - T_{m+1,n})/\Delta x$$

$$q_{n,n-1} = k\Delta x(T_{m,n} - T_{m,n-1})/\Delta y$$

The storage term may be written as:

$$Es_{m,n} = \rho c \Delta x \Delta y (dT_{m,n}/dt)$$

Substituting the above rate equations into the energy balance gives:

$$\begin{aligned} k\Delta x(T_{m,n+1} - T_{m,n})/\Delta y &= k\Delta y(T_{m,n} - T_{m-1,n})/\Delta x + \\ &+ k\Delta y(T_{m,n} - T_{m+1,n})/\Delta x + k\Delta x(T_{m,n} - T_{m,n-1})/\Delta y + \rho c \Delta x \Delta y (dT_{m,n}/dt) \end{aligned}$$

Rearranging terms gives:

$$\begin{aligned} \rho c \Delta x \Delta y (dT_{m,n}/dt) &= k(\Delta x/\Delta y)(T_{m,n+1} - 2T_{m,n} + T_{m,n-1}) + \\ &+ k(\Delta y/\Delta x)(T_{m-1,n} - 2T_{m,n} + T_{m+1,n}) \end{aligned} \quad 3.43$$

Each of the interior nodes can be represented by a similar equation.

Nodes along the axis of symmetry must be treated separately since no energy is transferred across the face (Figure 3.4), the energy balance therefore is:

$$q_{n+1,n} = q_{0,1} + q_{n,n-1} + Es_{1,n}$$

The equations describing rate of heat flow are:

$$q_{n+1,n} = k\Delta x(T_{0,n+1} - T_{0,n})/\Delta y$$

$$q_{0,1} = k\Delta y(T_{0,n} - T_{1,n})/\Delta x$$

$$q_{n,n-1} = k\Delta x(T_{0,n} - T_{0,n-1})/\Delta y$$

The storage term may be written as:

$$Es_{0,n} = \rho c \Delta x \Delta y (dT_{0,n}/dt)$$

Substituting the rate equations into the energy balance gives:

$$k\Delta x(T_{0,n+1} - T_{0,n})/\Delta y = k\Delta y(T_{0,n} - T_{1,n})/\Delta x + k\Delta x(T_{0,n} - T_{0,n-1})/\Delta y + \rho c \Delta x \Delta y (dT_{0,n}/dt)$$

Rearranging terms gives:

$$\rho c \Delta x \Delta y (dT_{0,n}/dt) = k\Delta y(T_{1,n} - T_{0,n})/\Delta x + k(\Delta x/\Delta y)(T_{0,n+1} - 2T_{0,n} + T_{0,n-1}) \quad 3.44$$

Nodes along the base of the tank and along the ground surface are also treated separately from the interior nodes due to convection across the boundary (Figure 3.5), the energy balance is therefore:

$$q(\text{conv}) = h\Delta x(T(\text{ambient}) - T_{m,n})$$

$$q_{m,m-1} = k\Delta y(T_{m,n} - T_{m-1,n})/\Delta x$$

$$q_{m,m+1} = k\Delta y(T_{m,n} - T_{m+1,n})/\Delta x$$

$$q_{n,n-1} = k\Delta x(T_{m,n} - T_{m,n-1})/\Delta y$$

The storage term may be written as:

$$Es_{m,n} = \rho c \Delta x \Delta y (dT_{m,n}/dt)$$

Substituting the rate equations into the energy balance gives:

$$h\Delta x(T(\text{ambient}) - T_{m,n}) = k\Delta y(T_{m,n} - T_{m-1,n})/\Delta x + k\Delta y(T_{m,n} - T_{m+1,n})/\Delta x + k\Delta x(T_{m,n} - T_{m,n-1})/\Delta y + \rho c \Delta x \Delta y (dT_{m,n}/dt)$$

Rearranging terms gives:

$$\rho c \Delta x \Delta y (dT_{m,n}/dt) = k(\Delta y/\Delta x)(T_{m-1,n} - 2T_{m,n} + T_{m+1,n}) + k\Delta x(T_{m,n} - T_{m,n-1})/\Delta y + h\Delta x(T(\text{ambient}) - T_{m,n}) \quad 3.45$$

Equations 3.43, 3.44 and 3.45 form the system of ordinary differential equations which must be solved

simultaneously for each time increment starting with the initial condition.

3.4 Coupling of Heat and Fluid Flow

The expressions presented in section 3.1.1 allow the performance of an oil sand mass when heated to be evaluated under fully drained and undrained conditions. When heat flow theory (section 3.3) is coupled to the fluid flow expression (section 3.2), the state of drainage or heat consolidation can be determined; that is, whether the oil sand mass will be fully drained, fully undrained, or partially drained. If partial drainage occurs, the volume change and pore pressure change can be calculated.

In this study a simplified approach was taken in the coupling of heat and fluid flow. The procedure adopted involves evaluating for each time increment the rate at which the heat from the structure propagates into the oil sand strata, calculating the change in pore fluid pressure and change in engineering properties of the oil sand strata in response to the change in temperature, and subsequently determining the state of drainage in the oil sand strata. Complete coupling was not achieved since the influence fluid flow has on the rate of heat flow was neglected. The effects of convection, however, are small considering that little fluid flows from the oil sand strata. The coupling method is discussed in detail in Chapter 6.

3.5 Conclusions

An expression was developed to calculate the net volume change of an oil sand mass subjected to a change in temperature under fully drained conditions. The volume change of the oil sand mass arises from the thermal expansion of the individual sand grains and structural changes in the sand skeleton.

An equation which allows the volume change of oil sand subjected to increases in temperatures under completely undrained conditions to be calculated was presented. The volume change of the oil sand mass is due to expansion of the individual sand grains and pore fluids as well as structural changes in the sand skeleton.

An expression was derived which expresses the volume of pore fluid which would drain from a fully saturated oil sand mass experiencing a change in temperature. The amount of fluid expelled from an oil sand mass during a drained thermal expansion test is the sum of the volume change of the pore fluids less the change in void volume and structural volume changes.

An expression was developed to calculate the increase in pore fluid pressure in a fully saturated oil sand mass subjected to a temperature change under fully undrained conditions.

The theoretical expressions to evaluate the rate of fluid from heating were derived and are presented. The method utilized to solve the governing differential fluid

flow equation for two dimensional transient fluid flow beneath a heated foundation using the finite element technique is described.

The theoretical formulations to determine the rate of heat flow were derived and are presented. The solution to the heat equation for two dimensional transient heat flow beneath a heated foundation utilizing the finite difference technique is illustrated.

The expressions developed in this study provide a method to analyze the rate at which heat flows through an oil sands mass, the rate at which excess pore fluid pressure resulting from an increase in temperature dissipates, and the amount of volume change which occurs.

4. LABORATORY APPARATUS AND PROCEDURES

4.1 Introduction

Inherent in the processing of oil sands at surface mining projects is the requirement of storage of heated bitumen in large retaining tanks. To experimentally investigate the problems which arise when these structures and other structures generating heat (e.g., hot water extraction plant, cokers, etc.) must be situated above oil sand strata, equipment has been built at the University of Alberta, Department of Civil Engineering.

The apparatus has the capability to explore the one-dimensional thermal expansion of oil sands and its constituent components at temperatures approaching 200 °C and pressures in excess of 3.5 Mpa. One-dimensional testing (zero lateral strain, i.e., volume change due to expansion in the vertical direction) is justified considering that the minor principal stress in the surface mineable area is believed to be vertical from the surface to a depth of approximately 330 m and is one-third that of the horizontal stress to a depth of about 100 m (Dusseault, 1977b).

Specifications and detailed dimensions of each component of the apparatus is given in Appendix B.

4.2 Laboratory Apparatus

The following is intended to be a brief summary of each constituent of the equipment.

4.2.1 Oedometer

The assembled apparatus is expressed schematically in Figure 4.1 and is shown in Figure 4.2. The oedometer is conceptually simple in design. The sample jacket which provides lateral confinement for the specimen is held stationary by a covering plate which is bolted to the base of the assembly. The specimen chamber is formed when the piston is lowered through the covering plate and is allowed to rest on the sample. This configuration ensures that vertical expansion or contraction of the specimen can be measured directly by recording the relative movement of the piston. Sealing of the sample chamber is accomplished with the aid of heat and petroleum resistant "O" rings, two of which are located on the lower part of the piston and one between the sample jacket and assembly base. A teflon *rider* ring is situated on the upper portion of the piston (Figure 4.1) to avert tilting and binding during vertical movement.

The oedometer has four drainage ports, two of which are contained within the piston and provide a drainage path from the top porous stone to the top of the piston, the other two provide a drainage path from the bottom porous stone and emerge through the base of the assembly below the sample chamber. One of the latter ports provides communication to

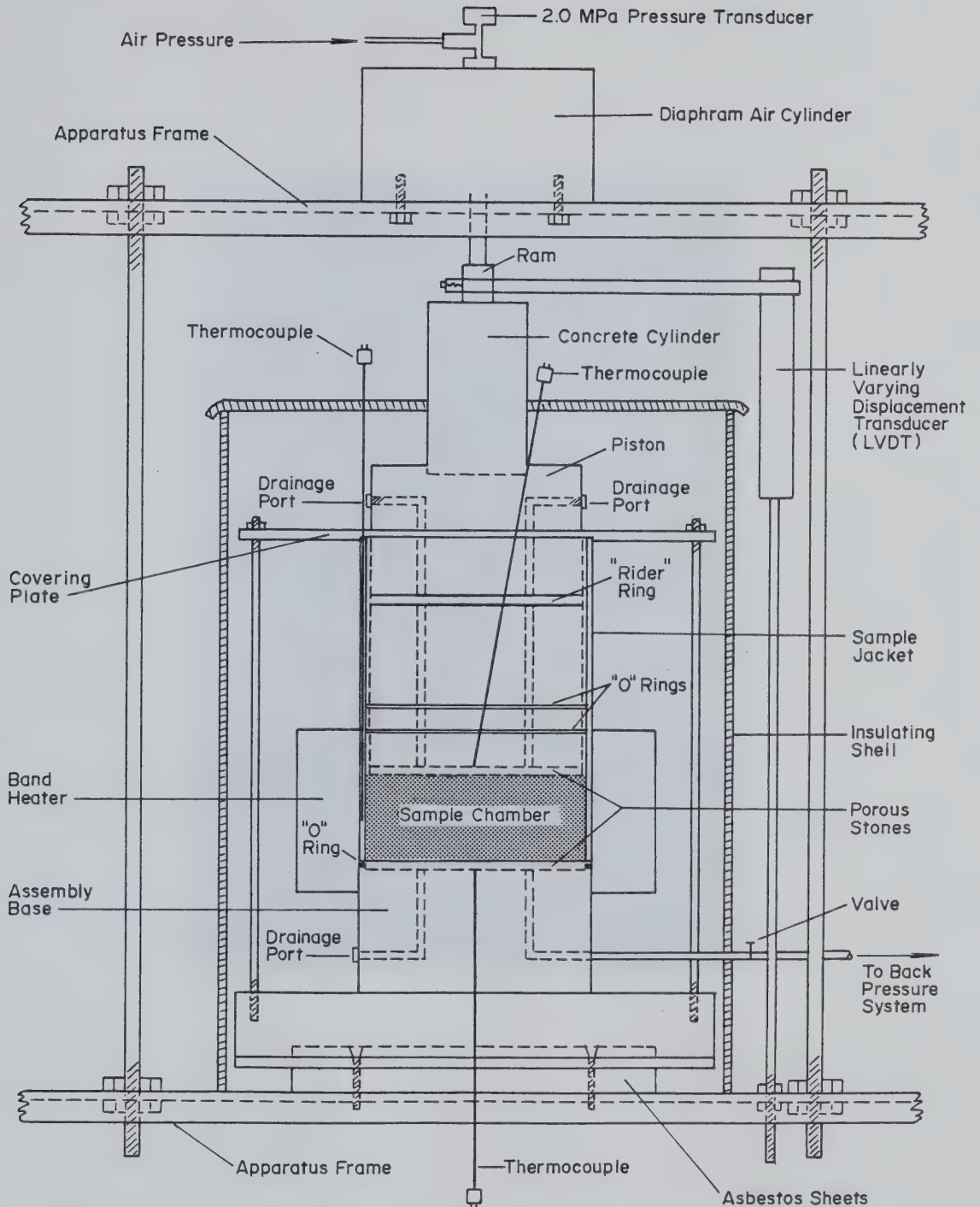


Figure 4.1 Drawing of Laboratory Apparatus

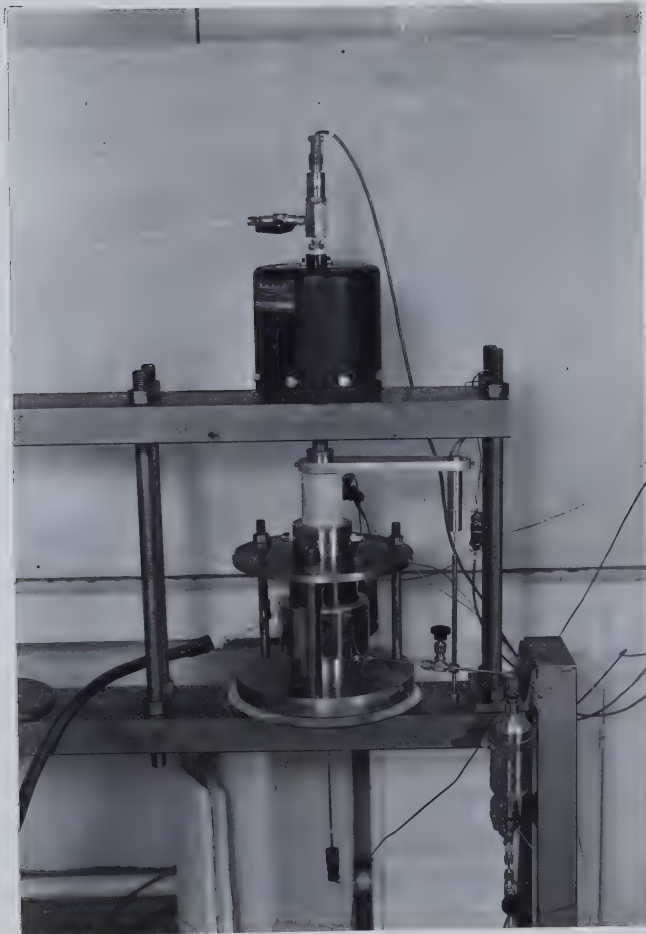


Figure 4.2 Laboratory Apparatus

the back pressure system. Located between the cell and the back pressure system is a stainless steel bottle, the purpose of which is to inhibit the flow of bitumen into the back pressure system. Valves are situated above and below the bottle.

4.2.2 Axial Loading and Back Pressure Systems

A diaphragm air cylinder is used to apply the axial load to the oedometer piston. Briefly, air under pressure is forced into the cylinder causing the diaphragm to expand against an internal piston producing the axial force. This force is transmitted to the oedometer piston through a small concrete cylinder, which retards the flow of heat from the oedometer to the air cylinder.

The back pressure system (Figure 4.3) performs on the same principal as the axial loading system. In this case, however, the diaphragm in the accumulator is nitrogen driven against silicon oil. The silicon oil in turn forces water under pressure to the oedometer.

4.2.3 Heating System

The heating system employed consists of three parts: a *sensing* thermocouple, a double coil electrical element band heater, and a digital temperature controller unit. The band heater is clamped to the sample jacket as shown in Figure 4.1.

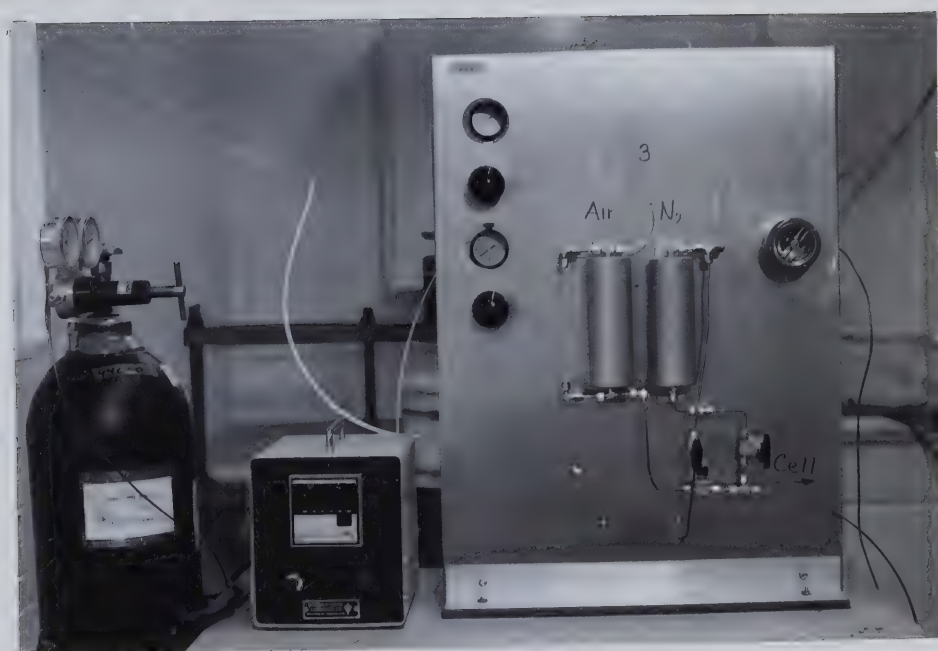


Figure 4.3 Back Pressure System and Temperature Controller Unit

The temperature controller unit (Figure 4.3) regulates the heat supplied to the sample chamber. The temperature controller once engaged will sense and display the temperature of the thermocouple. When a predetermined *set point* temperature is entered into the unit it will initially calculate and display the difference between the set point temperature and the temperature the thermocouple is sensing. If the set point temperature exceeds the thermocouple temperature the temperature controller will supply current to the elements of the band heater. Initially the cycle of heating is rapid but as the set point temperature is approached the cycle time will reduce and when it is reached the cycle time is proportioned to hold the temperature at the thermocouple constant. In operational use it was observed that the time to reach the set point temperature was extremely rapid and stabilization occurred generally after only a few minutes.

4.2.4 Measuring Devices - Data Logger System

The measuring devices associated with the oedometer consisted of two pressure transducers, one linearly varying displacement transducer (LVDT) and three *Type J* thermocouples. The specifications of each measuring device are discussed in Appendix B.

One pressure transducer is situated to measure the air pressure in the diaphragm of the air cylinder while the other is located in the line between the back pressure system and

the oedometer. One end of the LVDT is secured to the frame of the apparatus below the oedometer and the other end to the piston rod of the diaphragm air cylinder. The thermocouples are situated as follows: one in the oedometer piston with the measuring tip in contact with the top porous stone; one at mid-sample height in the sample jacket; and one in the base of the apparatus in contact with the bottom porous stone (Figure 4.1).

The data logging was performed by a *Hewlett - Packard 3497A Data Acquisition Control Unit* which electronically gathered and recorded the data during the testing program (Figure 4.4).

4.2.5 Insulation

The base of the oedometer is mounted on sheets of asbestos to reduce heat loss to the steel frame of the apparatus (Figure 4.1). During operational use, the oedometer itself is completely enclosed in an insulating shell composed of ceramic fiber insulation (Figure 4.5).

4.3 Test Procedures

4.3.1 Thermal Expansion of Water

Two thermal expansion tests were carried out on distilled water under pressures of 2000 and 3500 kPa. In both cases the sample chamber was filled at room temperature with water to a height of approximately 2.5 cm. All ports,



Figure 4.4 Data Logger System



Figure 4.5 Laboratory Apparatus Enclosed in Insulating Shell

passages and porous stones were saturated prior to testing.

Each test was performed under a constant back pressure. The back pressure was held constant during the test through manipulation of the applied load to the piston. The heating increment used for each test was 25 °C. After each application of heat, sufficient time was permitted to establish steady state conditions, i.e., the temperature readings had stabilized and the thermal expansion (volume change) ceased.

4.3.2 Thermal Expansion of Bitumen

Seven thermal expansion tests were performed on bitumen under pressures of 500 to 3500 kPa and temperature range of 22 to 200 °C. In all cases the sample chamber was filled at room temperature to a height of approximately 2.5 centimeters with bitumen and all ports, passages and porous stones saturated with distilled water. Prior to each test the system was permitted to *saturate* (gases driven into solution) for a period of up to 24 hours at the appropriate pressure level.

Each test was performed under a constant back pressure with heating increments varying from 5 to 25 °C. After each application of heat sufficient time was permitted to establish steady state conditions, i.e., the temperature readings had stabilized and the thermal expansion (volume change) ceased.

4.3.3 Thermal Expansion of Compacted Tailing Sand

Four tests were performed to investigate the thermal expansion of tailing sand at various densities. The temperature range for the testing was varied from room temperature to 200 °C. To eliminate any influence of induced pressure within the sample chamber, the sand was tested in the air dried state and during the testing the bottom drainage ports were held open to atmospheric pressure.

The initial test investigated the thermal expansion of sand in the loose state. To achieve a loose sample, sand was slowly poured into the sample chamber and carefully levelled using a small metal spatual. The piston was then placed inside the sample jacket and allowed to fall under its own weight to rest on the sample. Care was taken to avoid jarring of the apparatus. In order that the LVDT could be utilized to measure the vertical expansion (or contraction) of the specimen during the test, it was necessary to apply a small axial *seating* load of 50 kPa. The density obtained was 1.46 Mg/m³. Two subsequent tests were performed on sand under the same seating load of 50 kPa but at higher densities. Two procedures were utilized in achieving a dense sample. The first involved densifying the specimen by cycling the applied load from 50 to 3500 kPa. The second method involved placing the sand in the sample chamber in four lifts, vibrating between lifts under an applied load of 50 kPa. The methods produced densities of 1.57 and 1.62 Mg/m³ respectively.

The final thermal expansion test was performed on sand under an applied load of 3500 kPa. The sand was densified in the sample chamber by vibrating in four lifts. The density obtained was 1.65 Mg/m^3 .

The test procedure employed was the same for all four samples. It involved heating the sample in 25°C increments allowing sufficient time for temperature stabilization to occur at each desired level.

4.3.4 Thermal Expansion of Oil Sand

4.3.4.1 Sample Preparation

The oil sand specimens used in the testing program were obtained from 94.5 mm core samples taken from an oil sand outcrop at Saline Creek, approximately 1 km south of Fort McMurray, Alberta. The oil sand core samples prior to sample preparation were sealed in plastic and stored in a cold room at -20 to -25°C .

When an oil sand sample was required for testing a piece of core was taken and sealed in an air-tight metal container. The container was then placed in a styrofoam receptacle and covered with dry ice. Sealing the sample in the metal container prevents disturbance of the sample from the carbon dioxide gas emitted from the dry ice. The container was left in the dry ice (approximately -78°C) for several hours.

To obtain a test sample of the proper dimensions (7.62 cm in diameter; approximately 2.5 cm in height)

the following procedure was employed (between each step, to inhibit swelling of the specimen from heat developed during machining, the sample was sealed in the metal container and placed in dry ice for a minimum of 30 minutes):

- The piece of core was placed in the lathe (situated in the cold room), gripped at one end by the jaws of the chuck and supported at the other end by a freely rotating disc (tail stock). The surface of the specimen at the end supported by the disc was machined using a tungsten carbide bit until round and smooth. The specimen was removed from the lathe and an adjustable metal clamp (2.5 cm wide) placed on the trimmed section.
- The specimen was placed in the lathe with the end having the metal clamp gripped in the chuck. Reference marks were placed on the chuck and metal band. Similarly at the opposite end a reference mark on the support disc was aligned with a notch on the specimen. The surface of the sample was then machined from the metal band to within 2.5 cm of the opposite end (Figure 4.6). Ten passes were made, reducing the diameter by approximately 0.5 mm each time.
- The sample was returned to the lathe, realigned with respect to the reference marks and 10 more passes made.
- The previous step was repeated until the correct diameter was reached.



Figure 4.6 Trimming Sample to Correct Diameter

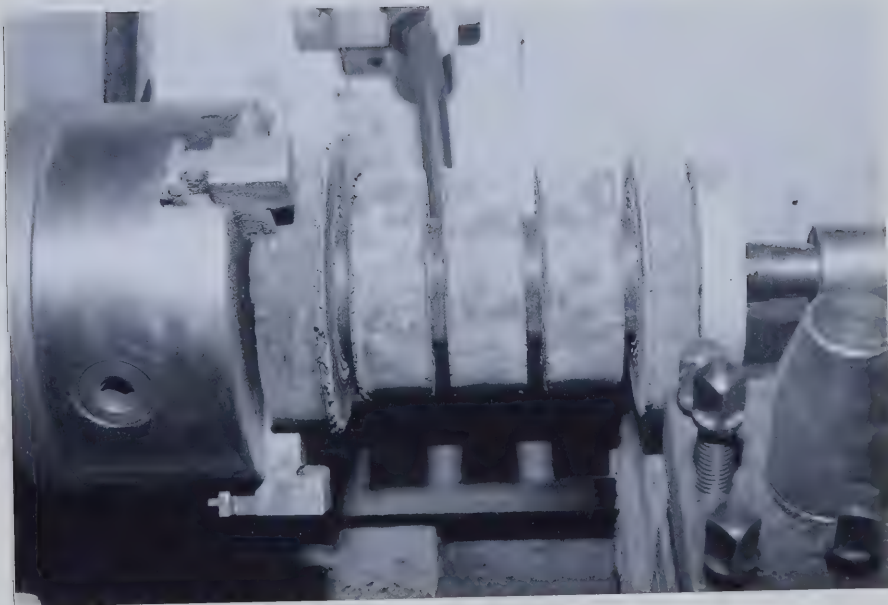


Figure 4.7 Notching Sample

- The specimen was returned to the lathe, aligned and square notches (about 2 cm deep) cut at 2.5 cm spacings (corresponding to the sample height). The notching ensured the sample ends would be parallel and square. A notched specimen is shown in Figure 4.7.
- The specimen was cut with a diamond saw at the notches.
- The test sample supported by a split metal ring was placed in the lathe and the central portion (cut by the saw) at each end machined flush (Figure 4.8).

4.3.4.2 Undrained Test Procedure

The prepared oil sand sample was inserted into the sample jacket in the cold room. The sample jacket was then transferred to the laboratory where the apparatus was quickly assembled and a 100 kPa seating load placed on the sample. The sample was allowed to thaw for approximately 4 hours after which time water was allowed to percolate up through the sample to saturate the passages and ports in the piston. The piston pressure was increased to slightly above the required test pressure. The back pressure was then increased incrementally to the desired level. The system was then allowed to *saturate* for about 24 hours to ensure all gases were dissolved in the liquid phases.

The test was performed under a constant back pressure. The back pressure was held constant during the

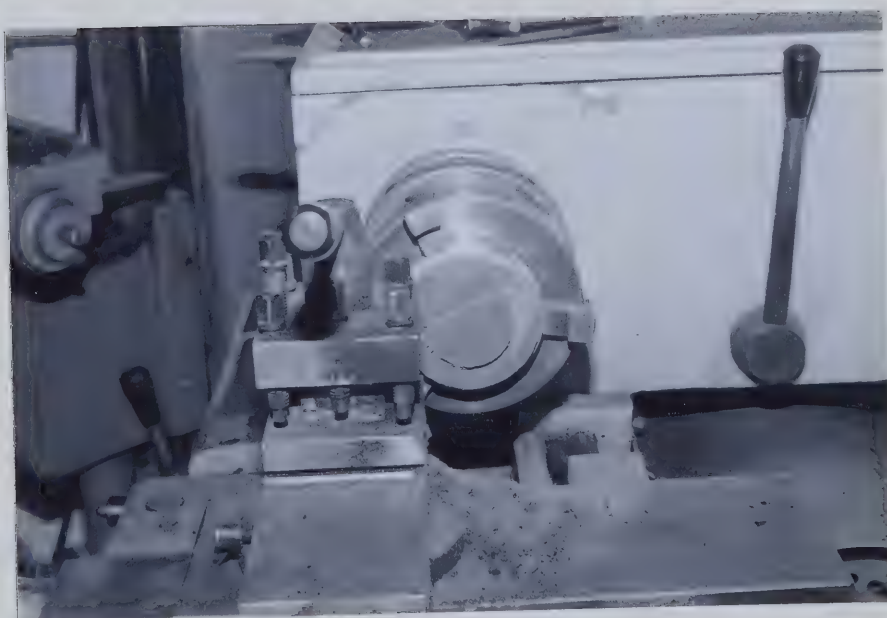
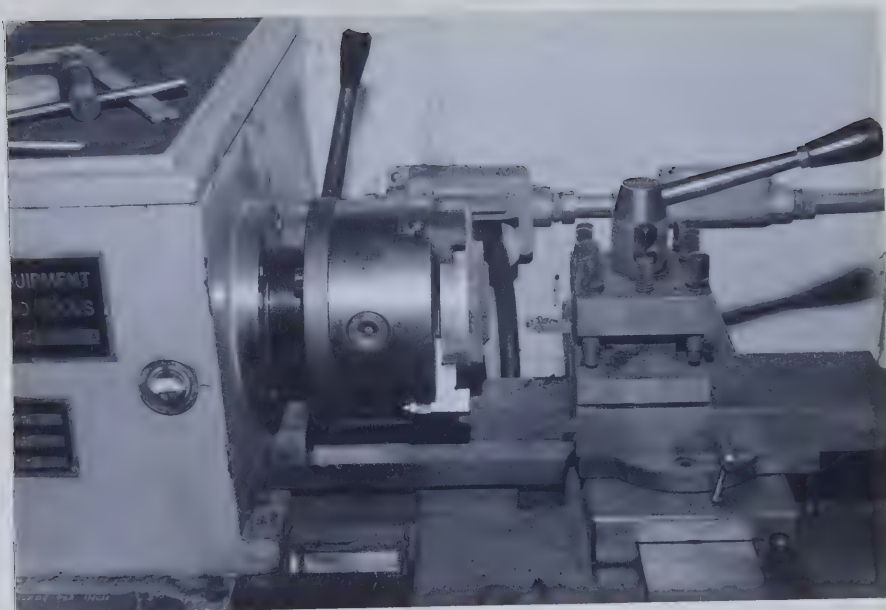


Figure 4.8 Machining Ends Flush

test through manipulation of the applied load to the piston. The heating increment used for the test was 20 °C. After each application of heat, sufficient time was permitted to establish steady state conditions, i.e., the temperature readings had stabilized and the thermal expansion (volume change) ceased.

4.3.4.3 Drained Test Procedure

The methods employed to mount and saturate the test sample were the same as those adopted for the undrained test (Section 4.3.4.2).

The drained test was performed under a constant effective confining pressure (difference between back pressure and piston pressure) of 240 kPa. A volume change measuring device was inserted between the back pressure system and the fluid trap to electronically monitor the fluid drainage during the test. The heating increment used for the test was 20 °C. After each application of heat, sufficient time was permitted to establish steady state conditions, i.e., the temperature readings had stabilized and the thermal expansion (volume change) ceased.

4.4 Conclusions

Equipment was successfully designed and constructed with the capability to explore the one-dimensional thermal expansion of oil sands and its constituent components to temperatures approaching 200 °C and pressures in excess of

3.5 MPa. A brief summary of each constituent of the equipment is presented.

The test procedures which were developed for use in the laboratory program worked successfully and are described. The method utilized to prepare oil sand samples from frozen core resulted in very high quality test specimens. The procedure adopted is illustrated.

5. EXPERIMENTAL RESULTS

5.1 Thermal Expansion of Water

5.1.1 Introduction

Due to the amount of emphasis placed on data obtained in the testing program, it is critical to ensure that the experimental information derived from the apparatus proves precise and reliable. To establish this confidence in the apparatus, it was necessary to test a substance whose behavior under temperature and pressure is well documented. Water was selected as the testing material owing to the vast amount of information contained in the literature.

5.1.2 Test Results

Two thermal expansion tests were performed on water under pressures of 2000 and 3500 kPa and temperature range of 22 to 200 °C (Figures 5.1 and 5.2). For completeness, all data gathered from the tests are plotted on the figures. It should be noted that steady state conditions for a particular temperature level were only reached when the temperature readings had stabilized and the thermal expansion (volume change) ceased. This condition is reflected on the plot where there is a high density of data points.

For comparative purposes theoretical curves were calculated based on information obtained from the 1968

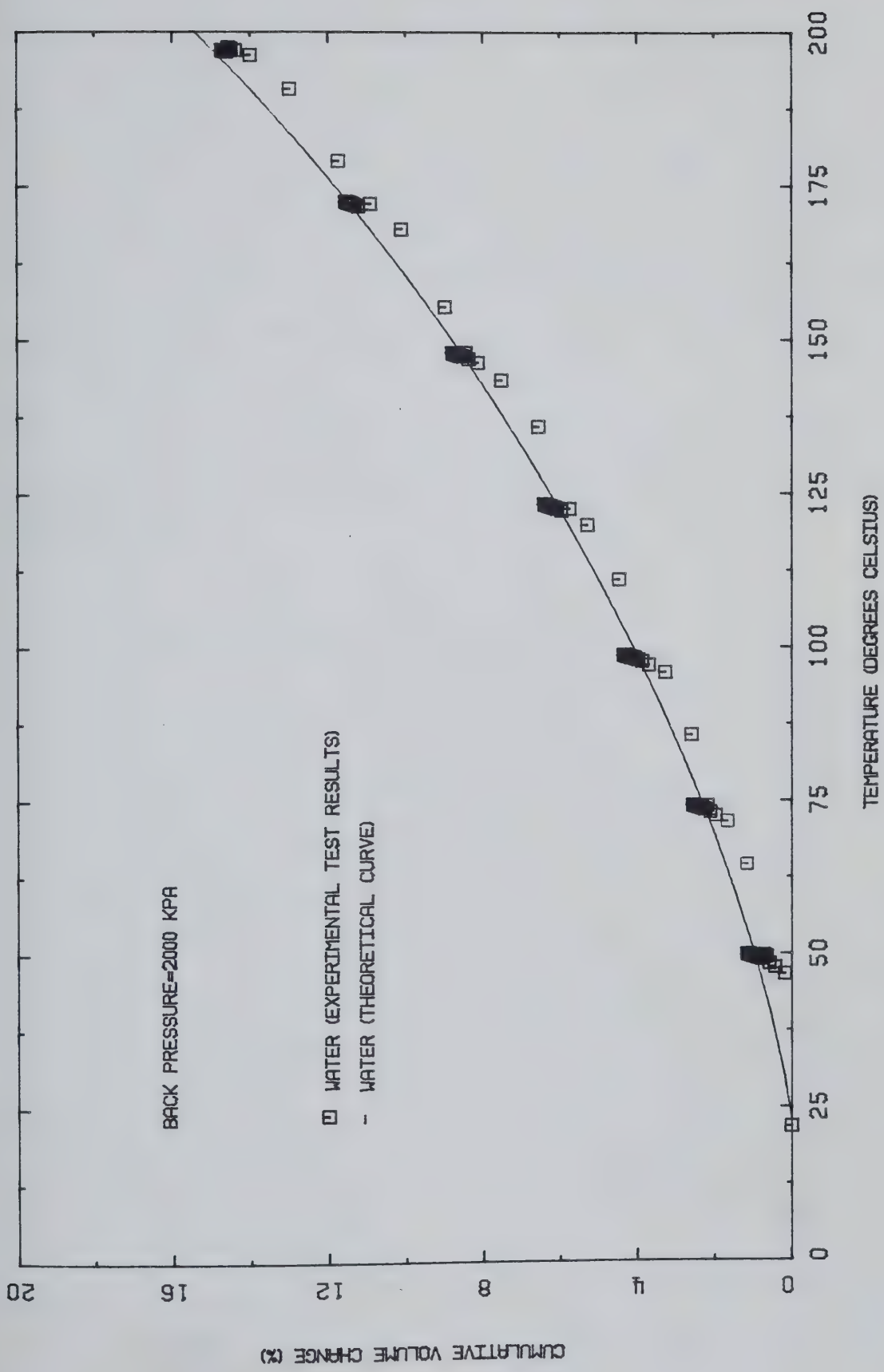


Figure 5.1 Thermal Expansion of Water: Test 1

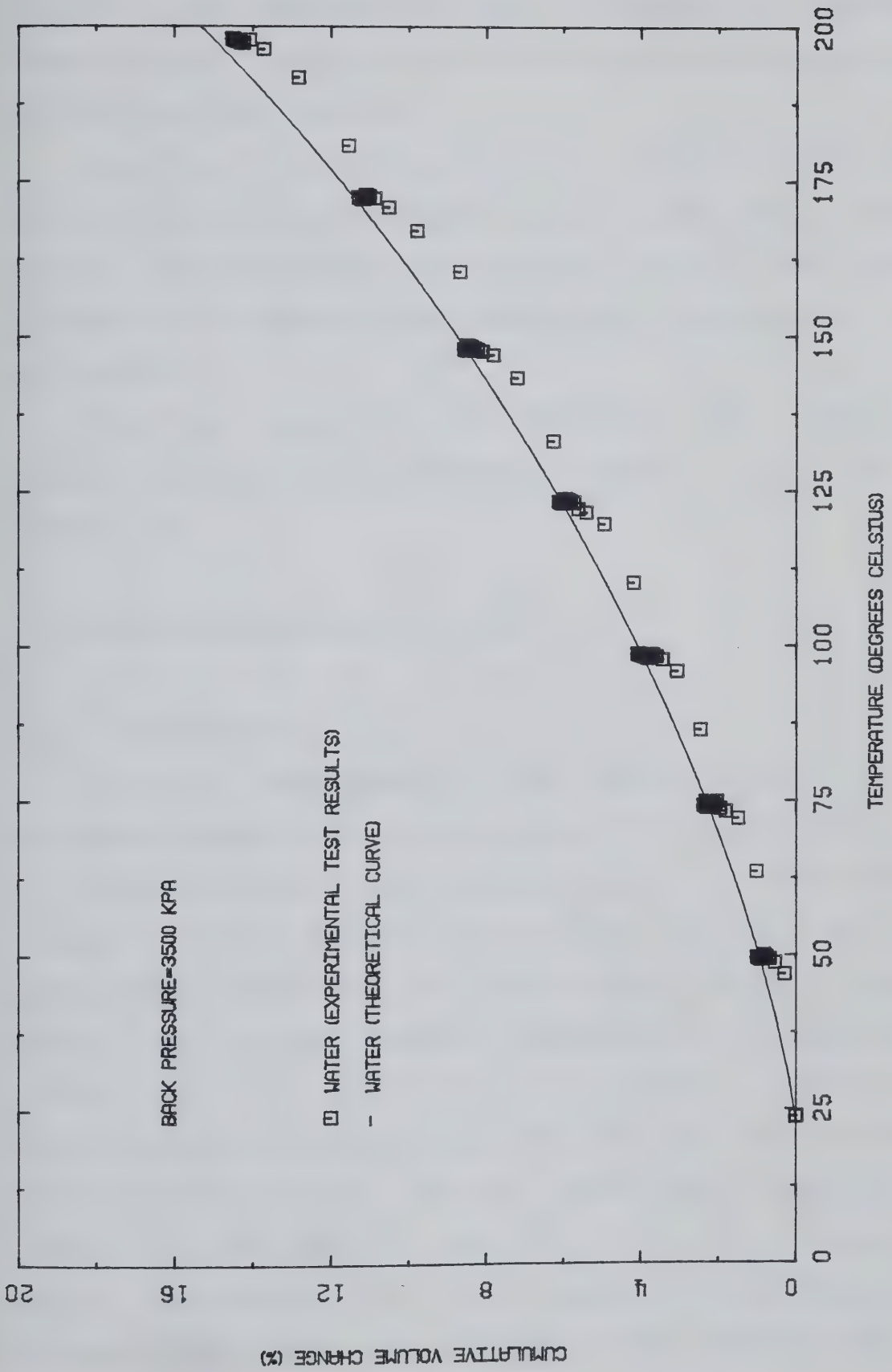


Figure 5.2 Thermal Expansion of Water: Test 2

edition of the *Japanese Society of Mechanical Engineers Steam Tables*. These curves reflect steady state conditions and are drawn on the plots.

Based on the steady state criteria (stabilized readings for each temperature increment) there is excellent agreement between theoretical and experimental results in both cases, indicating the apparatus performance and calibrations are satisfactory.

The data reduction calculations, data reduction computer programs and experimental results are contained in Appendix D.

5.2 Thermal Expansion of Bitumen

5.2.1 Introduction

The oil sands present in the mineable portions of the Athabasca Deposit have bitumen saturations ranging from 0 to 18 weight percent (up to approximately 36 volume percent [Mossop, 1978]). Present within this bitumen may be appreciable quantities of free and dissolved gases (mainly methane and carbon dioxide [Dusseault and Morgenstern, 1977]). The hot water extraction method is utilized to separate the bitumen from the other oil sand constituents. Briefly, the process involves subjecting oil sand to hot water, steam and caustic and collecting the bitumen as froth. Subsequent centrifuging completes the separation process. The bitumen obtained from this process can be

expected to be relatively free of dissolved gases and to have a slightly higher density (resulting from the lighter components being driven off during the process).

5.2.2 Test Material

Since no technology exists which allows undisturbed sampling of pure bitumen, bitumen obtained from the Syncrude extraction facility was used as the test material. Prior to testing, the bitumen was stored at room temperature in a sealed container.

5.2.3 Test Results

The data reduction calculations, data reduction computer programs and experimental results are contained in Appendix D. Points representing steady state conditions for each pressure and temperature level are shown in Figure 5.3. Figure 5.4 provides a comparative plot of the experimental thermal expansion of bitumen and the theoretical curves for water under pressures of 500 kPa and 3500 kPa (as given in the previous section). Figure 5.5 gives a comparative plot of the density change of bitumen with temperature with that of water.

Figure 5.3 indicates that the cumulative volume change of bitumen over the temperature range of room temperature to 200 °C is not dependent on pressure. The thermal expansion of the bitumen tested is greater than that of water up to a temperature of 125 °C and is slightly lower over the

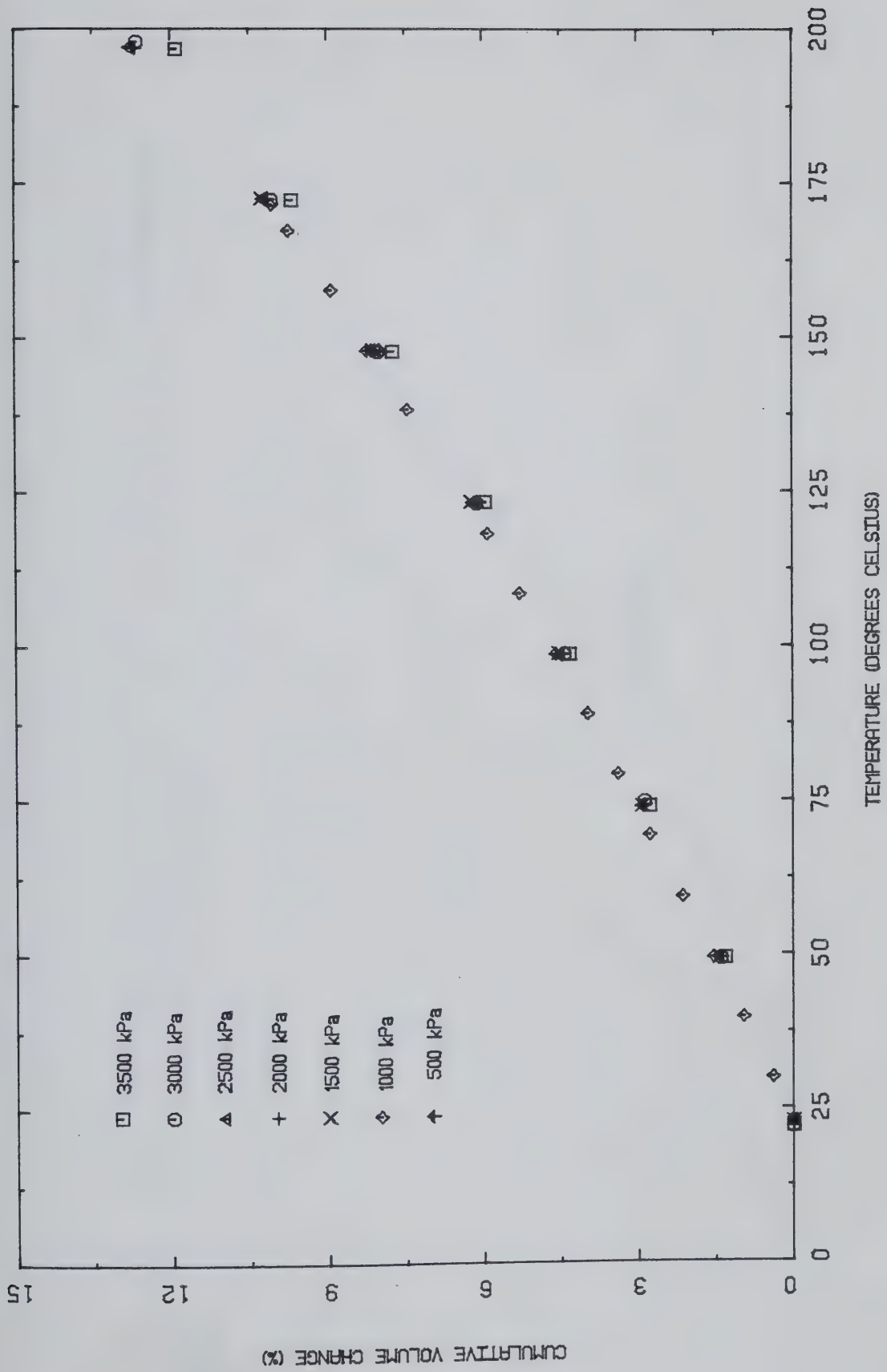


Figure 5.3 Thermal Expansion of Bitumen

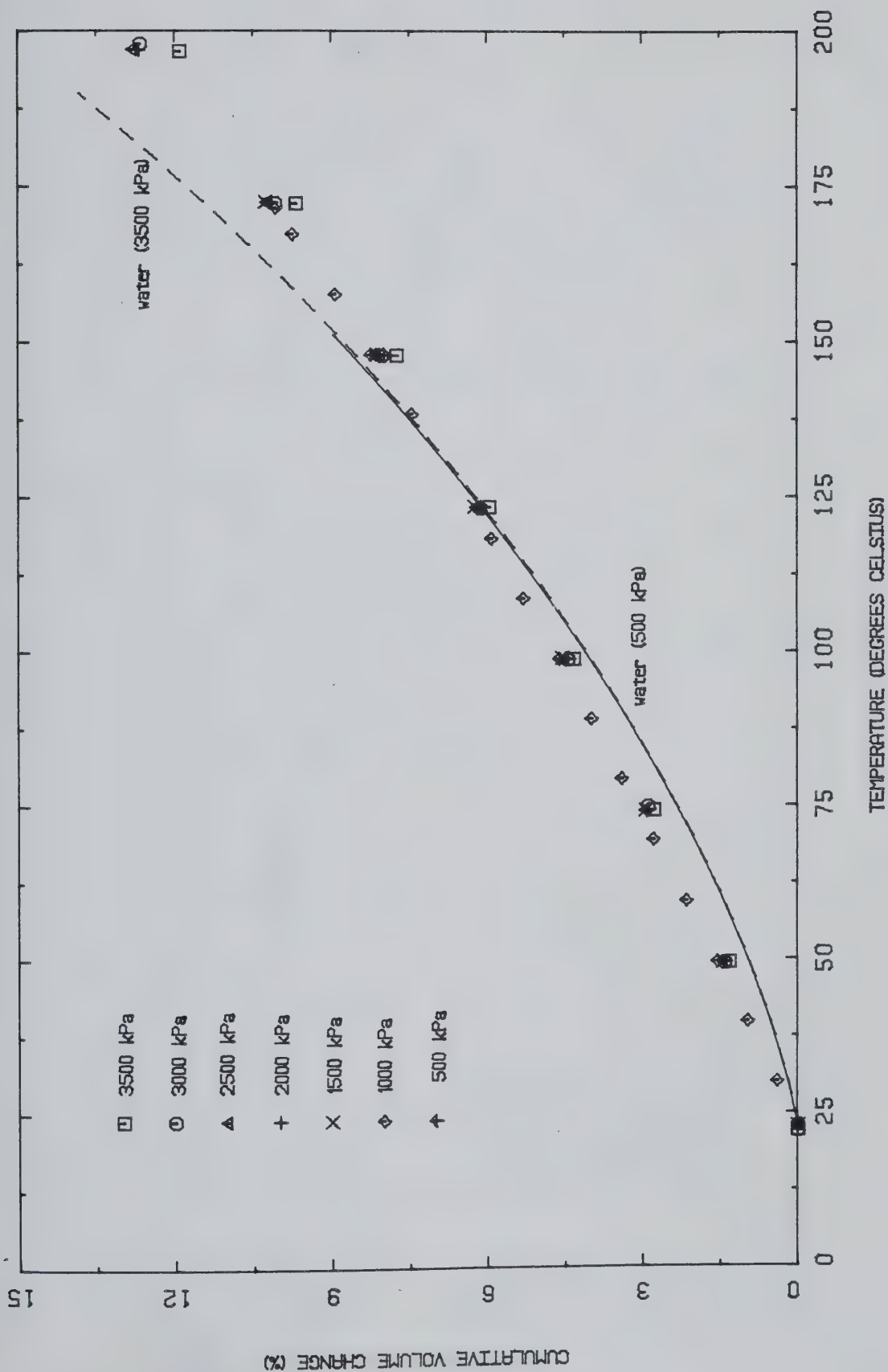


Figure 5.4 Thermal Expansion of Bitumen (Experimental Results) vs. Water (Theoretical Curves)

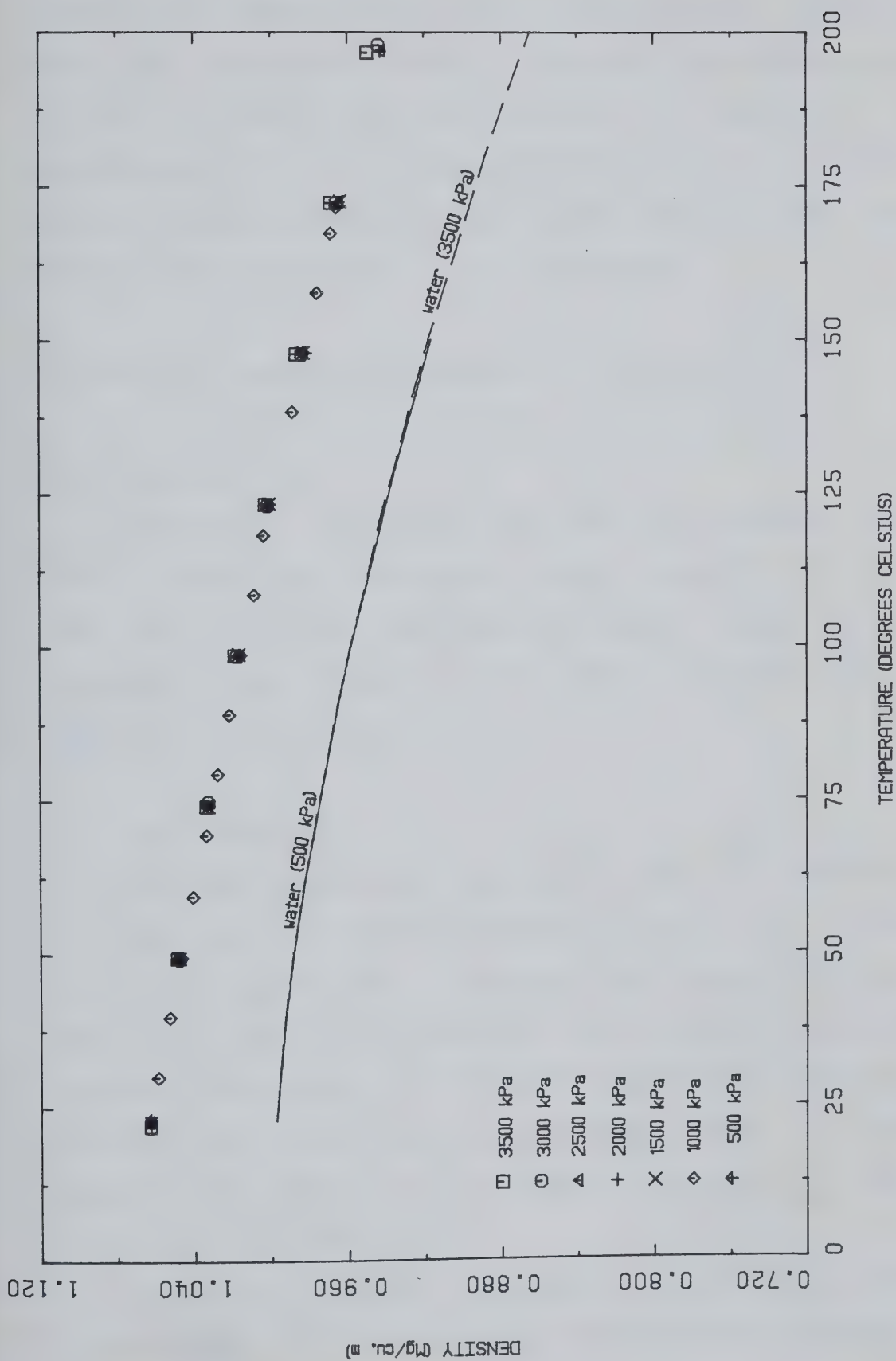


Figure 5.5 Thermal Expansion of Bitumen: Change in Density with Temperature

temperature range of 125 to 200 °C (Figure 5.4). Figure 5.5 shows that the density change of bitumen with temperature is similar to water from room temperature to about 125 °C and decreases at a slightly slower rate from 125 ° to 200 °. Figure 5.5 also shows that the bitumen had the same initial density for all pressure levels considered.

5.3 Thermal Expansion of Compacted Tailing Sand

5.3.1 Introduction

Laboratory tests were performed on compacted tailing sand to investigate the overall thermal expansion of the oil sand skeletal grains. The measured thermal expansion is the combined volume change of the soil structure and the individual sand grains.

5.3.2 Test Material

The sand used in the testing program was obtained from the Suncor operation and consisted of light brown, uniform, sub-angular quartz sand. The grain size analysis produced a distribution shown in Figure 5.6. Following the recommended A.S.T.M. Procedures (D 2049-69) the maximum and minimum densities were found to be 1.65 Mg/m³ and 1.41 Mg/m³, respectively. The minimum void ratio (e_{min}) was 0.61 and the maximum void ratio (e_{mx}) 0.87.

Hardy (1974) reports testing on sand tailings yielding a void ratio of 0.60 for sand in its most dense state and a

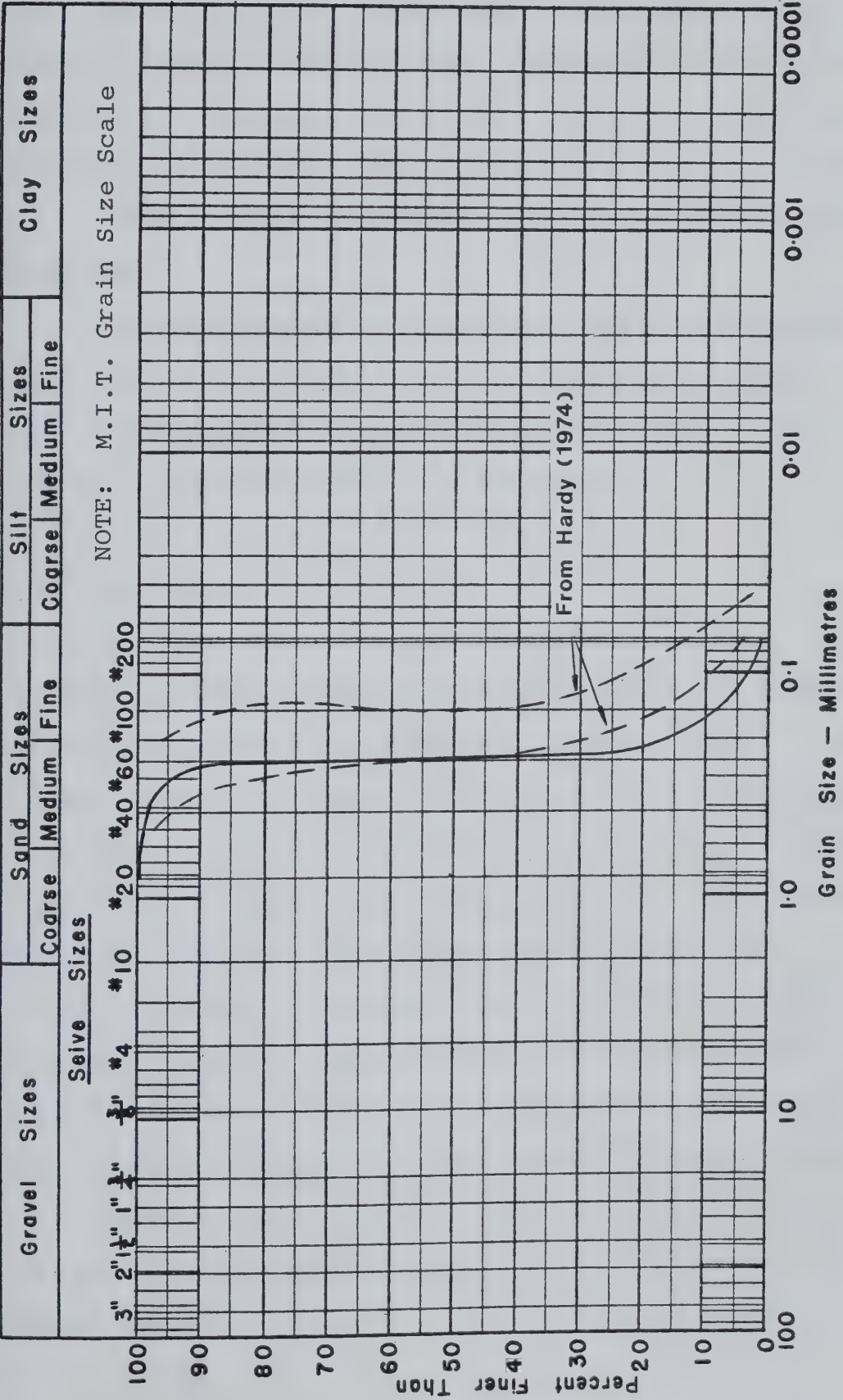


Figure 5.6 Grain Size Distribution of Oil Sand Tailings

void ratio of 0.87 in the most loose state. Hardy (1974) also provides two curves which encompass the majority of grain size distributions found in laboratory tests. For comparative purposes, these curves have been drawn on Figure 5.6. Hardy (1974) describes the sand grains as *sharp* and *abrasive*.

The visual properties and densities are consistent with those reported by Hardy (1974). Comparison between grain size distributions indicate the sand used in the testing program contained less silt size material.

5.3.3 Test Results

The data reduction calculations, data reduction computer program and experimental results are contained in Appendix D. Points representing steady state cumulative volume change at each temperature level (with respect to room temperature) for each particular density are shown in Figure 5.7. Figure 5.7 also contains, for comparative purposes, the cumulative volume change curve for an alpha quartz crystal. A typical sand grain may be composed of a number of randomly orientated quartz crystals and would expand thermally with no voids forming. Therefore, the thermal volume change of a sand grain can be approximated by the expansion of a single quartz crystal. Figure 5.8 contains plots of density change versus temperature for each sample tested.

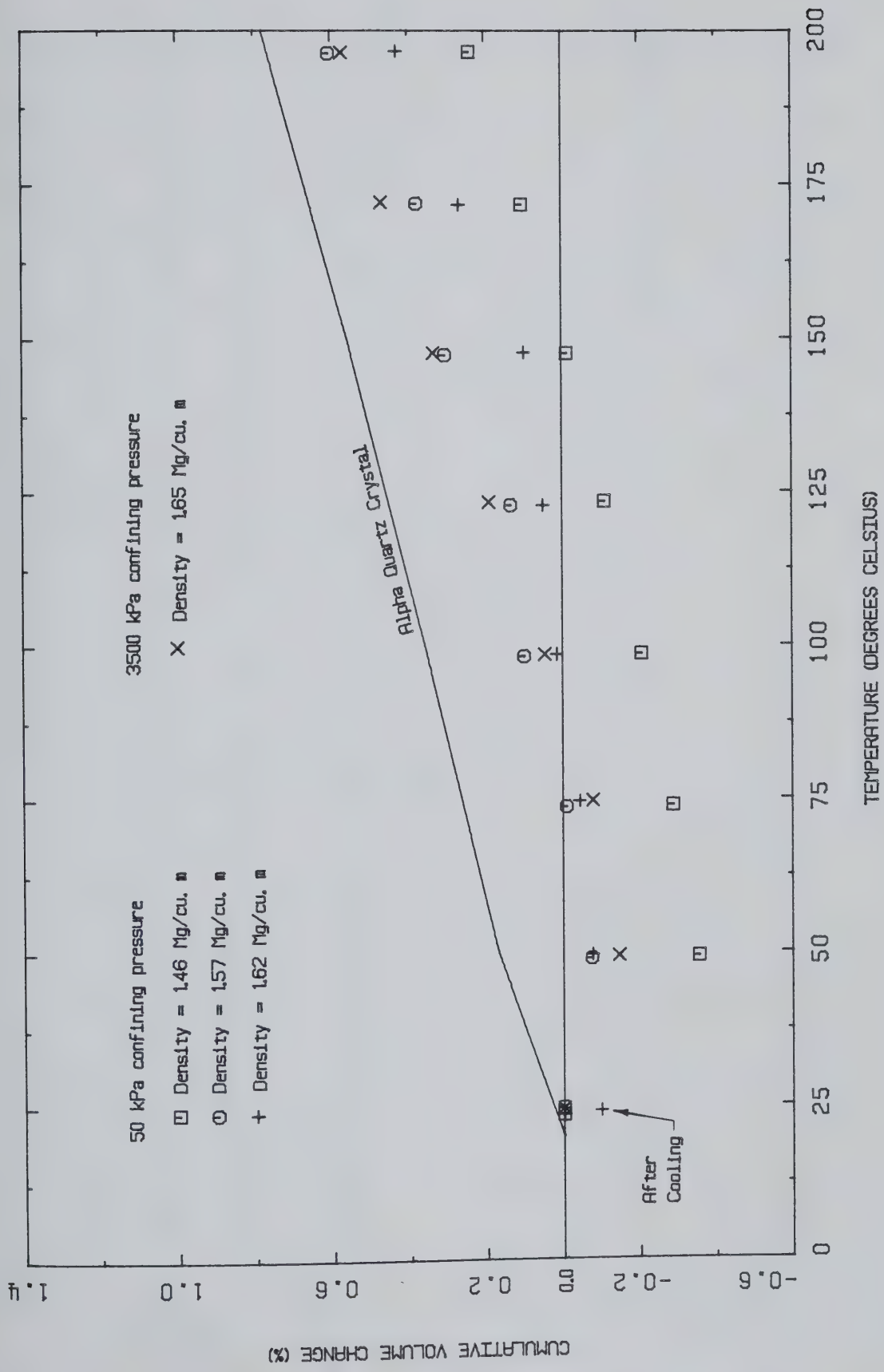


Figure 5.7 Thermal Expansion of Sand at Different Densities

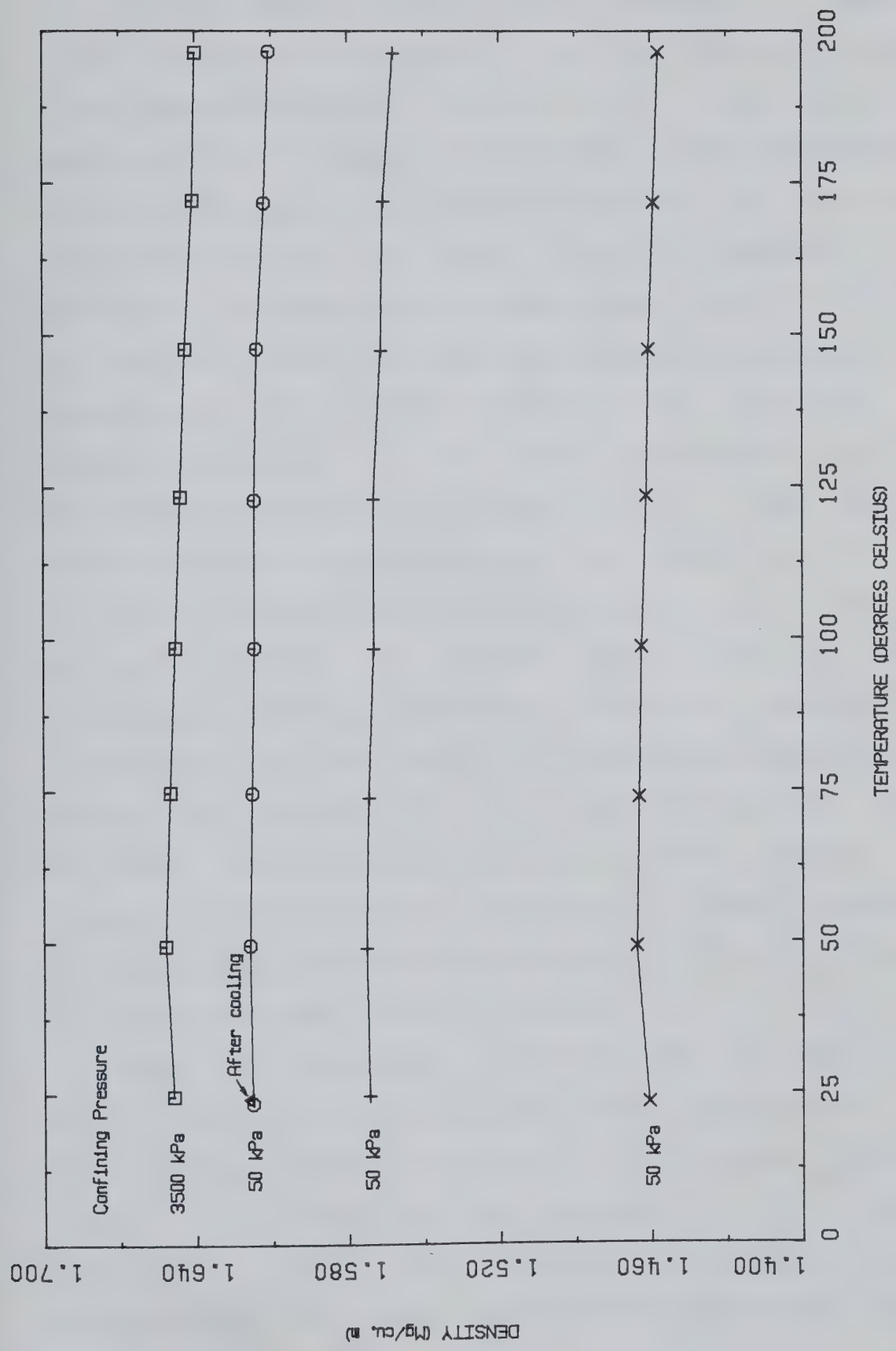


Figure 5.8 Thermal Expansion of Sand: Change in Density With Temperature

For each thermal expansion test conducted, a negative volume change was observed for the first heating increment (room temperature to 50 °C [Figure 5.7]). The loose sand sample (initial density of 1.46 Mg/m³ at room temperature) displayed the greatest volume decrease (0.36 %) over this temperature range. The sample initially compacted to a density of 1.62 Mg/m³ at room temperature showed a volume decrease of 0.08 % over the temperature increase from room temperature to 50 °C. After completion of this test (to approximately 200 °C) the sample was allowed to cool. At room temperature a volume decrease of 0.10 % was measured relative to the original volume at room temperature.

Since the sand was tested in the dry state with the grains in mineral to mineral contact and each grain undergoing thermal expansion, relative movement or reorientation of sand grains must have occurred during the temperature increase to 50 °C to allow an overall volume decrease. Campanella and Mitchell (1968) suggest such behavior results from a temperature induced change in interpartical forces that occurs to allow the sand structure to support the same effective stress.

Over the temperature range of 50 °C to 200 °C all samples display a volume increase roughly paralleling that of a quartz crystal (Figure 5.7). This behavior tends to suggest the soil structure has achieved a tight packing arrangement (grain slippage no longer occurring or negligible) and the volume increase with temperature result

from thermal expansion of the individual grains.

Figure 5.8 illustrates the change in density of each sand specimen with temperature. All samples tested display the same general trend, the density increasing over the temperature range of room temperature to 50 °C and gradually falling off to below the original density (at room temperature) over the temperature range of 50 °C to 200 °C. The sample originally at a room temperature density of 1.62 Mg/m³ shows a slight increase in density upon cooling back to room temperature.

5.4 Thermal Expansion of Oil Sand

5.4.1 Introduction

Oil sand subjected to increases in temperature will experience volume increases, the magnitude of which is dependent on the amount of pore fluid drainage which is permitted. The maximum thermal expansion occurs under undrained conditions and the minimum under conditions of full drainage of pore fluids.

Thermal expansion tests performed on oil sand under undrained conditions generates volume increases of mineral grains, pore fluids and mineral skeleton. Thermal expansion tests carried out on oil sand under drained conditions causes volume increase of mineral grains and mineral skeleton. In either case, if adequate back pressure is not provided, exsolution of gases dissolved in the liquid phases

will occur.

5.4.2 Test Material

The oil sand samples used in the experimental testing were obtained from core samples taken from an oil sand outcrop at Saline Creek, approximately 1 km south of Fort McMurray. The pertinent test sample data is given in table 5.1.

5.4.3 Test Results

The results of undrained and drained thermal expansion tests performed on oil sand under a constant back pressure of 2000 kPa (confining pressure of 2240 kPa) are given in Figure 5.9. Also contained within this figure is a plot of volume of fluid drained from the sample and a curve of the combined volume of fluid drained and volume change of the drained sample. Figure 5.10 illustrates the change in bulk density with temperature for both the undrained and drained cases.

Two additional drained thermal expansion tests were performed on Saline Creek oil sand under a back pressure of 5000 kPa (confining pressures of 11000 kPa and 5200 kPa). The results of these tests are given in Figure 5.11. Also contained in this figure is the drained test carried out under a back pressure of 2000 kPa (confining pressure of 2240 kPa). Figure 5.12 gives the results of the drained thermal expansion tests in terms of dry density. For

Table 5.1 Test and Sample Data

	1	Test 2	Number 3	4
Type of Test	Undrained	Drained	Drained	Drained
Back Pressure (kPa)	2000	2000	5000	5000
Vertical Confining Pressure (kPa)	2000	2240	11000	5200
Effective Confining Pressure (kPa)	0	240	6000	200
Bulk Density (Mg/m ³)	2.027	2.021	1.968	1.990
Percent Bitumen by Weight	11.19	11.19	15.55	15.58
Percent Sand by Weight	84.93	84.93	82.34	82.36
Percent Water by Weight	3.88	3.88	2.11	2.06
Void Ratio	0.539	0.539	0.634	0.617
Dry Density (Mg/m ³)	1.721	1.721	1.621	1.640

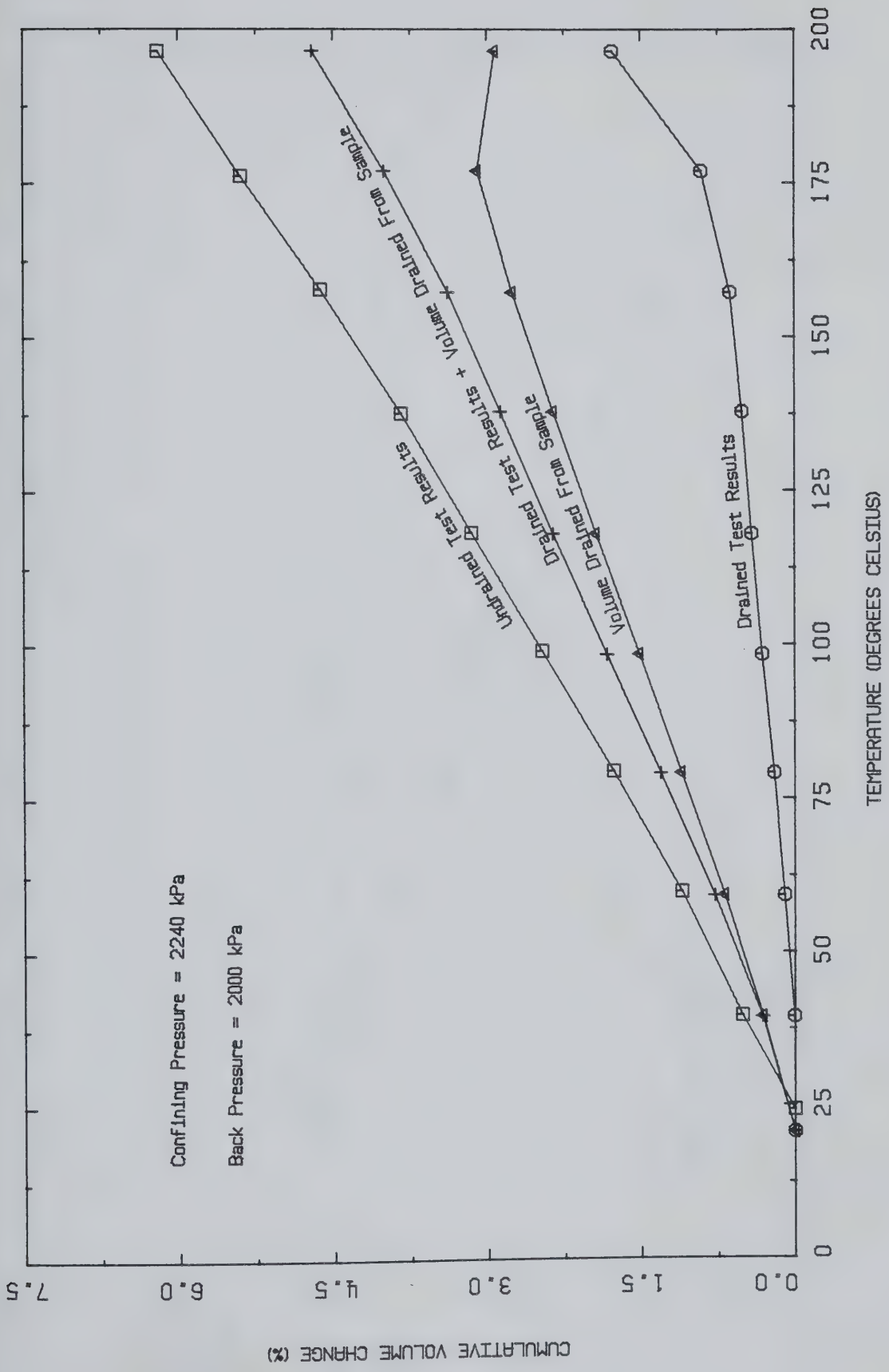


Figure 5.9 Thermal Expansion of Oil Sand Samples

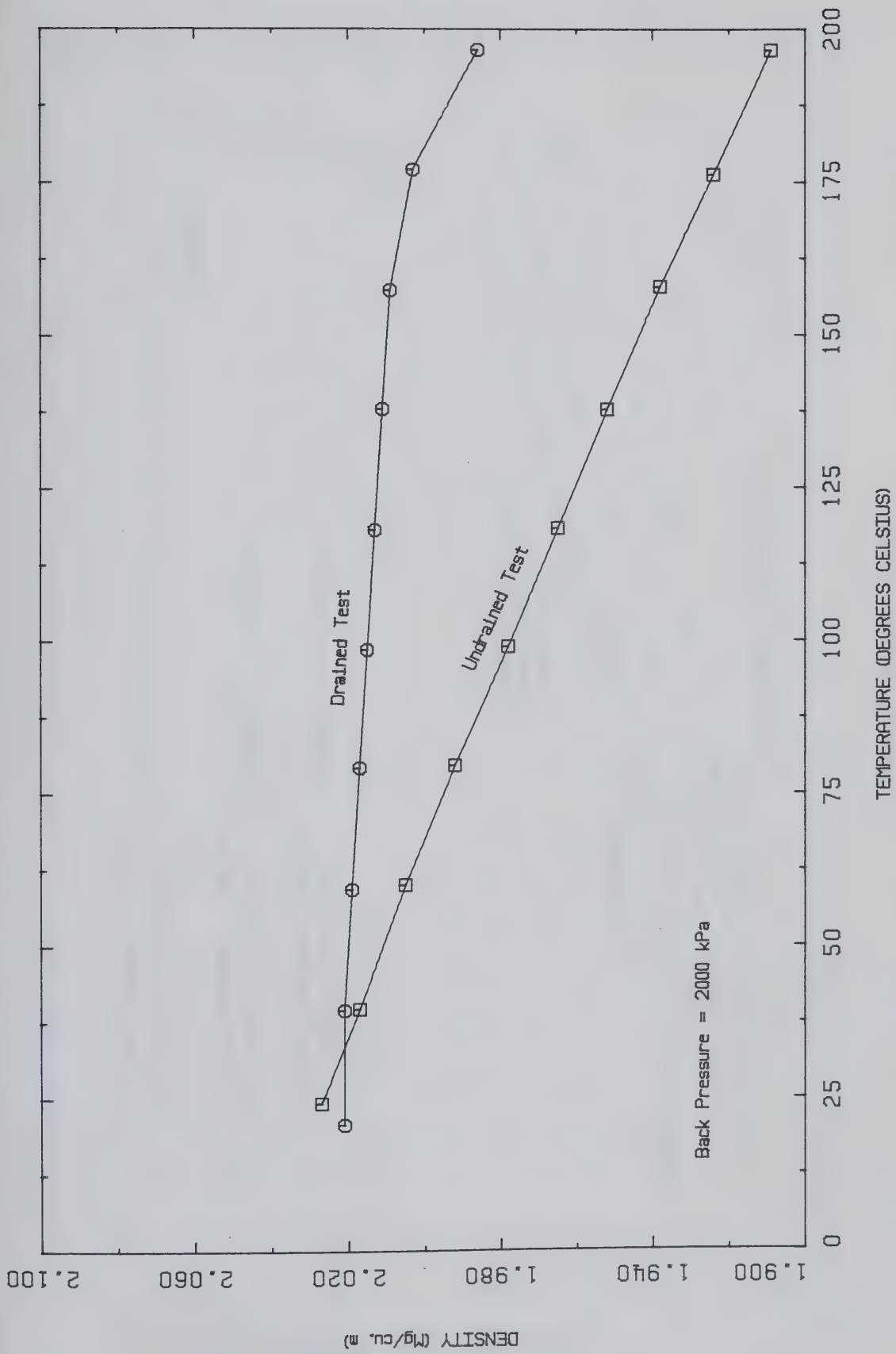


Figure 5.10 Thermal Expansion of Oil Sand: Change in Density With Temperature

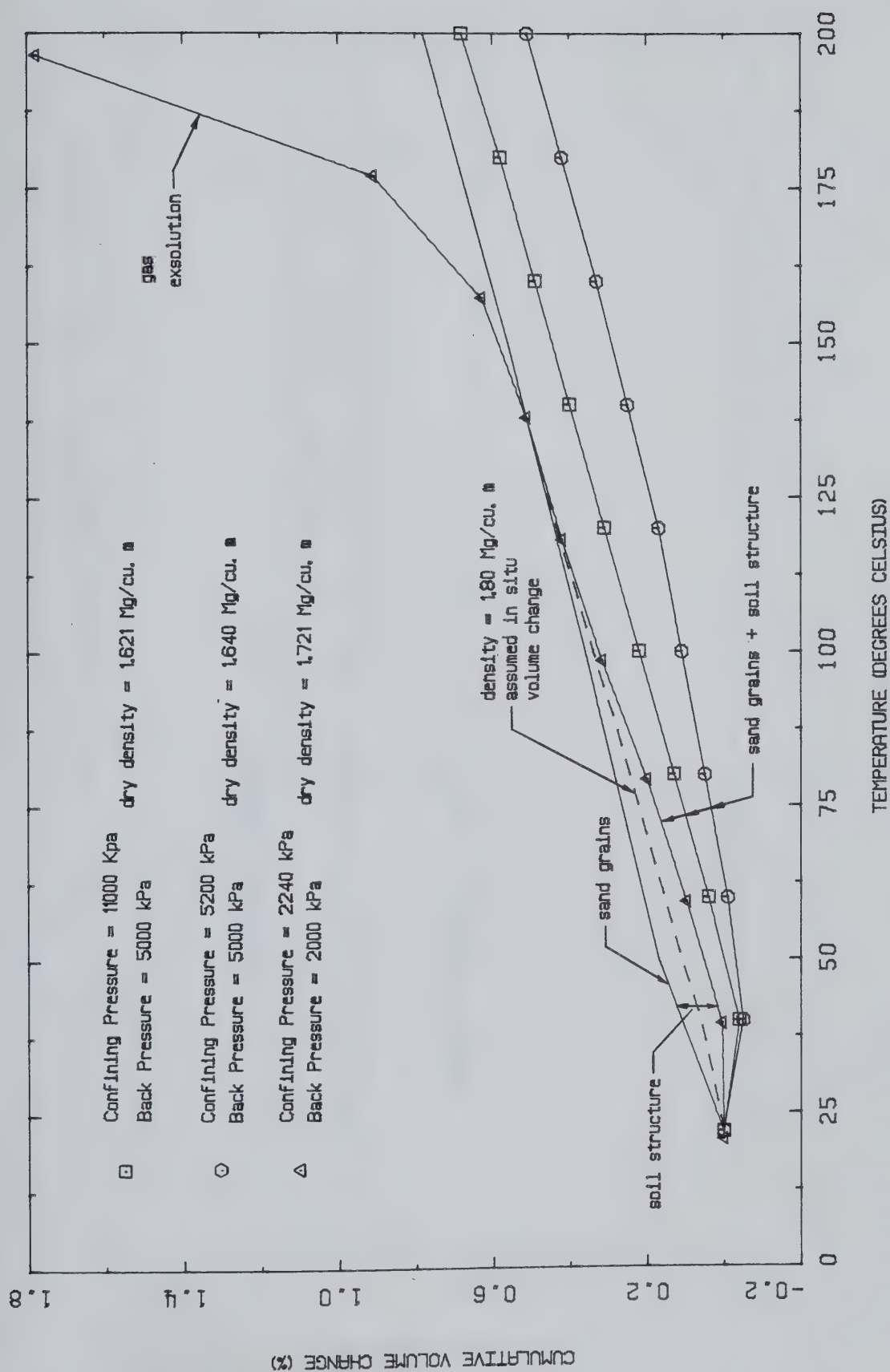


Figure 5.11 Thermal Expansion of Sand Grains and Soil Structure in Drained Oil Sand Tests

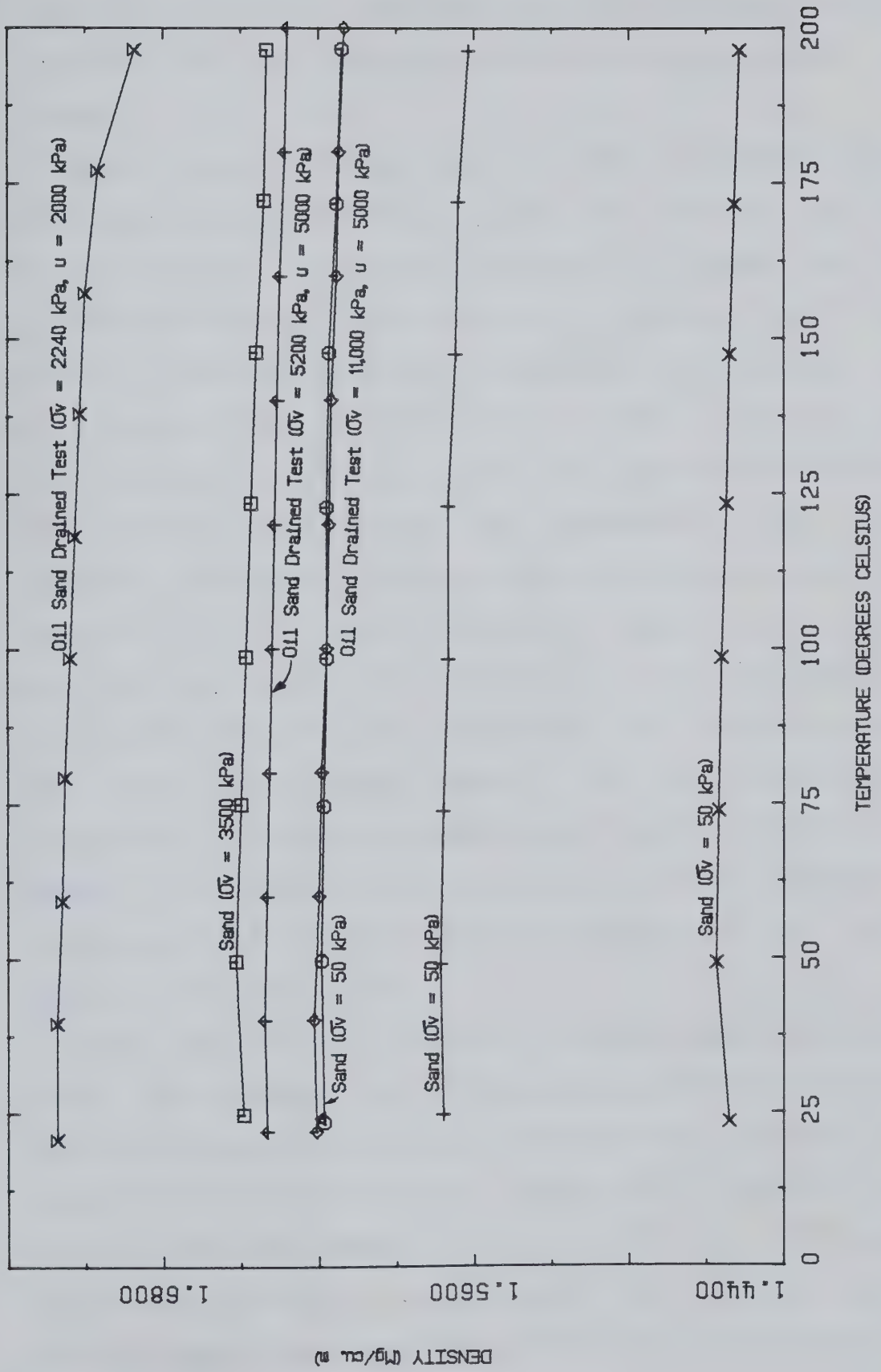


Figure 5.12 Drained Oil Sand Tests in Terms of Dry Density

comparitive purposes, the results of the tests performed on compacted tailing sand (Section 5.3.3) are included in the figure.

The drained thermal expansion test carried out on oil sand under a back pressure of 2000 kPa (Figures 5.9 and 5.11) displays a rapid increase in volume over the temperature range of 180 °C to 200 °C. Prior to 180 °C the rate of volume increase with temperature is consistant with the results of the two other drained tests (Figure 5.11). This observation tends to suggest the back pressure was not sufficiently high enough over this temperature range to keep gases in solution. If gas exsolution did occur over this temperature range, the gas bubbles at time of formation must have been at pressures exceeding the vertical confining stress (2240 kPa) in order to disrupt the skeletal grains and force the piston upward. The gas bubbles would theoretically continue to expand until pressure equilization between the fluid and gas phases was achieved resulting in the steady state points (temperature stable and zero volume change) at 180 and 200 °C.

The undrained and drained thermal expansion tests (under back pressure of 2000 kPa) were performed on similar oil sand samples obtained from the same core specimen. This implies the measured volume change of the drained sample combined with the volume of fluid drained from the sample should theoretically approximate the results of the undrained test (Section 5.4.1). The curve reflecting the

combined volume of fluid drained and volume change of the drained sample, although approximately parallel to the undrained test results, is consistently lower. The difference is due primarily to the contraction of the pore fluid as it leaves the sample chamber and is collected and cooled at room temperature in the fluid trap. The volume change apparatus does not take into account the contraction of expelled fluid and as a result consistently under estimates the amount of fluid drained during the test. The undrained test in contrast to the drained test shows no evidence of gas exsolution.

Several observations are made from the drained thermal expansion tests performed on oil sand. For the tests conducted under vertical confining pressures of 5200 and 11000 kPa negative volume changes were observed after the initial heating increments (Figure 5.11). Similar behavior was observed for the tests on compacted sand (Figure 5.7). Figure 5.12 shows the dry density change with temperature of these drained tests are consistent with those of the compacted sand. The initial densities were also similar indicating appreciable swelling occurred during sample preparation. The drained test performed under 2000 kPa back pressure did not display contraction during application of initial heat increments and had a significantly higher initial dry density (1.72 Mg/m^3) reflecting less sample disturbance.

Also shown on Figure 5.11 is the cumulative volume change with temperature of the quartz sand grains. Since the result of a fully drained thermal expansion test on oil sand is a measure of the volume change of both the sand grains and soil structure, the difference between the two curves is the volume change of the soil structure (Figure 5.11). A plot of the cumulative volume change of the soil structure with temperature for the drained tests performed is given in Figure 5.13.

An assumed cumulative volume change with temperature curve for in situ oil sand (average bulk density of 2.12 Mg/m^3 ; dry density of 1.80 Mg/m^3 [Dusseault, 1977]) is given in Figure 5.13. It is evident from Figure 5.13 that temperature induced changes in the soil structure is significant over the temperature range of room temperature to 140°C and is greatest at approximately 50°C . The more disturbed samples (bulk density of 1.968 and 1.990) showed a higher degree of contraction of the soil structure.

Figure 5.14 gives the change in the incremental coefficient of thermal expansion of soil structure with temperature. The incremental coefficient of thermal expansion for oil sand tested increases rapidly over the temperature range of room temperature to 50°C and becomes somewhat constant over the range of 50 to 200°C . The amount of change in the incremental coefficient of thermal expansion of the soil structure during the initial heating increments (to 50°C) is more pronounced for the disturbed

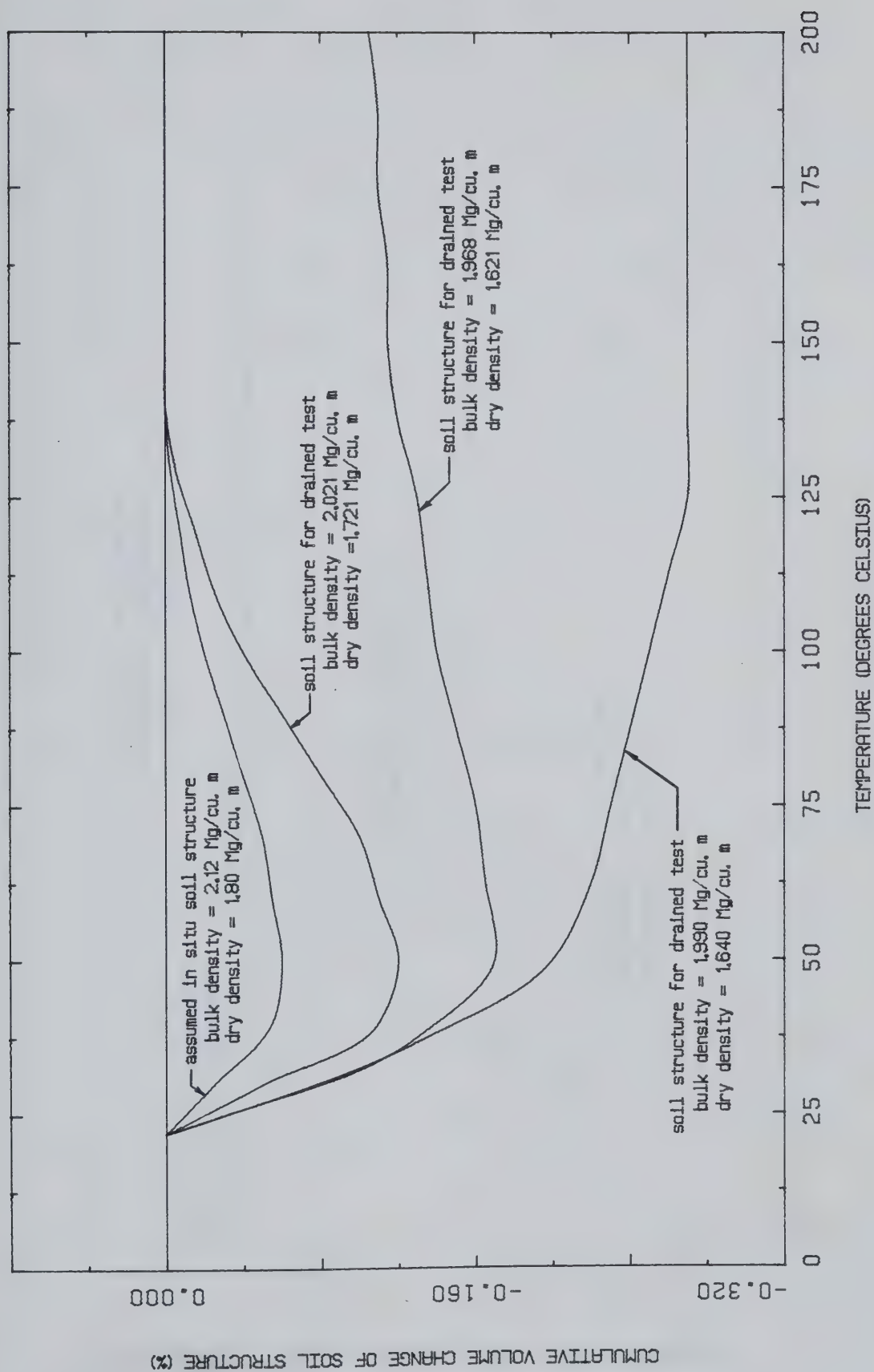


Figure 5.13 Thermal Volume Change of Soil Structure

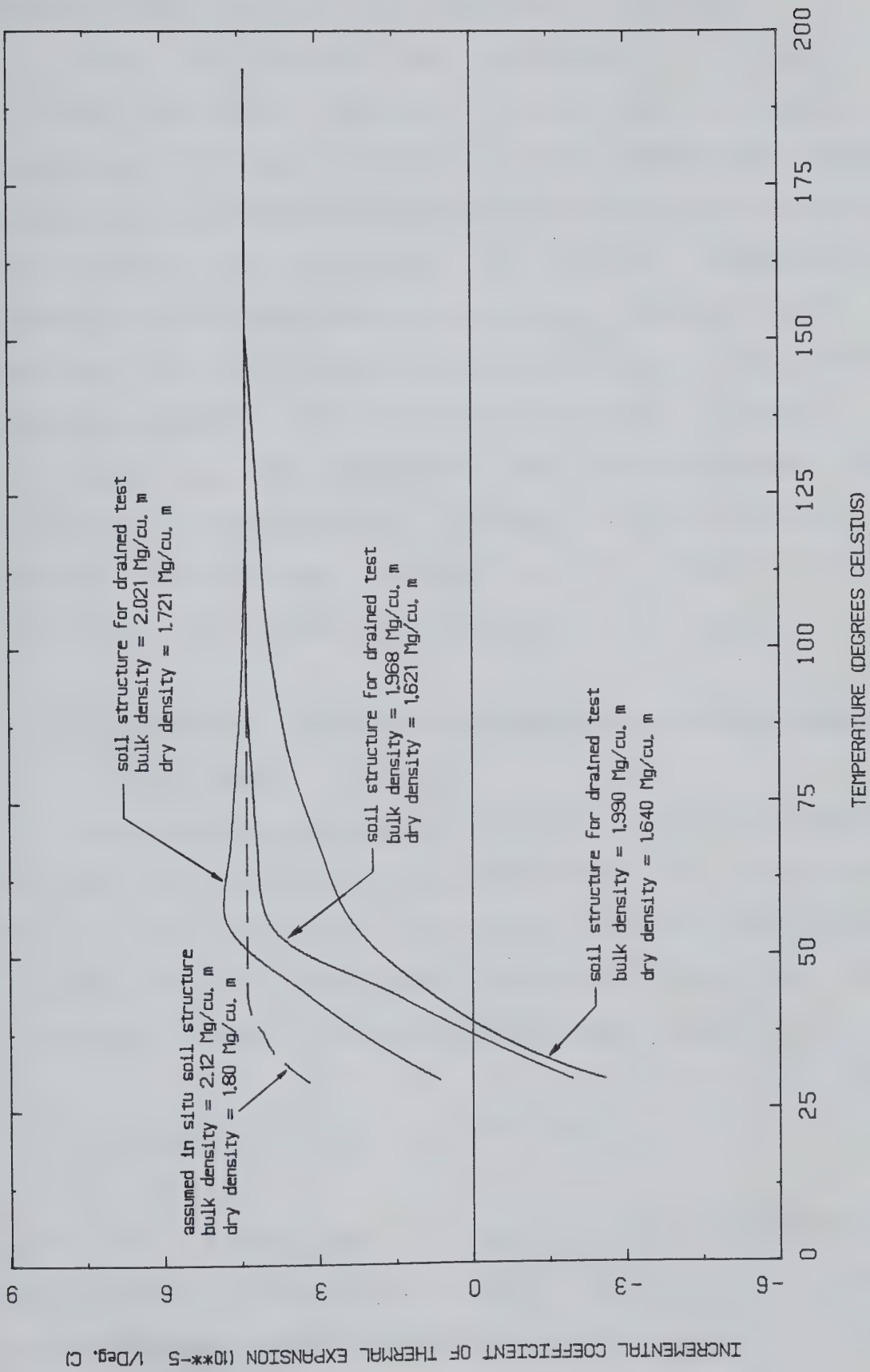


Figure 5.14 Coefficient of Thermal Expansion of Soil Structure

samples (bulk densities of 1.968 and 1.990 Mg/m³).

From the drained test conducted on oil sand it is evident that volume increase of less than 1 percent is likely for drained conditions over the temperature range of 20 to 200 °C provided adequate back pressures are maintained to prevent gas exsolution. The thermal volume increase appears to be independent of pressure (Figure 5.11). For Saline Creek oil sand significant thermal volume increases would be expected under back pressures below 2000 kPa.

Based on the undrained test results thermal volume increases of approximately 6 percent would be expected when Saline Creek oil sand is heated to 200 °C (assuming the back pressure is sufficient to keep gases in solution).

5.4.4 Theoretical Analysis to Predict the Undrained Behavior of Oil Sand

A theoretical analysis for predicting volume changes of oil sand due to temperature variations was presented in Chapter 3. From the theoretical analysis the change in volume of oil sand under undrained conditions and at constant effective stress was determined to be:

$$(\Delta V_m)_{\Delta T} = \alpha_w V_w \Delta T + \alpha_b V_b \Delta T + \alpha_s V_s \Delta T + (\Delta V_{s,t})_{\Delta T}$$

The above formulation is used to approximate the results obtained from the undrained thermal expansion test carried out on Saline Creek oil sand.

The coefficients of thermal expansion for bitumen and water used in the analysis was obtained from tests performed at the same back pressure as the undrained oil sand test (2000 kPa). Data collected from the drained test performed on oil sand obtained from the same core sample and tested at the same back pressure was used as input for the sand grain and sand structure terms. Figure 5.15 shows the experimental results of the undrained thermal expansion test along with the results of the theoretical analysis.

The theoretical analysis provided an underestimation of the thermal volume change obtained from the undrained test. Since the results obtained from the thermal expansion tests performed on water displayed excellent agreement with published data and results of the drained test (with regard to behavior of the sand grains and sand structure) were consistent with thermal expansion tests on similar oil sand (as well as tailing sand) then questions arise as to the validity of assuming results obtained from tests performed on extracted bitumen are representative of in situ bitumen. It is feasible that bitumen extracted by the hot water extraction process may have undergone some physical and chemical alteration. In addition, the compositional nature of bitumen may vary with respect to location (i.e., depositional environment).

If it is assumed that extracted bitumen is not representative of in situ bitumen, then results obtained from undrained and drained tests can be used as input in the

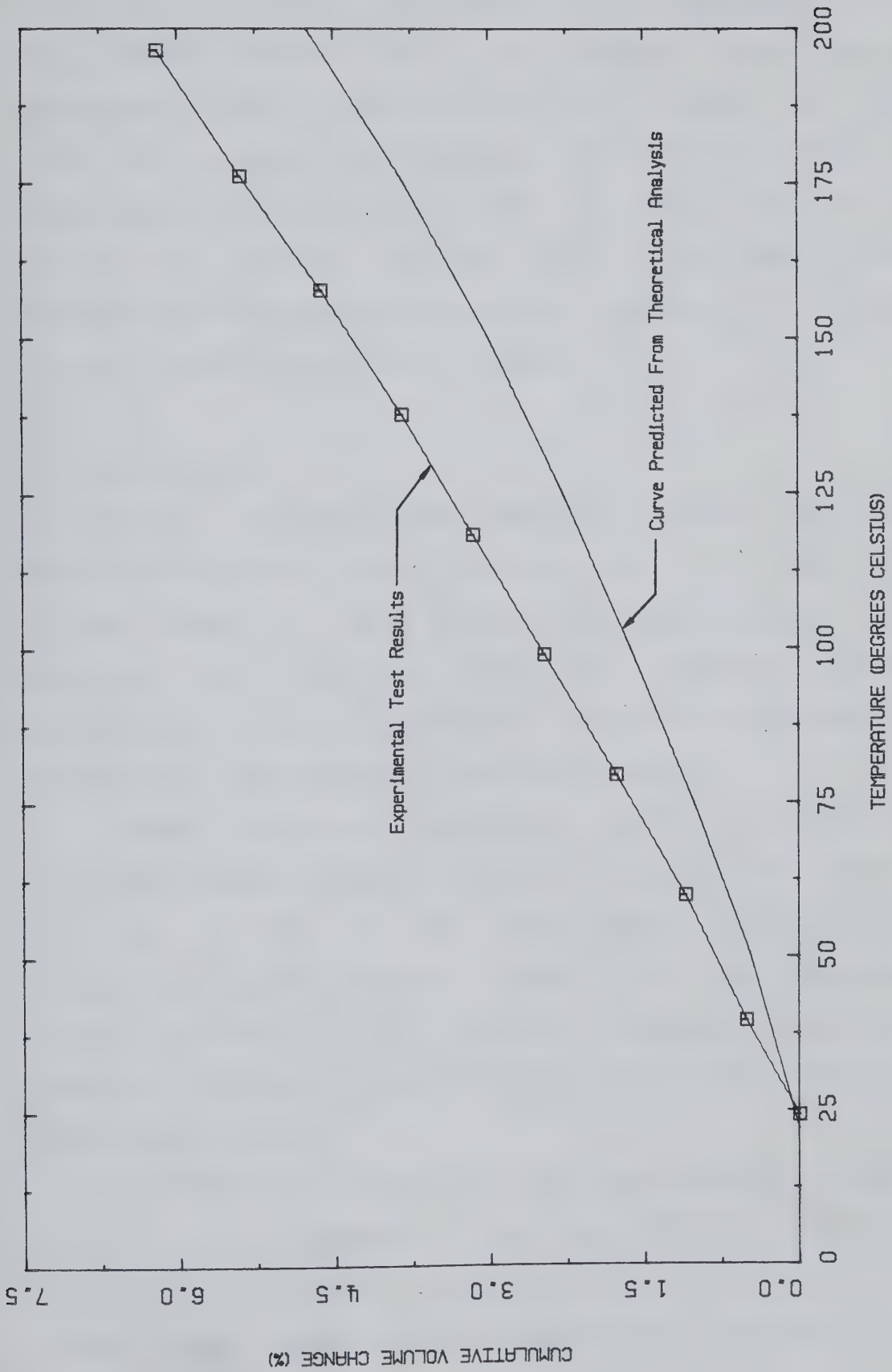


Figure 5.15 Thermal Volume Change of Oil Sand

theoretical analysis to generate a curve representative of the thermal expansion of in situ bitumen. Such a curve was developed for Saline Creek oil sand and is shown in Figure 5.16. For comparative purposes the results of the test performed on the extracted bitumen is also shown in the figure. The results indicate that in situ gas saturated bitumen may show temperature volume increases 50% greater than the extracted gas free bitumen.

5.5 Conclusions

Thermal expansion tests performed on water resulted in volume increases of about 15 per cent at 200 °C. The thermal volume change of water did not vary significantly for the pressure levels employed. Excellent agreement between experimental and published data indicates the pressure cell employed was calibrated and operating properly.

Thermal expansion experiments carried out on hot water extracted bitumen resulted in volume increases of about 15 per cent at 200 °C. The test results indicate that the cumulative volume change of bitumen over the temperature range considered is not pressure dependent. The volume change of this dead bitumen is more linear with temperature than that of water.

For each thermal expansion test conducted on compacted tailing sand, a negative volume change was observed for the first heating increment (room temperature to 50 °C). The loosest sand sample (initial density of 1.46 Mg/m³ at room

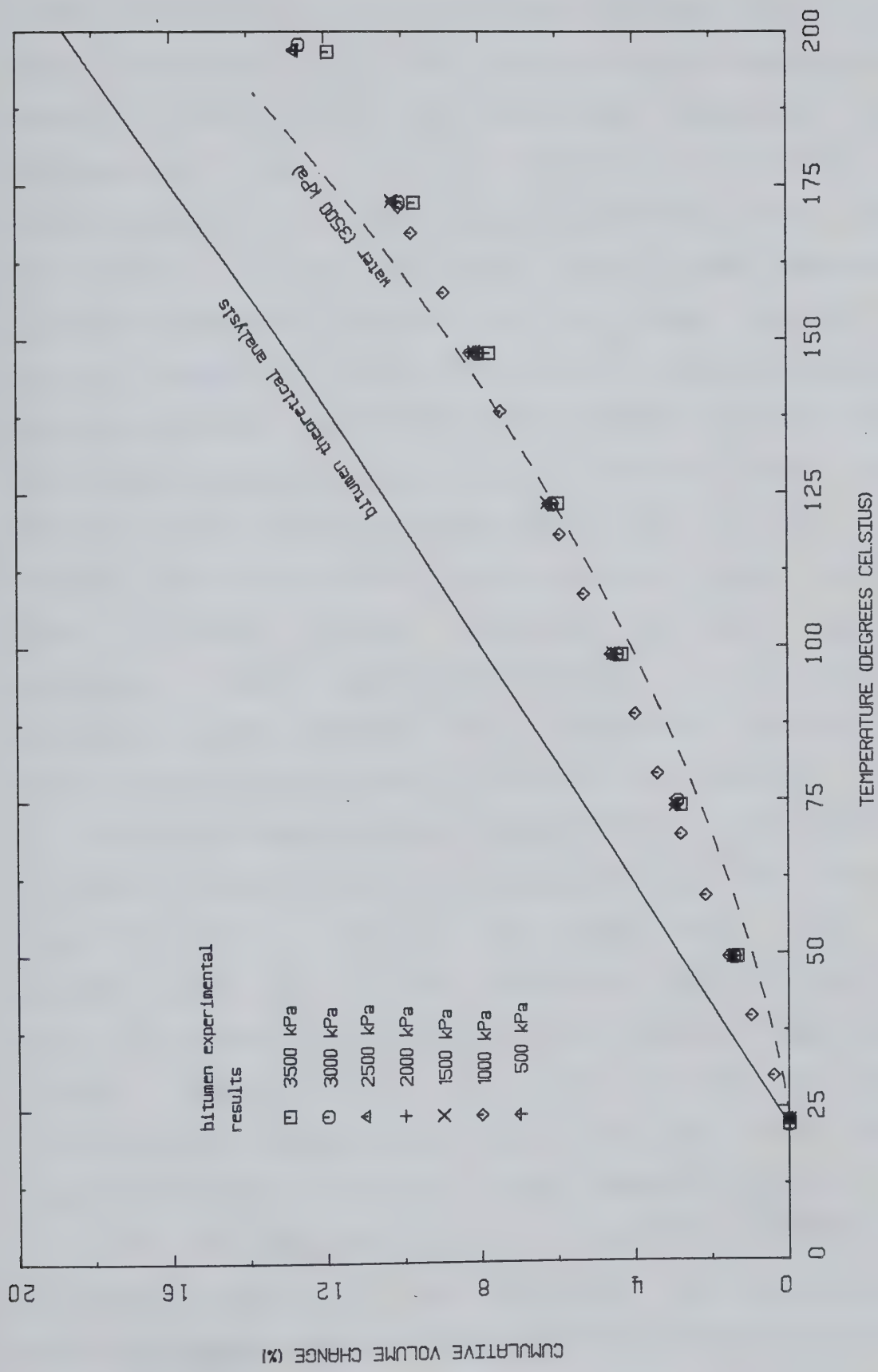


Figure 5.16 Theoretical Expansion of Bitumen

temperature) gave the greatest volume decrease (0.36%) over this temperature range. The sample initially compacted to a density of 1.62 Mg/m^3 at room temperature showed a volume decrease of 0.08% over the temperature range from room temperature to 50°C . After heating to 200°C , this sample was cooled to room temperature and a volume decrease of 0.10% was measured indicating that the volume decrease was due to a compaction of the soil structure. Relative movement or reorientation of sand grains must have occurred during the temperature increase to 50°C to allow an overall volume decrease. Over the temperature range of 50 to 200°C all samples tested displayed a volume increase roughly paralling that of a quartz crystal, indicating the soil structure achieved a tight packing arrangement at 50°C and the subsequent volume increase with temperature results only from the thermal expansion of the individual grains.

Undrained heating of oil sand to 200°C will result in a volume increase of about 6 percent. Most of this increase, over 5 percent, is due to the pore fluids, water and bitumen, with the bitumen expanding slightly more than water. The remainder of the volume increase is due to the thermal expansion of the sand grains. The dense, impenetrative structure of in situ oil sand will show a negligible amount of thermal volume change by itself.

From the tests performed on oil sand the thermal volume increase appears to be independent of the effective confining pressure for the pressure range considered in this

study. For the oil sand tested here, significant thermal volume increases would be expected under back pressures below 2000 kPa because of gas exsolution at temperatures above 180 °C.

Results obtained from the undrained and drained thermal expansion tests performed on oil sand were used to generate a plot representative of the thermal expansion of in situ bitumen. The results indicate that in situ gas saturated bitumen may show temperature volume increases 50% greater than the extracted gas free bitumen.

6. NUMERICAL ANALYSIS

6.1 Introduction

To determine the amount of heave which would occur beneath a structure where the oil sand foundation experiences a temperature increase, it is necessary to assess the spatial temperature increase with time and estimate the amount of drainage which might occur. Since such field observations are absent in the published literature, the rate of heat flow beneath the heated foundation and the amount of drainage which occurs are evaluated using numerical methods for a general stratigraphy.

The analytical model put forth here investigates the heat flow from an 80 m diameter storage tank resting on a 2 m crushed rock and sand foundation pad. The tank is assumed to be held at a constant temperature of 175 °C. The general stratigraphy chosen for this study consists of the granular pad on top of 3 m of clayey till overlying rich oil sand.

The analytical model developed in this study couples heat flow theory to the fluid flow expression to assess the state of drainage in the oil sand strata below the heated foundation and calculates the change in pore pressure and the volume change (or heave). The analytical model consists of four computer programs. *FEHT2-1*, developed by G. E. Myers at the University of Colorado, was used to evaluate the rate at which the heat from the foundation propagates through the

oil sand strata. *VARTEST5*, developed by the author, was used to calculate the change in pore pressure and change in engineering properties of the oil sand strata in response to the change in temperature (as predicted by *FEHT2-1*). *VARTEST5* then compiled the information and formatted the data for direct input into the fluid flow program. In other words, *VARTEST5* served to couple the heat flow analysis to the fluid flow analysis. *ADINAT*, developed by K. J. Bathe at M.I.T., was used to determine the state of drainage in the oil sand strata. The above three computer programs were executed in succession at predetermined time intervals to simulate simultaneous heating and draining of the oil sand strata.

A fourth computer program, *VOLTEST5* (also developed by the author) was utilized to determine the amount of volume change occurring after each heating and draining cycle and to calculate the amount of heave occurring under the foundation.

6.2 Heat Flow

The thermal analysis was performed utilizing a computer program (*FEHT2-1*) developed by G. E. Myers at the University of Colorado in 1972 (Appendix E). *FEHT2-1* (Finite Element Heat Transfer - 2 dimensions) evaluates problems of heat conduction in two dimensions by a finite element method. The method involves the use of linear triangular elements. The computer program has the capability of handling steady and

transient states. The transient states can be analyzed by any of three methods: Eulers; Crank-Nicholson; or pure-implicit. The program considers three boundary conditions: time independent convection; time independent heat flux; and time independent temperature. The program was originally dimensioned to accommodate 50 nodal points but has been altered to handle in excess of 280.

The finite element mesh utilized for the numerical analyses is shown in Figure 6.1. The finite element mesh consists of 500 triangular elements and 284 nodes. The elements were proportioned in size to provide greater accuracy in critical areas.

The Crank-Nicholson method (a central finite difference scheme) was utilized to determine the transient temperature variation beneath the heated foundation. Myers (1971) provides an in-depth discussion of the Crank-Nicholson scheme. The transient temperature variation was calculated using *FEHT2-1* based on a time increment of 12 hours for the first year and a time increment of 60 hours for years 1 to 30. The thermal properties used in the thermal numerical analysis were taken from Boga et al. (1980) and are given in Table 6.1.

The transient temperature variation was determined based on the following assumptions:

(i) the thermal properties given in Table 6.1 did not vary significantly with time

Table 6.1 Thermal Properties Used in Numerical Analysis

	Thermal Conductivity (k) kJ/hr m °K (Btu/hr ft °R)	Density (ρ) kg/m ³ (lbs/ft ³)	Specific Heat (c) kJ/kg °K (Btu/lb °R)
Crushed Rock/Sand	7.289 (1.17)	2162.4 (135.0)	0.838 (0.20)
Overburden (Till)	6.230 (1.00)	2082.3 (130.0)	1.173 (0.28)
Oil Sand	6.230 (1.00)	2162.4 (135.0)	1.131 (0.27)

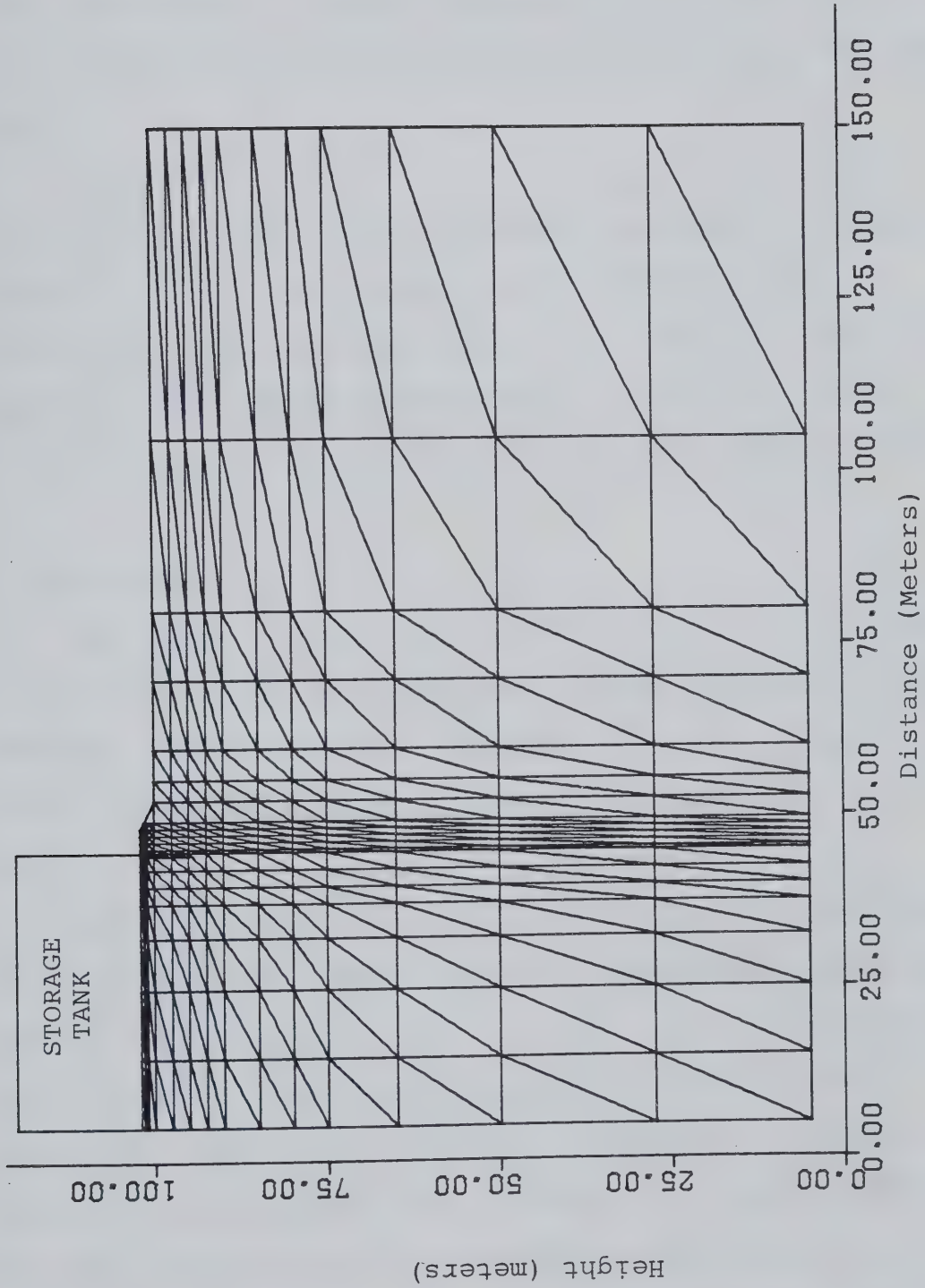


Figure 6.1 Finite Element Mesh Utilized for Thermal Analyses

- (ii) the thermal properties were independent of the direction of heat flow
- (iii) the ambient air temperature was constant at 10 °C
- (iv) the ambient oil sand temperature was constant at 5 °C
- (v) fluid flow in the strata did not influence the flow of heat

The results of the thermal analysis are shown in Figures 6.2 through 6.11. The figures are representative of the temperature distribution into the depth of the strata underlying the heated foundation at times 0.25, 0.5, 0.75, 1, 5, 10, 15, 20, 25 and 30 years as predicted by *FEHT2-1*.

6.3 Drainage

The state of drainage in the oil sand strata below the heated foundation was calculated using computer programs: *VARTEST5* (Appendix E), developed by the author for this study; and *ADINAT*, developed by K. J. Bathe at M.I.T. in 1977.

VARTEST5 calculates the increase in pore fluid pressure due to temperature change from the formulations developed in section 3.1.3 for each node in the finite element mesh employed in the thermal analysis. This program also calculates the coefficient of hydraulic conductivity, thermal generation rate and the specific storage coefficient for each element required as input to the fluid flow program *ADINAT*. The material properties required in the above

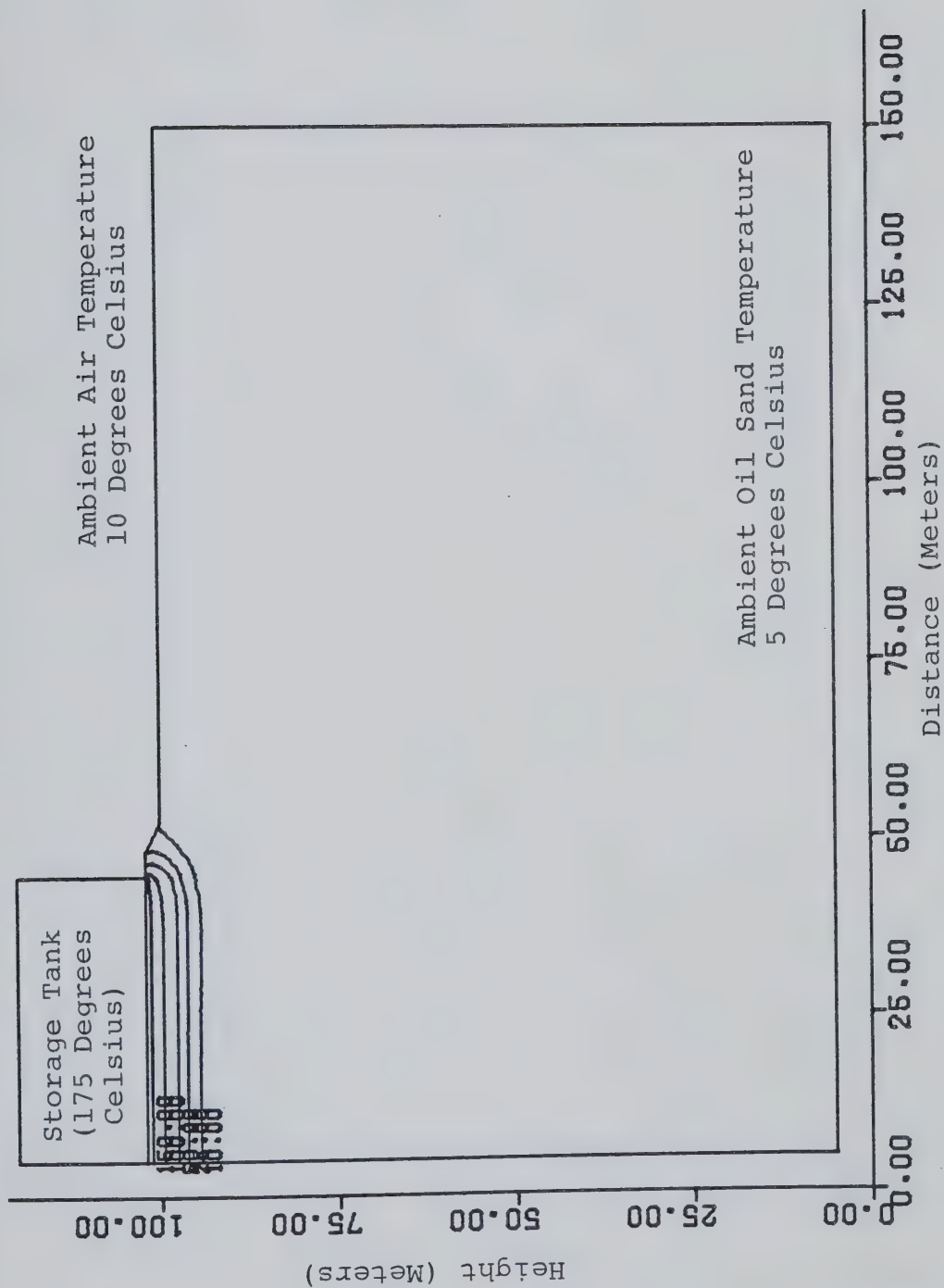


Figure 6.2 Isotherm Plot after 3 Months

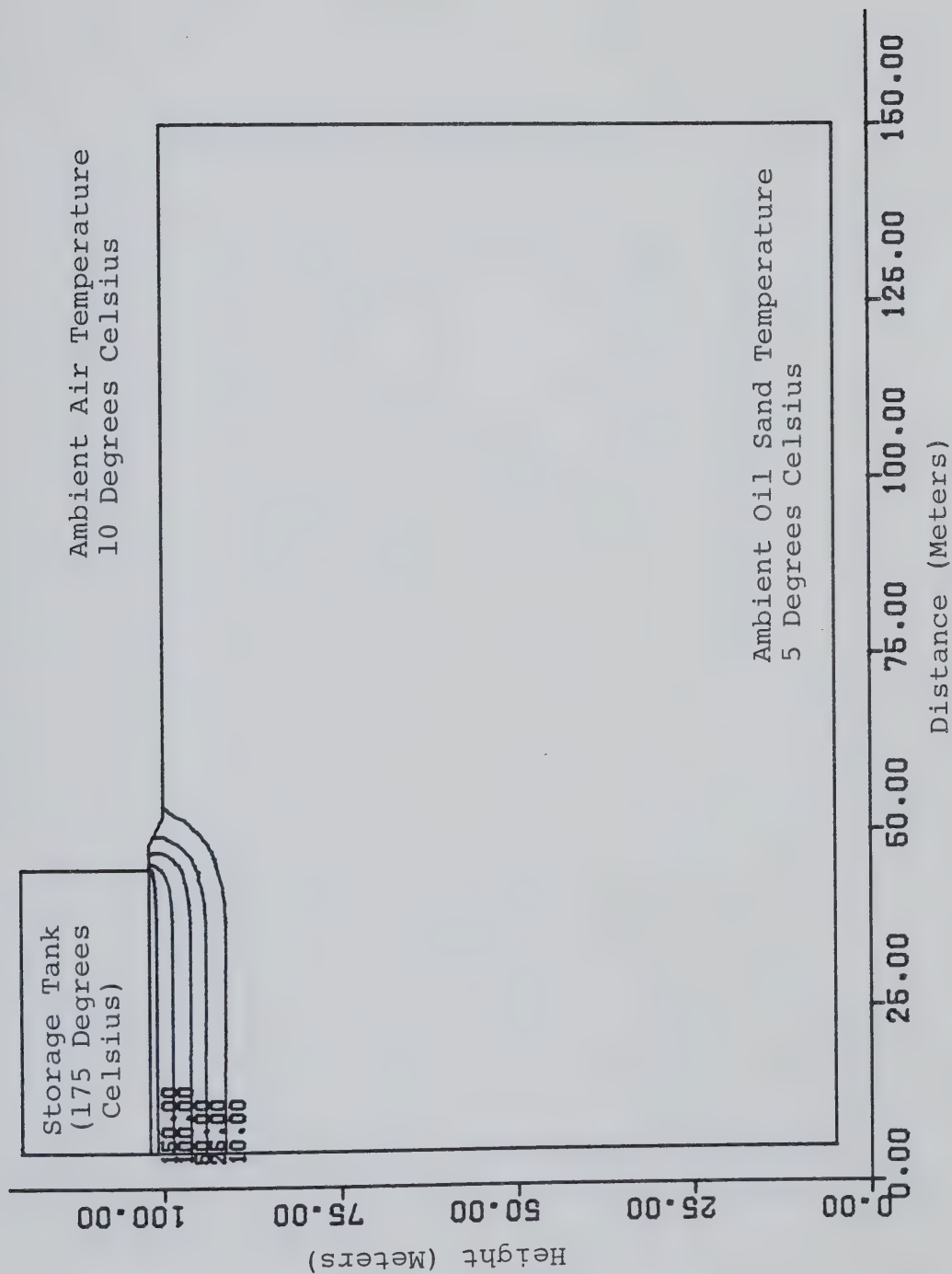


Figure 6.3 Isotherm Plot after 6 Months

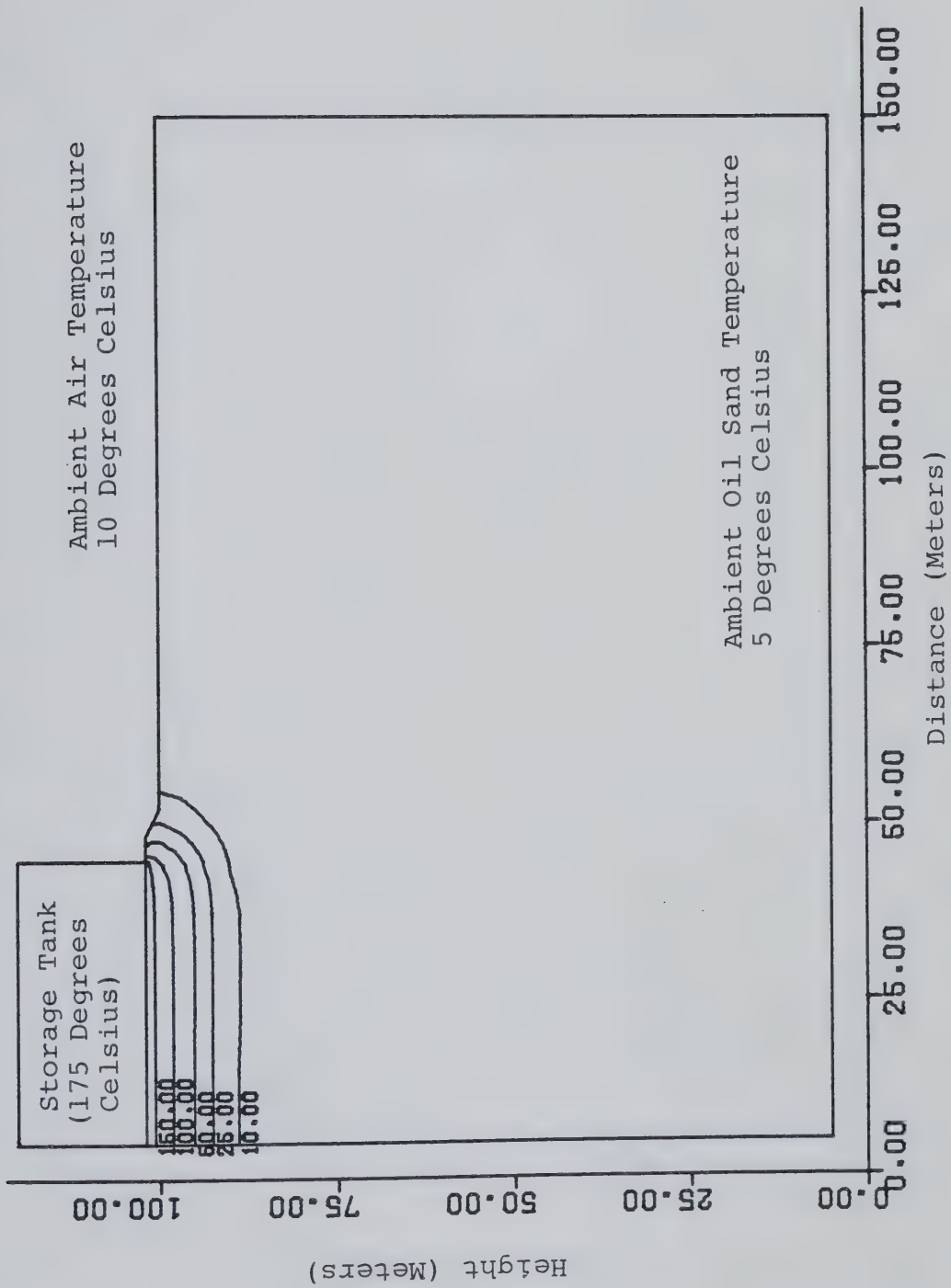


Figure 6.4 Isotherm Plot after 9 Months

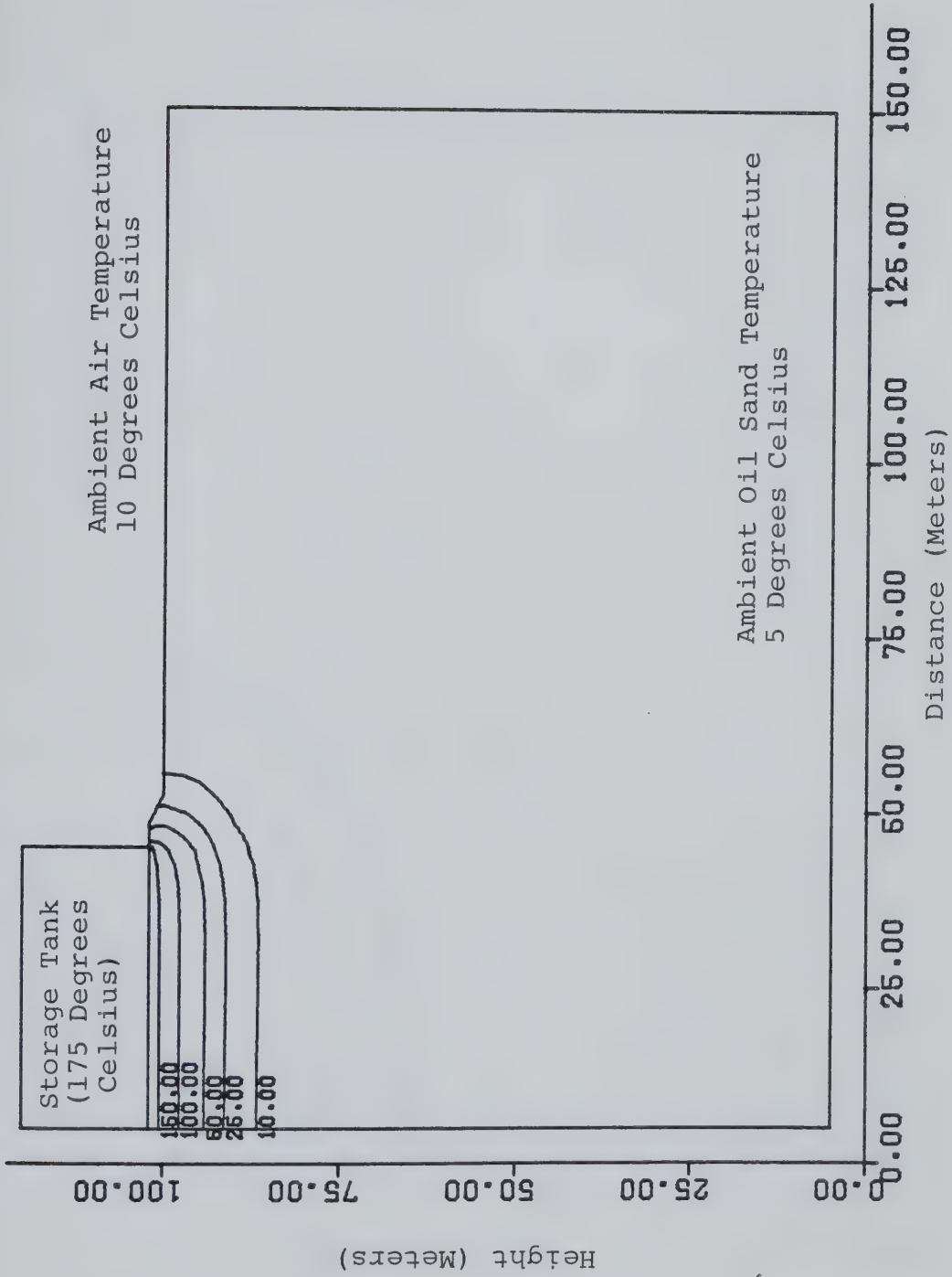


Figure 6.5 Isotherm Plot after 1 Year

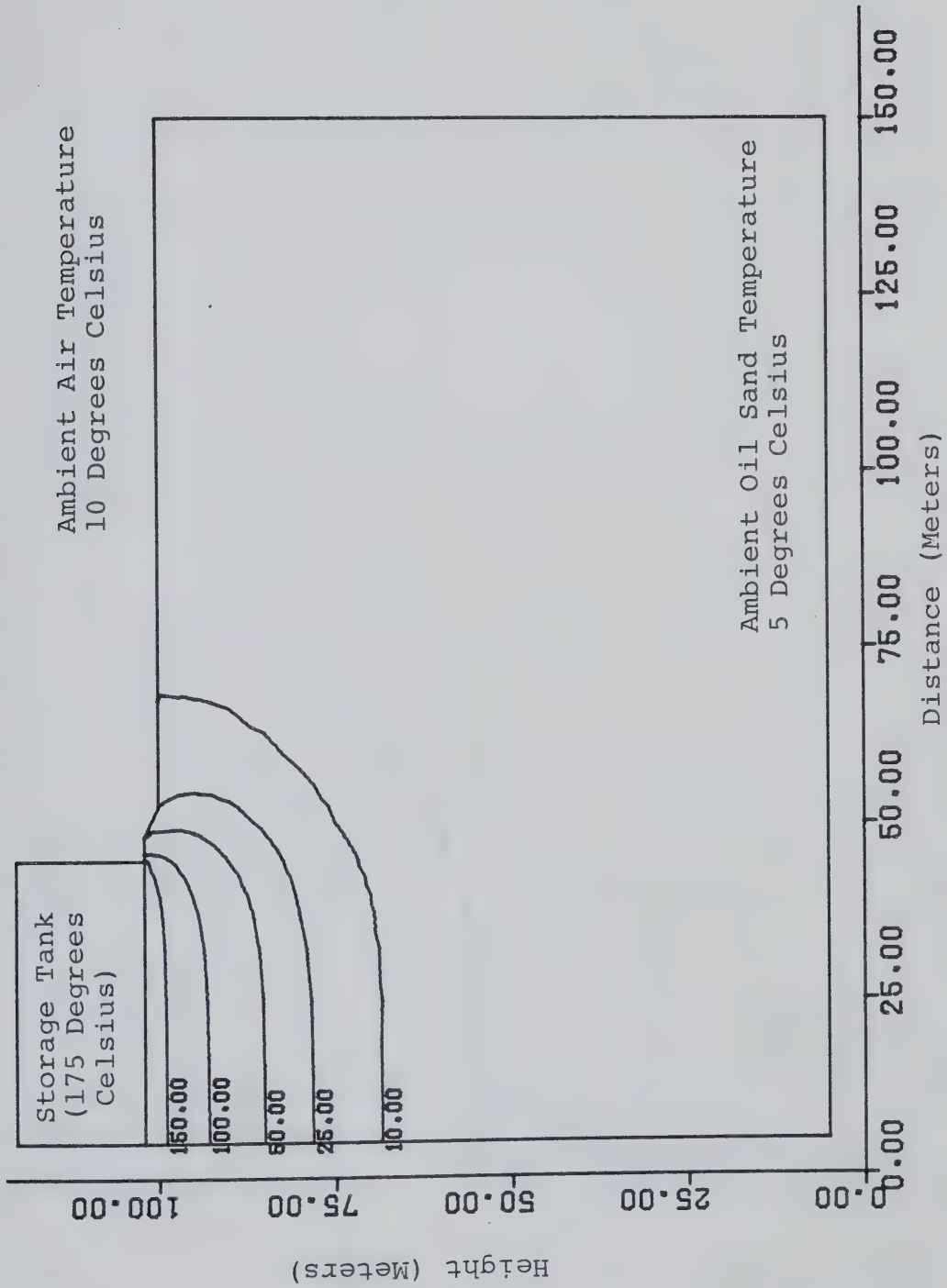


Figure 6.6 Isotherm Plot after 5 Years

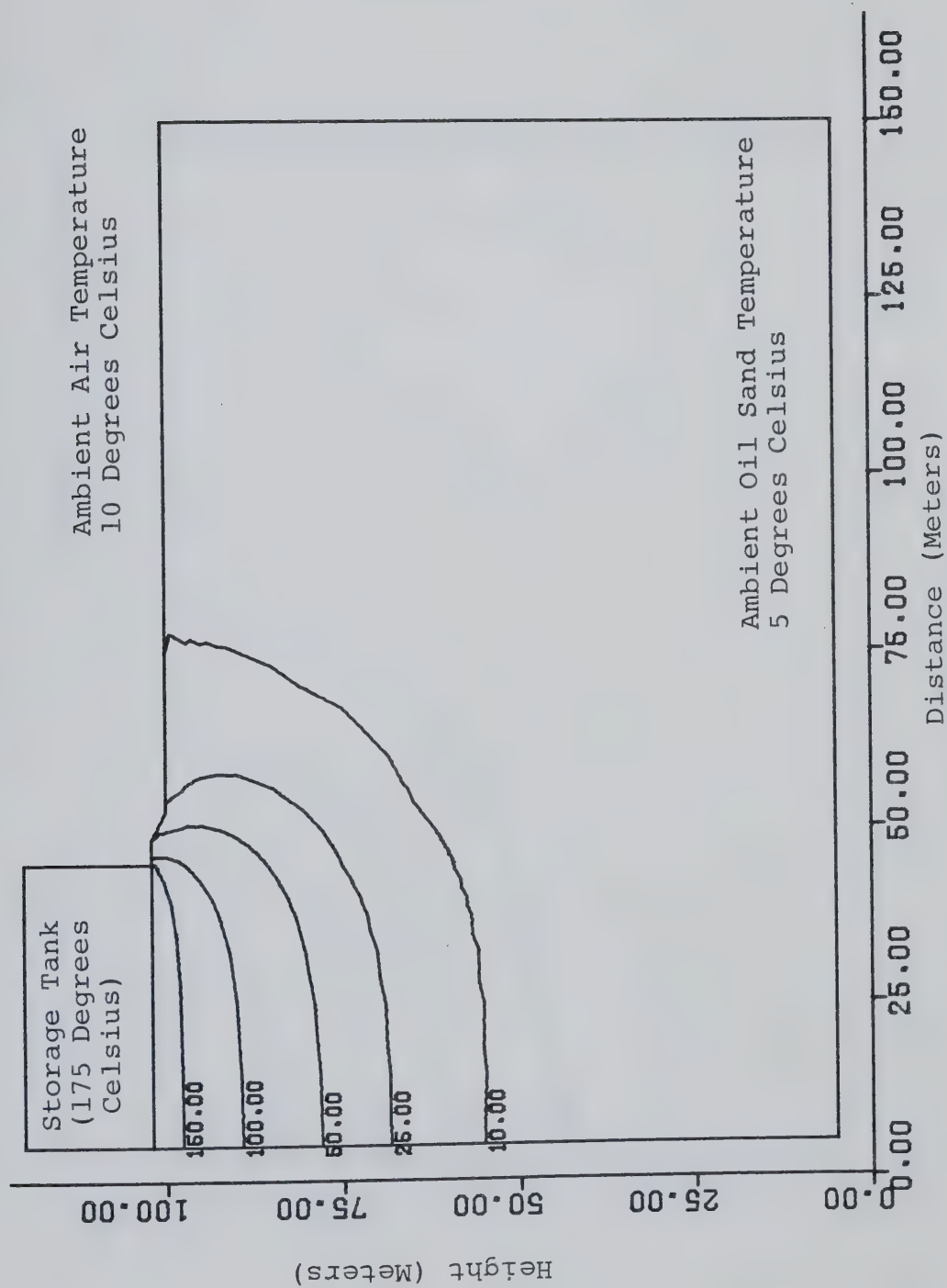


Figure 6.7 Isotherm Plot after 10 Years

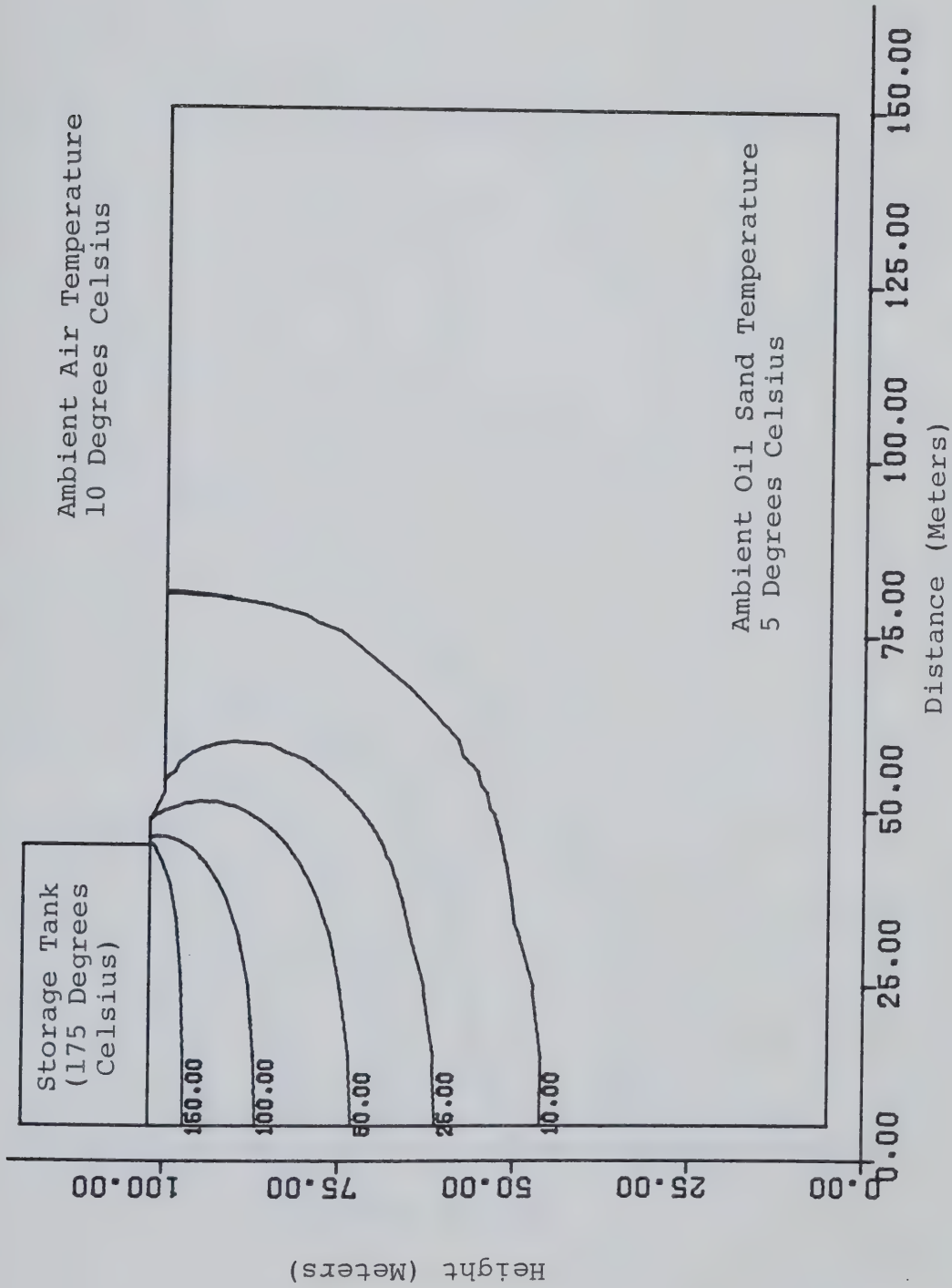


Figure 6.8 Isotherm Plot after 15 Years

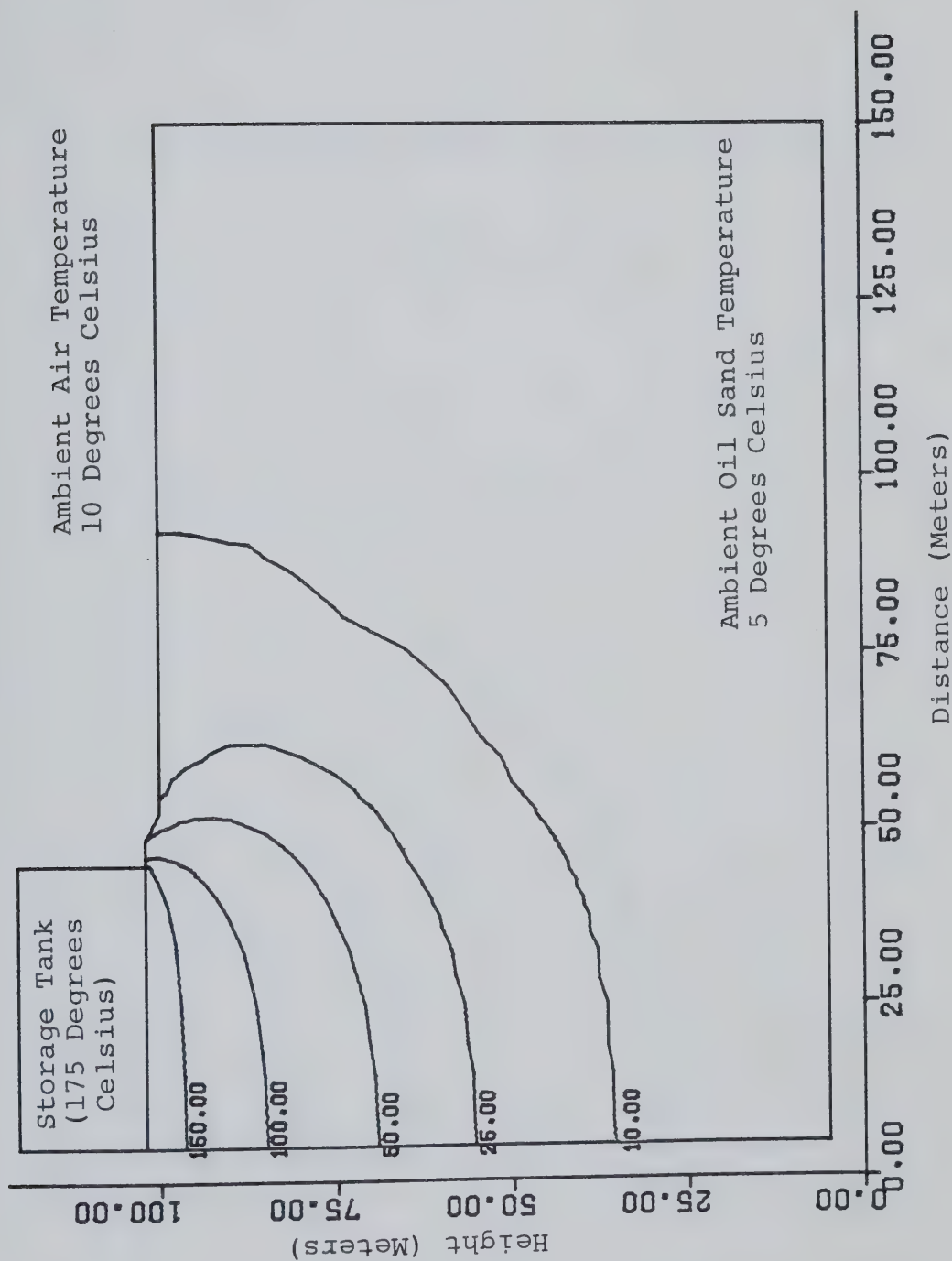


Figure 6.9 Isotherm Plot after 20 Years

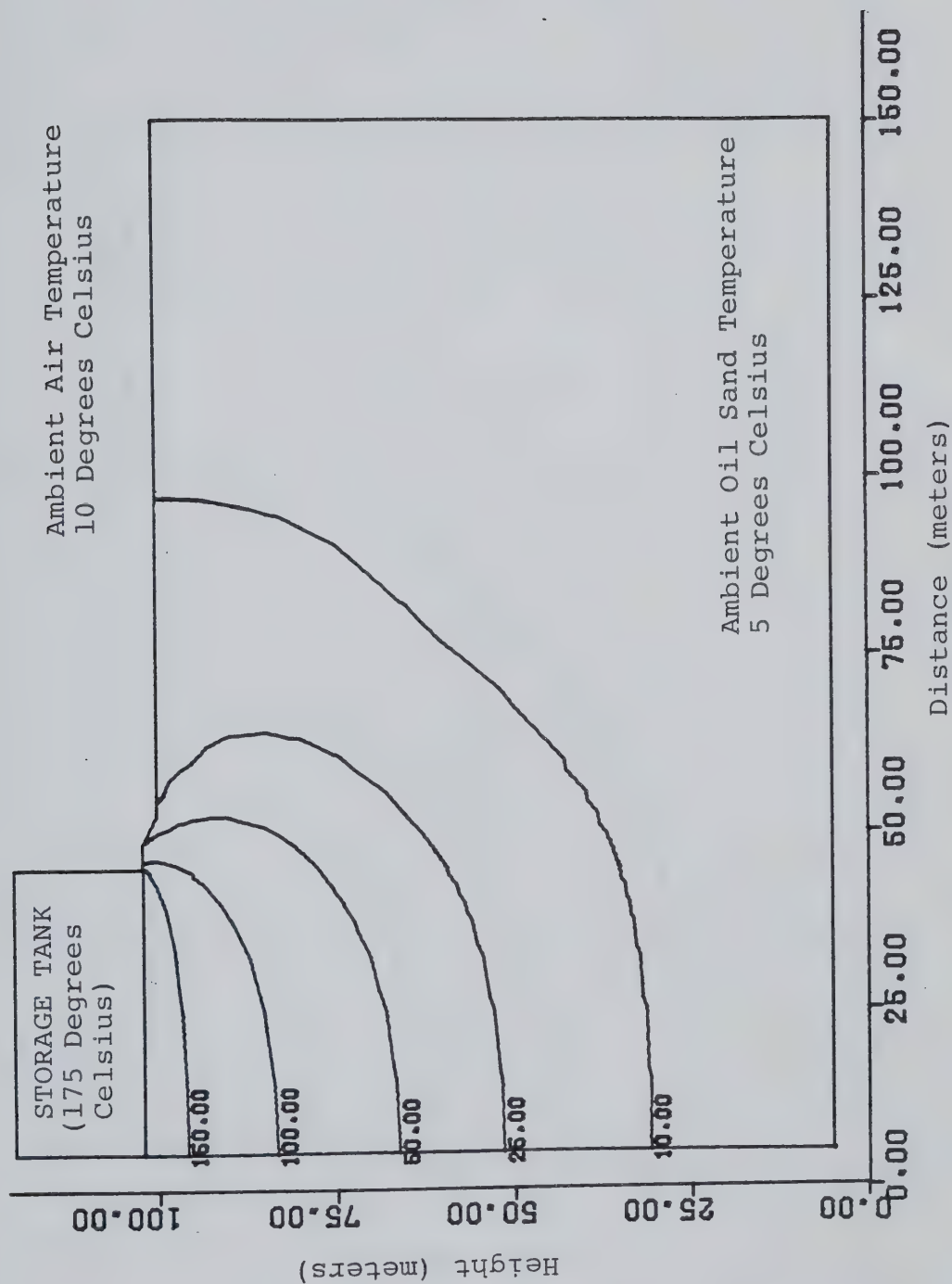


Figure 6.10 Isotherm Plot after 25 Years

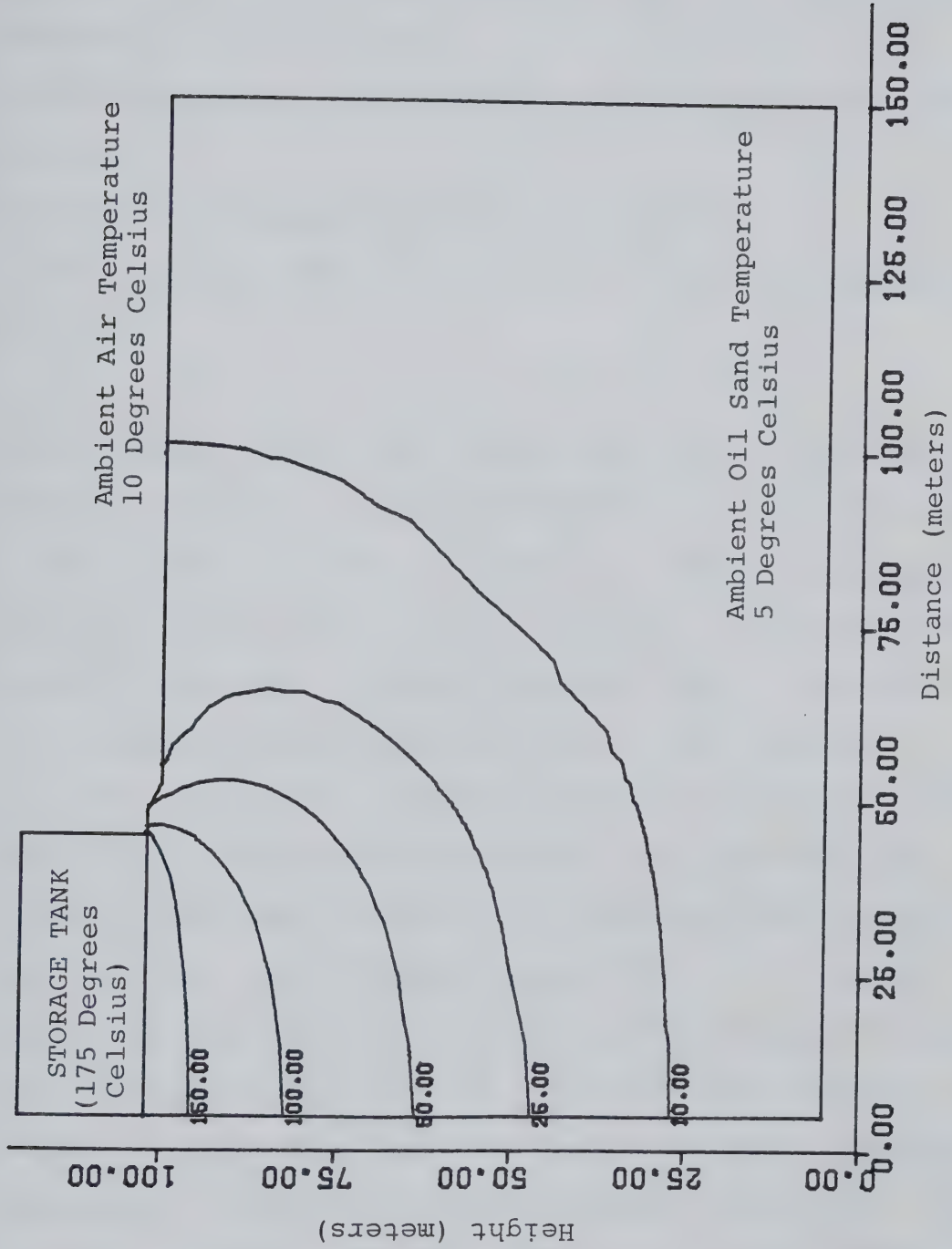


Figure 6.11 Isotherm Plot after 30 Years

formulations include:

- coefficients of thermal volume change for each of the components of the oil sand
- coefficients of compressibility of the components of the oil sand
- dynamic viscosity of the bitumen and water
- unit weight (density) of the bitumen, water and sand grains

These values have been determined experimentally or taken from the literature and are discussed in detail in Appendix A. The step by step operation of *VARTEST5* is summarized graphically in Figure 6.12. The method in which *VARTEST5* couples the heat transfer program (*FEHT2-1*) and the fluid flow program (*ADINAT*) is also shown in the figure.

The fluid flow analysis was performed with a finite element mesh consisting of 209 four-node elements. The mesh (total of 240 nodes) differs from the heat transfer analysis mesh in that the elements comprising the crushed rock foundation pad are neglected (the foundation pad is assumed to be free draining). In the analysis the elements were assumed to be linear, that is, having constant permeability properties in the iteration process. Two-point Gauss numerical integration was employed for the elements. The Euler backward method was the numerical time integration scheme employed in the transient fluid flow analysis. Bathe

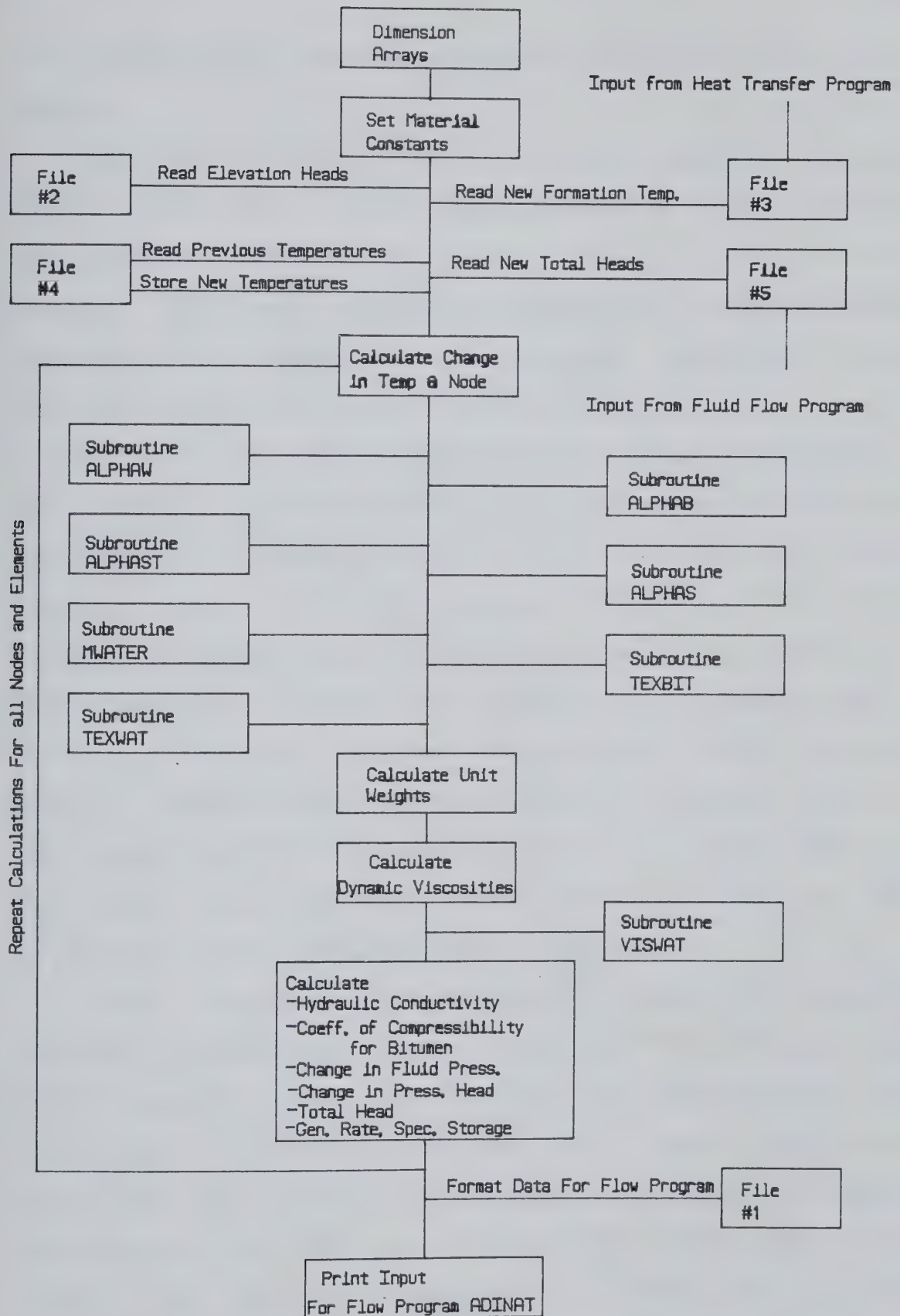


Figure 6.12 Computer Program Vartest5

(1977) derived the governing equations used with the Euler method.

Two natural boundary conditions were assumed. In the first, fluid flow was not permitted normal to the surface represented by the axis of symmetry (center of tank). In the second, the ground surface was taken as a surface of free seepage. Initial conditions were assumed hydrostatic with the water table coinciding with the ground surface.

Under actual field conditions the oil sand mass beneath the heated foundation is experiencing simultaneous heating and drainage. To ideally simulate these conditions the heat transfer and fluid flow program should be executed frequently using a very small time increment. To accomplish this, however, requires an extremely large computational effort at unrealistic expense. To provide an optimal balance between computational cost and analysis accuracy, the oil sand strata below the heated foundation was permitted to heat and drain in one month cycles up to the first year and in one year cycles from one year to 30 years.

A heat and drain cycle begins with the coupling program (VARTEST5) reading the elevation heads for each node in the finite element mesh. The program then receives the new temperature distribution in the oil sand foundation reflecting the propagation of heat from the overlying structure for the time increment used for that particular cycle. The program subsequently reads the previous temperature and total head for each node representing the

distributions at the end of the prior heat and drain cycle. For the first cycle the previous temperature of all nodes is 5 °C and the pressure distribution is hydrostatic. The new temperature distribution is then stored for use in the next heat and drain cycle.

The coupling program then makes a series of calculations which include calculating for each node: the change in temperature; incremental coefficients of thermal expansion for water, bitumen, soil structure and sand grains; coefficient of compressibility of water, bitumen and soil structure; cumulative volume change of water and bitumen at new and previous temperature; unit weight of water and bitumen at new and previous temperature; change in unit weight due to temperature change for water and bitumen; in situ viscosity of bitumen, water and fluid; in situ hydraulic conductivity (permeability); change in pore fluid pressure; change in pressure head; new total head; thermal generation rate; and specific storage coefficient. The program then calculates the hydraulic conductivity, thermal generation rate and specific storage coefficient for each element in the mesh.

The total head, hydraulic conductivity, thermal generation rate and specific storage coefficient distributions are fed into the fluid flow program which determines the total head distribution after the time increment of the cycle. The resulting total head distribution is converted to excess pore pressure.

The results of the analysis are shown in Figures 6.13 through 6.22, expressed in terms of excess pore pressure (pressure exceeding original hydrostatic conditions) with depth at times 0.25, 0.5, 0.75, 1, 5, 10, 15, 20, 25 and 30 years. Figures 6.13 through 6.22 show a *band* of excess pore pressure propagating into the oil sand strata beneath the heated foundation. The shape of these pore pressure bands roughly mimic the shape of the isotherms shown in Figures 6.2 through 6.11. The bands of excess pore pressure in figures 6.13 through 6.22 appear to be symmetrical beneath the tank (diameter of 40 meters) with a region of high pore pressure in the center bounded by closely spaced lines of equal pore pressure. The center of the excess pore pressure bands represent zones of oil sand where drainage is slow and the temperature increase is causing pore fluid pressure increases. Above the center of the bands the viscosity of the bitumen is sufficiently low enough to make it mobile and to permit drainage to occur.

The presence of two thin regions in which the pressure gradients are extremely high may be accounted for in the following manner. The high pressure gradient above the bands is due in part to the initial rapid change of hydraulic conductivity of oil sand with temperature. Referring to Figure A.8 in Appendix A, it is observed that the hydraulic conductivity of oil sand changes by over 3 orders of magnitude over the temperature range of 5 °C to 25 °C. Below the center of the bands of high pore pressure the high

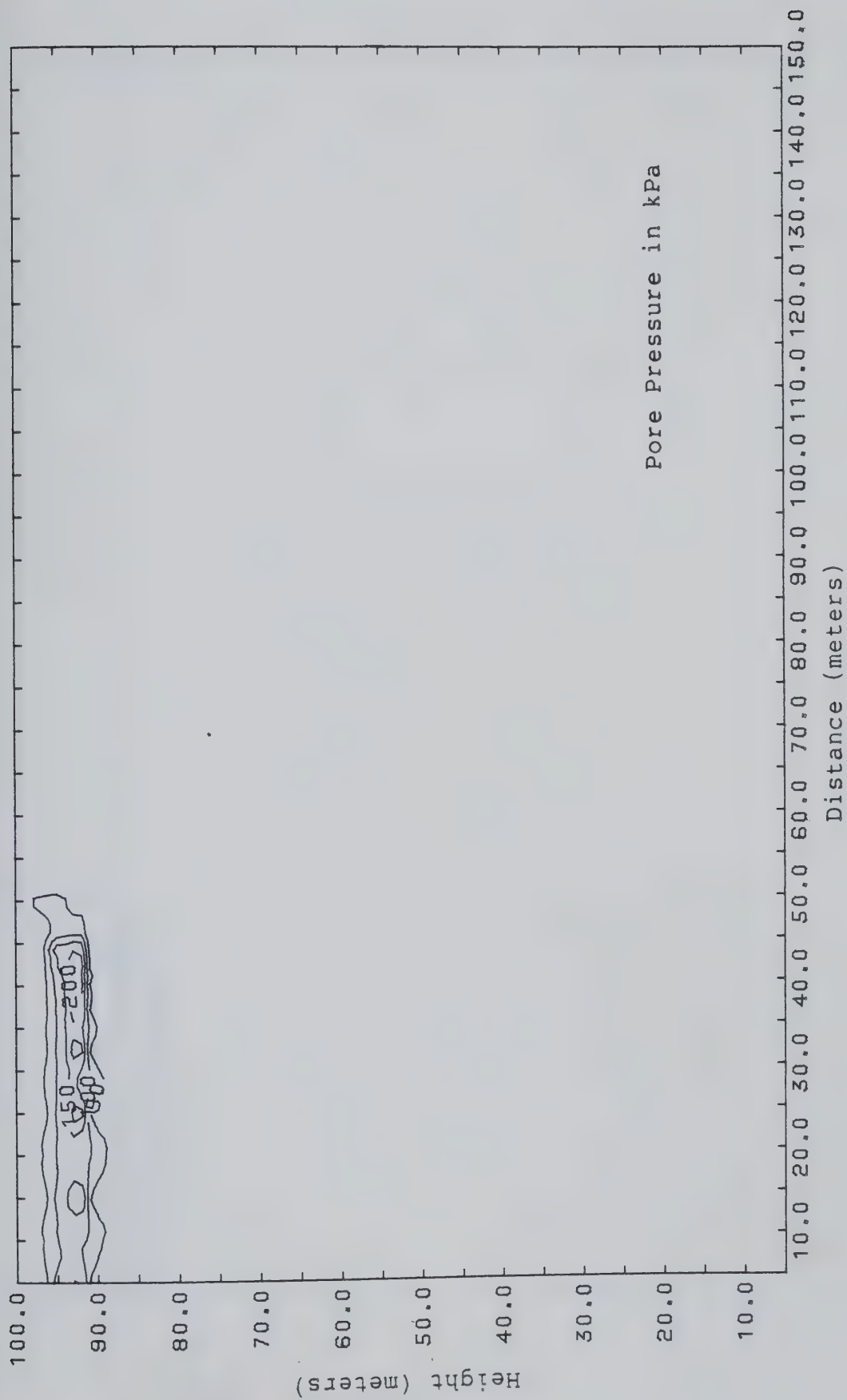


Figure 6.13 Excess Pore Pressure after 3 Months

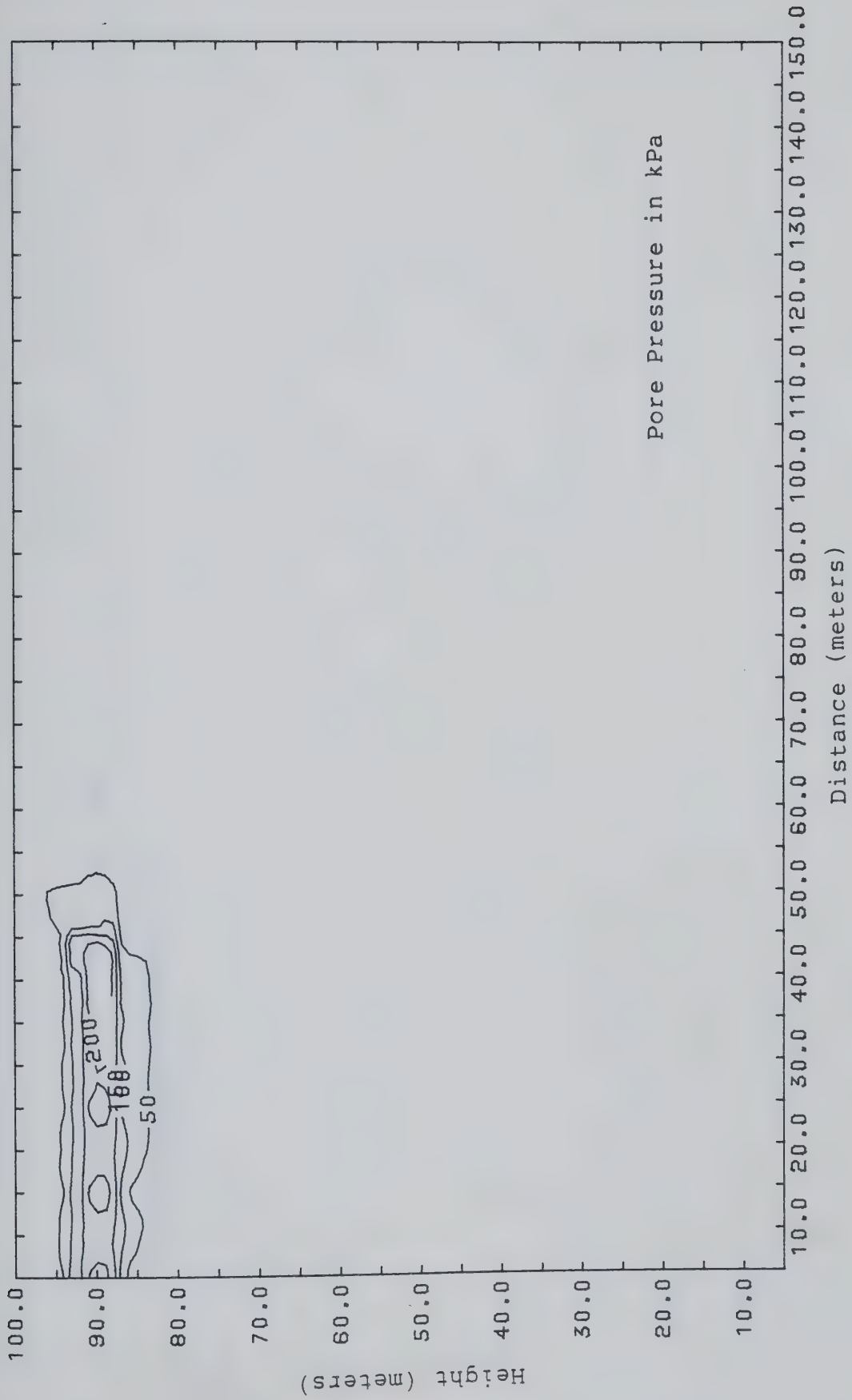


Figure 6.14 Excess Pore Pressure after 6 Months

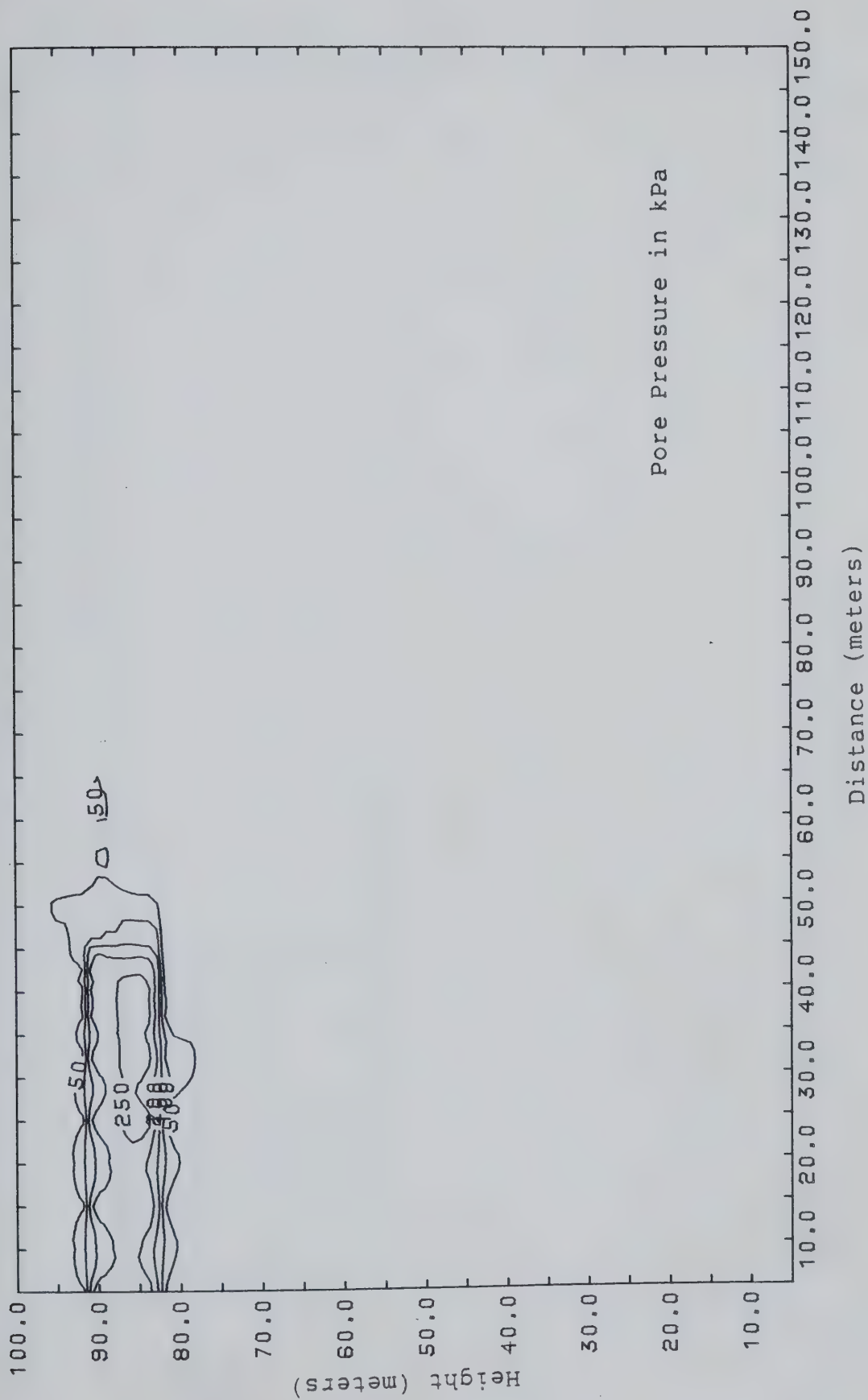


Figure 6.15 Excess Pore Pressure after 9 Months

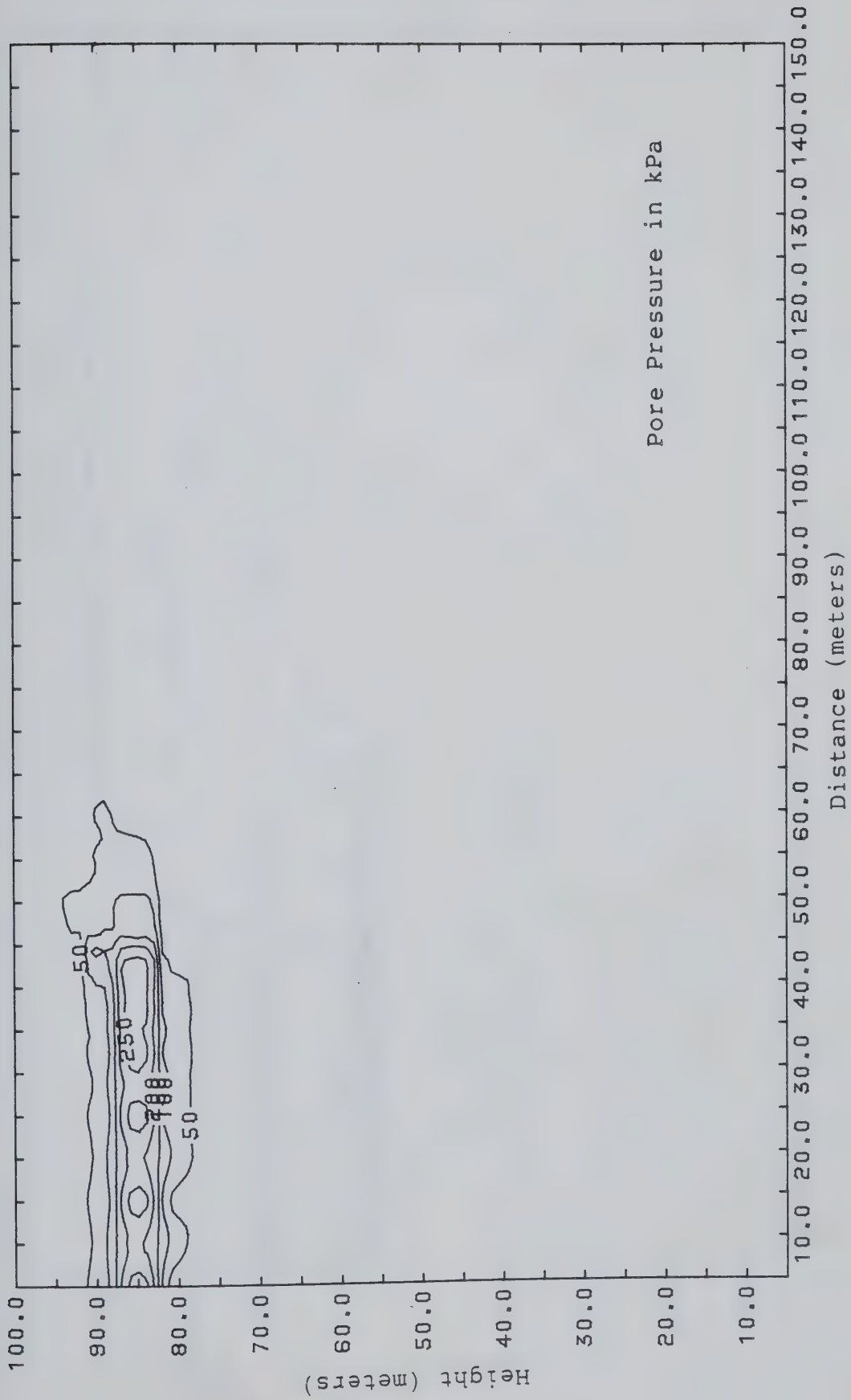


Figure 6.16 Excess Pore Pressure after 1 Year

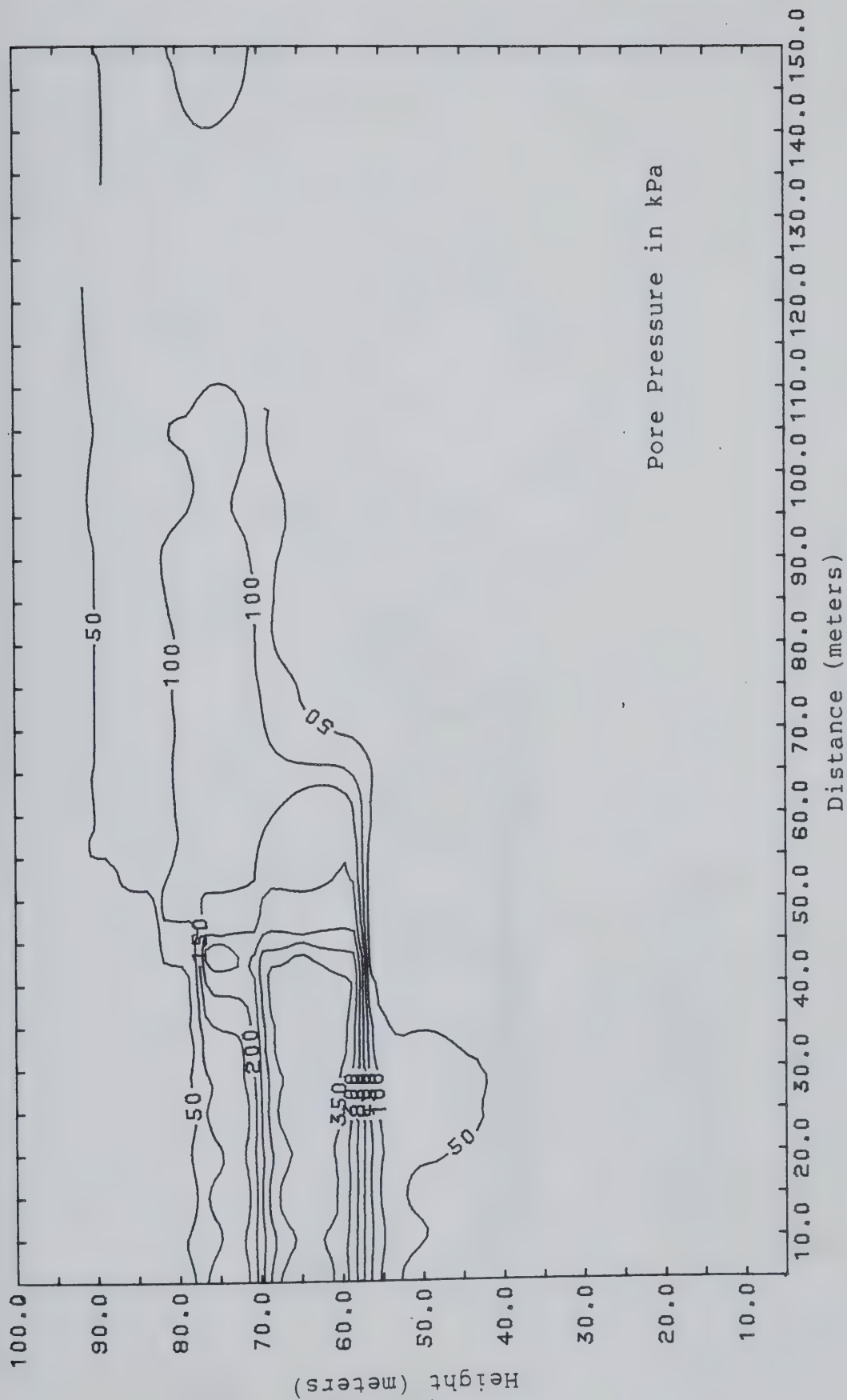


Figure 6.17 Excess Pore Pressure after 5 Years

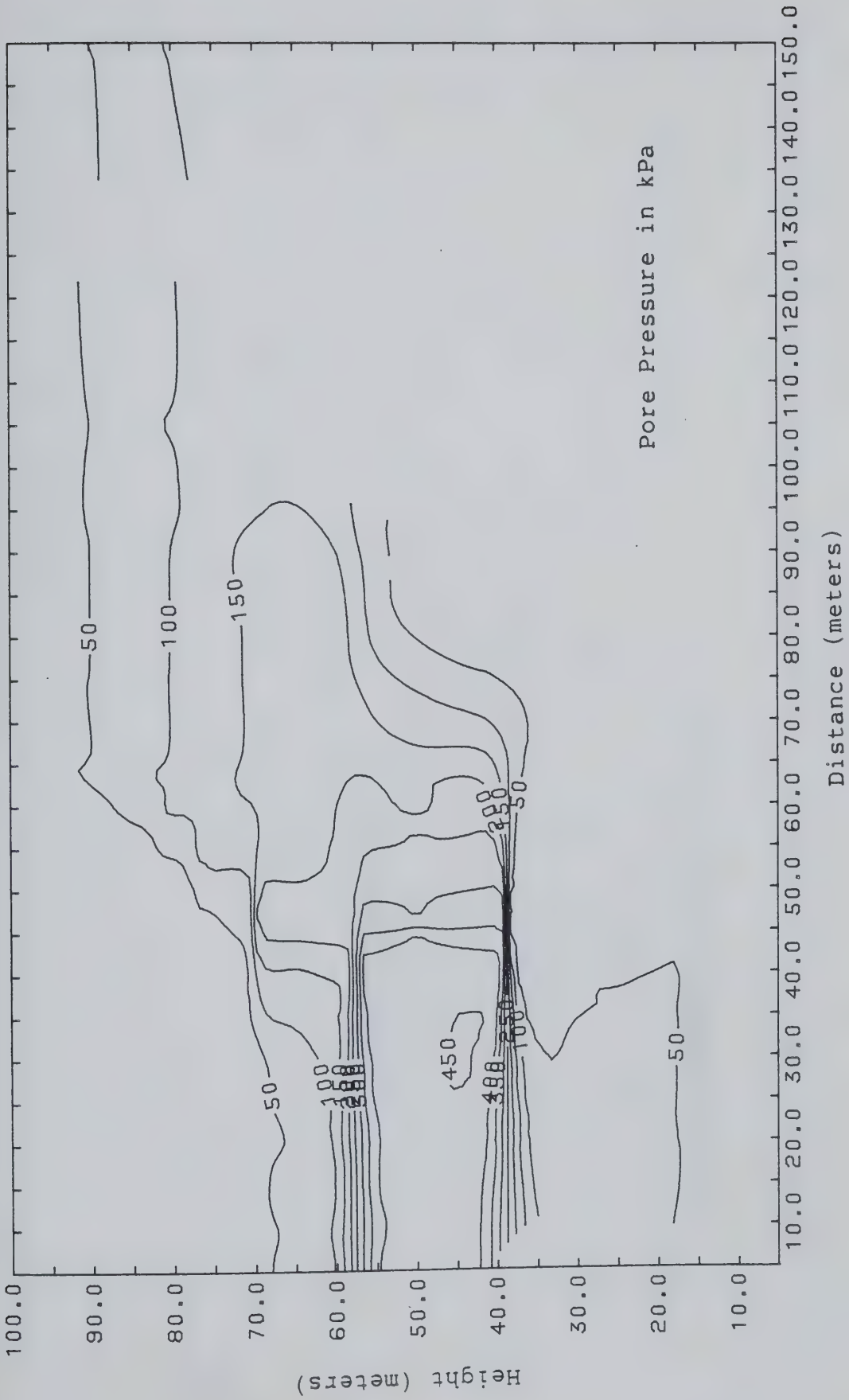


Figure 6.18 Excess Pore Pressure after 10 Years

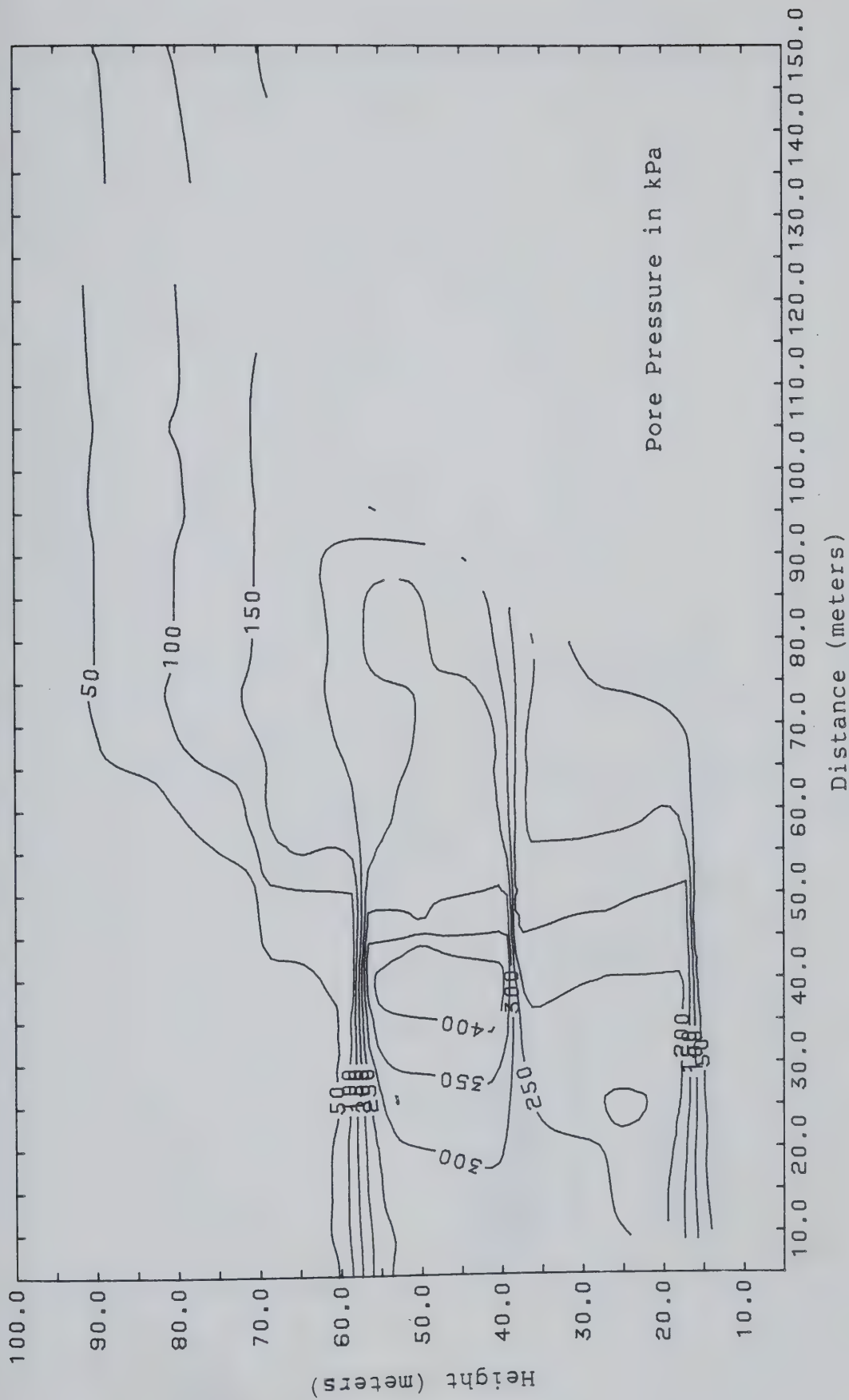


Figure 6.19 Excess Pore Pressure after 15 Years

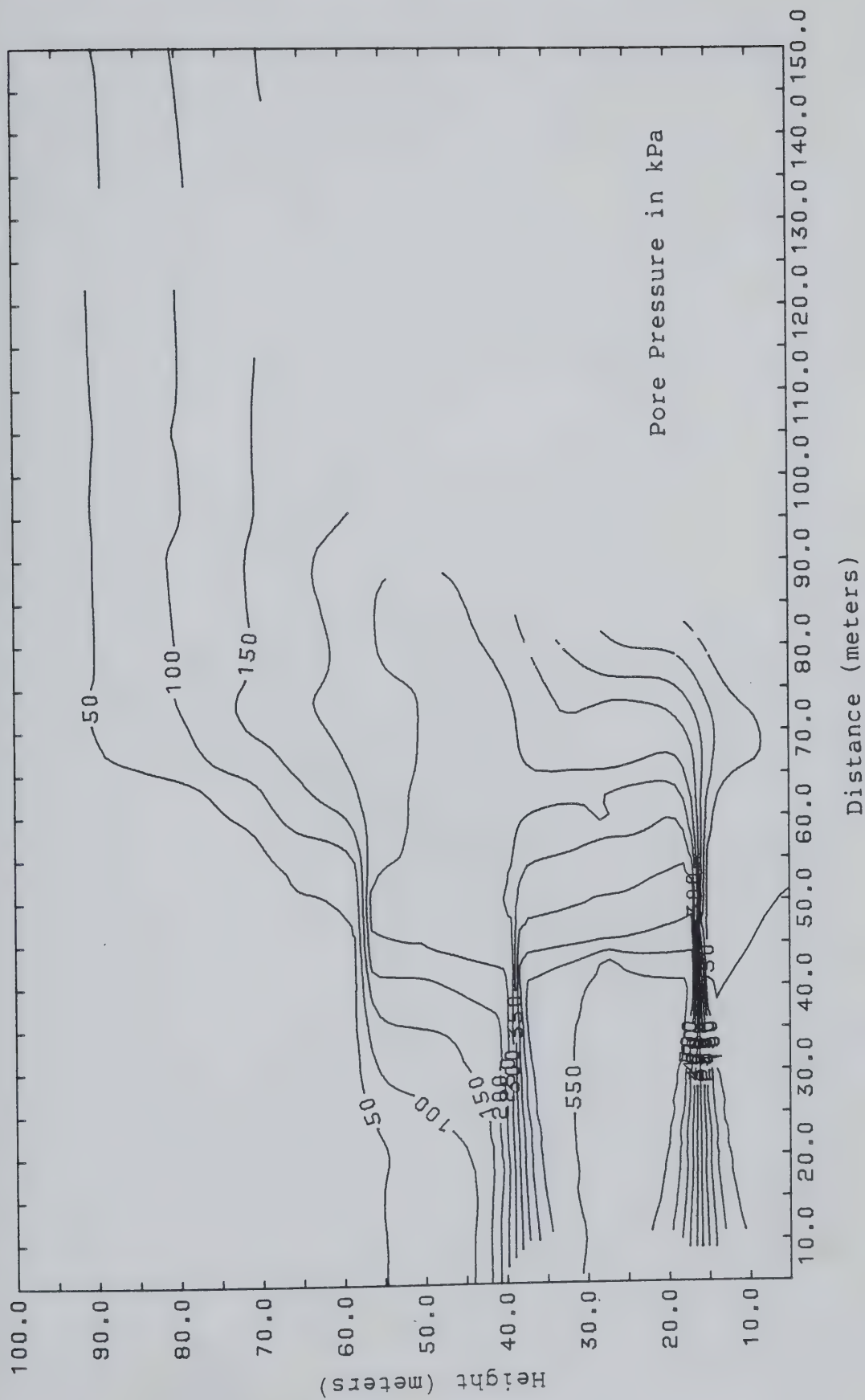


Figure 6.20 Excess Pore Pressure after 20 Years

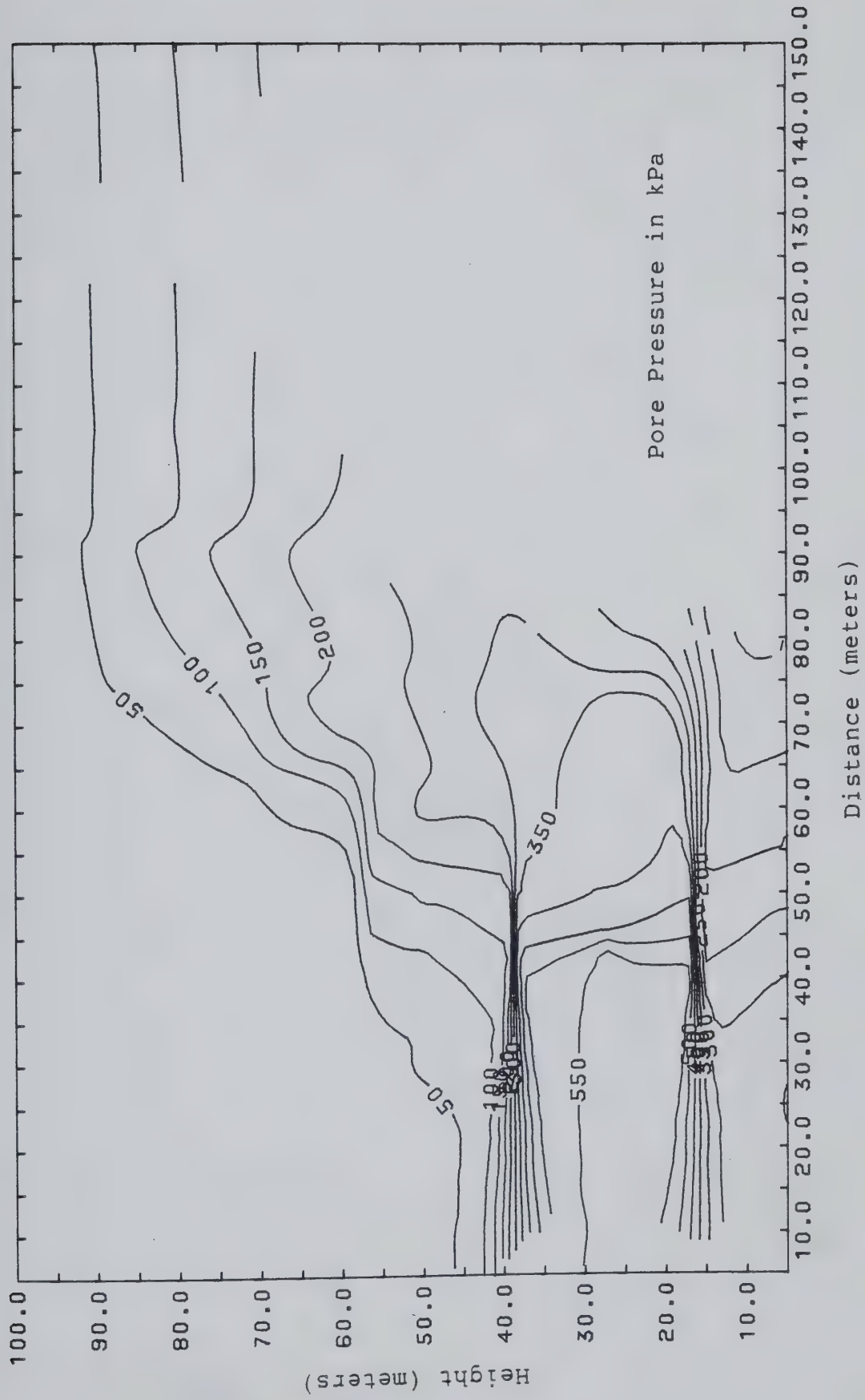


Figure 6.21 Excess Pore Pressure after 25 Years

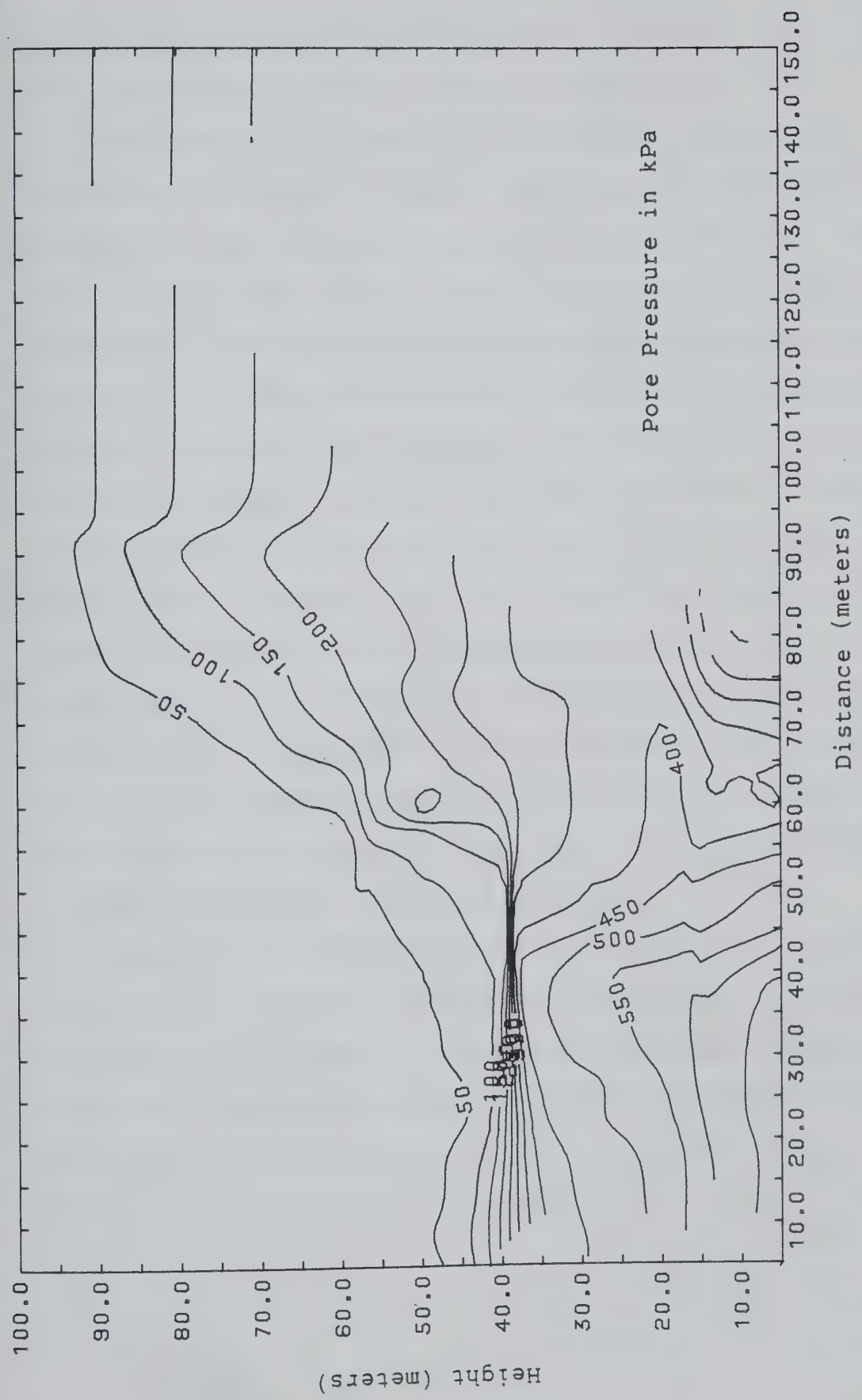


Figure 6.22 Excess Pore Pressure after 30 Years

pressure gradients reflect the sensitivity of the thermal pore pressure generation term with temperature.

The excess pore pressure distribution with time show significant drainage of the oil sand mass is occurring. Even during the time interval of one to 30 years when the length of the heat and drain cycles are large (resulting in significant amounts of pore pressure being generated due to heating) a large porportion of the oil sand strata beneath the tank is almost fully drained. After 5 years the oil sand beneath the heated foundation is fully drained to a depth of over 20 meters and after 30 years to a depth exceeding 50 meters (tank center). If the time of the heat and drain cycles were reduced to the one month increment used for the first year, the porportion of the oil sand mass which is drained would be expected to be even greater. The results of the analysis indicate that although the rate of pore fluid flow is slower than that of heat flow, it is sufficient to provide a significant amount of drainage.

Figures 6.13 through 6.22 also show that the bands of excess pore pressure in the oil sand strata are generally horizontal with respect to the base of the tank (diameter of 40 meters). This would appear to indicate the heaving due to excess pore fluid pressure is fairly uniform and severe differential heave is not occurring.

6.4 Volume Change

Volume changes occurring in the oil sand strata was assumed to produce only vertical movement (heave) beneath the heated structure (Chapter 4). The magnitude of heave was calculated by considering volume changes resulting from volume change of pore fluid in response to relief of pore fluid pressure which exceeds the total vertical confining stress (weight of structure and overlying sediment) and thermal volume change of the sand grains and soil structure.

The pore fluid pressure distribution was calculated twice for each increment of time, after the heating cycle and after the draining cycle. During the heating cycle the pore fluid pressure response was determined assuming undrained conditions with no volume change using equation 3.24. The pore fluid pressure distribution during the drainage cycle was predicted by the fluid flow analysis. In either case, if the pore fluid pressure exceeded the total vertical confining pressure the strata was permitted to expand such that the pore fluid pressure balanced the total stress. This volumetric expansion was converted to heave by assuming no lateral strain. If during subsequent time increments, zones of pore fluid pressure exceeding the total

 'An inconsistency is apparent since calculation of pore fluid pressure from equation 3.24 ignores the volume change due to the thermal expansion of sand grains and soil structure. This error, however, is slight since the thermal volume change of sand grains and soil structure is relatively small (less than 1% at 175 °C, Figure 5.11) and thus the bitumen and water porosities (ratio of volume of bitumen or water to volume of oil sand mass) in equation 3.24 would change only slightly.

vertical confining stress became sufficiently permeable to permit full drainage of pore fluid, the heave associated with this zone of pore pressure was neglected (i.e., the soil structure was allowed to collapse). In other words, the heave associated with pore fluid pressure relief was determined incrementally with each heating and draining cycle. A plot of heave beneath the heated tank resulting from pore fluid pressure relief is shown in Figure 6.23.

Figure 6.23 indicates that heave resulting from pore fluid pressure relief is sensitive to the time increment employed in the analysis. For the first year when the heat and drain cycles were limited to one month, a maximum heave in the order of 0.7 cm (tank center) was observed at 3 months and steadily decreased with time to one year. However, when the heat and drain cycles were increased to one year a heave of about 3 cm (tank center) was found after 5 years and decreased with time to approximately 0.1 cm after 30 years. This dependence on the time increment is due almost entirely to the amount of pore fluid pressure calculated during the heating portion of the heat and drain cycle. Examination of equation 3.24 indicates that the pore fluid pressure change, Δu , is dependent on the temperature change, ΔT . During the one year time increment the temperature change is much greater than for a one month time increment and, as a result, significantly more pore fluid pressure is generated. One would expect if the time increment was held constant throughout the analysis at one

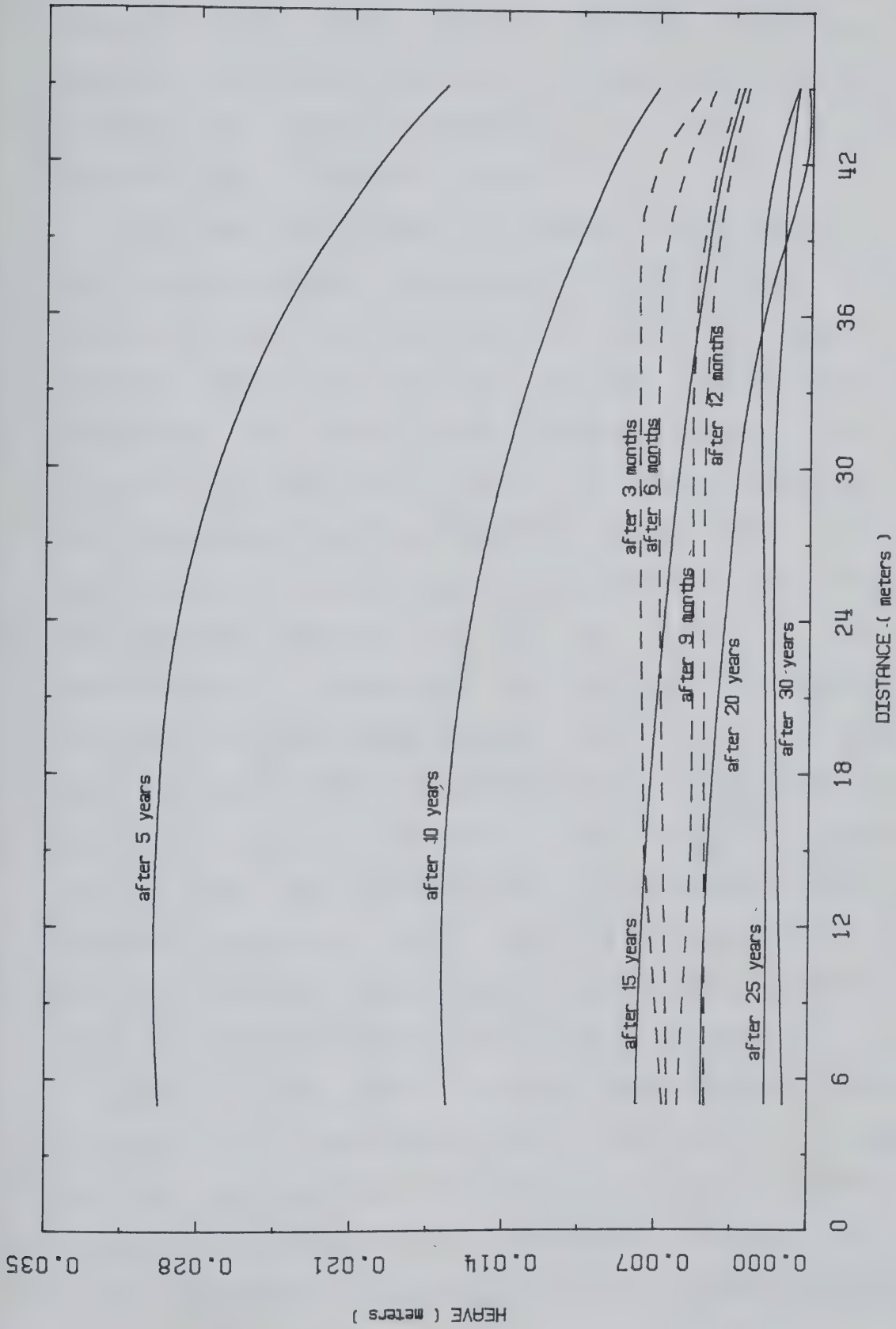


Figure 6.23 Heave Beneath Tank Due to Pore Fluid Pressure

month, the amount of heave resulting from pore fluid pressure relief would decline steadily throughout the analysis. The maximum differential heave resulting from pore fluid pressure relief was found to be about 1.4 cm and occurred after 5 years of heating.

The heave associated with thermal volume change of the sand grains and soil structure with time is shown in Figure 6.24. A maximum heave of about 35 cm (tank center) was observed after 30 years of heating. Unlike the heave associated with pore fluid pressure relief, the heave increases at any point under the tank progressively with time and appears far less dependent on the time increment. This is because the thermal volume change of sand grains and soil structure depends only on the volume of oil sand experiencing a temperature increase and is independent of the amount of pore fluid drainage occurring. It is apparent that the heave associated with thermal volume change of the sand grains and soil structure is one order of magnitude greater than that due to pore fluid pressure relief. The maximum differential heave resulting from thermal volume change of the sand grains and soil structure was found to be about 14 cm and occurred after 30 years of heating.

Figure 6.25 shows the total heave beneath the heated foundation with time. Comparison of this plot with Figures 6.23 and 6.24 shows the vast majority of heave is due to the thermal volume change of the sand grains and soil structure. A maximum differential heave of 14 cm was observed after 30

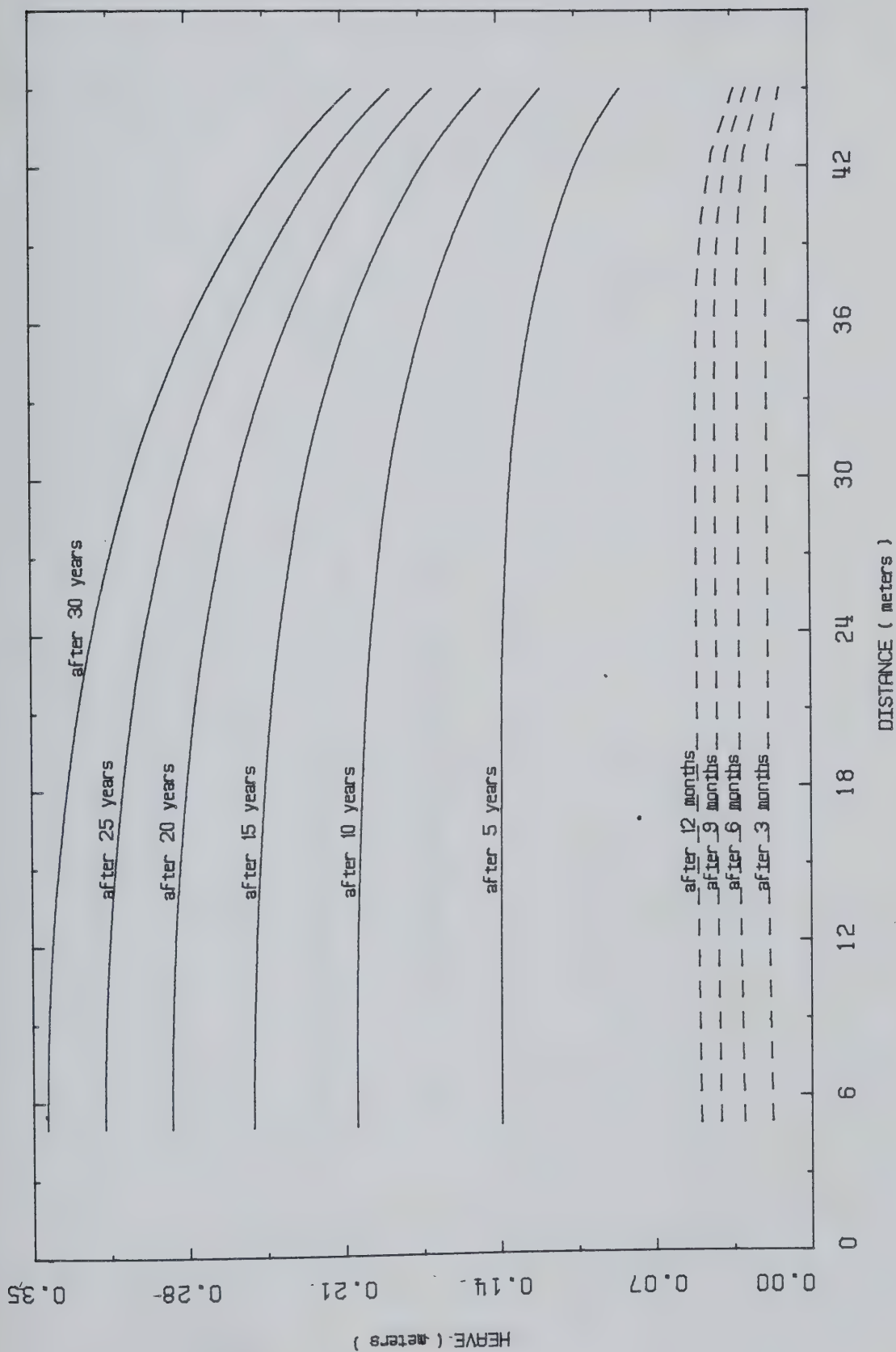


Figure 6.24 Heave Beneath Tank Due to Thermal Volume Change of Sand Grains and Soil Structure

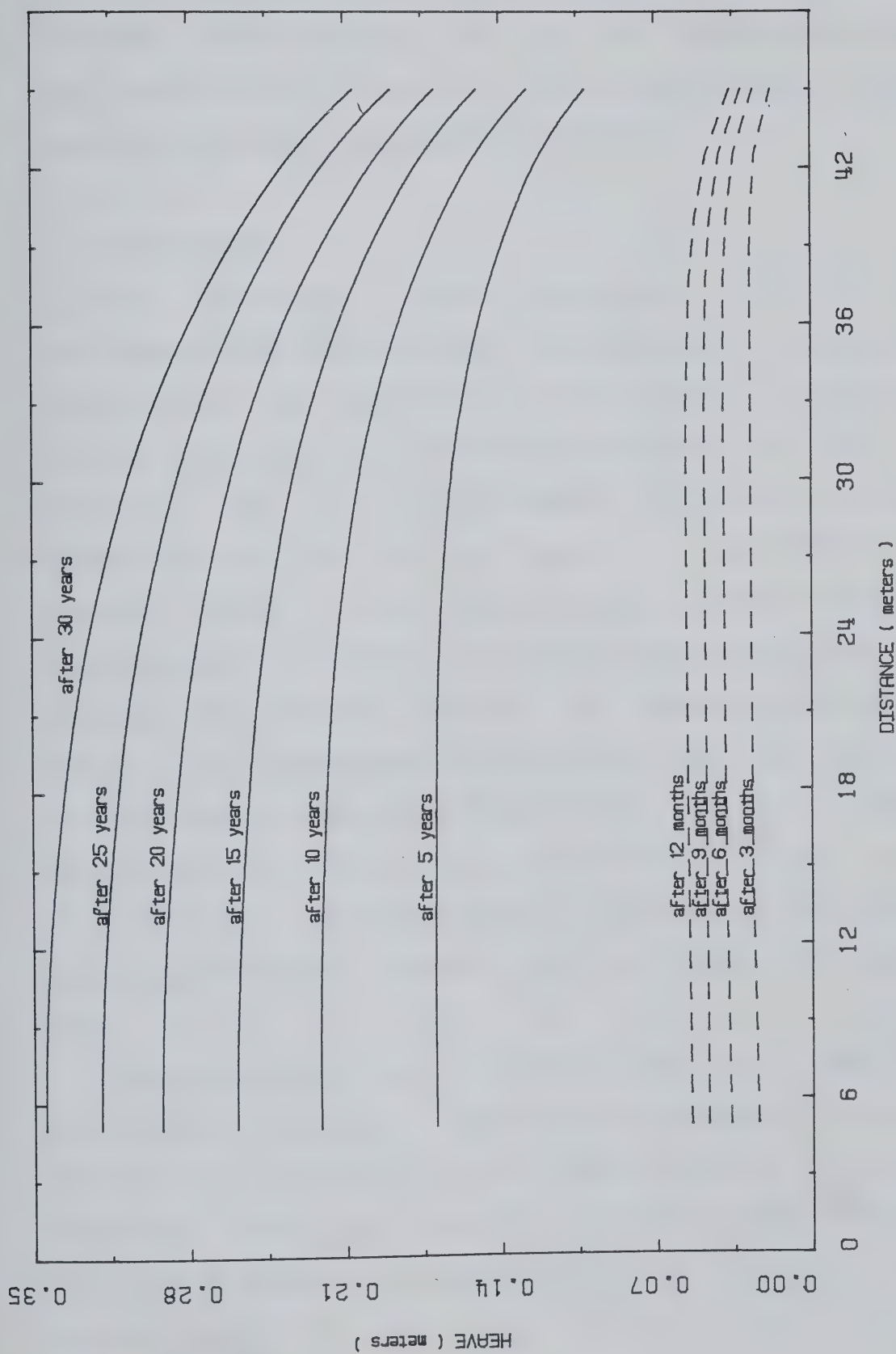


Figure 6.25 Total Heave Beneath Tank

years of heating. This indicates pore fluid pressure developed during heating of the oil sand strata drains sufficiently quickly enough to negate large volume changes associated with the undrained condition.

6.5 Conclusions

The analytical model presented in this study investigated the effect of heat flow from an 80 m diameter storage tank on underlying oil sand strata. The tank was assumed to rest on a conventional crushed rock and sand foundation pad, 2 m in thickness, and held at a constant temperature of 175 °C. The results of the theoretical analysis showed a band of excess pore pressure (pressure exceeding original hydrostatic conditions) propagating into the oil sand strata beneath the heated foundation. The center of the excess pore pressure bands represent zones of oil sand where drainage is slow and the temperature increase is causing pore fluid pressure increases. Above the center of the bands the viscosity of the bitumen is sufficiently low enough to make it mobile and to permit drainage to occur.

The excess pore pressure distribution with time show significant drainage of the oil sand mass is occurring. After 5 years of heating the oil sand beneath the heated foundation is fully drained to a depth of over 20 meters, and after 30 years to a depth exceeding 50 meters (tank center).

The bands of excess pore pressure in the oil sand strata are generally horizontal with respect to the base of the tank indicating the heaving due to excess pore fluid pressure is fairly uniform and severe differential heave is not occurring.

The results of the analysis indicate that although the rate of pore fluid flow is slower than that of heat flow, it is sufficient to provide a significant amount of drainage.

Volume changes occurring in the oil sand strata was assumed to produce vertical movement (heave) beneath the heated structure. The magnitude of heave was calculated by considering volume changes resulting from volume change of pore fluid in response to relief of pore fluid pressure which exceeds the total vertical confining stress (weight of structure and overlying sediment) and thermal volume change of the sand grains and soil structure.

The heave resulting from pore fluid pressure relief was found sensitive to the time increment employed in the analysis. For the first year when the heat and drain cycles were limited to one month, a heave in the order of 0.7 cm (tank center) was observed at 3 months and steadily decreased with time to one year. When the heat and drain cycles were increased to one year, a heave of about 3 cm (tank center) was found after 5 years and decreased with time to approximately 0.1 cm after 30 years. This dependence on the time increment is due almost entirely to the amount of pore fluid pressure generated during the heating portion

of the heat and drain cycle. If the time increment was held constant throughout the analysis at one month, the amount of heave resulting from pore fluid pressure relief would decline steadily throughout the analysis. The maximum differential heave resulting from pore fluid pressure relief was found to be about 1.4 cm and occurred after 5 years of heating.

The heave associated with thermal volume change of the sand grains and soil structure with time showed a maximum heave of about 35 cm (tank center) occurred after 30 years of heating. Unlike the heave associated with pore fluid pressure relief, the heave increases at any point under the tank progressively with time and is far less dependent on the time increment. The heave associated with thermal volume change of sand grains and soil structure is one order of magnitude greater than that due to pore fluid pressure relief. The maximum differential heave resulting from thermal volume change of the sand grains and soil structure was found to be approximately 14 cm and occurred after 30 years of heating.

When considering the total heave beneath the heated foundation with time, the vast majority of heave is due to the thermal volume change of the sand grains and soil structure. A maximum differential heave of 14 cm was found after 30 years of heating. This indicates pore fluid pressure generated during heating of the oil sand strata drains fast enough to negate large volume changes associated

with the undrained condition.

The theoretical analyses used in this study did not include the influence of gas exsolution. The amount of gas driven out of solution from the fluid phase of oil sand is dependent on the kind and amount of gas in solution, the increase in temperature and the pore fluid pressure. The amount of gas initially in solution in the fluid phase of the oil sand is dependent on the initial pore pressure. Since hydrostatic pore pressure conditions initially exist in the surface mineable area little gas is expected to be in solution near the ground surface but the amount increases progressively with depth. The increase in total stress exerted by the weight of the structure and foundation pad reduces the pore volume increase from an increase in temperature and therefore has a significant effect on the amount of gas driven from solution. Since the propagation of heat from the structure is extremely slow when compared to that experienced in the laboratory, it would be difficult to experimentally assess the amount of gas drainage which would occur under actual field conditions. The permeability of oil sand to gas would also be difficult to assess but may be significant. It would appear that some amount of volume change due to gas exsolution could be expected to contribute to heaving beneath the heated structure, the amount of which would be difficult to determine. Since the isotherms beneath the tank were shown to be somewhat horizontal the contribution to differential heave may not prove to be of

major concern. For the above reasons, it was decided to not include gas exsolution in this first analysis of the performance of heated foundations on oil sand.

Variations in stratigraphy beneath the heated structure may have a significant influence on the amount of heave which occurs. A simplified stratigraphy consisting of a thin till layer overlying rich oil sand was assumed for this study. This stratigraphy was selected because rich oil sand which contains a large percentage of bitumen has an extremely low permeability under formation temperatures and therefore when subjected to an increase in temperature would generate large amounts of pore pressures and possibly represent a worse case. It was of concern to assess the rate at which these high pore pressures would dissipate. The results of the analyses shows a significant portion of this pore fluid pressure was dissipating and the heave associated with pore fluid volume increase was not significant.

Should clay shale layers be present in the oil sand, drainage would initially be impeded, however, the permeability of the clay shale layer would possibly increase dramatically through fracturing due to thermal volume changes of the underlying oil sand. In contrast, the presence of lean or bitumen free sand would significantly improve the hydraulic conductivity of the strata since the dynamic viscosity of water is much lower than that of bitumen. In addition, the amount of pore fluid pressure generated in lean oil sand would be less than for rich oil

sand.

Complex stratigraphy such as discontinuous layers adversely affect the amount of differential heave which would occur and would have to be modelled for the specific conditions.

7. SUMMARY AND CONCLUSIONS

7.1 Summary

The extraction and upgrading of bitumen at surface mining projects may require the construction of heat generating structures above oil sand strata. To date, the design procedure adopted involves limiting the temperature in the oil sand beneath the structure to 45 °C. The design criteria was based on undrained triaxial testing of disturbed oil sand over the temperature range of room temperature to 90 °C. For structures generating large amounts of heat, such as heated bitumen storage tanks, the design criteria results in very complex and expensive foundation pads utilizing ventilation systems.

The purpose of this study was to provide a better understanding of the geotechnical behavior of oil sands under conditions that develop after the placement of heated structures on oil sand and to provide a rational basis of design for foundation pads for these structures.

The analytical concepts presented in this study provide the rationale to assess the influence of heat on oil sand (thermal volume change and pore fluid pressure response), rate of heat flow and rate and extent of fluid flow (or drainage). These concepts give the basis for the theoretical analysis of the geotechnical behavior of oil sand underlying heated foundations. The theoretical analysis serves to couple heat flow theory to the fluid flow expression to

determine whether the oil sand mass will be fully drained, fully undrained, or partially drained. If partial drainage occurs, the pore fluid pressure change and volume change can be calculated. The theoretical analysis can be further refined by considering the influence of gas exsolution and pore fluid vaporization or distillation and by considering the three dimensional case.

The material properties required for the analyses are coefficients of thermal volume change and the coefficients of compressibility for each of the components of oil sand, heat flow parameters, as well as the dynamic viscosity of the bitumen and water and the density of bitumen, water and sand grains. These values have been determined experimentally or taken from the literature.

The analytical model presented in this study investigated the effect of heat flow from an 80 m diameter storage tank on underlying oil sand strata. The tank was assumed to rest on a conventional crushed rock and sand foundation pad, 2 m in thickness, and held at a constant temperature of 175 °C. The general stratigraphy chosen consisted of the granular pad on top of 3 m of till overlying oil sand.

The results found in this study are based on a specific stratigraphy and measured properties for one oil sand. If different stratigraphy and properties of oil sand, such as significant gas exsolution, exist then those particular conditions would have to be modelled.

7.2 Conclusions

The results of this study showed that when examining the foundation performance beneath a heated structure, heave and differential heave is the sole factor affecting the foundation performance of the oil sand. The possibility of shear failure and lateral movement of the oil sand and structure are extremely remote. Settlement of the structure does not take place even under successive heating and cooling cycles.

An expression was developed to calculate the net volume change of an oil sand mass subjected to a change in temperature under fully drained conditions. The volume change of the oil sand mass arises from the thermal expansion of the individual sand grains and structural changes in the sand skeleton.

An equation which allows the volume change of oil sand subjected to increases in temperatures under completely undrained conditions to be calculated was presented. The volume change of the oil sand mass is due to expansion of the individual sand grains and pore fluids as well as structural changes in the sand skeleton.

An expression was derived which expresses the volume of pore fluid which would drain from a fully saturated oil sand mass experiencing a change in temperature. The amount of fluid expelled from an oil sand mass during a drained thermal expansion test is the sum of the volume change of the pore fluids less the change in void volume and

structural volume changes.

An expression was developed to calculate the increase in pore fluid pressure in a fully saturated oil sand mass subjected to a temperature change under fully undrained conditions.

The theoretical expressions to evaluate the rate of fluid from heating were derived and are presented. The method utilized to solve the governing differential fluid flow equation for two dimensional transient fluid flow beneath a heated foundation using the finite element technique is described.

The theoretical formulations to determine the rate of heat flow were derived and are presented. The solution to the heat equation for two dimensional transient heat flow beneath a heated foundation utilizing the finite difference technique is illustrated.

The expressions developed in this study provide a method to analyze the rate at which heat flows through an oil sands mass, the rate at which excess pore fluid pressure resulting from an increase in temperature dissipates, and the amount of volume change which occurs.

Equipment was successfully designed and constructed with the capability to explore the one-dimensional thermal expansion of oil sands and its constituent components to temperatures approaching 200 °C and pressures in excess of 3.5 MPa. A brief summary of each constituent of the equipment is presented.

The test procedures which were developed for use in the laboratory program worked successfully and are described. The method utilized to prepare oil sand samples from frozen core resulted in very high quality test specimens. The procedure adopted is illustrated.

Thermal expansion tests performed on water resulted in volume increases of about 15 per cent at 200 °C. The thermal volume change of water did not vary significantly for the pressure levels employed. Excellent agreement between experimental and published data indicates the pressure cell employed was calibrated and operating properly.

Thermal expansion experiments carried out on hot water extracted bitumen resulted in volume increases of about 15 per cent at 200 °C. The test results indicate that the cumulative volume change of bitumen over the temperature range considered is not pressure dependent. The volume change of this dead bitumen is more linear with temperature than that of water.

For each thermal expansion test conducted on compacted tailing sand, a negative volume change was observed for the first heating increment (room temperature to 50 °C). The loosest sand sample (initial density of 1.46 Mg/m³ at room temperature) gave the greatest volume decrease (0.36%) over this temperature range. The sample initially compacted to a density of 1.62 Mg/m³ at room temperature showed a volume decrease of 0.08% over the temperature range from room temperature to 50 °C. After heating to 200 °C, this sample

was cooled to room temperature and a volume decrease of 0.10% was measured indicating that the volume decrease was due to a compaction of the soil structure. Relative movement or reorientation of sand grains must have occurred during the temperature increase to 50 °C to allow an overall volume decrease. Over the temperature range of 50 to 200 °C all samples tested displayed a volume increase roughly paralling that of a quartz crystal, indicating the soil structure achieved a tight packing arrangement at 50 °C and the subsequent volume increase with temperature results only from the thermal expansion of the individual grains.

Undrained heating of oil sand to 200 °C will result in a volume increase of about 6 percent. Most of this increase, over 5 percent, is due to the pore fluids, water and bitumen, with the bitumen expanding slightly more than water. The remainder of the volume increase is due to the thermal expansion of the sand grains. The dense, impenetrative structure of in situ oil sand will show a negligible amount of thermal volume change by itself.

From the tests performed on oil sand the thermal volume increase appears to be independent of the effective confining pressure for the pressure range considered in this study. For the oil sand tested here, significant thermal volume increases would be expected under back pressures below 2000 kPa because of gas exsolution at temperatures above 180 °C.

Results obtained from the undrained and drained thermal expansion tests performed on oil sand were used to generate a plot representative of the thermal expansion of in situ bitumen. The results indicate that in situ gas saturated bitumen may show temperature volume increases 50% greater than the extracted gas free bitumen.

The results of the theoretical analysis showed a band of excess pore pressure (pressure exceeding original hydrostatic conditions) propagating into the oil sand strata beneath the heated foundation. The center of the excess pore pressure bands represent zones of oil sand where drainage is slow and the temperature increase is causing pore fluid pressure increases. Above the center of the bands the viscosity of the bitumen is sufficiently low enough to make it mobile and to permit drainage to occur.

The excess pore pressure distribution with time show significant drainage of the oil sand mass is occurring. After 5 years of heating the oil sand beneath the heated foundation is fully drained to a depth of over 20 meters, and after 30 years to a depth exceeding 50 meters (tank center).

The bands of excess pore pressure in the oil sand strata are generally horizontal with respect to the base of the tank indicating the heaving due to excess pore fluid pressure is fairly uniform and severe differential heave is not occurring.

The results of the analysis indicate that although the rate of pore fluid flow is slower than that of heat flow, it is sufficient to provide a significant amount of drainage.

Volume changes occurring in the oil sand strata was assumed to produce vertical movement (heave) beneath the heated structure. The magnitude of heave was calculated by considering volume changes resulting from volume change of pore fluid in response to relief of pore fluid pressure which exceeds the total vertical confining stress (weight of structure and overlying sediment) and thermal volume change of the sand grains and soil structure.

The heave resulting from pore fluid pressure relief was found sensitive to the time increment employed in the analysis. For the first year when the heat and drain cycles were limited to one month, a heave in the order of 0.7 cm (tank center) was observed at 3 months and steadily decreased with time to one year. When the heat and drain cycles were increased to one year, a heave of about 3 cm (tank center) was found after 5 years and decreased with time to approximately 0.1 cm after 30 years. This dependence on the time increment is due almost entirely to the amount of pore fluid pressure generated during the heating portion of the heat and drain cycle. If the time increment was held constant throughout the analysis at one month, the amount of heave resulting from pore fluid pressure relief would decline steadily throughout the analysis. The maximum differential heave resulting from pore fluid pressure relief

was found to be about 1.4 cm and occurred after 5 years of heating.

The heave associated with thermal volume change of the sand grains and soil structure with time showed a maximum heave of about 35 cm (tank center) occurred after 30 years of heating. Unlike the heave associated with pore fluid pressure relief, the heave increases at any point under the tank progressively with time and is far less dependent on the time increment. The heave associated with thermal volume change of sand grains and soil structure is one order of magnitude greater than that due to pore fluid pressure relief. The maximum differential heave resulting from thermal volume change of the sand grains and soil structure was found to be approximately 14 cm and occurred after 30 years of heating.

When considering the total heave beneath the heated foundation with time, the vast majority of heave is due to the thermal volume change of the sand grains and soil structure. A maximum differential heave of 14 cm was found after 30 years of heating. This indicates pore fluid pressure generated during heating of the oil sand strata drains fast enough to negate large volume changes associated with the undrained condition.

The results of the study showed significant drainage of the oil sand mass was occurring and that the vast majority of vertical surface movement or heave was due to the thermal expansion of the sand grains and soil structure. The amount

of differential heave predicted from the theoretical analysis appears manageable when incorporated into a structural design of a storage tank.

7.3 Recommendations for Future Work

The oil sand used in the experimental testing was obtained from core samples taken from an oil sand outcrop at Saline Creek, approximately 1 km south of Fort McMurray. It is apparent that the stresses in this outcrop of oil sand have been reduced at a very slow rate during geologic time and therefore, significant portion of the gas initially present in the oil sand has drained. When considering the design of a heated structure on oil sand, testing of the oil sand should be conducted on a site specific basis to determine if similar amount of gas drainage has occurred. It is possible with the apparatus used in this testing program to monitor and sample gases from oil sand tested at high temperatures.

Experimental testing should be undertaken to provide a better understanding of the heat flow properties of oil sand and to measure the change in hydraulic conductivity of oil sand with temperature.

Should strata other than oil sand be present in the foundation beneath the heated structure, similar testing on these soils should be conducted.

The theoretical analysis used in this study can be further refined by considering the influence of gas

exsolution and pore fluid vapourization or distillation and by considering the three dimensional case. The influence of closely spaced heated structures should also be investigated.

BIBLIOGRAPHY

- Agar, J.G., 1982. Personnel communication. University of Alberta
- Alsands Project Group, 1978. *Application to the Alberta Energy Resources Conservation Board for an Oil Sands Mining Project.*
- American Society for Metals, 1978. *Metals Handbook*. Prepared under the direction of the ASM Handbook Committee, 9th ed., Metals Park, Ohio.
- American Society for Testing Materials, 1975. *Proceedures for Testing Soils*. (D 2049-69).
- Bathe, K.J., 1977. *ADINAT - A Finite Element Program for Automatic Dynamic Incremental Nonlinear Analysis of Temperatures*. AVL Report 82448-5, Mechanical Engineering Department, M.I.T., (May 1977).
- Bathe, K.J. and Wilson, E.L., 1976. *Numerical Methods in Finite Element Analysis*. Prentice-Hall Inc., Englewood Cliffs, N.J..
- Bayley, F.J., Owen, J.M., and Turner, A.B. 1972. *Heat Transfer*. Thomas Nelson & Sons.
- Boga, S.K., Hwang, C.T. and Krishnayya, A.K.G., 1980. *Thermal Foundation Design for Syncrude's Hot Bitumen Tanks*. Proceedings of Applied Oilsands Geosciences Conference, University of Alberta, Edmonton, Alberta, 40 pages.
- Brown, A.I. and Marco, S.M., 1958. *Introduction To Heat Transfer*. McGraw-Hill.
- Byrne, P.M., Smith, L.B., Grigg, R., Stewart, W.P., 1980. *Computer Model for Stress-Strain Analysis of Oilsands*. Conference on Applied Oilsands Geoscience, June, 1980, Edmonton Alberta.

- Carrigy, M.A. and Kramers, J.W., 1974. *Geology of Alberta Oil Sands*. In *Athabasca Oil Sands*, Conference Proceedings, 1974: Engineering Institute of Canada, Western Region, pp. 13-24.
- Cedergren, H.R., 1977. *Seepage, Drainage, and Flow Nets*. John Wiley & Sons, Inc., New York.
- Charlwood, R.G., Byrne, P.M., McKinley, D.Wm., Varoglu, E., 1980. *Thermal-Geomechanical Analyses and Criteria for the Design of a Mine Assisted Heavy Oil Facility*. Applied Oilsands Geosciences Conference, Edmonton, Alberta, June 1980.
- Chatterji, P.K., Smith, L.B., Insley, A.E., Sharma, L. 1979. *Construction of Saline Creek Tunnel in Athabasca Oil Sand*. Can. Geol. Journal, Vol. 16, No. 1, pp 90-107.
- Devenny, D.W. and Raisbeck, J.M., 1980. *Rock Mechanics Considerations for In-Situ Development of Oil Sands*. CIM Special Volume 22, Underground Rock Engineering, The Canadian Institute of Mining and Metallurgy, pp. 90-96.
- Dusseault, M.B., 1980. *Sample Disturbance in Athabasca Oil Sands*. Journal of Canadian Petroleum Technology, 18(2), pp. 85-92.
- Dusseault, M.B., 1977. *The Geotechnical Characteristics of Oil Sands*. Ph.D. Thesis, University of Alberta.
- Dusseault, M.B. and Morgenstern, N.R., 1977. *Sampling and Testing of Athabasca Oil Sands for Stability Studies*. The Oil Sands of Canada-Venezuela, The Canadian Institute of Mining and Metallurgy, Special Volume 17, pp. 260-269.
- Freeze, R.A. and Cherry, J.A., 1979. *Groundwater*. Prentice-Hall, Inc., Englewood Cliffs, N.J.
- Geological Society of America, 1966. *Handbook of Physical Constants*. S.P. Clark, Jr., Editor, Memoir 97, Yale University, New Haven, Connecticut.
- Hackbarth, D.A., 1978. *Regional Hydrology of the Athabasca*

Oil Sands Area, Alberta Canada. The Oil Sands of Canada-Venezuela, D.A. Redford and A.G. Winestock (eds.), CIM Special Volume 17, pp. 87-102.

Hackbarth, D.A., 1978. *Hydrogeological Concerns in Underground Excavation Athabasca Oil Sands Area.* Proceedings of AOSTRA Seminar on Underground Excavation in Oil Sands, University of Alberta, May. (including questions and responses), 35 pages.

Hackbarth, D.A., 1980. *Regional Aqifer Parameters Evaluated During Mine Depressurization in the Athabasca Oil Sands, Alberta.* Proceedings of Applied Oilsands Geoscience Conference, Edmonton, 15 pages.

Halliday, D. and Resnick, R., 1974. *Fundamentals of Physics.* John Wily and Sons, 827 pp.

Hardy, R.M., 1974. *Tailings Dams.* Proceedings First Regional Conference, Western Regoin, Engineering Institute of Canada, Edmonton, 17-19 April, pp. 99 112.

Harr, M.E., 1962. *Groundwater and Seepage.* McGraw-Hill, New York.

Harris, M.C. and Sobkowicz, J.C., 1977. *Engineering Behavior of Oil Sand.* The Oil Sands of Canada-Venezuela, The Canadian Institute of Mining and Metallurgy, Special Volume 17, pp. 270-281.

Lambe, T.W. and Whitman, R.V., 1969. *Soil Mechanics* John Wiley & Sons, Inc., New York.

Mitchell, J.K., 1976. *Fundamentals of Soil Behavior.* John Wiley & Sons, Inc., New York.

Mitchell, J.K., 1969. *Temperature Effects on Engineering Properties and Behavior of Soils.* HRB Spec. Rept. 103, pp. 9-28.

Mitchell J.K., and Campanella R.G., 1968. *Influence of Temperature Variations on Soil Behavior.* Proceedings of The American Society of Civil Engineers, Journal of the Soil Mechanics and Foundation Division, v. 94, no. SM3,

May 1968, pp. 709-734.

- Morgenstern, N.R., 1981. *Geotechnical Engineering and Frontier Resource Development*. Twenty-first Rankine Lecture, *Geotechnique*, 31, pp. 303-365.
- Mossop, G.D., 1980. *Geology of the Athabasca Oil Sands*. *Science*, v. 207, no. 11, Jan., 1980, pp. 145-152.
- Mossop, G.D., 1978. *Facies Control on Bitumen Saturation in The Athabasca Oil Sands*. Canadian Society of Petroleum Geologists, Memoir 6, Calgary, June 1978.
- Mossop, G.D., 1978. *Geological Controls on Reservoir Hetrogenity, Athabasca Oil Sands*. In Dusseault, M.B. (ed.), *Proceedings of AOSTRA Seminar on Subsurface Excavation in Oil Sands*, Edmonton, Department of Extension, University of Alberta, Edmonton, Paper no. 1, 26 pp.
- Myers, G.E., 1971. *Analytical Methods in Conduction Heat Transfer*. McGraw-Hill Book Company, New York.
- Nihon Kikaigakki, 1968. *JSME Steam Tables*. 3rd ed., Tokyo.
- Outtrim, C.P. and Evans R.G., 1978. *Alberta's Oil Sands Reserves and Their Evaluation*. In Redford, D.A. and Winestock, A.G. (eds.), *The Oil Sands of Canada-Venezuela*, The Canadian Institute of Mining and Metallurgy Special Volume 17, pp.36-66.
- Paaswell, R.E., 1967. *Temperature Effects on Clay Soil Consolidation*. *Journal of the Soil Mechanics and Foundation Division, ASCE*, Vol 93, No. SM3, Proc. Paper 5225, May, 1967, pp. 9-22.
- Scott, J.D. and Kosar, K.M., 1982. *Thermal Expansion of Oil Sands*. *Proceedings of Forum on "Subsidence Due to Fluid Withdrawal"*, U.S. Dept. of Energy and the Republic of Venezuela Ministry of Energy and Mines, Oklahoma USA, November 14-17, 1982, 30 pages.
- Smith, L. and Chapman, D.S., 1983. *On the Thermal Effects of Groundwater Flow : 1. Regional Scale Systems*. *Journal of*

Geophysical Research, Vol 88, No. B1, pp. 593-608.

Svrcek, W.Y. and Mehrotra, A.K., 1981. *Measurement and Correlation of the Density, Viscosity, and Gas Solubility For Athabasca Bitumen*. Department of Petroleum and Chemical Engineering, University of Calgary, AOSTRA Report, AOSTRA Agreement #147.

Svrcek, W.Y., 1979. AOSTRA/University Agreement #13, Department of Chemical Engineering, University of Calgary.

APPENDIX A - THEORETICAL DEVELOPMENT

Introduction

The engineering properties of the oil sand constituent components which were required as input for the numerical analyses were determined either from the experimental testing or from published information. This appendix outlines briefly the source of the data used to derive each property and how each property varies with temperature and pressure.

Incremental Coefficient of Thermal Expansion

(i) Water

The incremental coefficient of thermal expansion for water was derived from both experimental and published data. The coefficient, calculated based on 10 °C temperature increments, did not vary significantly over the pressure range of 0 to 3500 kPa (temperature range of 5 to 200 °C). As a result, it was possible to derive a unique relationship between the incremental coefficient of thermal expansion and temperature. This relationship is shown graphically in Figure A.1.

(ii) In Situ Bitumen

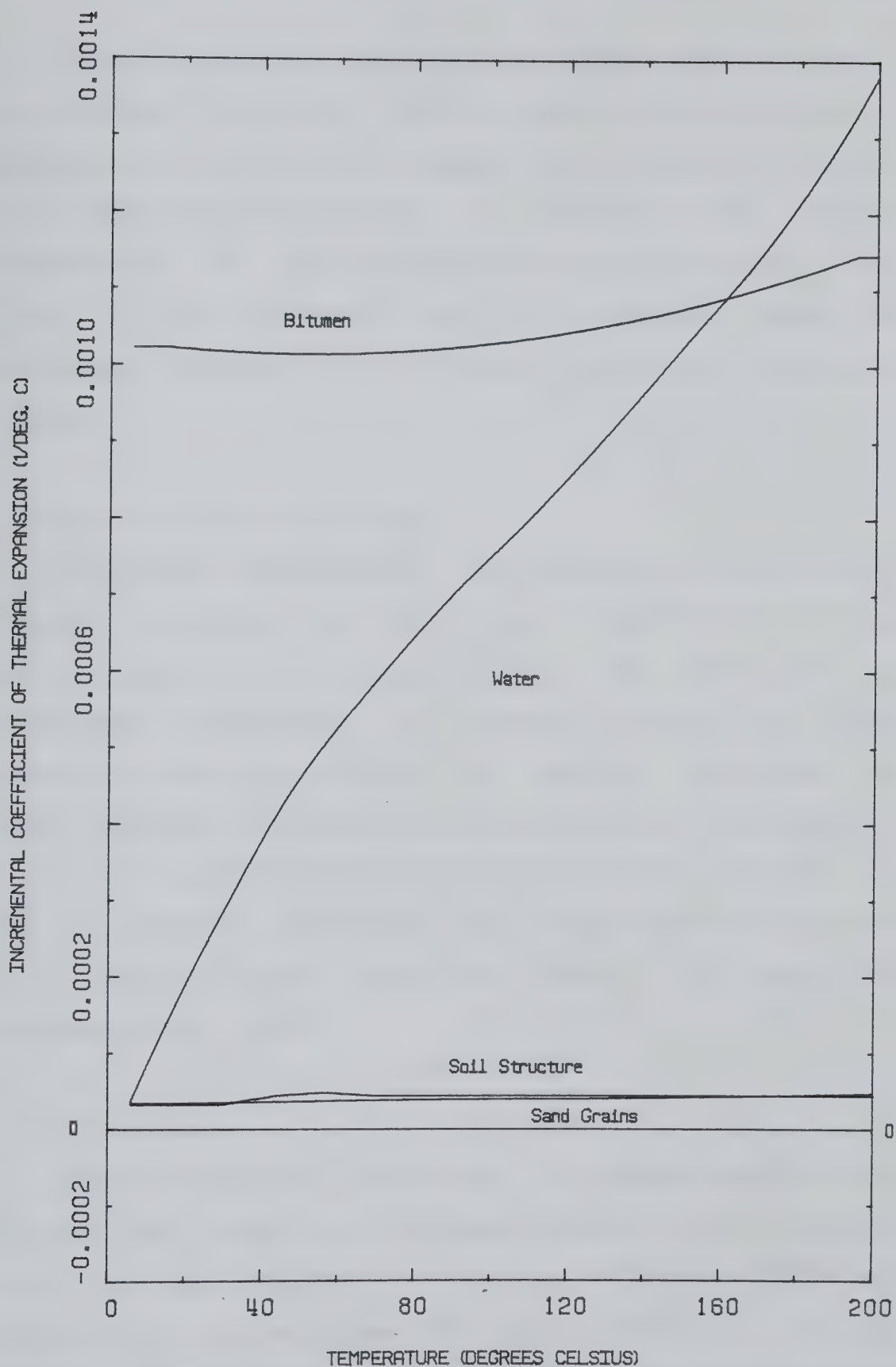


Figure A.1 Coefficient of Thermal Expansion of Oil Sand Components

The incremental coefficient of thermal expansion for in situ bitumen was derived solely on data collected during the experimental testing. The coefficient, calculated based on 10 °C temperature increments, is assumed to be pressure independent over the temperature range considered in this study (5 to 200 °C). A plot of the incremental coefficient of thermal expansion with increasing temperature is shown in Figure A.1.

(iii) In Situ Soil Structure

The relationship between the incremental coefficient of thermal expansion for the in situ oil sand soil structure and temperature is given in Figure A.1. The coefficient was calculated considering data obtained from drained thermal expansion tests performed on high quality undisturbed oil sand samples and adapting these results to approximate in situ conditions through density extrapolation (Chapter 5). The incremental coefficient of thermal expansion for the soil structure was calculated based on temperature increments of 12.5 °C.

(iv) Sand Grains

The incremental coefficient of thermal expansion for the oil sand grains was calculated based on data extracted from the 1966 edition of the *Handbook of Physical Constants* published by the Geological Society of America, Inc. A plot of the incremental coefficient of thermal expansion with

increasing temperature is shown in Figure A.1.

Incremental Coefficient of Compressibility

(i) *Water*

The coefficient of compressibility for water was calculated based on data taken from the 1968 edition of the *Japanese Society of Mechanical Engineers Steam Tables*. Over the pressure range of 0 to 3500 kPa the coefficient did not vary for temperature levels up to and including 200 °C. Therefore, it was possible to derive a unique relationship between the incremental coefficient of compressibility and temperature. This relationship is shown graphically on Figure A.2.

(ii) *In Situ Bitumen*

The incremental coefficient of compressibility for in situ bitumen was calculated based on information extracted from the work done by Svrcek and Mehrotra (1981). In situ bitumen was assumed to be gas saturated with 80 percent methane and 20 percent carbon dioxide. As with the case of water, over the pressure range under consideration the coefficient is not pressure sensitive and as a result it was possible to derive a unique relationship between the incremental coefficient of compressibility and temperature (Figure A.2). Since only data to 100 °C was available, the curve was extrapolated to 200 °C as shown in the figure.

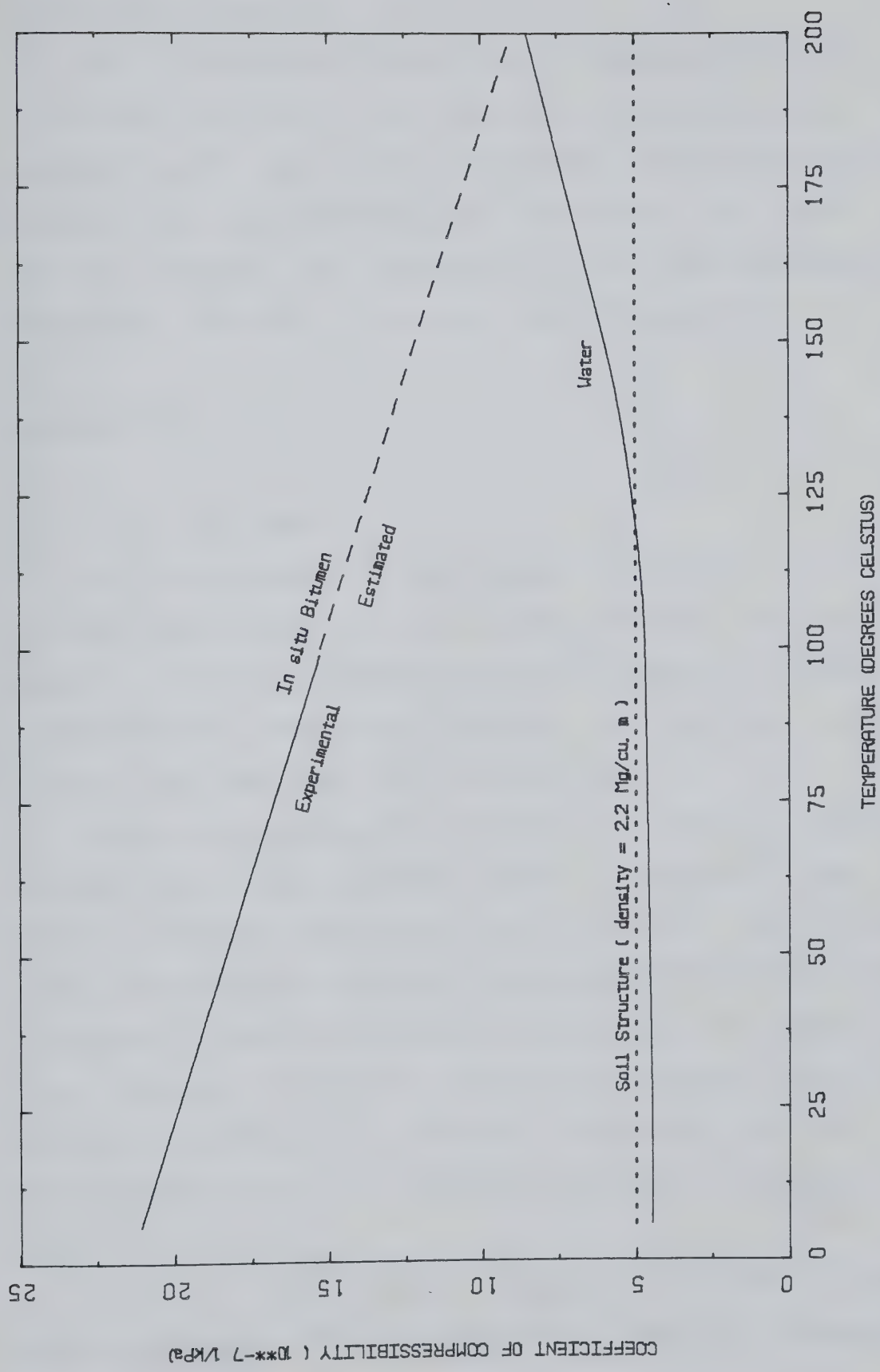


Figure A.2 Coefficient of Compressibility of Oil Sand Components

(iii) Soil Structure

The incremental coefficient of compressibility for the in situ oil sand soil structure was assumed to be both pressure and temperature independent for the pressure and temperature ranges utilized for this study. The value used in the analysis was selected from the range suggested by Dusseault (1980) for in situ oil sand (Figure A.2).

Dynamic Viscosity

(i) In Situ Bitumen

In situ bitumen, in this study, is assumed to obtain 80 percent methane and 20 percent carbon dioxide in solution. Dynamic viscosity-temperature relationships for methane and carbon dioxide saturated bitumens, for various pressure levels, have been reported by Svrcek (1979).

Plots of the dynamic viscosity of methane saturated bitumen over the pressure range of atmospheric (gas free oil) to 2.5 MPa is shown in Figure A.3. Over this pressure range the dynamic viscosity of methane saturated bitumen is relatively insensitive to pressure changes. As a result, it was possible to derive a unique relationship between the dynamic viscosity of methane saturated bitumen and temperature (Figure A.3) without introducing any appreciable amount of error.

Plots of the dynamic viscosity of carbon dioxide saturated bitumen over the pressure range of atmospheric

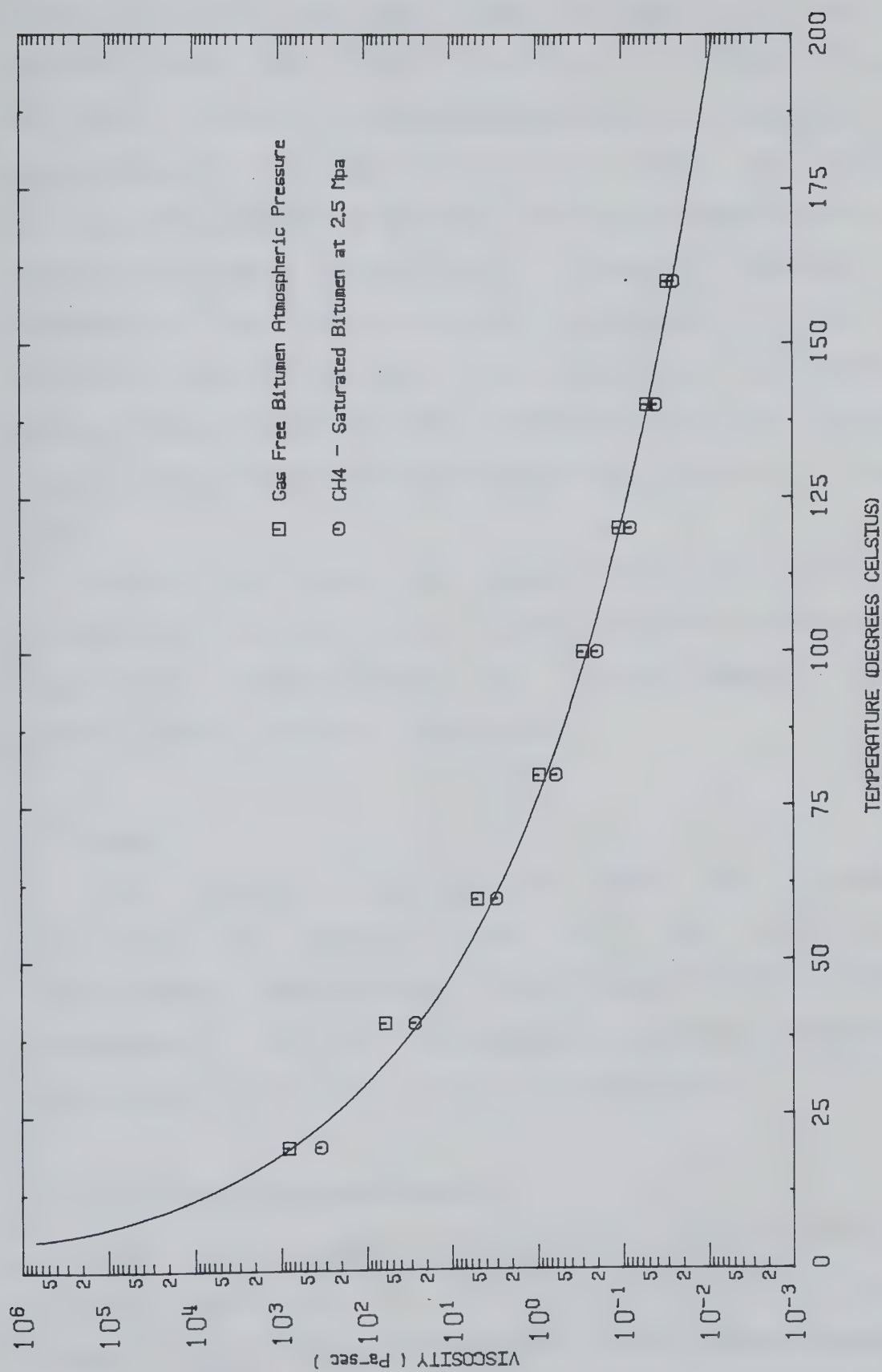


Figure A.3 Dynamic Viscosity of Methane Saturated Bitumen

(gas free oil) to 2.34 MPa is shown in Figure A.4. Over this pressure range the dynamic viscosity of carbon dioxide saturated bitumen is significantly pressure dependent over the temperature interval of 5 to 75 °C. Since the majority of pressure dependency occurs in the room temperature range (where the bitumen is known to be virtually immobile) and considering that in situ bitumen is assumed to contain only 20 percent carbon dioxide, it is reasonable to assume a unique relationship between the dynamic viscosity of carbon dioxide saturated bitumen and temperature as shown in Figure A.4.

Figure A.5 gives the dynamic viscosity-temperature relationship for in situ bitumen based on the assumption that in situ bitumen contains 80 percent methane and 20 percent carbon dioxide in solution.

(ii) Water

The dynamic viscosity of water with increasing temperature was obtained from the 1980 edition of *Thermodynamics and Transport Properties of Fluids* by Rogers and Mayhew. A plot of the dynamic viscosity-temperature relationship for water is given in Figure A.6.

(iii) Fluid (Bitumen and Water)

The dynamic viscosity-temperature relationship for the fluid was based on an oil sand having 15 weight percent bitumen (31 volume percent) and 2 weight percent water (4

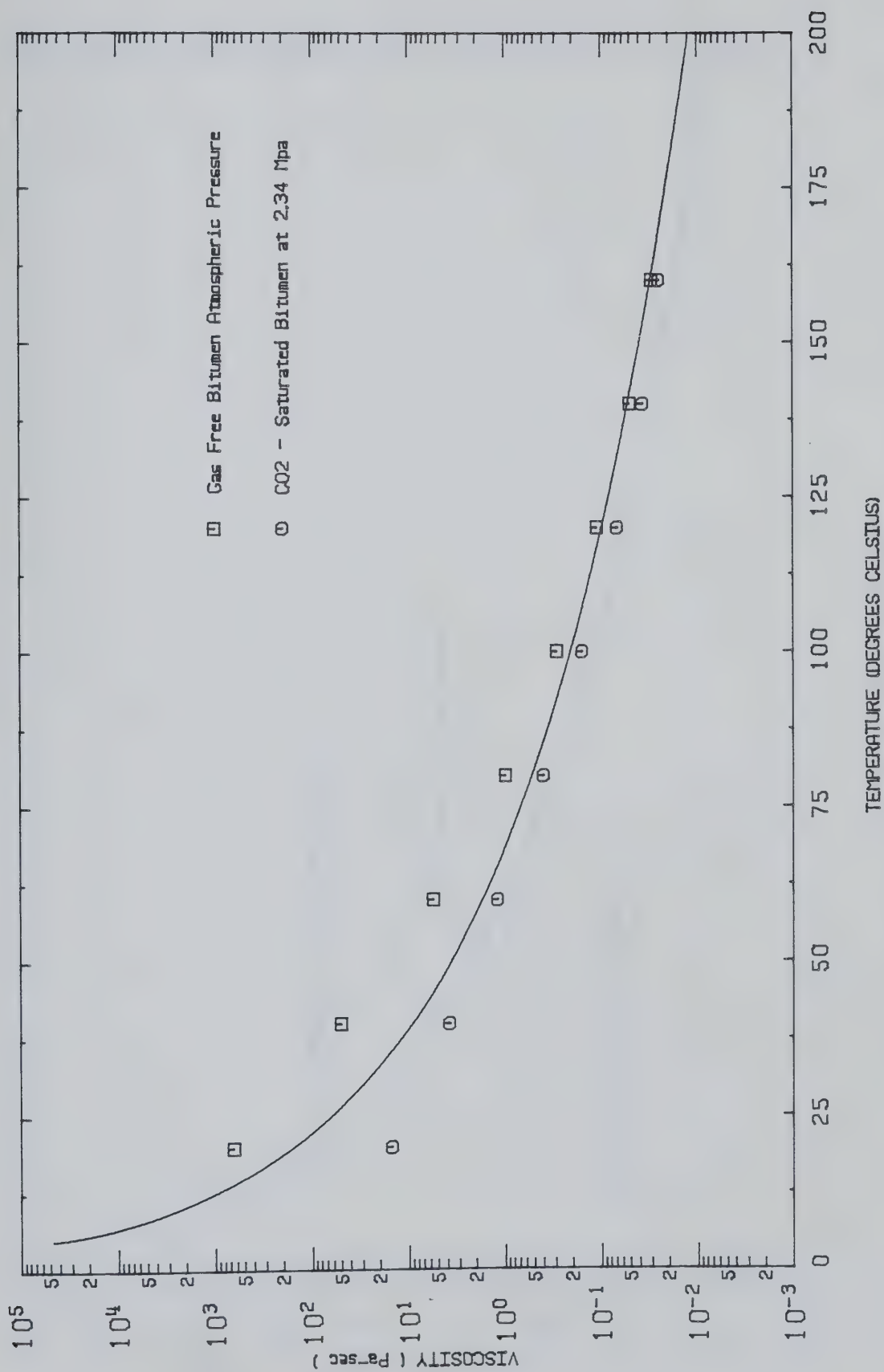


Figure A.4 Dynamic Viscosity of Carbon Dioxide Saturated Bitumen

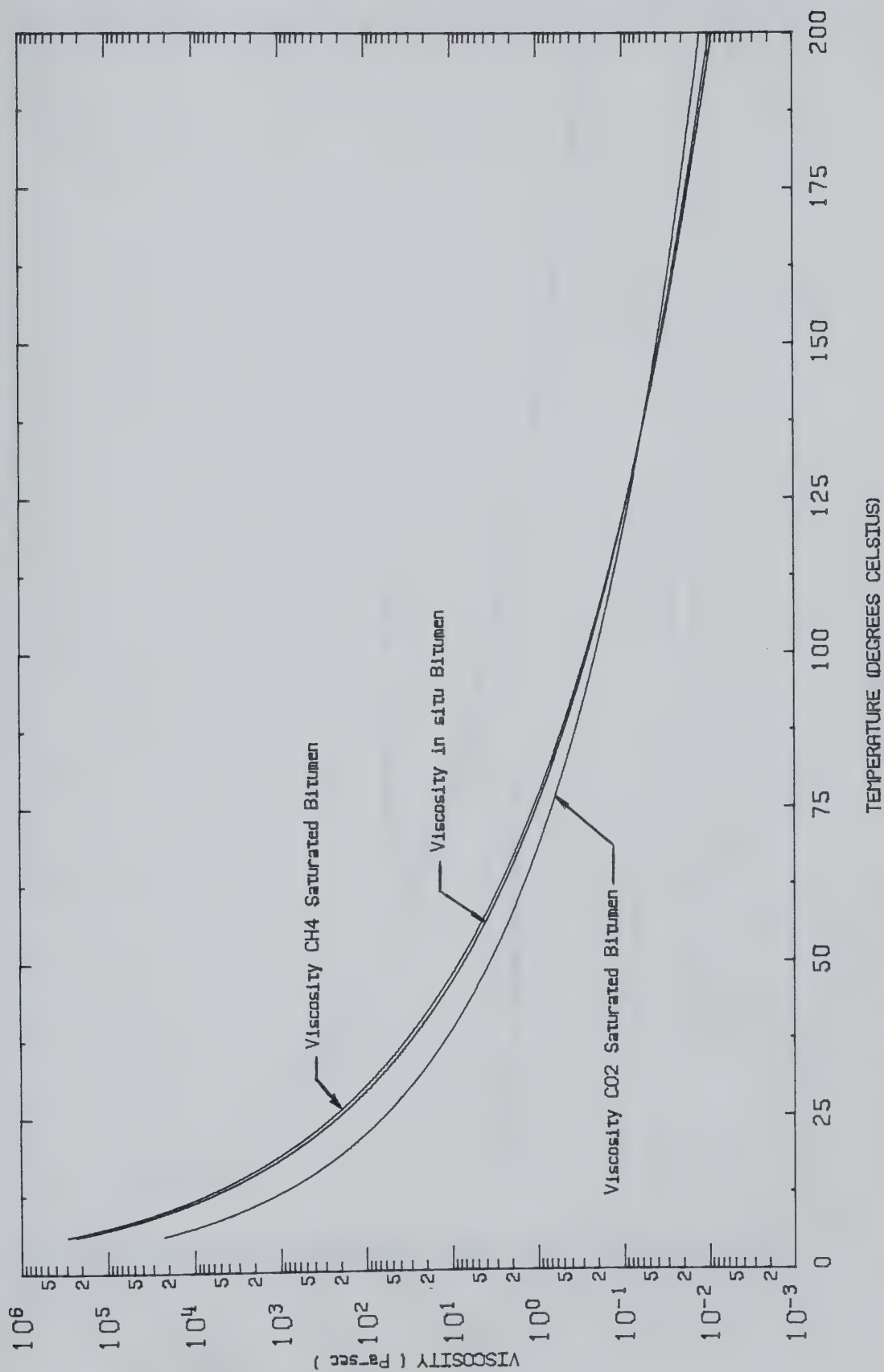


Figure A.5 Dynamic Viscosity of In Situ Bitumen

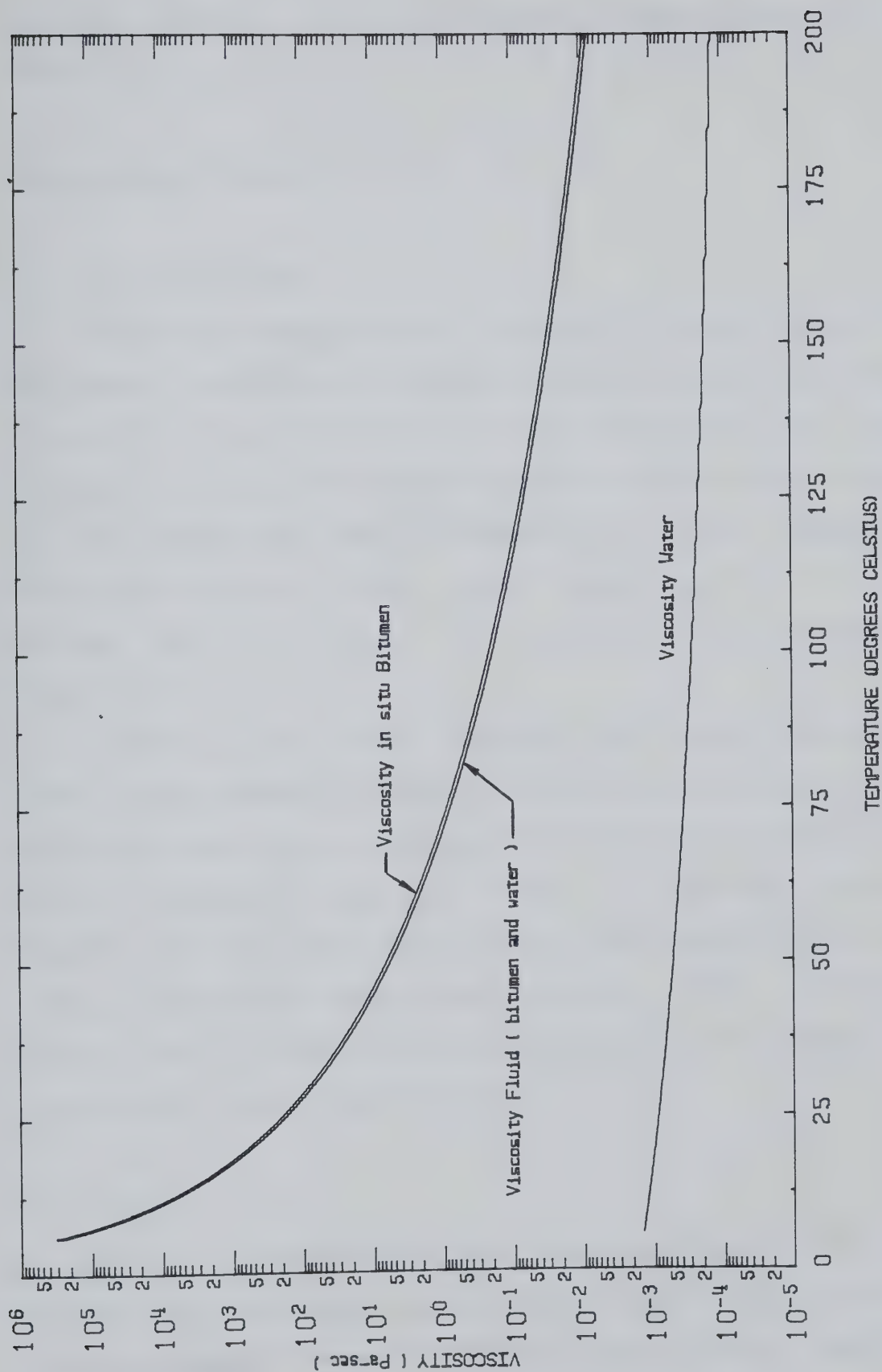


Figure A.6 Dynamic Viscosity of Bitumen, Water and Fluid

volume percent). This relationship is shown graphically in Figure A.6.

Unit Weight (Density)

(i) In Situ Bitumen

The room temperature unit weight for bitumen containing 80 percent methane and 20 percent carbon dioxide was assumed to be 10.104 kN/m^3 (1.03 g/cm^3) (Svrcek and Mehrotra, 1981). Utilizing the volume change-temperature relationship derived in the laboratory testing (Chapter 5) a curve representing the change in unit weight with temperature for in situ bitumen was calculated. This relationship is presented in Figure A.7.

Based on the data reported by Svrcek and Mehrotra (1981) the presence of carbon dioxide in solution has little effect on density over the pressure range considered in this study. Similarly, the unit weight of methane saturated bitumen does not vary significantly over the pressure range used in this study (Svrcek and Mehrotra, 1981). Therefore, the unit weight-temperature relationship given in Figure A.7 is valid for analytical purposes.

(ii) Water

The unit weight-temperature relationship for water was derived from both experimental and published data. Since the volume change of water did not vary significantly over the

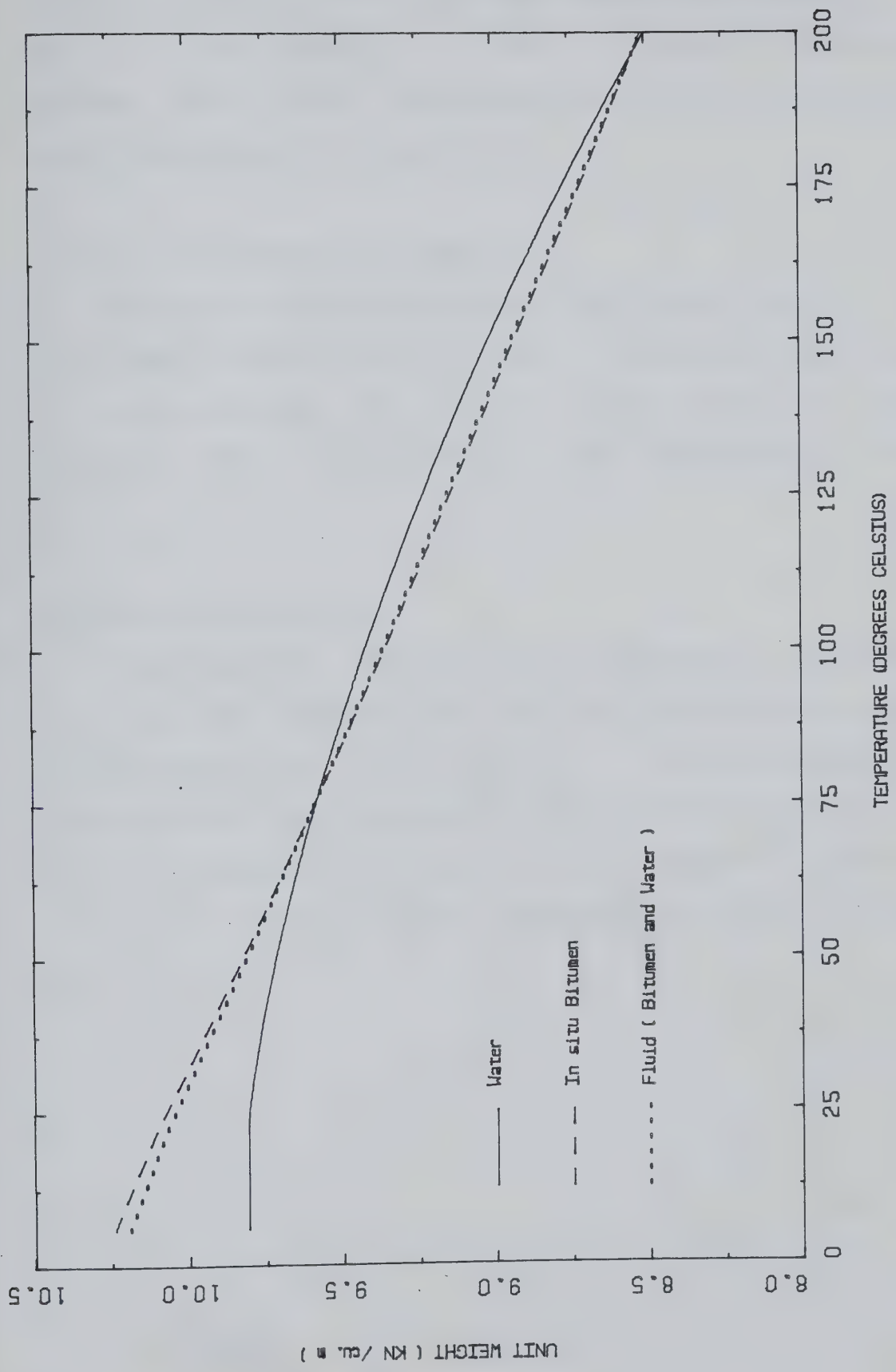


Figure A.7 Unit Weight of Bitumen, Water and Fluid

pressure range of 0 to 3500 kPa (temperature range of 5 to 200 °C) it was possible to derive a unique relationship between unit weight and temperature. This relationship is shown graphically in Figure A.7.

(iii) Fluid (Bitumen and Water)

The unit weight-temperature relationship for the fluid was based on an oil sand having a 15 weight percent bitumen (31 volume percent) and 2 weight percent water (4 volume percent). This relationship is shown graphically in Figure A.7.

Hydraulic Conductivity

The hydraulic conductivity- temperature relationship for the fluid (bitumen and water) was derived from the unit weight-temperature and dynamic viscosity-temperature relationships and assuming an absolute permeability of $3 \times 10^{-12} \text{ m}^2$ (Chapter 3). A plot of the hydraulic hydraulic conductivity with increasing temperature is shown in Figure A.8.

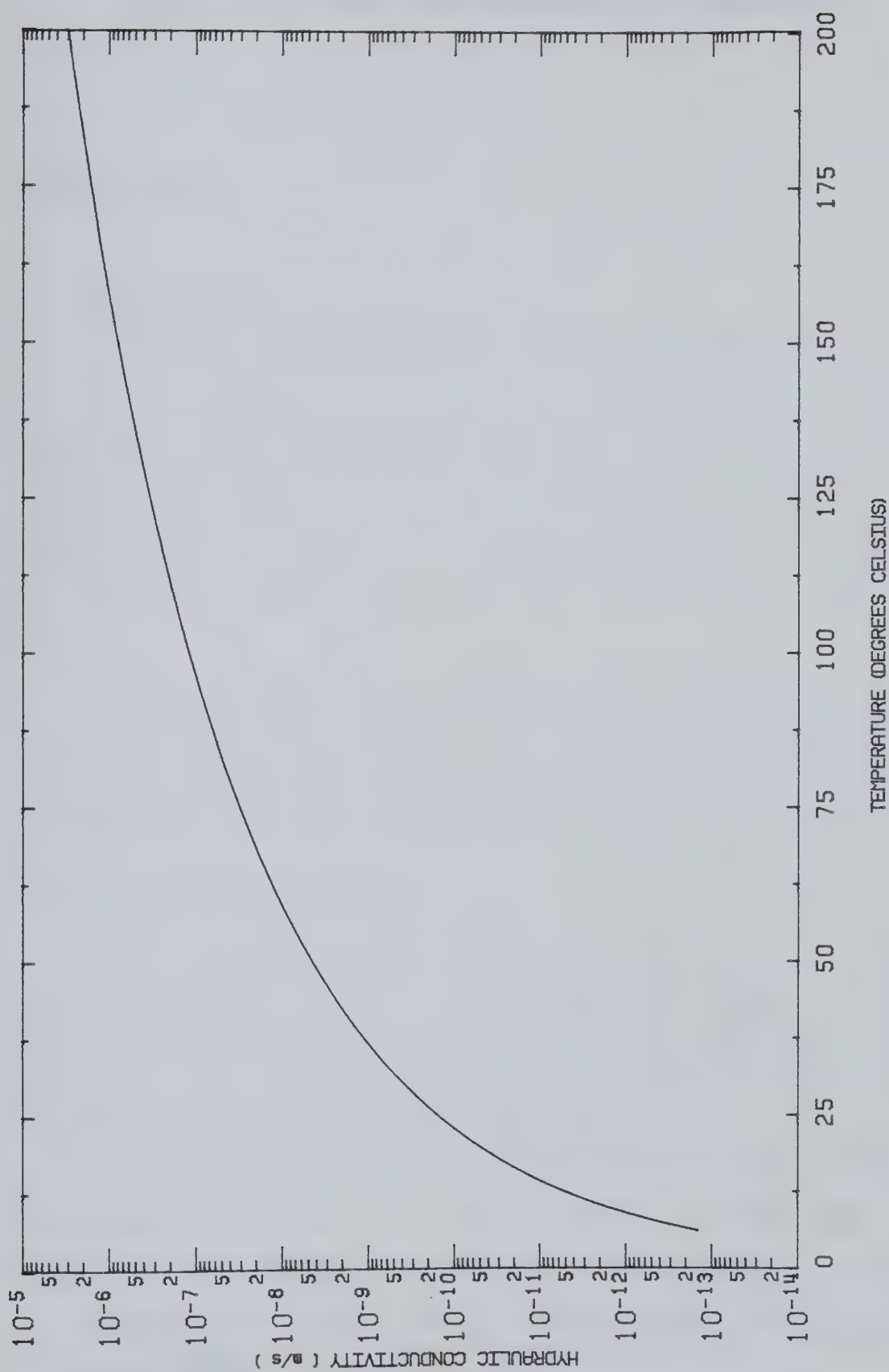


Figure A.8 Hydraulic Conductivity of Oil Sand With Temperature

APPENDIX B - DETAILED DESCRIPTION OF APPARATUS

Consolidometer

(i) Sample Jacket

The consolidometer sample jacket is composed of 420 series stainless steel with a coefficient of linear thermal expansion of 10.8 micrometers per meter per degrees celsius (Metals Handbook, Vol. 3, 9th Edition). The jacket was tempered to increase its hardness in order to prevent scratching of the metal by the sand grains. Also made smooth.

The sample jacket has an inside diameter of 7.63 cm and a wall thickness of 0.635 cm. The jacket was designed to accommodate specimens ranging in height from 2.0 to 4.0 cm.

(ii) Consolidometer Piston

The consolidometer piston consists of 304 series stainless steel with a coefficient of linear thermal expansion of 17.8 micrometers per meter per degrees celsius (Metals Handbook, Vol. 3, 9th Edition).

The clearance between the piston and sample jacket is approximately 0.025 cm. The overall weight of the consolidometer piston (including concrete cylinder) is 38.84 N. Location and dimensions of thermocouple and drainage ports are given in Appendix D.

There are two closely spaced sealing *O* rings located on the lower portion of the piston and a *rider* ring positioned on the upper portion. The purpose of the latter is to ensure vertical movement of the piston and to reduce frictional resistance between the piston and sample jacket.

(iii) *O* and Rider Rings

All *O* rings used with the apparatus are composed of a chemical compound commercially referred to as *Viton*. *Viton*, unlike conventional *o*-ring material, is resistant to degradation over the operational temperature range of the apparatus and in addition is compatible with petroleum products.

Teflon, a chemically stable, heat resistant plastic polymer, was selected as the material for the rider ring. Teflon proved to be an ideal material owing to its low coefficient of friction, good commercial availability and ease of machining.

(iv) *Pedestal*

The pedestal is composed of the same material as the piston and contains 2 drainage ports, location and dimensions of which are given in Appendix D.

(v) *Porous Stones*

The consolidometer contains three porous stones. Two 0.32 cm thick porous stones are imbedded within the piston

as shown in Figure 2.1 and one 0.64 cm thick porous stone in the pedestal.

(vi) Filter Paper

The filter paper used in the consolidometer consists of very finely woven glass fibers. Unlike conventional filter paper, glass fiber paper is heat resistant. The filter paper has the finest mesh (effective retention, 1.2×10^{-6} m) of those commercially available giving the greatest amount of flow resistance.

Measuring Devices

(i) Pressure Transducers

The transducers used to measure the back and air cylinder diaphragm pressures were commercially produced by the Viatran Corporation. Briefly, the transducers have diaphragms which deflect when subjected to fluid under pressure. This deflection is measured by foil strain gauges mounted on the diaphragm and converted to output voltage signals. The design is such that the output signal varies linearly with with applied pressure.

The air cylinder pressure transducer (Model 222) has an operational range of 0 through 2.0 MPa. The back pressure transducer (Model 108) has an operational range of 0 to 7.0 Mpa. Detailed specifications are readily available from the manufacturer.

(ii) Linearly Varying Displacement Transducer

The LVDT used in the apparatus was manufactured by the Hewlett Packard Company.

The LVDT performs on the following theory: the direct current input is transformed into alternating current by an oscillator. The alternating current excites the primary windings inducing voltage in the secondary windings, the amount of which is determined by the location of the axial core. Secondary circuits enable the output to be read as DC voltage which is linearly proportional to the axial core displacement.

The model used in the apparatus was the HP 24DCDT. Detailed specifications are readily available from the manufacturer.

(iii) Thermocouples

The thermocouples used in the apparatus were manufactured by the Barber-Colman Company. The thermocouples are Type J (iron-constantan element) with fiberglass insulation. The element is housed in 0.3175 cm stainless steel protective tube which is closed at the end. The operational temperature range of the thermocouple is from 0 to approximately 400 °C. Detailed specifications are readily available from the manufacturer.

Band Heater

The band heater used in the apparatus was obtained from Thermel Incorporated. The *ThermaStrip* heater band (Model CD-25350) contains two elements and is rated at 650 watts. The band has an inside diameter of 8.9 cm, is 6.35 cm wide and operates on 115 volts. The heater also has a 6.35 cm terminal box.

Diaphragm Air Cylinder

The diaphragm air cylinder was obtained from the Bellofram Corporation. Its theory of operation was discussed in Chapter 4. The following is a brief summary of the pertinent specifications:

TYPE:	5
SIZE:	24
SERIES:	E
ROD:	BP
BORE:	13.97 cm
STROKE:	6.60 cm
MAXIMUM APPLIED AIR PRESSURE:	1260 kPa

Further specifications are available from the manufacturer.

Temperature Controller

The temperature controller (Model 580) is microprocessor-based and manufactured by the Barber-Colman Company. The operational use of the instrument is discussed in Chapter 4.

The controller has a rated accuracy of $\pm(0.5\%$ of reading + 2 °C) and a temperature range of 0 to 400 °C. The controller has a temperature sampling time of 3 per second. Detailed specifications are available from the manufacturer.

Insulating Shell

The material composing the insulating shell was manufactured by the Carborundum Company Insulation Division. The *Fibrefrax Moist-Pack D* used to construct the shell is made of ceramic fiber and an inorganic binder which is easily workable but cures to a rigid structure. The insulation is composed primarily of Alumina-Silica with an operational limit of 1260 °C. The material has good thermal reflectance, low heat storage and low thermal conductivity.

The insulating shell itself is 1.27 cm thick and fully encompasses the consolidometer. Detailed specifications are available from the manufacturer.

Data Aquisition Unit

The data aquisition unit was manufactured by the Hewlett Packard Company. The unit consists of the *HP-85F Desktop Computer* and the *HP-3497A Data Aquisition Control Unit*.

The data logger is programmable to print measurements on paper as well as record on magnetic tape. During testing up to 3 channels can be monitored on the CRT display. The data recorded by the unit on the magnetic tape is

transferable directly to the University computer for processing.

The operational use, although not complex, is smewhat involved and will not be discussed here. Procedural instructions and unit specifications are available in the *Operator's Handbook* accompanying the equipment.

APPENDIX C - LABORATORY CALIBRATIONS

Calibration of Measuring Devices

To process the data collected by the data acquisition unit it was necessary to calibrate each of the measuring devices independent of the apparatus. Each of the measuring devices had an operational range far exceeding that utilized by the apparatus but, to precisely define the calibration functions for each instrument, each was taken to capacity.

(i) Calibration of Pressure Transducers

Each pressure transducer was calibrated using the Barnet Instruments Ltd. *Calibrator*. Documentation concerning its use is available with the instrument and will not be discussed here. Figure C.1 shows the calibration curve for the 7.0 MPa pressure transducer (used to monitor the back pressure within the apparatus), while Figure C.2 illustrates the curve for the 2.0 Mpa transducer. Since the 2.0 Mpa transducer cannot directly measure the consolidometer piston pressure but only the applied air pressure to the diaphragm air cylinder, an additional calibration was required. It involved calibrating the applied air pressure to the diaphragm air cylinder with the load exerted on the piston. This calibration was performed using a standard proving ring and is shown in Figure C.3.

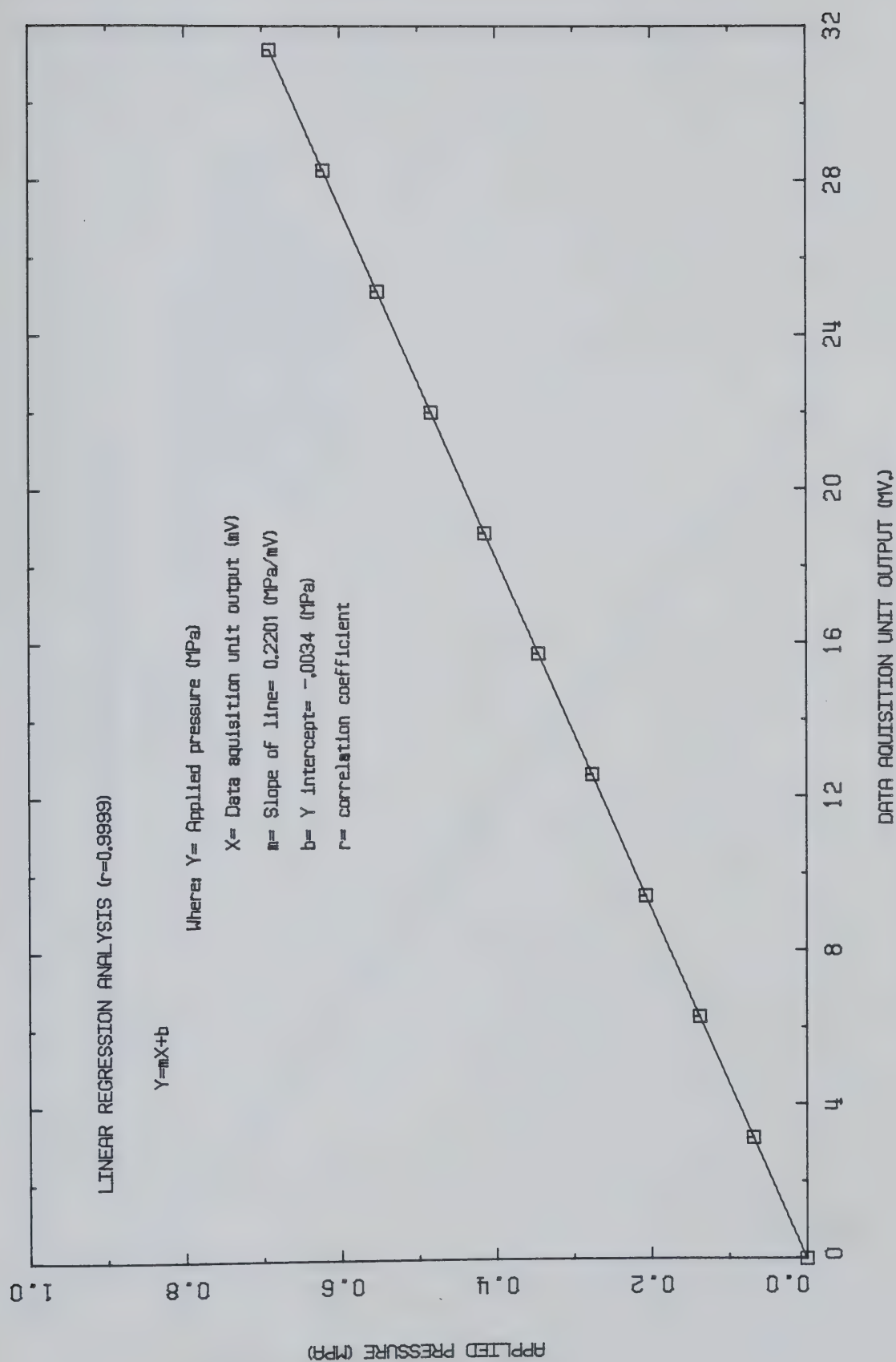


Figure C.1 Calibration Curve for 7.0 MPa Pressure Transducer

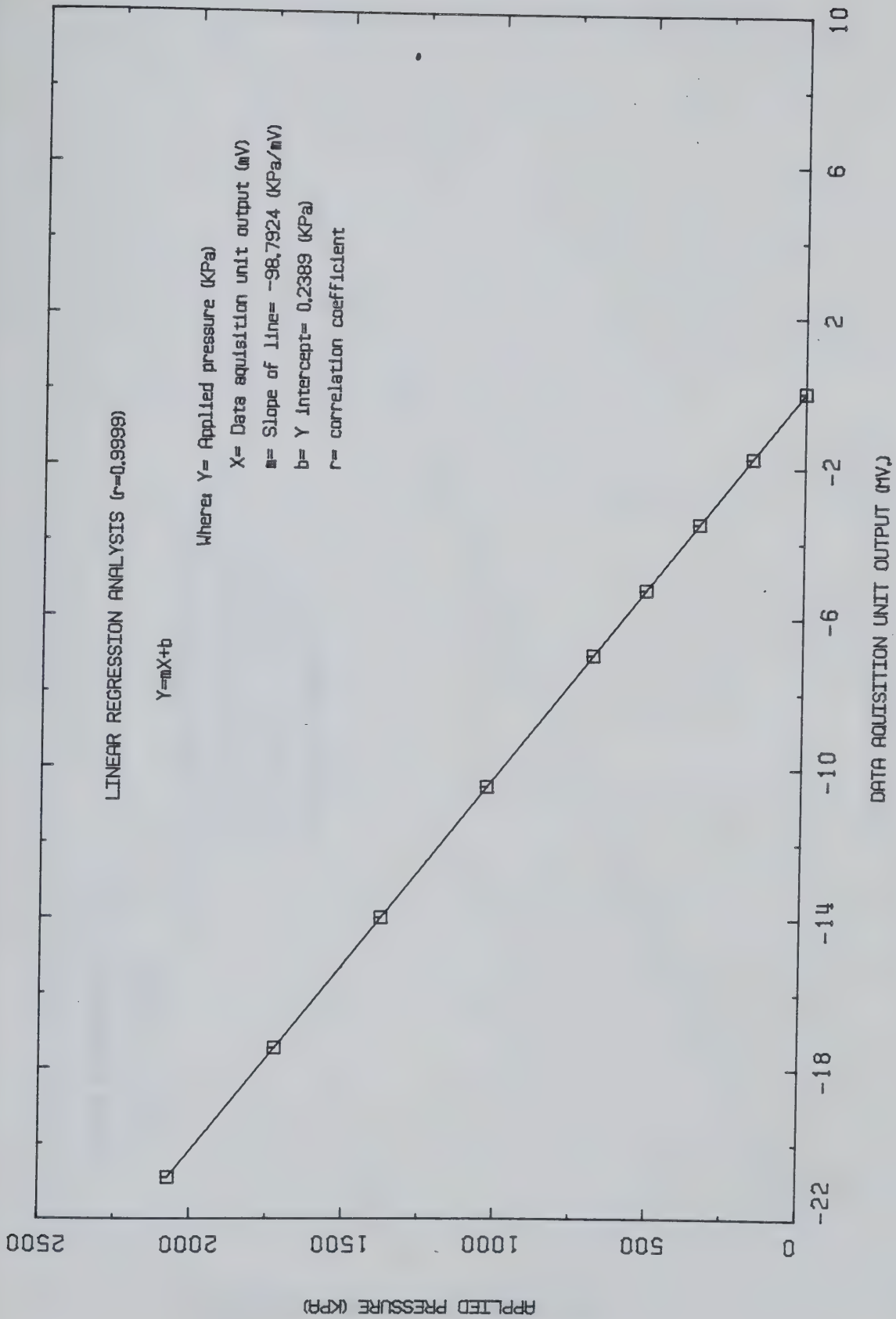
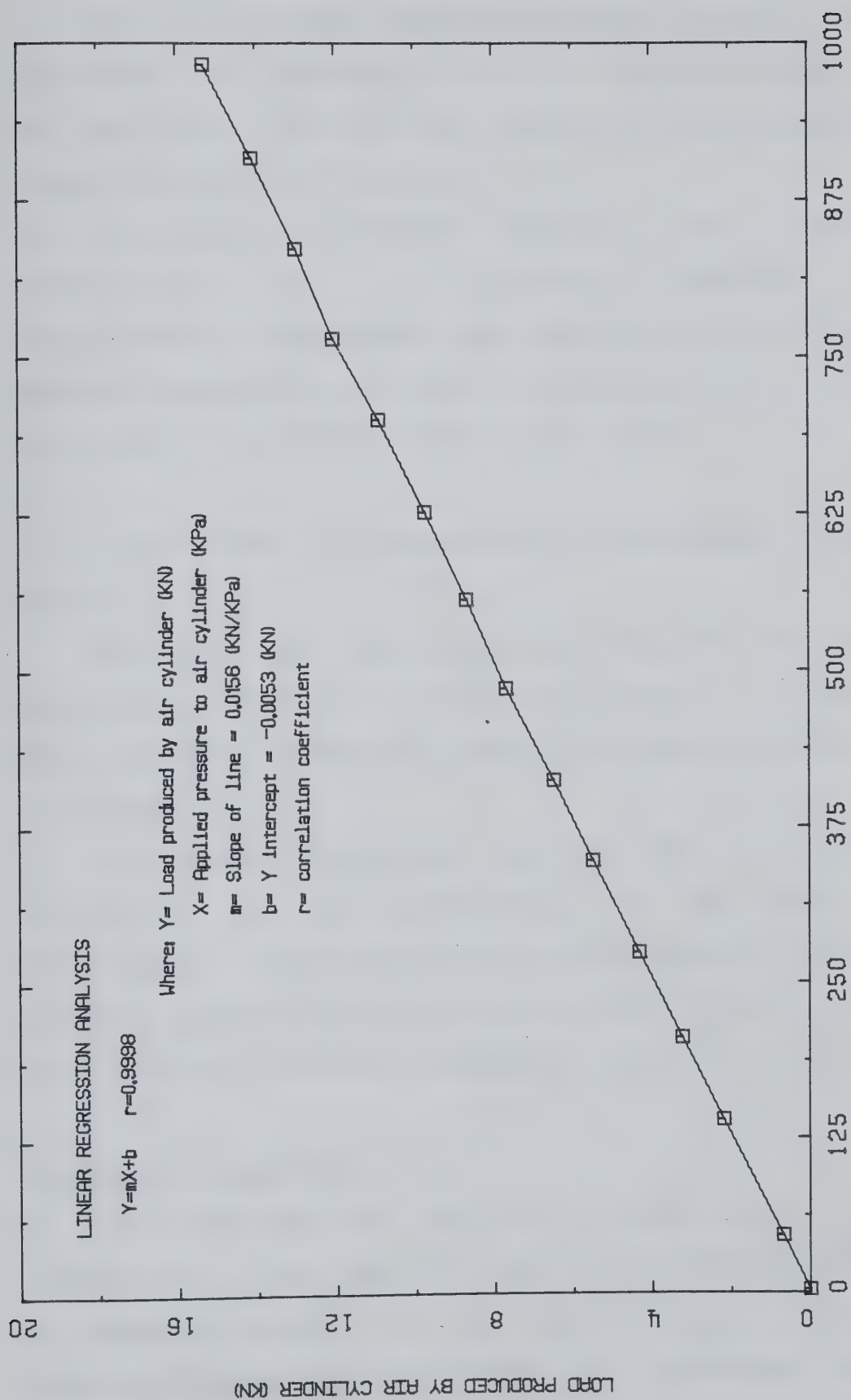


Figure C.2 Calibration Curve for 2.0 MPa Pressure Transducer



APPLIED PRESSURE TO AIR CYLINDER (KPa)

Figure C.3 Calibration Curve for Diaphragm Air Cylinder

Each of the above curves was plotted linearly and was subjected to a regression analysis to provide a *good fit* to the data points. The pertinent details of the analysis are contained within the figures.

all linear regression analyses gave correlation coefficients of 1.0 indicating excellent linear relationships. This implies data electronically collected by the data acquisition unit can be converted with an extremely high level of confidence (negligible error).

(ii) Calibration of Linear Varying Displacement Transducer (LVDT)

The LVDT was calibrated with the use of a precision micrometer, the results of which are shown in Figure C.4. The regression analysis results are also contained within the figure.

The linear regression analysis gave a correlation coefficient of 1.0 indicating an excellent linear relationship. This implies data electronically collected by the data acquisition unit can be converted with an extremely high level of confidence (negligible error).

Calibration Apparatus

The apparatus is subject to significant error in measurement in four specific areas: vertical compression due to operation loading; vertical expansion due to operational heating; horizontal expansion due to operational heating;

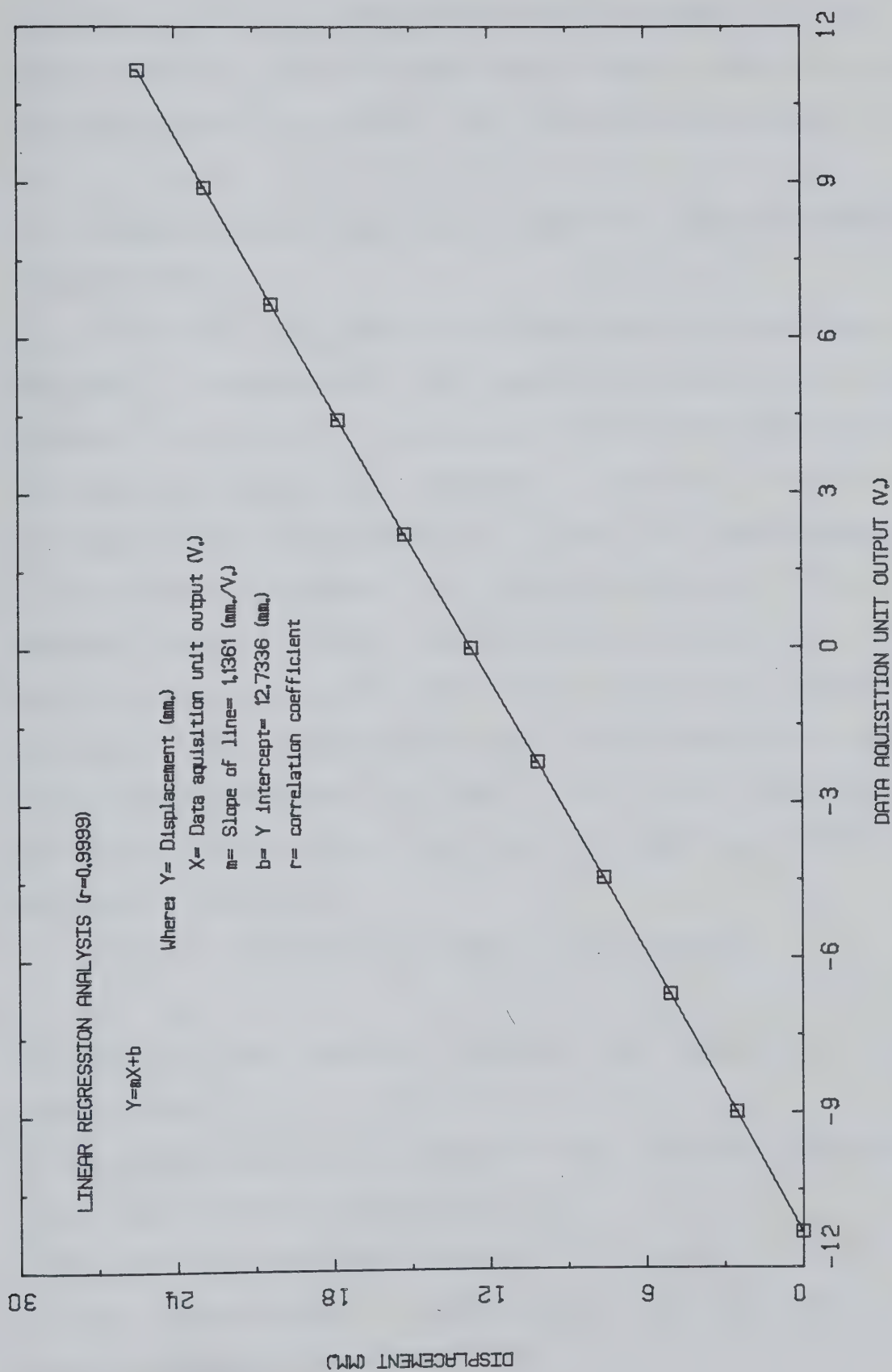


Figure C.4 Calibration Curve for Linearly Varying Displacement Transducer

and piston friction. To eliminate the influence of each of these factors from the experimental data a series of tests were performed to provide a set of correction curves.

(i) Compression of Apparatus by Applied Loads for Different Temperatures

A series of tests were performed to investigate the degree of compression the apparatus experiences during loading at different temperature levels. The specimen used in these experiments was composed of aluminum machined to the approximate dimensions of an actual oil sands sample. To eliminate any influence of induced pressure within the sample chamber, water was excluded from the test and the bottom drainage ports were kept open to atmospheric pressure. The temperature range for the testing was varied from room temperature to 200 °C and the consolidometer piston pressure from the 100 kPa *seating pressure* to a maximum of 3500 kPa.

The following test procedure was employed:

- The 100 kPa seating pressure was applied at room temperature
- The consolidometer was heated to the desired temperature level and allowed to stabilize
- The LVDT reading was recorded
- The consolidometer piston pressure was increased at 500 kPa increments to 3500 kPa

The results derived from this series of testing are presented in Figure C.5.

To account for compression of the apparatus during actual testing the vertical displacement as measured by the tests at room temperature, 100 °C and 200 °C were averaged. The test performed at 50 °C was discarded due to lack of similarity with respect to the other tests. From Figure C.5 it is evident that influence of temperature on the compression of the apparatus by the applied loads was not a significant factor.

(ii) Vertical Expansion of Apparatus with Temperature

The degree of vertical thermal expansion of the apparatus was determined for two seating pressures (100 kPa and 3500 kPa). As with the compression tests, the aluminum specimen was used and the sample chamber was held open to atmospheric pressure. The following test procedure was utilized:

- The seating pressure was applied at room temperature and the LVDT reading recorded
- Heat was applied to the consolidometer
- After temperature stabilization occurred at the desired level, the LVDT reading was recorded
- Steps 2 and 3 were repeated in 10 °C increments to 200 °C

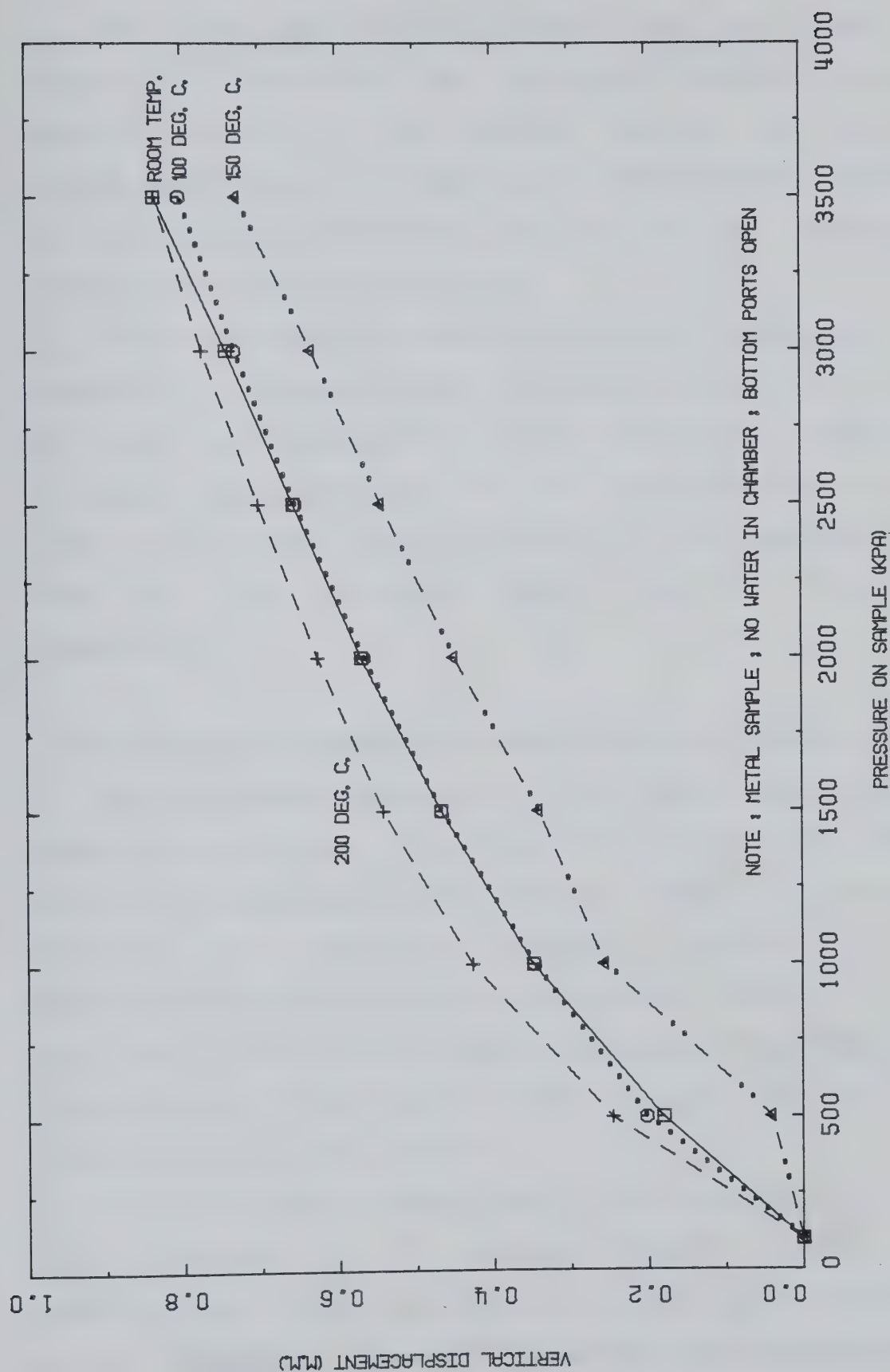


Figure C.5 Compression of Apparatus for Different Temperatures

The curves resulting from these tests are shown in Figure C.6 along with the theoretical vertical thermal expansion curve for the aluminum sample. The vertical thermal expansion of the apparatus is the difference between the expansion measured during the tests and the theoretical expansion of the aluminum sample.

During experimental testing to account for the vertical expansion of apparatus with temperature the results of the two tests were expressed by a linear relationship (Appendix D). Since the expansion of the aluminum sample is also linear, the vertical thermal expansion of the apparatus was taken as the difference between these two equations (Appendix D).

(iii) Horizontal Expansion of Apparatus with Temperature

The horizontal expansion of the sample chamber with temperature was taken into account by considering the sample chamber as an isotropic solid. When an isotropic solid is subjected to a temperature change it expands with the distance between any two points increasing in the ratio α (α being the coefficient of linear expansion). This means the inside diameter of the sample jacket enlarges in the same ratio as the external dimension.

It can be proven theoretically that the coefficient of area expansion of an isotropic solid is twice the coefficient of linear expansion (e.g., Halliday and Resnick [1974]). Therefore, the change in area of the sample chamber

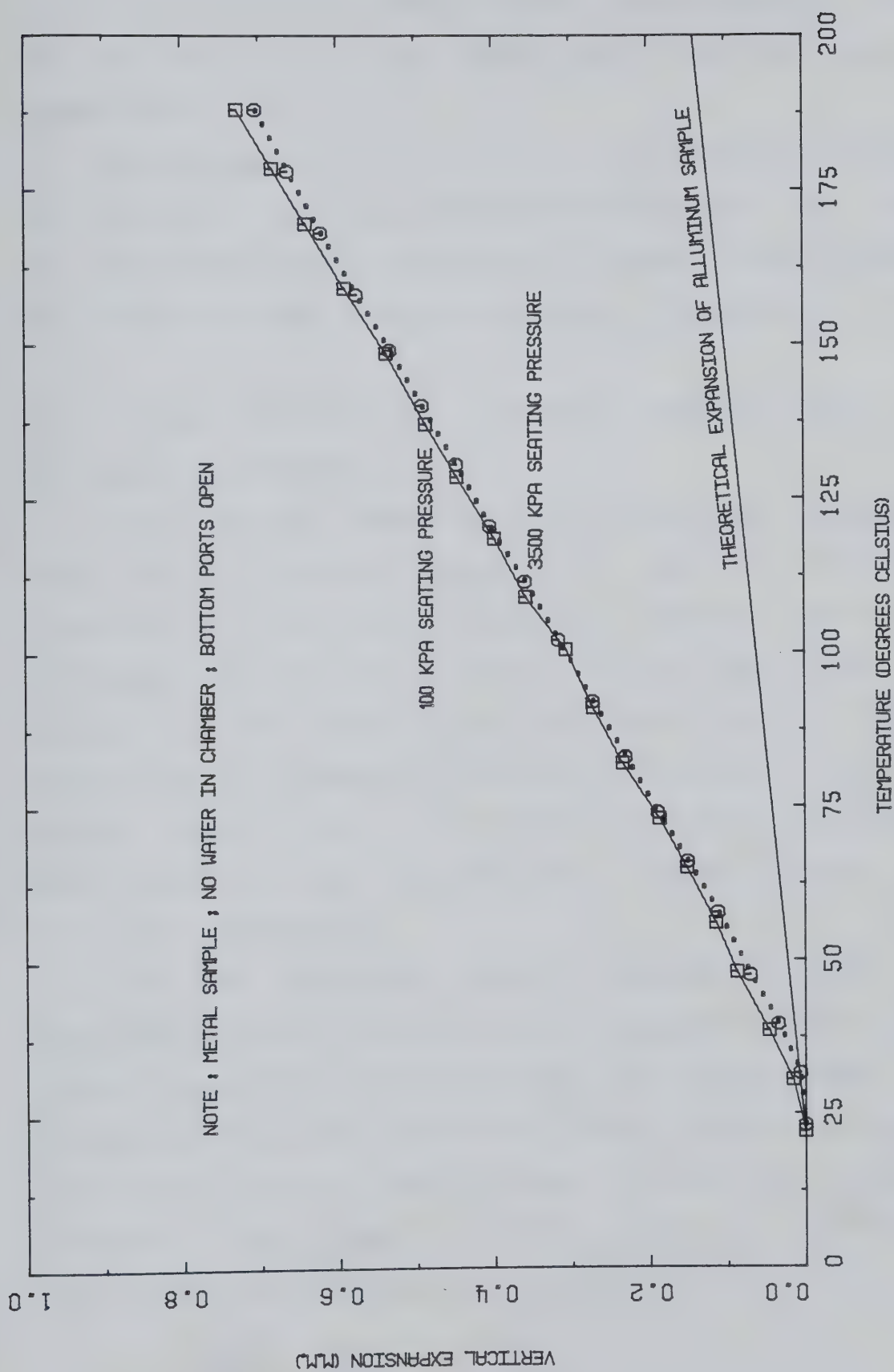


Figure C.6 Vertical Expansion of Apparatus with Temperature

is 2 times the linear coefficient of linear expansion times the original area (at room temperature) times the change in temperature.

The thermal volume change of the apparatus was taken into account in the measurements by multiplying the change in area of the sample chamber by the sample height. Details of the calculations involved are given in Appendix D.

(iv) Piston Friction for Different Pressure Level and Different Temperatures

The oedometer piston and sample jacket are composed of steel alloys differing slightly in material properties (Appendix B). As a result differential thermal expansion in the radial direction was of concern during operational use because of its direct effect on piston friction. Also of concern is the frictional resistance between the o ring and sample chamber wall. It was therefore necessary to examine piston friction for both different pressure levels and different temperatures.

The test procedure adopted involved holding the temperature constant and varying the pressure applied to the piston (Figure C.7). During the test the sample chamber was filled with water and the system totally deaired. The piston friction was taken as the difference between the pressure applied to the piston and the pressure in the water as measured by the back pressure transducer.

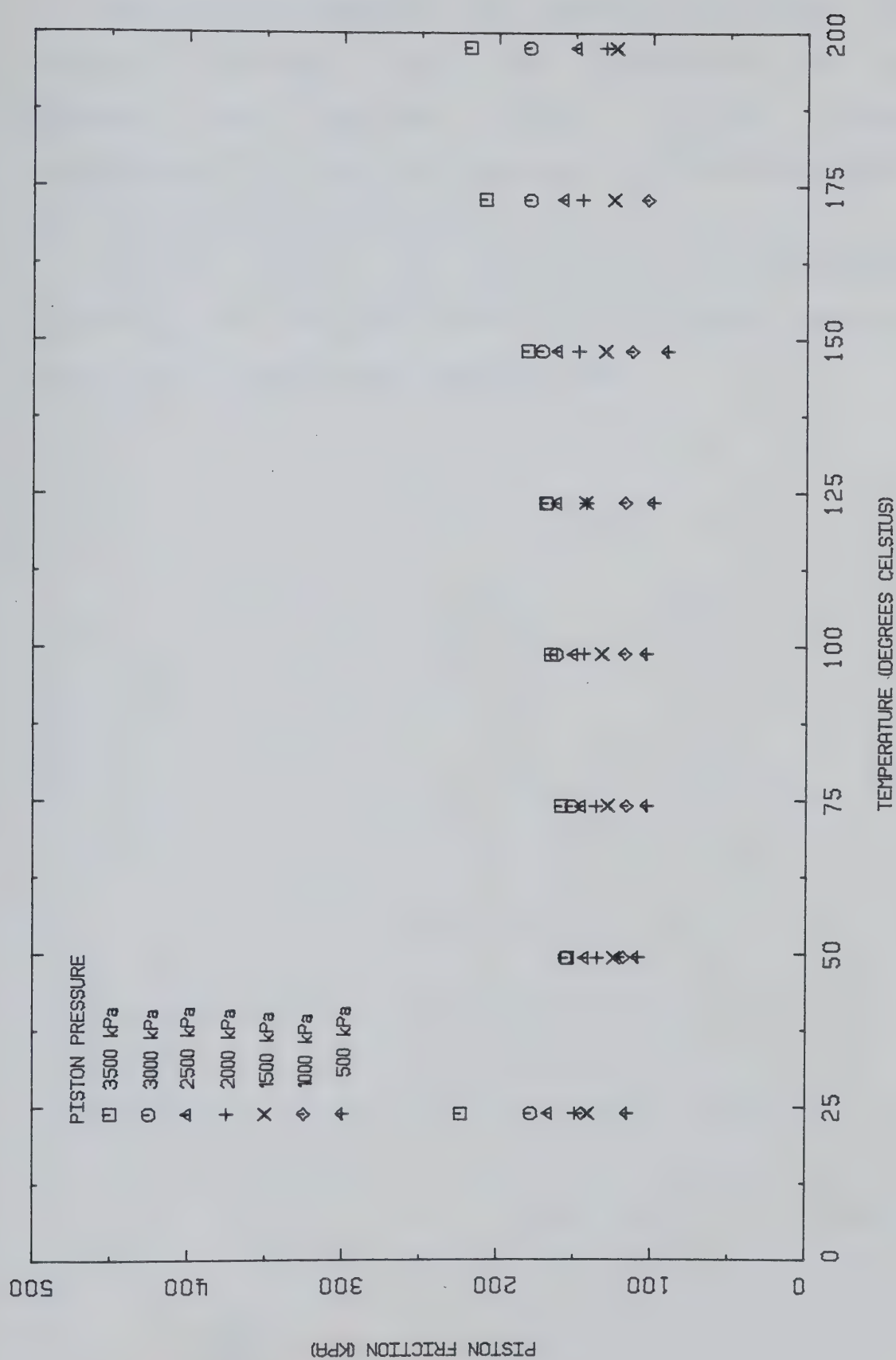


Figure C.7 Piston Friction For Different Pressure Levels and Temperatures

The results (Figure C.7) indicate that the piston friction increases with both temperature and piston pressure. The maximum piston friction pressure (approximately 230 kPa) was measured for the piston pressure of 3500 kPa at approximately 200 °C.

Piston friction was accounted for in experimental testing by utilizing the piston friction versus temperature curve for the appropriate applied load.

APPENDIX D - DATA REDUCTION CALCULATIONS

Volume of Extraneous Water

Extraneous water refers to water not in sample chamber, ie. water in porous stones, passages and ports.

(i) Porous Stones

Stone	Top (Inside)	Top (Outside)	Top* (Outside)	Bottom
Weight wet (g)	37.20	36.98	32.25	95.31
Weight dry (g)	32.54	32.29	37.25	85.56
Weight of water (g)	4.66	4.69	5.125	9.75
Volume of water (cm ³)	4.66	4.69	5.125	9.75

*Stone replaced after being damaged

Total Volume of Extraneous Water in Porous Stones

(a) initially:

$$4.66 + 4.69 + 9.75 = 19.10 \text{ cm}^3$$

(b) after top outside stone was replaced:

$$4.66 + 5.125 + 9.75 = 19.53 \text{ cm}^3$$

(ii) Piston

Thermocouple port:

Thermocouple:	length = 9.955 cm
	diameter = 0.318 cm
Port:	length = 9.955 cm
	diameter = 0.397 cm

Volume of extraneous water = Volume of port - Volume of thermocouple

$$VOE = \pi(9.955)(0.25)[(0.397)^2 - (0.318)^2] = 0.443 \text{ cm}^3$$

Port ccw of Thermocouple (viewing downward):

length	= 8.250 cm
diameter	= 0.318 cm
length less plug length	= 0.785 cm
diameter of plug	= 0.890 cm

$$VOE = \pi(0.25)(8.250)(0.318)^2 + \pi(0.25)(7.85)(0.890)^2 = 1.142 \text{ cm}^3$$

Port cw of Thermocouple (viewing downward):

length	= 8.250 cm
diameter	= 0.318 cm
length less plug length	= 0.860 cm
diameter of plug	= 0.890 cm

Plug: length = 1.435 cm
diameter = 0.238 cm

$$VOE = \pi(0.25)(1.435)(0.238)^2 = 0.064 \text{ cm}^3$$

Tubing: length = 8.905 cm
diameter = 0.159 cm

$$VOE = \pi(0.25)(8.905)(0.159)^2 = 0.176 \text{ cm}^3$$

Remaining drainage port:

length = 3.195 cm
diameter = 0.318 cm

$$VOE = \pi(0.25)(3.195)(0.318)^2 = 0.253 \text{ cm}^3$$

length less plug depth = 0.825 cm

diameter = 0.955 cm

$$VOE = \pi(0.25)(0.825)(0.955)^2 = 0.591 \text{ cm}^3$$

Total volume of extraneous water in pedestal including
tubing to first valve:

$$= 0.349 + 0.253 + 0.777 + 0.064 + 0.176 + 0.253 + 0.591 = 2.463 \text{ cm}^3$$

Total Volume of Extraneous Water:

Initially

After Top Outside

		Stone was Replaced
Porous Stones (cm ³)	19.10	19.535
Piston (cm ³)	2.773	2.773
Pedestal and Tubing (cm ³)	2.463	2.463
Total (cm ³)	24.336	24.771

Change in Sample due to Heating

$$\Delta A = 2 \alpha \Delta T$$

where:

ΔA = change in sample area

A = area of sample

α = thermal coefficient of linear expansion

ΔT = change in temperature

For the sample jacket (420 stainless steel)

$$\alpha = 10.8 \times 10^{-6}/^{\circ}\text{C} \text{ (Appendix B)}$$

$$2\alpha = 2.16 \times 10^{-5}/^{\circ}\text{C}$$

At room temperature (22 °C) the inside area of the sample chamber is:

$$A = \pi(76.2/2)^2 = 4560.37 \text{ mm}^2$$

At any temperature (T_1) the area (A_1) is as follows:

$$A_1 = A(1 + 2\alpha[T_1 - 22])$$

Therefore, the volume (V_1) at any temperature (T_1) is as follows:

$$V_1 = A H (1 + 2\alpha[T_1 - 22])$$

$$\text{i.e., } V_1 = 4560.37 H (1 + 2.16 \times 10^{-5}[T_1 - 22]) [\text{mm}^3]$$

$$\text{or, } V_1 = 4560.37 H + 0.0985 H(T_1 - 22) [\text{mm}^3]$$

where: H = height of sample (corrected for vertical expansion with temperature)

Therefore, the total volume of system at any temperature, T_1 , is:

$$V_t = \text{VOE} + 4560.37 H + 0.0985 H (T_1 - 22) [\text{mm}^3]$$

where:

VOE = volume of extraneous water

T_1 = temperature

H = height of sample

Vertical Expansion of Apparatus with Temperture

From linear regression analysis performed on calibration data the following results were obtained:

$$y = 0.00448 x - 0.1324$$

where:

y = vertical expansion of apparatus and aluminum sample (mm)

x = temperature ($^{\circ}\text{C}$)

Considering expansion of aluminum sample:

$$y' = 0.00079 x' - 0.0173$$

where:

y' = vertical expansion of aluminum sample (mm)

x' = temperature ($^{\circ}\text{C}$)

therefore,

$$y_t = y - y'$$

where:

y_t = net expansion of apparatus due to temperature

$$y_t = 0.0048 x - 0.1324 - 0.00079 x' + 0.0173$$

or,

$$y_t = 0.0048 x - 0.00079 x' - 0.1151$$

but $x = x'$, therefore,

$$y_t = 0.00401 x - 0.1151$$

Volume in Sample Chamber from LVDT Reading

To calculate the volume in the sample chamber from the LVDT reading an aluminum sample was placed in the chamber at room temperature and at the desired ram pressure.

From the LVDT calibration curve (Appendix C)

$$y = mx + b$$

where:

y = data acquisition unit reading (volts)

m = slope from linear regression analysis

b = y intercept from linear regression analysis

Since the height of the aluminum sample is known as well as the corresponding LVDT reading, the new y intercept can be calculated.

i.e. $H = x = 25.25 \text{ mm}$

LVDT Reading for Aluminum Sample = y

Therefore:

$b' = \text{LVDT Reading} - m (25.25) \text{ for aluminum sample}$

As a result, the height of the sample during testing is:

$H = (\text{LVDT Reading} - b')/m$

Correcting for vertical expansion of apparatus with temperature:

$H = (\text{LVDT Reading} - b')/m - 0.0040 T + 0.1151$

and as before:

$V_t = \text{VOE} + 4650.37 H + 0.0985 H (T - 22.0)$

Calculation of Applied Ram Pressure

From calibration curve for 2.0 MPa transducer:

$y = mx + b$

where:

y = applied pressure (kPa)

x = data aquisition unit output (mV)

m = slope of line (kPa/mV)

b = y intercept (kPa)

Diaphram air cylinder:

$$y' = m'x' + b'$$

where:

y' = load produced by air cylinder (kN)

x' = applied pressure to air cylinder (kPa)

m' = slope of line (kN/kPa)

b' = y intercept (kN)

Since $y = x'$:

$$y' = m' (mx + b) + b'$$

Therefore:

The applied room pressure = $y'H(1000)^2/V_1$ + Weight of piston and concrete cylinder (kPa)

where:

V_i = volume of sample chamber corrected for extraneous water and radial expansion of sample jacket

H = height of sample corrected for vertical expansion of apparatus with temperature

100

```
*****
FEHT2 (FINITE ELEMENT HEAT TRANSFER-2 DIMENSIONS) IS A PROGRAM
FOR THE ANALYSIS OF TWO-DIMENSIONAL HEAT CONDUCTION PROBLEMS BY A
FINITE ELEMENT TECHNIQUE USING LINEAR TRIANGULAR ELEMENTS.
```

- 1) STEADY STATE PROBLEMS.
- 2) TRANSIENT PROBLEMS BY THE FOLLOWING METHODS.
 - A) EULERS METHOD.
 - B) THE CRANK-NICHOLSON METHOD.
 - C) A PURE-IMPLICIT METHOD.

- 1) TIME INDEPENDENT CONVECTION.
- 2) TIME INDEPENDENT HEAT FLUX.
- 3) TIME INDEPENDENT TEMPERATURE.

- 1) THERMAL CONDUCTIVITY.
- 2) DENSITY.
- 3) SPECIFIC HEAT.
- 4) RATE OF HEAT GENERATION PER UNIT VOLUME.

THE PROGRAM IS DIMENSIONED TO ACCOMMODATE 500 NODAL POINTS PROVIDED THAT THEY ARE NUMBERED TO RESULT IN A BAND WIDTH OF 30 OR LESS. THE BAND WIDTH IS EQUAL TO 1 PLUS TWICE THE MAXIMUM DIFFERENCE BETWEEN NODAL POINT NUMBERS OF AN ELEMENT.

REFERENCE -

[illegible]


```

C
C *****
C DIMENSIONS
C *****
  IMPLICIT REAL*8(A-H,O-Z)
  COMMON BN(500,30),CN(500,30),SN(500,30),SP(500),Y(500),X(500),
  *T(500),GN(500),RN(500),GEN(50),CEE(50),RHO(50),CAY(50),TIMAX,
  *DTIME,TIME,NTOUT(500),MN(500),NRL(500),KN(500),JN(500),IN(500),JC,
  * ICOUNT,NTIME,NT,NQ,NH,NC,NG,NE,NN,IBW,IOUT,IIN

C
C *****
C SET INPUT/OUTPUT FILE NUMBERS AND INITIALIZE
C *****
  IIN = 5
  IOUT = 6
  LABEL=0
  IFLAG = 0

1
C
C *****
C MAIN PROGRAM
C *****
  CALL DATA(LABEL)
  IF (LABEL.EQ.1) GO TO 15
  CALL FORM
  IF (NH) 2,2,3
2   IF (NQ) 4,4,3
3   CALL BINT
4   IF (NC) 6,6,5
5   CALL INIT
  CALL TRANS
6   IF (NT) 8,8,7
7   CALL MODSN
8   CALL DBAND(NN,IBW,SN,LABEL)
  IF (LABEL.EQ.1) GO TO 14
9   CALL RHS
  IF (NT) 11,11,10
10  CALL MODRN
11  CALL SBAND(NN,IBW,SN,RN,T)
  CALL RESUL(IFLAG)
  IF (NC) 1,1,12
12  IF (TIME - TIMAX) 13,1,1
13  IF (IFLAG) 16,9,16
14  WRITE (IOUT,601)
15  STOP
16  WRITE (IOUT,602)
  GO TO 15

C
C *****
C FORMAT STATEMENTS
C *****
601  FORMAT (// 'O',15X,'DECOMPOSITION FAILS'//)
602  FORMAT ('O',15X,'OUTPUT TIME SPECIFICATION ERROR')
  END

```



```

SUBROUTINE DATA(LABEL)
IMPLICIT REAL*8(A-H,O-Z)
*****
* READ INPUT DATA *
*****

*****
ARGUMENT-

LABEL - END OF FILE INDICATOR
        = 0 IF EXECUTION IS TO CONTINUE
        = 1 IF EXECUTION IS TO TERMINATE
*****

*****
DIMENSIONS
*****
COMMON BN(500,30),CN(500,30),SN(500,30),SP(500),Y(500),X(500),
*T(500),GN(500),RN(500),GEN(50),CEE(50),RHO(50),CAY(50),TIMAX,
*DTIME,TIME,NTOUT(500),MN(500),NRL(500),KN(500),JN(500),IN(500),JC,
*   ICOUNT,NTIME,NT,NQ,NH,NC,NG,NE,NN,IBW,IOUT,IIN

DIMENSION TITLE(20)

*****
PROBLEM IDENTIFICATION
*****
READ (IIN,501,END=99) (TITLE(I),I=1,20)
WRITE (IOUT,601) (TITLE(I),I=1,20)

*****
PROBLEM INDICATORS
*****
WRITE (IOUT,602)
READ (IIN,502) NG,NC,NH,NQ,NT,NN,NE,NM
WRITE (IOUT,603) NG,NC,NH,NQ,NT,NN,NE,NM

*****
MATERIAL PROPERTIES
*****
WRITE (IOUT,604)
DO 1 K=1,NM
  READ (IIN,503) M,CAY(M),RHO(M),CEE(M),GEN(M)
  WRITE (IOUT,605) M,CAY(M),RHO(M),CEE(M),GEN(M)

*****
NODAL COORDINATES
*****
WRITE (IOUT,606)
DO 4 K=1,NN
  READ (IIN,504) J,X(J),Y(J)
  WRITE (IOUT,607) J,X(J),Y(J)

```



```

C
C *****
C ELEMENT INFORMATION
C *****
  WRITE (IDOUT,608)
  IBW = 0
  DO 11 K=1,NE
    READ (IIN,505) I,IN(I),JN(I),KN(I),MN(I)
    IF (IN(I)-JN(I)) 6,6,5
5      ITEM = IN(I)
      IN(I) = JN(I)
      JN(I) = ITEM
6      IF (JN(I)-KN(I)) 9,9,7
7      ITEM = JN(I)
      JN(I) = KN(I)
      KN(I) = ITEM
      IF (IN(I)-JN(I)) 9,9,8
8      ITEM = IN(I)
      IN(I) = JN(I)
      JN(I) = ITEM
9      ICMAX = KN(I) - IN(I) + 1
      IF (ICMAX-IBW) 11,11,10
10     IBW = ICMAX
11     WRITE (IDOUT,609) I,IN(I),JN(I),KN(I),MN(I)
  LABEL = 0
  RETURN
99 LABEL = 1
  RETURN
C
C *****
C FORMAT STATEMENTS
C *****
501 FORMAT (20A4)
502 FORMAT (8I5)
503 FORMAT (I5,4F10.0)
504 FORMAT (I5,2F10.0)
505 FORMAT (5I5)
601 FORMAT ('1',15X,20A4)
602 FORMAT ('O',15X,'NG  NC  NH  NQ  NT  NN  NE  NM')
603 FORMAT (' ',15X,I2,9I5)
604 FORMAT ('O',15X,'MATERIAL PROPERTIES'/
1      ' ',15X,'MATL.  CAY  RHO  CEE  GEN')
605 FORMAT (' ',15X,I3,4F9.2)
606 FORMAT ('O',15X,'COORDINATES OF NODES'/
1      ' ',15X,'NODE',4X,'X',8X,'Y')
607 FORMAT (' ',15X,I3,2F9.3)
608 FORMAT ('O',15X,'ELEMENT INFORMATION'/
1      ' ',15X,'ELM.  I  J  K  MATL.')
609 FORMAT (' ',15X,I3,I6,2I4,I5)
  END

```



```

SUBROUTINE FORM
IMPLICIT REAL*8(A-H,O-Z)
*****
C * FORM ELEMENT CONDUCTION, GENERATION, *
C * AND CAPACITANCE MATRICES *
C *****
C
C *****
C DIMENSIONS
C *****
COMMON BN(500,30),CN(500,30),SN(500,30),SP(500),Y(500),X(500),
*T(500),GN(500),RN(500),GEN(50),CEE(50),RHO(50),CAY(50),TIMAX,
*DTIME,TIME,NTOUT(500),MN(500),NRL(500),KN(500),JN(500),IN(500),JC,
* ICOUNT,NTIME,NT,NQ,NH,NC,NG,NE,NN,IBW,IOUT,IIN

C
C DIMENSION ID(3), SE(3,3)
C
C *****
C INITIALIZE
C *****
DO 1 J=1,NN
  GN(J) = 0.0
  SP(J) = 0.0
  DO 1 K=1,IBW
    CN(J,K) = 0.0
    SN(J,K) = 0.0
1
C
C *****
C ELEMENT CONDUCTION MATRICES
C *****
I = 0
4 I = I + 1
5 IF (I-NE) 5,5,99
  INN=IN(I)
  JNN=JN(I)
  KNN=KN(I)
  MNN=MN(I)
  XIJ=X(JNN)-X(INN)
  XIK=X(KNN)-X(INN)
  XJK=X(KNN)-X(JNN)
  YIJ=Y(JNN)-Y(INN)
  YIK=Y(KNN)-Y(INN)
  YJK=Y(KNN)-Y(JNN)
  AIJK = DABS(XIJ*YIK - XIK*YIJ)/2.0
  E2=(CAY(MNN))/(4.0*AIJK)
  SE(1,1) = E2*(XJK**2 + YJK**2)
  SE(1,2) = -E2*(XIK*XJK + YIK*YJK)
  SE(1,3) = E2*(XIJ*XJK + YIJ*YJK)
  SE(2,2) = E2*(XIK**2 + YIK**2)
  SE(2,3) = -E2*(XIJ*XIK + YIJ*YIK)
  SE(3,3) = E2*(XIJ**2 + YIJ**2)
  ID(1) = IN(I)
  ID(2) = JN(I)
  ID(3) = KN(I)
  DO 6 J=1,3
    IR = ID(J)

```



```

        DO 6 K=J,3
          IC = ID(K) - IR + 1
          SN(IR,IC) = SN(IR,IC) + SE(J,K)
6      C
      C
      C *****
      C ELEMENT GENERATION MATRICES
      C *****
      IF (NG) 9,9,7
7      E2=(GEN(MNN)*AIJK)/3.0
        DO 8 J=1,3
          IR = ID(J)
          GN(IR) = GN(IR) + E2
8      C
      C
      C *****
      C ELEMENT CAPACITANCE MATRICES
      C *****
9      IF (NC) 12,12,10
10     E2=((RHO(MNN))*(CEE(MNN))*AIJK)/12.0
        SE(1,1) = 2.0*E2
        SE(1,2) = E2
        SE(1,3) = E2
        SE(2,2) = 2.0*E2
        SE(2,3) = E2
        SE(3,3) = 2.0*E2
        DO 11 J=1,3
          IR = ID(J)
          DO 11 K=J,3
            IC = ID(K) - IR + 1
            CN(IR,IC) = CN(IR,IC) + SE(J,K)
11
12     GO TO 4
99     RETURN
      END

```



```

SUBROUTINE BINT
  IMPLICIT REAL*8(A-H,O-Z)
  *****
  * SET UP MATRICES FOR CONVECTION AND NON-ZERO *
  * HEAT FLUX BOUNDARY CONDITIONS *
  *****

  *****
  DIMENSIONS
  *****
  COMMON BN(500,30),CN(500,30),SN(500,30),SP(500),Y(500),X(500),
  *T(500),GN(500),RN(500),GEN(50),CEE(50),RHO(50),CAY(50),TIMAX,
  *DIME,TIME,NTOUT(500),MN(500),NRL(500),KN(500),JN(500),IN(500),JC,
  * ICOUNT,NTIME,NT,NQ,NH,NC,NG,NE,NN,IBW,IOUT,IIN

  *****
  CONVECTION BOUNDARY LINES
  *****
  IF (NH) 5,5,1
    WRITE (IOUT,603)
    DO 4 J=1,NH
      READ (IIN,502) IS,JS,H,TAMB
      IF (IS - JS) 3,3,2
        ITEM = IS
        IS = JS
        JS = ITEM
        WRITE (IOUT,604) J,IS,JS,H,TAMB
        IC = JS - IS + 1
        XIJ = X(JS) - X(IS)
        YIJ = Y(JS) - Y(IS)
        SIJ = DSQRT(XIJ**2 + YIJ**2)
        E2 = (H*SIJ)/6.0
        SN(IS,1) = SN(IS,1) + 2.0*E2
        SN(IS,IC) = SN(IS,IC) + E2
        SN(JS,1) = SN(JS,1) + 2.0*E2
        E2 = (H*SIJ*TAMB)/2
        GN(IS) = GN(IS) + E2
        GN(JS) = GN(JS) + E2
    CONTINUE

  *****
  NON-ZERO HEAT FLUX BOUNDARY LINES
  *****
  IF (NQ) 10,10,6
    WRITE (IOUT,605)
    DO 9 J=1,NQ
      READ (IIN,503) IS,JS,Q
      IF (IS - JS) 8,8,7
        ITEM = IS
        IS = JS
        JS = ITEM
        WRITE (IOUT,606) J,IS,JS,Q
        XIJ = X(JS) - X(IS)
        YIJ = Y(JS) - Y(IS)
        SIJ = DSQRT(XIJ**2 + YIJ**2)
        E2 = (Q*SIJ)/2.0
        GN(IS) = GN(IS) + E2

```



```

          GN(JS) = GN(JS) + E2
9         CONTINUE
10        RETURN
C
C
C *****
C  FORMAT STATEMENTS
C *****
502       FORMAT (2I5,2F10.0)
503       FORMAT (2I5,F10.0)
603       FORMAT ('O',15X,'CONVECTION BOUNDARY LINES'/
1         ' ',15X,'LINE   I   J   HCON   TAMB')
604       FORMAT (' ',15X,I3,I6,I4,F8.2,F10.3)
605       FORMAT ('O',15X,'NON-ZERO HEAT FLUX BOUNDARY LINES'/
1         ' ',15X,'LINE   I   J   FLUX')
606       FORMAT (' ',15X,I3,I6,I4,F8.2)
        END

```



```

SUBROUTINE INIT
IMPLICIT REAL*8(A-H,O-Z)
*****
C   * READ INITIAL CONDITIONS *
C   *****
C
C   *****
C   DIMENSIONS
C   *****
C   COMMON BN(500,30),CN(500,30),SN(500,30),SP(500),Y(500),X(500),
*   T(500),GN(500),RN(500),GEN(50),CEE(50),RHO(50),CAY(50),TIMAX,
*   DTIME,TIME,NTOUT(500),MN(500),NRL(500),KN(500),JN(500),IN(500),JC,
*   ICOUNT,NTIME,NT,NQ,NH,NC,NG,NE,NN,IBW,IOUT,IIN
C
C   *****
C   INITIAL AND MAXIMUM TIME
C   *****
C   READ (IIN,501) TIME,TIMAX
C   WRITE (IOUT,601) TIME, TIMAX
C
C   *****
C   INITIAL CONDITIONS
C   *****
C   DO 1 J=1,NN
C       READ (IIN,502) K,T(K)
1       WRITE (IOUT,602) K,T(K)
C   RETURN
C
C   *****
C   FORMAT STATEMENTS
C   *****
501  FORMAT (2F10.0)
502  FORMAT (I5,F10.0)
601  FORMAT ('O',15X,'INITIAL TIME=',E13.6,4X,'MAXIMUM TIME=',E13.6/
1      'O',15X,'INITIAL TEMPERATURES'/
2      ' ',15X,'NODE    TEMP. ')
602  FORMAT (' ',15X,I3,F10.3)
END

```



```

SUBROUTINE TRANS
IMPLICIT REAL*8(A-H,O-Z)
*****
C      * SET UP TRANSIENT ALGORITHMS *
C      *****
C
C      *****
C      DIMENSIONS
C      *****
COMMON BN(500,30),CN(500,30),SN(500,30),SP(500),Y(500),X(500),
*T(500),GN(500),RN(500),GEN(50),CEE(50),RHO(50),CAY(50),TIMAX,
*DTIME,TIME,NTOUT(500),MN(500),NRL(500),KN(500),JN(500),IN(500),JC,
*   ICOUNT,NTIME,NT,NQ,NH,NC,NG,NE,NN,IBW,IOUT,IIN
C
C      *****
C      TIME INCREMENT
C      *****
READ (IIN,501) DTIME
WRITE (IOUT,601) DTIME
C
C      *****
C      PRINTOUT TIMES
C      *****
READ (IIN,502) NTIME
WRITE (IOUT,602) NTIME
READ (IIN,503) (NTOUT(I),I=1,NTIME)
WRITE (IOUT,603)
WRITE (IOUT,604) (NTOUT(I),I=1,NTIME)
C
C      *****
C      TRANSIENT COMPUTATIONAL METHOD
C      *****
ICOUNT = 0
JC = 1
GO TO (1,3,5), NC
C
C      *****
C      EULERS METHOD - NC=1
C      *****
1   DO 2 J=1,NN
      DO 2 K=1,IBW
        BN(J,K) = CN(J,K) - DTIME*SN(J,K)
        SN(J,K) = CN(J,K)
2   WRITE (IOUT,605)
      GO TO 7
C
C      *****
C      CRANK-NICHOLSON METHOD - NC=2
C      *****
3   DT2 = DTIME/2.0
      DO 4 J=1,NN
        DO 4 K=1,IBW
          BN(J,K) = CN(J,K) - DT2*SN(J,K)
          SN(J,K) = CN(J,K) + DT2*SN(J,K)
4

```



```

WRITE (IOUT,606)
GO TO 7

C
C
C *****
C PURE-IMPLICIT METHOD - NC=3
C *****
5 DO 6 J=1,NN
    DO 6 K=1,IBW
        BN(J,K) = CN(J,K)
6        SN(J,K) = CN(J,K) + DTIME*SN(J,K)
    WRITE (IOUT,607)
7    RETURN
C
C
C *****
C FORMAT STATEMENTS
C *****
501 FORMAT (F10.0)
502 FORMAT (I5)
503 FORMAT (16I6)
601 FORMAT ('O',15X,'TIME INCREMENT =',E13.6)
602 FORMAT ('O',15X,'NUMBER OF OUTPUT TIMES=',I5)
603 FORMAT ('O',15X,'MULTIPLES OF TIME INCREMENT AT WHICH RESULTS ',
1      'ARE BEING PRINTED')
604 FORMAT (' ',15X,16I6)
605 FORMAT ('O',15X,'EULERS METHOD IS BEING USED')
606 FORMAT ('O',15X,'CRANK-NICHOLSON METHOD IS BEING USED')
607 FORMAT ('O',15X,'PURE-IMPLICIT METHOD IS BEING USED')
END

```



```

SUBROUTINE MODSN
IMPLICIT REAL*8(A-H,O-Z)
*****
* READ SPECIFIED TEMPERATURES *
* AND MODIFY MATRICES *
*****

*****
DIMENSIONS
*****
COMMON BN(500,30),CN(500,30),SN(500,30),SP(500),Y(500),X(500),
*T(500),GN(500),RN(500),GEN(50),CEE(50),RHO(50),CAY(50),TIMAX,
*DTIME,TIME,NTOUT(500),MN(500),NRL(500),KN(500),JN(500),IN(500),JC,
* ICOUNT,NTIME,NT,NQ,NH,NC,NG,NE,NN,IBW,IOUT,IIN

*****
SPECIFIED NODAL TEMPERATURES
*****
WRITE (IOUT,605)
DO 12 J=1,NN
  12  NRL(J) = 0
DO 13 J=1,NT
  13  READ (IIN,504) K,T(K)
     13  NRL(K) = 1
     13  WRITE (IOUT,606) K,T(K)

*****
MODIFY SN AND SP MATRICES FOR SPECIFIED NODAL TEMPERATURES
*****
DO 14 J=1,NN
  14  IF (NRL(J)) 14,14,2
     14  IF (J-1) 7,7,3
     14  IL = 1
     14  IU = J - 1
     14  IF (J-IBW) 5,5,4
     14  IL = J - IBW + 1
     14  DO 6 I=IL,IU
     14  K = J - I + 1
     14  SP(I) = SP(I)-SN(I,K)*T(J)
     14  SN(I,K) = 0.0
     14  IF (NN-J) 15,15,8
     14  KL = 2
     14  KU = IBW
     14  IF (J-NN+IBW-1) 10,10,9
     14  KU = NN - J + 1
     14  DO 11 K=KL,KU
     14  I = J + K - 1
     14  SP(I) = SP(I)-SN(J,K)*T(J)
     14  SN(J,K) = 0.0
     14  SN(J,1) = 1.0
15  CONTINUE
14  RETURN

*****
FORMAT STATEMENTS
*****

```



```
504  FORMAT (I5,F10.0)
605  FORMAT ('O',15X,'SPECIFIED NODAL TEMPERATURES'/
1    ' ',15X,'NODE    TEMP. ')
606  FORMAT (' ',15X,I3,F10.3)
      END
```



```

SUBROUTINE DBAND(N,IBW,U,LABEL)
IMPLICIT REAL*8(A-H,O-Z)
C *****
C * DECOMPOSE SYMMETRIC BANDED MATRIX *
C *****
C
C *****
C ARGUMENTS-
C
C N      - NUMBER OF NODAL POINTS
C IBW    - UPPER BAND WIDTH
C U      - RESULT OF DECOMPOSITION ALGORITHM
C LABEL  - END OF FILE INDICATOR
C          = 0 IF EXECUTION IS TO CONTINUE
C          = 1 IF EXECUTION IS TO TERMINATE
C *****
C
C *****
C DIMENSION
C *****
C DIMENSION U(500,30)
C
C *****
C DOUBLE PRECISION DSUM, D1, D2, D3, DSQRT
C *****
C
C *****
C DECOMPOSE BAND (MAY REQUIRE DOUBLE PRECISION ACCUMULATORS. CHANGE
C SQRT TO DSQRT ON CARD FHT20649 AND ACTIVATE DOUBLE PRECISION
C DECLARATION ON CARD FHT20619.)
C *****
C DO 13 I=1,N
C   IP = N - I + 1
C   IF (IBW - IP) 2,3,3
C 2   IP = IBW
C 3   DO 13 J=1,IP
C     IQ = IBW - J
C     IF (I - IQ - 1) 4,5,5
C 4     IQ = I - 1
C 5     DSUM = U(I,J)
C     IF (IQ - 1) 8,6,6
C 6     DO 7 K=1,IQ
C       IMK = I - K
C       KP1 = K + 1
C       JPK = J + K
C       D1 = U(IMK,KP1)
C       D2 = U(IMK,JPK)
C       DSUM = DSUM - D1*D2
C 7     IF (J - 1) 12,9,12
C 8     IF (DSUM) 10,10,11
C 9     LABEL = 1
C 10    GO TO 14
C 11    D3 = 1.0/DSQRT(DSUM)
C     U(I,J) = D3
C     GO TO 13
C 12    U(I,J) = DSUM*D3

```



```
13  CONTINUE  
    LABEL = 0  
14  RETURN  
    END
```



```

SUBROUTINE RHS
IMPLICIT REAL*8(A-H,O-Z)
*****
C      * UPDATE RIGHT HAND SIDE *
C      *****
C
C      *****
C      DIMENSIONS
C      *****
COMMON BN(500,30),CN(500,30),SN(500,30),SP(500),Y(500),X(500),
*T(500),GN(500),RN(500),GEN(50),CEE(50),RHO(50),CAY(50),TIMAX,
*DTIME,TIME,NTOUT(500),MN(500),NRL(500),KN(500),UN(500),IN(500),JC,
*   ICOUNT,NTIME,NT,NQ,NH,NC,NG,NE,NN,IBW,IOUT,IIN
C
C      *****
C      STEADY STATE PROBLEMS
C      *****
IF (NC) 20,20,22
DO 21 J=1,NN
21   RN(J) = GN(J) + SP(J)
GO TO 9
C
C      *****
C      INCREASE TIME
C      *****
22   TIME = TIME + DTIME
ICOUNT = ICOUNT + 1
C
C      *****
C      COMPUTE NEW RIGHT HAND SIDE
C      *****
DO 8 J=1,NN
RN(J) = GN(J)*DTIME + SP(J)
KL = 1
KU = IBW
IF (J-NN+IBW-1) 2,2,1
1   KU = NN - J + 1
2   DO 3 K=KL,KU
JJ = J + K - 1
3   RN(J) = RN(J) + BN(J,K)*T(JJ)
IF (J-1) 8,8,4
4   KL = 2
KU = IBW
IF (J - IBW) 5,6,6
5   KU = J
6   DO 7 K=KL,KU
JJ = J - K + 1
7   RN(J) = RN(J) + BN(JJ,K)*T(JJ)
8   CONTINUE
9   RETURN
END

```



```

SUBROUTINE MODRN
IMPLICIT REAL*8(A-H,O-Z)
C *****
C * MODIFY RIGHT HAND SIDE FOR *
C * SPECIFIED TEMPERATURES *
C *****
C
C *****
C DIMENSIONS
C *****
COMMON BN(500,30),CN(500,30),SN(500,30),SP(500),Y(500),X(500),
*T(500),GN(500),RN(500),GEN(50),CEE(50),RHO(50),CAY(50),TIMAX,
*DTIME,TIME,NTOUT(500),MN(500),NRL(500),KN(500),JN(500),IN(500),JC,
* ICOUNT,NTIME,NT,NQ,NH,NC,NG,NE,NN,IBW,IOUT,IIN
C
C *****
C MODIFY RN MATRIX FOR SPECIFIED NODAL TEMPERATURES
C *****
DO 2 J=1,NN
  IF (NRL(J)) 2,2,1
    RN(J) = T(J)
1
2 CONTINUE
RETURN
END

```



```

SUBROUTINE RESUL(IFLAG)
IMPLICIT REAL*8(A-H,O-Z)
*****
C
C * PRINT RESULTS *
C *****
C
C *****
C ARGUMENT-
C
C IFLAG - PRINTOUT TIME FLAG
C      = 0 IF OUTPUT TIME SPECIFICATIONS ARE CORRECT
C      = 1 IF CALCULATIONS EXTEND BEYOND THE RANGE OF THE OUTPUT
C      = 2 IF THE NUMBER OF OUTPUT TIMES DOES NOT MATCH THE
C          NUMBER OF MULTIPLES OF THE TIME INCREMENT INPUT
C *****
C
C *****
C DIMENSIONS
C *****
COMMON BN(500,30),CN(500,30),SN(500,30),SP(500),Y(500),X(500),
*T(500),GN(500),RN(500),GEN(50),CEE(50),RHO(50),CAY(50),TIMAX,
*DTIME,TIME,NTOUT(500),MN(500),NRL(500),KN(500),JN(500),IN(500),JC,
*   ICOUNT,NTIME,NT,NQ,NH,NC,NG,NE,NN,IBW,IOUT,IIN
C
C *****
C STEADY STATE OR TRANSIENT PROBLEM
C *****
IF (NC) 1,1,3
C
C *****
C PRINT NODAL TEMPERATURES - STEADY STATE PROBLEMS
C *****
1  WRITE (IOUT,601)
   DO 2 J=1,NN
2   WRITE (IOUT,602) J,T(J)
   GO TO 7
C
C *****
C PRINT NODAL TEMPERATURES - TRANSIENT PROBLEMS
C *****
3  IF (TIME - DTIME) 4,4,5
4   WRITE (IOUT,603)
5   CONTINUE
   IF (ICOUNT - NTOUT(JC)) 7,10,9
10  WRITE (IOUT,604) TIME
   DO 6 J=1,NN
6   WRITE (IOUT,605) J,T(J)
   JC = JC + 1
   IF (JC - NTIME - 1) 7, 7, 11
7   CONTINUE
8   RETURN
C
C *****
C SET PRINTOUT TIME FLAG

```



```

C      *****
9      IFLAG = 1
      GO TO 8
11     IFLAG = 2
      GO TO 8

C
C
C      *****
C      FORMAT STATEMENTS
C      *****
601    FORMAT ('O',15X,'STEADY STATE TEMPERATURE DISTRIBUTION'/
1      ' ',15X,'NODE          TEMP. ')
602    FORMAT (' ',15X,I3,E17.6)
603    FORMAT ('O',15X,'TRANSIENT TEMPERATURE VARIATION')
604    FORMAT ('O',15X,'TIME =',E13.6,'      NODE          TEMP. ')
605    FORMAT (' ',15X,I25,E17.6)
      END

```



```

C      file #2 - "ELEV.HEAD2" and Calculate
C      Depth to node
C      -----
C
      DO 3000 I=1,240
      READ(2,3001)Z(I)
3000  D(I)=100.0-Z(I)
3001  FORMAT(G20.0)
C
C      Read New Formation Temperatures
C      from file #3 - "TEMP.IN2"
C      -----
C
      DO 3002 I=1,260
      READ(3,3003)NODEN(I),TNUT(I)
3002  IF(TNUT(I).LT.5.0)TNUT(I)=5.0
3003  FORMAT(2G20.0)
C
      LSOD=-1
      LOG=0
      DO 3411 J=1,20
      LSOD=LSOD+1
        DO 3412 L=1,12
        LOG=LOG+1
        LSOD=LSOD+1
        NODE(LOG)=NODEN(LSOD)
        T(LOG)=TNUT(LSOD)
3412  CONTINUE
3411  CONTINUE
C
C      Read Previous Formation Temperatures
C      from file #4 - "TEMP.PREV2"
C      -----
C
      DO 3004 I=1,240
      READ(4,3003)NODE(I),TPREV(I)
3004  IF(TPREV(I).LT.5.0)TPREV(I)=5.0
      REWIND 4
C
C      Read New Total Heads From
C      File #5 - "TOTAL.HEAD2"
C      -----
C
      DO 6000 I=1,240
      READ(5,6001)THEAD(I)
6000  READ(5,6001)THEAD(I)
6001  FORMAT(G20.0)
C
C      Store New Formation Temperatures
C      in file #4 - "TEMP.PREV2"
C      -----
C
      DO 3005 I=1,240
      WRITE(4,3006)NODE(I),T(I)
3005  WRITE(4,3006)NODE(I),T(I)
3006  FORMAT(I5,',',F10.5,',')
C
C      Variable Calculations
C      -----
C
      DO 1 I=1,240
      TEMP=T(I)

```



```

C      TEMPVS=TPREV(I)
C
C      Calculate change in temperature at each node
C      -----
C
C      DT(I)=T(I)-TPREV(I)
C
C      Calculate Incremental coefficient of
C      Thermal Expansion for Water
C      -----
C
C      CALL ALPHAW(TEMP,AWSPC)
C      AW(I)=AWSPC
C
C      Calculate Incremental Coeffiecient of
C      Thermal Expansion for Bitumen
C      -----
C
C      CALL ALPHAB(TEMP,ABSPC)
C      AB(I)=ABSPC
C
C      Calculate Incremental Coeffiecient of
C      Thermal Expansion for Soil Structure
C      -----
C
C      CALL ALPHST(TEMP,ASTSPC)
C      AST(I)=ASTSPC
C
C      Calculate Incremental Coefficient of
C      Thermal Expansion for Sand Grains
C      -----
C
C      CALL ALPHAS(TEMP,ASSPC)
C      AS(I)=ASSPC
C
C      Calculate Coefficient of Compressibility
C      of Water
C      -----
C
C      CALL MWATER(TEMP,MWSPC)
C      MW(I)=MWSPC
C
C      Calculate Cummulative Volume Change of
C      Bitumen at new Temperature
C      -----
C
C      CALL TEXBIT(TEMP,BITSPC)
C      BIT(I)=BITSPC
C
C      Calculate Cummulative Volume Change of
C      Bitumen at Previous Temperature
C      -----
C
C      CALL TEXBIT(TEMPVS,BITS)
C      BITVS(I)=BITS
C
C      Calculate Cummulative Volume Change of
C      Water at new Temperature
C      -----
C

```



```

      CALL TEXWAT(TEMP,WATSPC)
      WAT(I)=WATSPC
C
C      Calculate Cummulative Volume Change of
C      Water at Previous Temperature
C      -----
C
      CALL TEXWAT(TEMPVS,WATS)
      WATVS(I)=WATS
C
C      Calculate Unit Weight of Bitumen and
C      Water at New Temperature
C      -----
C
      VOB(I)=100.+BIT(I)
      VOW(I)=100.+WAT(I)
      GAMMAW(I)=981./VOW(I)
      GAMMAB(I)=1010.43/VOB(I)
      VOBB(I)=VOB(I)*0.886
      VOWW(I)=VOW(I)*0.114
      GAMMAF(I)=VOBB(I)/(VOBB(I)+VOWW(I))*GAMMAB(I)+
&      VOWW(I)/(VOBB(I)+VOWW(I))*GAMMAW(I)
C
C      Calculate Unit Weight of Bitumen and
C      Water at Previous Temperature
C      -----
C
      VOBVS(I)=100.+BITVS(I)
      VOWVS(I)=100.+WATVS(I)
      GAWVS(I)=981./VOWVS(I)
      GABVS(I)=1010.43/VOBVS(I)
      VOBBVS(I)=VOBVS(I)*0.886
      VOWWVS(I)=VOWVS(I)*0.114
      GAFVS(I)=VOBBVS(I)/(VOBBVS(I)+VOWWVS(I))*GABVS(I)+
&      VOWWVS(I)/(VOBBVS(I)+VOWWVS(I))*GAWVS(I)
C
C      Calculate Change in Unit Weight due to
C      Temperature Change
C      -----
C
      DGAMF(I)=GAMMAF(I)-GAFVS(I)
      DGAMB(I)=GAMMAB(I)-GABVS(I)
      DGAMW(I)=GAMMAW(I)-GAWVS(I)
C
C      Calculate in situ Viscosity for Bitumen
C      -----
C
      VISCH4(I)=(1.9661227*10.**9.)*(T(I)**(-4.936318))
      VISCO2(I)=(3.5066118*10.**7.)*(T(I)**(-4.107852))
      VSITU(I)=(VISCH4(I)*.8)+(VISCO2(I)*.2)
C
C      Calculate Viscosity for Water
C      -----
C
      CALL VISWAT(TEMP,VWSPC)
      VISW(I)=VWSPC
C
C

```


C Calculate Viscosity for Fluid (bitumen & water)
 C -----
 C

$$\text{VISF(I)} = .886 * \text{VSITU(I)} + .114 * \text{VISW(I)}$$

C Calculate in situ Hydraulic Conductivity
 C -----
 C

$$\text{PERM(I)} = (\text{GAMMAF(I)} * 3.0\text{E-}12) / (\text{VISF(I)} / 1000.)$$

C Calculate Coefficient of Compressibility
 C For Bitumen
 C -----
 C

$$\text{MB(I)} = (-6.25\text{E-}9 * \text{T(I)}) + 2.15\text{E-}6$$

C Calculate change in pore fluid pressure
 C -----
 C

$$\begin{aligned} & \text{DU(I)} = (\text{NB} * \text{DT(I)} * (\text{AB(I)} - \text{AS(I)}) + \text{NW} \\ & \& * \text{DT(I)} * (\text{AW(I)} - \text{AS(I)}) - \text{AST(I)} * \text{DT(I)} + \text{MV} * (\text{NB} \\ & \& * \text{DGAMB(I)} * \text{D(I)} + \text{NW} * \text{DGAMW(I)} * \text{D(I)})) / (\text{MV} + \text{NB} \\ & \& * (\text{MB(I)} + \text{NW} * (\text{MW(I)}))) \end{aligned}$$

C Set pore pressure change at surface nodes
 C to zero
 C -----
 C

```

IF(I.EQ.12)DU(I)=0.0
IF(I.EQ.24)DU(I)=0.0
IF(I.EQ.36)DU(I)=0.0
IF(I.EQ.48)DU(I)=0.0
IF(I.EQ.60)DU(I)=0.0
IF(I.EQ.72)DU(I)=0.0
IF(I.EQ.84)DU(I)=0.0
IF(I.EQ.96)DU(I)=0.0
IF(I.EQ.108)DU(I)=0.0
IF(I.EQ.120)DU(I)=0.0
IF(I.EQ.132)DU(I)=0.0
IF(I.EQ.144)DU(I)=0.0
IF(I.EQ.156)DU(I)=0.0
IF(I.EQ.168)DU(I)=0.0
IF(I.EQ.180)DU(I)=0.0
IF(I.EQ.192)DU(I)=0.0
IF(I.EQ.204)DU(I)=0.0
IF(I.EQ.216)DU(I)=0.0
IF(I.EQ.228)DU(I)=0.0
IF(I.EQ.240)DU(I)=0.0

```

C Calculate change in pressure Head
 C -----
 C

$$\text{DPHEAD(I)} = \text{DU(I)} / \text{GAMMAF(I)}$$

C Calculate new total Head
 C -----
 C

$$\text{THEAD(I)} = \text{THEAD(I)} + \text{DPHEAD(I)}$$


```

C
C      Check if Pore Fluid Pressure > Total Stress
C      if so, set Pore Fluid Pressure = Total Stress
C      Calculate New Total Head
C      -----
C
C      Total Stress due to tank
C      = 14.63 m * 8.713 KN/m3 + .3048 m * 76.979 KN/m3
C      = 150.93 KPa
C
C      Total Stress due to Gravel Pad
C      = 2 m * 21.21 KN/m3 = 42.42 KPa
C
C      TANK=0.0
C      PAD=0.0
C      IF(I.LE.96)TANK=150.93
C      IF(I.LE.156)PAD=42.42
C      NS=1.0-NB-NW
C      TSTRES(I)=D(I)*(NB*GAMMAB(I)+NW*GAMMAW(I)+NS*GAMMAS)+TANK
&      +PAD
C      IF(((THEAD(I)-Z(I))*GAMMAF(I)).LE.TSTRES(I))GO TO 9000
C      THEAD(I)=TSTRES(I)/GAMMAF(I)+Z(I)
C
C      Calculate generation rate
C      -----
C
C      9000      G(I)=(NW*AW(I)*DT(I)+NB*AB(I)*DT(I)
&      +AS(I)*DT(I)*(NB+NW)-AST(I)*DT(I))/TIMEIN
C
C      Calculate specific storage coefficient
C      -----
C
C      SS(I)=((NW*MW(I)*GAMMAW(I))+(NB*MB(I)*GAMMAB(I))
&      -(MV*GAMMAF(I))*GAMMAF(I)
C      1 CONTINUE
C
C      Set Generation rate for surface nodes equal to
C      zero
C      -----
C
C      DO 51 J=12,240,12
C      51 G(J)=0.0
C
C      Calculate hydraulic conductivity, generation rate and
C      specific storage for each element
C      -----
C      WRITE(9,3085)
C      3085  FORMAT(3X,'ELEM',2X,'NODE',2X,'NODE',2X,'NODE',2X,
&      *'NODE',2X,'PERMEL',10X,'GEL',12X,'SSEL',/)
C
C      DO 4000 I=1,209
C      READ(7,4001)MNK1,MNK2,MNK3,MNK4
C      PERMEL(I)=(PERM(MNK1)+PERM(MNK2)+PERM(MNK3)
&      +PERM(MNK4))/4.
C      GEL(I)=(G(MNK1)+G(MNK2)+G(MNK3)+G(MNK4))/4.
C      SSEL(I)=(SS(MNK1)+SS(MNK2)+SS(MNK3)+SS(MNK4))/4.
C      WRITE(9,2298)I,MNK1,MNK2,MNK3,MNK4,PERMEL(I),GEL(I),SSEL(I)
C      2298  FORMAT(3X,5I5,3X,E12.6,3X,E12.6,3X,E12.6)
C      4000 CONTINUE

```



```

4001 FORMAT(4I5)
C
C
C   PRINT OUTPUT
C   -----
C
C   DATA CHECK
C
      WRITE(9,9600)
9600  FORMAT('1',2X,'I',8X,'T',10X,'TPREV',9X,'DT',13X,'D',14X,
* 'AB',12X,'AS',12X,'AW',10X,'AST',//)
      DO 8989 I=1,240
        WRITE(9,96)I,T(I),TPREV(I),DT(I),D(I),AB(I),AS(I),AW(I),
&AST(I)
8989  CONTINUE
      WRITE(9,9700)
9700  FORMAT('1',2X,'I',5X,'DGAMB',9X,'DGAMW',12X,'MB',10X,'MW',
*12X,'DU',12X,'GAMMAF',//)
      DO 8976 I=1,240
8976  WRITE(9,96)I,DGAMB(I),DGAMW(I),MB(I),MW(I),DU(I),GAMMAF(I)
      WRITE(9,9800)
9800  FORMAT('1',2X,'I',6X,'DPHEAD',8X,'TSTRES',8X,'THEAD',10X,
* 'G',12X,'SS',12X,'PERM'//)
      DO 8977 I=1,240
8977  WRITE(9,96)I,DPHEAD(I),TSTRES(I),THEAD(I),G(I),SS(I),PERM(I)
96   FORMAT(G5,2X,E12.6,2X,E12.6,2X,E12.6,2X,E12.6,2X,E12.6,
*2X,E12.6,2X,E12.6,2X,E12.6)
C
      READ(1,100)(HED(I),I=1,16)
100  FORMAT(20A4)
      WRITE(6,100)(HED(I),I=1,16)
      READ(1,101)NUMNP,NEGL,NEGNL,MODEX,NPER,TSTART,IPRI,ITP56
101  FORMAT(5I5,F10.2,2I5)
      WRITE(6,101)NUMNP,NEGL,NEGNL,MODEX,NPER,TSTART,IPRI,ITP56
      READ(1,102)IHEAT,IHEATN
102  FORMAT(2I5)
      WRITE(6,102)IHEAT,IHEATN
      READ(1,103)IEIG
103  FORMAT(I5)
      WRITE(6,103)IEIG
      READ(1,104)ISREF,IEQUIT,ITEMAX,RTOL
104  FORMAT(3I5,E10.4)
      WRITE(6,104)ISREF,IEQUIT,ITEMAX,RTOL
      READ(1,105)IOPE,ALPHA
105  FORMAT(I10,F10.1)
      WRITE(6,105)IOPE,ALPHA
      READ(1,106)NPB
106  FORMAT(I5)
      WRITE(6,106)NPB
      READ(1,107)IPNODE
107  FORMAT(I5)
      WRITE(6,107)IPNODE
      READ(1,108)NSPER
108  FORMAT(I5)
      WRITE(6,108)NSPER
      READ(1,109)DTPER
109  FORMAT(F10.2)
      WRITE(6,109)DTPER
      DO 1000 I=1,240
        READ(1,110)IT(I),N(I),JPR(I),ID(I),X(I),Y(I),Z(I),KN(I)

```



```

110 FORMAT(A1,I4,A1,I4,3F10.1,I5)
WRITE(6,110)IT(I),N(I),JPR(I),ID(I),X(I),Y(I),Z(I),KN(I)
1000 CONTINUE
READ(1,111)ICON,IPRIC
111 FORMAT(2I5)
WRITE(6,111)ICON,IPRIC
LNNN=0
LMNO=-1
DO 9990 J=1,19
  LMNO=LMNO+1
  DO 9991 I=1,11
    LNNN=LNNN+1
    LMNO=LMNO+1
    THIN(LNNN)=THEAD(LMNO)
9991 CONTINUE
9990 CONTINUE
WRITE(6,112)(THEAD(K),K=1,240)
112 FORMAT(6E12.6)
READ(1,113)NTTF,NPTM,ILCOV,NTEMP,NOCV,NORA,NLOAD,NIHT,NTOT
113 FORMAT(9I5)
WRITE(6,113)NTTF,NPTM,ILCOV,NTEMP,NOCV,NORA,NLOAD,NIHT,NTOT
DO 9944 KK=1,2
  READ(1,114)NTF,NPTS
114 FORMAT(2I5)
WRITE(6,114)NTF,NPTS
READ(1,115)TIMV1,RV1,TIMV2,RV2
115 FORMAT(4F10.1)
9944 WRITE(6,115)TIMV1,RV1,TIMV2,RV2
DO 4465 IB=1,2
  READ(1,4466)NUD,NCOR,FUC,BSTRT,KNKN
4466 FORMAT(2I5,2F10.1,I5)
WRITE(6,4466)NUD,NCOR,FUC,BSTRT,KNKN
4465 CONTINUE
READ(1,116)NEG(I),NGL(I),NTE(I)
WRITE(6,116)NEG(I),NGL(I),NTE(I)
DO 1003 J=1,209
  READ(1,117)M(J),NCUR(J),FAC(J),STRT(J),KNN(J)
  IF(GEL(J).EQ.0.0)NCUR(J)=2
  WRITE(6,127)M(J),NCUR(J),GEL(J),STRT(J),KNN(J)
1003 CONTINUE
116 FORMAT(3I5)
117 FORMAT(2I5,2F10.0,I5)
127 FORMAT(2I5,E10.4,F10.1,I5)
READ(1,118)NPAR1,NPAR2,NPAR3,NPAR4,NPAR5,NPAR7,NPAR10,
&NPAR15,NPAR16,NPAR17,NPAR18
118 FORMAT(5I4,I8,I12,I20,3I4)
LLL=0
KKK=0
DO 2000 J=1,2
  NNNN=209
  IF(J.EQ.2)NPAR2=19
  IF(J.EQ.2)GO TO 2000
  IF(J.EQ.2)NPAR16=1
  IF(J.EQ.2)NPAR3=1
  IF(J.EQ.2)NPAR4=1
  WRITE(6,118)NPAR1,NPAR2,NPAR3,NPAR4,NPAR5,NPAR7,NPAR10,
&NPAR15,NPAR16,NPAR17,NPAR18
  DO 1008 I=1,NNNN
    LLL=LLL+1
    IF(LLL.GT.210)GO TO 1008

```



```

      READ(1,119)NN(LL)
1008 CONTINUE
      DO 1007 L=1,NNNN
      KKK=KKK+1
      IF(KKK.GT.210)GO TO 1007
      WRITE(6,119)NN(KKK)
119  FORMAT(I5)
      WRITE(6,122)PERMEL(KKK)
122  FORMAT(E10.4)
      WRITE(6,122)SSEL(KKK)
1007 CONTINUE
      DO 1005 K=1,NNNN
      READ(1,120)M2,IEL,MTYP,KG,BET,THIC,ETIME
120  FORMAT(4I5,3G10.0)
      WRITE(6,128)M2,IEL,MTYP,KG,BET,THIC,ETIME
128  FORMAT(4I5,3F10.1)
      READ(1,121)NOD1,NOD2,NOD3,NOD4,NOD5,NOD6,NOD7,NOD8
121  FORMAT(8I5)
      WRITE(6,121)NOD1,NOD2,NOD3,NOD4,NOD5,NOD6,NOD7,NOD8
1005 CONTINUE
2000 CONTINUE
C     WRITE(6,10)
C 10  FORMAT(12X,'T(C)',6X,'ALPHAW',9X,'ALPHAB',9X'ALPHAST',
C     *8X'ALPHAS',9X'MWATER')
C     DO 2 I=6,200
C 2  WRITE(6,11)T(I),AW(I),AB(I),AST(I),AS(I),MW(I)
C 11  FORMAT(10X,F5.1,4F15.8,F16.9)
      READ(1,7777)NUT1,NUT2,NUT3,NUT4,NUT5,NUT6,NUT7,NUT8,NUT9,
&NUT10
7777 FORMAT(I4,I8,4I4,I8,20X,I4,2I4)
      WRITE(6,7777)NUT1,NUT2,NUT3,NUT4,NUT5,NUT6,NUT7,NUT8,NUT9,
&NUT10
      READ(1,7778)NICE,CONVN
7778 FORMAT(I5,E10.4)
      WRITE(6,7778)NICE,CONVN
      DO 7779 III=1,2
      READ(1,7780)MUD,NODC1,NODC2,NODC3,ICTYP,KGLL,THUC,EATIME
7780 FORMAT(6I5,2F10.1)
      WRITE(6,7780)MUD,NODC1,NODC2,NODC3,ICTYP,KGLL,THUC,EATIME
7779 CONTINUE
      PRINT 2001
2001 FORMAT('STOP')
      STOP
      END

C
C
C  * * * * *
C  *      SUBROUTINE  ALPHAW      *
C  * * * * *
C
C
C  This subroutine calculates the incremental
C  coefficient of thermal expansion of water
C  for a given temperature
C
C
C  SUBROUTINE ALPHAW (TSPEC,AWSPC)
C  DIMENSION AW(35),TW(35)
C  DATA TW(1)/5.5/,TW(2)/8./,TW(3)/9.5/,TW(4)/10.5/,
C  *TW(5)/11.5/,TW(6)/12.5/,TW(7)/13.5/,TW(8)/14.5/,

```



```

*TW(9)/15.5/,TW(10)/16.5/,TW(11)/17.5/,TW(12)/18.5/,
*TW(13)/19.5/,TW(14)/21./,TW(15)/23.5/,TW(16)/26./,
*TW(17)/28.5/,TW(18)/35./,TW(19)/45./,TW(20)/55./,
*TW(21)/65./,TW(22)/75./,TW(23)/85./,TW(24)/95./,
*TW(25)/105./,TW(26)/115./,TW(27)/125./,TW(28)/135./,
*TW(29)/145./,TW(30)/155./,TW(31)/165./,TW(32)/175./,
*TW(33)/185./,TW(34)/195./,TW(35)/205.1/,AW(1)/3.34E-5/,
*AW(2)/5.E-5/,AW(3)/1.001E-4/,AW(4)/1.001E-4/,AW(5)/1.E-4/,
*AW(6)/1.001E-4/,AW(7)/1.001E-4/,AW(8)/2.E-4/,AW(9)/2.002E-4/,
*AW(10)/2.003E-4/,AW(11)/1.993E-4/,AW(12)/2.002E-4/,
*AW(12)/2.002E-4/,AW(13)/2.001E-4/,AW(14)/2.496E-4/,
*AW(15)/2.663E-4/,AW(16)/2.493E-4/,AW(17)/2.66E-4/,
*AW(18)/3.488E-4/,AW(19)/4.27E-4/,AW(20)/4.944E-4/,
*AW(21)/5.609E-4/,AW(22)/6.164E-4/,AW(23)/6.71E-4/,
*AW(24)/7.341E-4/,AW(25)/7.768E-4/,AW(26)/8.278E-4/,
*AW(27)/8.872E-4/,AW(28)/9.355E-4/,AW(29)/1.0009E-3/,
*AW(30)/1.0553E-3/,AW(31)/1.1077E-3/,AW(32)/1.1855E-3/,
*AW(33)/1.2603E-3/,AW(34)/1.3323E-3/,AW(35)/1.4274E-3/
AWSPC=-1.0
IF(TSPEC-TW(1)) 90,90,91
90 AWSPC=AW(1)
RETURN
91 IF(TSPEC-TW(35)) 93,92,92
92 AWSPC=AW(35)
RETURN
93 DO 100 J=1,35
IF(TSPEC-TW(J)) 100,94,100
94 AWSPC=AW(J)
RETURN
100 CONTINUE
MIN=1
MAX=35
102 CONTINUE
IF((MAX-MIN)-1) 200,200,104
104 NEXT=(MIN+MAX)/2
IF(TSPEC-TW(NEXT)) 105,105,107
105 MAX=NEXT
GO TO 102
107 MIN=NEXT
GO TO 102
200 I=MIN
TWFAC=(TSPEC-TW(I))/(TW(I+1)-TW(I))
AWSPC=AW(I)+TWFAC*(AW(I+1)-AW(I))
RETURN
END

```

C
C
C
C
C
C
C
C
C
C

```

* * * * *
*   SUBROUTINE  ALPHAB   *
* * * * *

```

This subroutine calculates the incremental
coefficient of thermal expansion of bitumen
for a given temperature

```

SUBROUTINE ALPHAB (TSPEC,ABSPC)
DIMENSION AB(19),TB(19)
DATA TB(1)/15./,TB(2)/25./,TB(3)/35./,TB(4)/45./,
*TB(5)/55./,TB(6)/65./,TB(7)/75./,

```



```

*TB(8)/85./,TB(9)/95./,TB(10)/105./,TB(11)/115./,
*TB(12)/125./,TB(13)/135./,TB(14)/145./,TB(15)/155./,
*TB(16)/165./,TB(17)/175./,TB(18)/185./,TB(19)/195./,
*AB(1)/1.0225E-3/,AB(2)/1.0185E-3/,AB(3)/1.0159E-3/,
*AB(4)/1.0143E-3/,AB(5)/1.0142E-3/,AB(6)/1.0153E-3/,
*AB(7)/1.0177E-3/,AB(8)/1.0212E-3/,AB(9)/1.0263E-3/,
*AB(10)/1.0323E-3/,AB(11)/1.0399E-3/,AB(12)/1.0486E-3/,
*AB(13)/1.0585E-3/,AB(14)/1.0699E-3/,AB(15)/1.0824E-3/,
*AB(16)/1.0962E-3/,AB(17)/1.1112E-3/,AB(18)/1.1277E-3/,
*AB(19)/1.1453E-3/
  ABSPC=-1.0
  IF(TSPEC-TB(1)) 90,90,91
90  ABSPC=AB(1)
  RETURN
91  IF(TSPEC-TB(19)) 93,92,92
92  ABSPC=AB(19)
  RETURN
93  DO 100 J=1,19
  IF(TSPEC-TB(J)) 100,94,100
94  ABSPC=AB(J)
  RETURN
100 CONTINUE
  MIN=1
  MAX=19
102 CONTINUE
  IF((MAX-MIN)-1) 200,200,104
104 NEXT=(MIN+MAX)/2
  IF(TSPEC-TB(NEXT)) 105,105,107
105 MAX=NEXT
  GO TO 102
107 MIN=NEXT
  GO TO 102
200 I=MIN
  TBFAC=(TSPEC-TB(I))/(TB(I+1)-TB(I))
  ABSPC=AB(I)+TBFAC*(AB(I+1)-AB(I))
  RETURN
END

```

```

C
C      * * * * *
C      *   SUBROUTINE  ALPHAST   *
C      * * * * *
C

```

```

C      This subroutine calculates the incremental
C      coefficient of thermal expansion of soil
C      structure for a given temperature
C
C

```

```

SUBROUTINE ALPHST (TSPEC,ASTSPC)
  DIMENSION AST(14),TST(14)
  DATA TST(1)/29.75/,TST(2)/43.75/,TST(3)/56.25/,
*TST(4)/68.75/,TST(5)/81.25/,TST(6)/93.75/,
*TST(7)/106.25/,TST(8)/118.75/,TST(9)/131.25/,
*TST(10)/143.75/,TST(11)/156.25/,TST(12)/168.75/,
*TST(13)/181.25/,TST(14)/193.75/,
*AST(1)/3.2E-5/,AST(2)/4.4E-5/,AST(3)/4.8E-5/,
*AST(4)/4.4E-5/,AST(5)/4.4E-5/,AST(6)/5.2E-5/,
*AST(7)/4.8E-5/,AST(8)/4.4E-5/,AST(9)/4.4E-5/,
*AST(10)/4.0E-5/,AST(11)/4.0E-5/,AST(12)/4.8E-5/,
*AST(13)/4.0E-5/,AST(14)/4.8E-5/

```



```

      ASTSPC=-1.0
      IF(TSPEC-TST(1)) 90,90,91
90    ASTSPC=AST(1)
      RETURN
91    IF(TSPEC-TST(14)) 93,92,92
92    ASTSPC=AST(14)
      RETURN
93    DO 100 J=1,14
      IF(TSPEC-TST(J)) 100,94,100
94    ASTSPC=AST(J)
      RETURN
100   CONTINUE
      MIN=1
      MAX=14
102   CONTINUE
      IF((MAX-MIN)-1) 200,200,104
104   NEXT=(MIN+MAX)/2
      IF(TSPEC-TST(NEXT)) 105,105,107
105   MAX=NEXT
      GO TO 102
107   MIN=NEXT
      GO TO 102
200   I=MIN
      TSTFAC=(TSPEC-TST(I))/(TST(I+1)-TST(I))
      ASTSPC=AST(I)+TSTFAC*(AST(I+1)-AST(I))
      RETURN
      END

```

C
C
C
C
C
C
C
C
C
C
C

```

* * * * *
*   SUBROUTINE  ALPHAS   *
* * * * *

```

This subroutine calculates the incremental
coefficient of thermal expansion of sand
grains for a given temperature

```

      SUBROUTINE ALPHAS (TSPEC,ASSPC)
      DIMENSION AS(5),TS(5)
      DATA TS(1)/20./,TS(2)/75./,TS(3)/125./,TS(4)/175./,
      *TS(5)/225./,
      *AS(1)/3.4E-5/,AS(2)/3.8E-5/,AS(3)/4.E-5/,
      *AS(4)/4.4E-5/,AS(5)/5.0E-5/
      ASSPC=-1.0
      IF(TSPEC-TS(1)) 90,90,91
90    ASSPC=AS(1)
      RETURN
91    IF(TSPEC-TS(5)) 93,92,92
92    ASSPC=AS(5)
      RETURN
93    DO 100 J=1,5
      IF(TSPEC-TS(J)) 100,94,100
94    ASSPC=AS(J)
      RETURN
100   CONTINUE
      MIN=1
      MAX=5
102   CONTINUE
      IF((MAX-MIN)-1) 200,200,104

```



```

104 NEXT=(MIN+MAX)/2
    IF(TSPEC-TS(NEXT)) 105,105,107
105 MAX=NEXT
    GO TO 102
107 MIN=NEXT
    GO TO 102
200 I=MIN
    TSFAC=(TSPEC-TS(I))/(TS(I+1)-TS(I))
    ASSPC=AS(I)+TSFAC*(AS(I+1)-AS(I))
    RETURN
END

C
C      * * * * *
C      *   SUBROUTINE  MWATER   *
C      * * * * *
C
C      This subroutine calculates the incremental
C      coefficient of thermal compressibility of
C      sand grains for a given temperature
C
C      SUBROUTINE MWATER (TSPEC,MWSPC)
C      REAL MW(5),TW(5),MWSPC
C      DATA TW(1)/20./,TW(2)/100./,TW(3)/125./,
C      *TW(4)/150./,TW(5)/200./,
C      *MW(1)/4.5E-7/,MW(2)/4.73E-7/,MW(3)/5.15E-7/,
C      *MW(4)/6.04E-7/,MW(5)/8.54E-7/
C      MWSPC=-1.0
C      IF(TSPEC-TW(1)) 90,90,91
90  MWSPC=MW(1)
    RETURN
91  IF(TSPEC-TW(5)) 93,92,92
92  MWSPC=MW(5)
    RETURN
93  DO 100 J=1,5
    IF(TSPEC-TW(J)) 100,94,100
94  MWSPC=MW(J)
    RETURN
100 CONTINUE
    MIN=1
    MAX=5
102 CONTINUE
    IF((MAX-MIN)-1) 200,200,104
104 NEXT=(MIN+MAX)/2
    IF(TSPEC-TW(NEXT)) 105,105,107
105 MAX=NEXT
    GO TO 102
107 MIN=NEXT
    GO TO 102
200 I=MIN
    TWFAC=(TSPEC-TW(I))/(TW(I+1)-TW(I))
    MWSPC=MW(I)+TWFAC*(MW(I+1)-MW(I))
    RETURN
END

C
C      * * * * *
C      *   SUBROUTINE  TEXBIT   *
C      * * * * *
C

```


C
C This subroutine calculates the thermal
C expansion (volume change) of in situ
C bitumen for a given temperature
C

```

SUBROUTINE TEXBIT (TSPEC,BITSPC)
  REAL BIT(9),TB(9),BITSPC
  DATA TB(1)/5./,TB(2)/22./,TB(3)/50./,TB(4)/75./,
  *TB(5)/100./,TB(6)/125./,TB(7)/150./,
  *TB(8)/175./,TB(9)/200./,BIT(1)/-1.4215/,
  *BIT(2)/0.0/,BIT(3)/2.851/,BIT(4)/5.373/,
  *BIT(5)/7.975/,BIT(6)/10.514/,BIT(7)/13.158/,
  *BIT(8)/15.971/,BIT(9)/18.737/
  BITSPC=-2.0
  IF(TSPEC-TB(1)) 90,90,91
90  BITSPC=BIT(1)
  RETURN
91  IF(TSPEC-TB(9)) 93,92,92
92  BITSPC=BIT(9)
  RETURN
93  DO 100 J=1,9
    IF(TSPEC-TB(J)) 100,94,100
94  BITSPC=BIT(J)
  RETURN
100 CONTINUE
  MIN=1
  MAX=9
102 CONTINUE
  IF((MAX-MIN)-1) 200,200,104
104  NEXT=(MIN+MAX)/2
  IF(TSPEC-TB(NEXT)) 105,105,107
105  MAX=NEXT
  GO TO 102
107  MIN=NEXT
  GO TO 102
200  I=MIN
  TBFAC=(TSPEC-TB(I))/(TB(I+1)-TB(I))
  BITSPC=BIT(I)+TBFAC*(BIT(I+1)-BIT(I))
  RETURN
END

```

C
C * * * * *
C * SUBROUTINE TEXWAT *
C * * * * *
C
C

C This subroutine calculates the thermal
C expansion (volume change) of water
C for a given temperature
C

```

SUBROUTINE TEXWAT (TSPEC,WATSPC)
  DIMENSION WAT(19),TW(19)
  DATA TW(1)/23./,TW(2)/30./,TW(3)/40./,TW(4)/50./,
  *TW(5)/60./,TW(6)/70./,TW(7)/80./,
  *TW(8)/90./,TW(9)/100./,TW(10)/110./,TW(11)/120./,
  *TW(12)/130./,TW(13)/140./,TW(14)/150./,TW(15)/160./,
  *TW(16)/170./,TW(17)/180./,TW(18)/190./,TW(19)/200./,
  *WAT(1)/0.0/,WAT(2)/0.182/,WAT(3)/0.531/,

```



```

*WAT(4)/0.960/,WAT(5)/1.470/,WAT(6)/2.029/,
*WAT(7)/2.668/,WAT(8)/3.357/,WAT(9)/4.106/,
*WAT(10)/4.924/,WAT(11)/5.793/,WAT(12)/6.731/,
*WAT(13)/7.730/,WAT(14)/8.798/,WAT(15)/9.946/,
*WAT(16)/11.174/,WAT(17)/12.492/,WAT(18)/13.900/,
*WAT(19)/15.428/
WATSPC=-1.0
IF(TSPEC-TW(1)) 90,90,91
90 WATSPC=WAT(1)
RETURN
91 IF(TSPEC-TW(19)) 93,92,92
92 WATSPC=WAT(19)
RETURN
93 DO 100 J=1,19
IF(TSPEC-TW(J)) 100,94,100
94 WATSPC=WAT(J)
RETURN
100 CONTINUE
MIN=1
MAX=19
102 CONTINUE
IF((MAX-MIN)-1) 200,200,104
104 NEXT=(MIN+MAX)/2
IF(TSPEC-TW(NEXT)) 105,105,107
105 MAX=NEXT
GO TO 102
107 MIN=NEXT
GO TO 102
200 I=MIN
TWFAC=(TSPEC-TW(I))/(TW(I+1)-TW(I))
WATSPC=WAT(I)+TWFAC*(WAT(I+1)-WAT(I))
RETURN
END

```

C
C
C
C
C
C
C
C
C

```

* * * * *
*   SUBROUTINE  VISWAT   *
* * * * *

```

This subroutine calculates the viscosity
of water for a given temperature

```

SUBROUTINE VISWAT (TSPEC,VWSPC)
DIMENSION VW(35),TW(35)
DATA TW(1)/5./,TW(2)/10./,TW(3)/15./,TW(4)/20.0/,
*TW(5)/25.0/,TW(6)/30.0/,TW(7)/35.0/,TW(8)/40.0/,
*TW(9)/45.0/,TW(10)/50.0/,TW(11)/55.0/,TW(12)/60.0/,
*TW(13)/65.0/,TW(14)/70./,TW(15)/75.0/,TW(16)/80./,
*TW(17)/85.0/,TW(18)/90./,TW(19)/95./,TW(20)/100./,
*TW(21)/105./,TW(22)/110./,TW(23)/115./,TW(24)/120./,
*TW(25)/125./,TW(26)/130./,TW(27)/135./,TW(28)/140./,
*TW(29)/145./,TW(30)/150./,TW(31)/160./,TW(32)/170./,
*TW(33)/180./,TW(34)/190./,TW(35)/200./,VW(1)/1.501E-3/,
*VW(2)/1.3E-3/,VW(3)/1.136E-3/,VW(4)/1.002E-3/,VW(5)/8.9E-4/,
*VW(6)/7.97E-4/,VW(7)/7.18E-4/,VW(8)/6.51E-4/,VW(9)/5.94E-4/,
*VW(10)/5.44E-4/,VW(11)/5.01E-4/,VW(12)/4.63E-4/,
*VW(13)/4.30E-4/,VW(14)/4.E-4/,VW(15)/3.74E-4/,
*VW(16)/3.51E-4/,VW(17)/3.3E-4/,VW(18)/3.11E-4/,
*VW(19)/2.94E-4/,VW(20)/2.79E-4/,VW(21)/2.65E-4/,

```



```

    *VW(22)/2.52E-4/,VW(23)/2.41E-4/,VW(24)/2.3E-4/,
    *VW(25)/2.2E-4/,VW(26)/2.11E-4/,VW(27)/2.03E-4/,
    *VW(28)/1.95E-4/,VW(29)/1.88E-4/,VW(30)/1.81E-4/,
    *VW(31)/1.69E-4/,VW(32)/1.59E-4/,VW(33)/1.49E-4/,
    *VW(34)/1.41E-4/,VW(35)/1.34E-4/
    VWSPC=-1.0
    IF(TSPEC-TW(1)) 90,90,91
90  VWSPC=VW(1)
    RETURN
91  IF(TSPEC-TW(35)) 93,92,92
92  VWSPC=VW(35)
    RETURN
93  DO 100 J=1,35
    IF(TSPEC-TW(J)) 100,94,100
94  VWSPC=VW(J)
    RETURN
100 CONTINUE
    MIN=1
    MAX=35
102 CONTINUE
    IF((MAX-MIN)-1) 200,200,104
104  NEXT=(MIN+MAX)/2
    IF(TSPEC-TW(NEXT)) 105,105,107
105  MAX=NEXT
    GO TO 102
107  MIN=NEXT
    GO TO 102
200  I=MIN
    TWFAC=(TSPEC-TW(I))/(TW(I+1)-TW(I))
    VWSPC=VW(I)+TWFAC*(VW(I+1)-VW(I))
    RETURN
END

```


B30365